

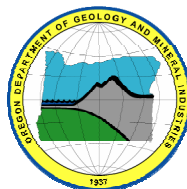
State of Oregon  
Department of Geology and Mineral Industries  
Vicki S. McConnell, State Geologist

**OPEN-FILE REPORT  
OFR O-06-02**

**INTERIM REPORT:  
JOHNSON CREEK LANDSLIDE PROJECT,  
LINCOLN COUNTY, OREGON**



By  
George R. Priest<sup>1</sup>, Jonathan Allan<sup>1</sup>, Alan Niem<sup>1</sup>, Samuel R. Christie<sup>2</sup>, and Stephen E. Dickenson<sup>2</sup>



**2006**

<sup>1</sup>Oregon Department of Geology and Mineral Industries, Coastal Field Office, 313 SW Second Street, Suite D, Newport, OR 97365

<sup>2</sup>Geotechnical Engineering Group, Department of Civil, Construction and Environmental Engineering, Oregon State University, Corvallis

---

#### **NOTICE**

This paper is being published as received from the author(s). No warranty, expressed or implied, is made regarding the accuracy or utility of the information described and/or contained herein, nor shall the act of distribution constitute any such warranty. This disclaimer applies both to individual use of the data and aggregate use with other data. The Oregon Department of Geology and Mineral Industries shall not be held liable for improper or incorrect use of this information

Oregon Department of Geology and Mineral Industries Open File Report O-06-02  
Published in conformance with ORS 516.030

For copies of this publication or other information about Oregon's geology and natural resources, contact:

Nature of the Northwest Information Center  
800 NE Oregon Street #5  
Portland, Oregon 97232  
(503) 872-2750  
<http://www.naturenw.org>

## TABLE OF CONTENTS

<b>Executive Summary</b> .....	1
<b>Introduction</b> .....	5
Purpose and Scope of Work.....	8
Background Information and Previous Investigation.....	8
<b>Geology and Surface Conditions</b> .....	9
Surface Features .....	9
Geology .....	12
Surface Water and Groundwater .....	24
<b>Field Investigation</b> .....	25
Topographic Survey.....	25
Exploratory Drilling and Borehole Instrumentation.....	25
Precipitation .....	30
Test Pits.....	30
Surface Ground Movement Survey.....	30
Erosion .....	30
Sand Movement.....	31
<b>Laboratory Testing</b> .....	32
Soil Classification.....	32
Natural Moisture Content.....	32
In-Place Density.....	32
Residual Shear Strength.....	33
<b>Geotechnical Data</b> .....	35
Subsurface Materials/Conditions .....	35
Landslide Movements.....	35
Groundwater and Precipitation .....	50
Erosion and Beach Sand Movement .....	63
<b>Landslide Stability Evaluation</b> .....	64
Back Analysis (from Landslide Technology, 2004) .....	64
Sensitivity Analysis .....	66
<b>Conceptual Mediation Options</b> .....	68
Option 1 – Unload Upper Slide .....	69
Option 2 – Toe Buttress.....	71
Option 3 – Horizontal Drains.....	72
Option 4 – Tied-Back Shear Pile Wall.....	73
Option 5 – Road Maintenance .....	74
Summary of Remediation Options .....	74
Discussion of Stability Analysis .....	75
<b>Discussion</b> .....	76
<b>Recommendations</b> .....	80
<b>Acknowledgements</b> .....	84
<b>References</b> .....	85
 <b>Appendix A. Preliminary Borehole to Sea Cliff Correlations, X-ray Diffraction and SEM Analysis of Slip Plane, and Grain Size Study of Sedimentary Units of the Johnson Creek Landslide on US 101, Central Coast of Oregon, North of Newport</b>	
<b>Appendix B. Borehole Logs</b>	
<b>Appendix C. Test Pits at the Toe of the Johnson Creek Landslide</b>	
<b>Appendix D. Slide Movement from Surveys of Iron Marker Pins, October 24, 2002 and April 17, 2003</b>	
<b>Appendix E. Line-of-Sight Surveys on Highway 101</b>	
<b>Appendix F. Erosion Pin Data at The Sea Cliff</b>	
<b>Appendix G. Movement Data from Reference Nails on Fresh Landslide Scarps</b>	
<b>Appendix H. Beach Sand Movement</b>	
<b>Appendix I. Ring Shear Test Results</b>	
<b>Appendix J. Geotechnical Modeling of Slope Stability, Johnson Creek Landslide Investigation, Lincoln County, Oregon</b>	

## LIST OF FIGURES

Figure 1.	Location of study area.....	6
Figure 2.	Site map of the Johnson Creek landslide.....	7
Figure 3.	Astoria Formation Sandstone.....	10
Figure 4.	Highly sheared dark gray sandy siltstone unit at the toe of the Johnson Creek Landslide.....	11
Figure 5.	Pleistocene marine terrace sand exposed in the northeast headwall of the landslide.....	12
Figure 6.	Geologic map of the Johnson Creek Landslide.....	14
Figure 7.	Simplified geologic cross section A-A .....	15
Figure 8.	Map explanation for geologic map .....	15
Figure 9.	Geologic map illustrating general continuity of bedding along the large block at the toe of the landslide ..	16
Figure 10.	View north at white marker bed that is easily traced for hundreds of feet along the toe of the Johnson Creek Landslide.....	17
Figure 11.	Blue lines are structure contours in meters of elevation (relative to geodetic mean sea level NAVD88) on the slide plane .....	19
Figure 12.	Detailed geologic map of the southwest end of the Johnson Creek Landslide .....	20
Figure 13.	Detailed geologic map at northwest margin of the landslide at Miner Creek.....	21
Figure 14.	Soft wet silty gouge at slide plane in borehole LT-1 at 27.4 m (90 ft) depth.....	23
Figure 15.	Schematic diagram of extensometer construction in boreholes LT-1, LT-2, and LT-3 .....	28
Figure 16.	Automated data collection system installed November 20, 2004 .....	29
Figure 17.	Topographic contours at 0.25-m intervals on the beach west of the Johnson Creek Landslide.....	31
Figure 18.	Sample used for ring shear test at a depth of 59 feet in borehole LT-2. ....	33
Figure 19.	Results of ring shear test on sample from 59 ft depth in borehole LT-2. ....	34
Figure 20.	Inclinometer data for borehole LT-1 .....	37
Figure 21.	Inclinometer data for borehole LT-2 .....	38
Figure 22.	Inclinometer data for borehole LT-3 .....	39
Figure 23.	Inclinometer, Extensometer, and rainfall data. ....	40
Figure 24.	Total movement from combined inclinometer and extensometer data (cm) versus piezometer (pressure head in meters above the slide plane) data and rainfall (mm/hour). ....	41
Figure 25.	Piezometric head elevation above geodetic mean sea level (NAVD 88) at the LT-2p borehole, January 2003 .....	41
Figure 26.	January 31 to February 3, 2003 movement event versus head and rainfall. ....	26
Figure 27.	March 2003 movement versus piezometer, and rainfall data. ....	42
Figure 28.	November 17, 2003 to January 2, 2004 movement versus head and rainfall. ....	43
Figure 29.	January 27 to February 7, 2004 movement versus head and rainfall.....	43
Figure 30.	Correlation of slide movement and pressure head above the slide plane in each movement event with cumulative antecedent rainfall 1, 2, 4, 8, 16, and 48.7 days before the event .....	44
Figure 31.	Compression (- values) and extension (+ values) between boreholes based on the 2002-2004 inclinometer and extensometer data .....	45
Figure 32.	Change of distance between boreholes LT-1 and LT-3 .....	45
Figure 33.	Re-survey data for steel rods east of active slide movement for determination of error.....	47
Figure 34.	Horizontal movement (cm) at steel stakes (blue crosses) in northern part of landslide between October 2002 and April 2003 .....	48
Figure 35.	Horizontal movement (cm) at steel stakes (blue crosses) landslide between October 2002 and April 2003 in southern part of landslide .....	48
Figure 36.	Schematic illustration of groundwater circulation .....	51
Figure 37.	Cross section illustrates inclinometer holes, piezometer holes, piezometer tip locations and the minimum water level (red dashed line) that initiates movement on the Johnson Creek slide relative to the February 1, 2003 maximum and summer minimum.....	51
Figure 38.	Schematic illustration of progressive rise in piezometric head from east-to-west after a typical rainfall event.....	56
Figure 39.	Positive correlation of hourly rainfall to same-hour pressure head rise for five 2003 rainfall events .....	59
Figure 40.	Generalized cross section used by Landslide Technology (2004) for stability analysis .....	65
Figure 41.	Decrease of factor of safety at the Johnson Creek Landslide from erosion of the slide toe (sea cliff).....	67
Figure 42.	All remediation alternatives summarized by Landslide Technology (2003).....	70
Figure 43.	Remediation by unloading the head of the slide and buttressing the slide (taken from Landslide Technology, 2003) .....	70
Figure 44.	Remediation by horizontal drains and shear pile wall with tiebacks (taken from Landslide Technology, 2003) .....	73
Figure 45.	Schematic illustration of probable water level changes in the landslide fracture system before, at, and after a sharp rise in pressure head from a rainfall event .....	79



## LIST OF TABLES

Table 1. Depths and elevations of boreholes, piezometers, and the slide plane at each hole .....	27
Table 2. Summary of In-place density testing. ....	32
Table 3. Re-survey of steel stake markers at the headwall for error analysis (all horizontal and vertical values should be zero). ....	46
Table 4. Slide movement between October 2002 and April 2003 from re-survey of steel stakes .....	49
Table 5. Detailed correlation of piezometric head versus slide movement for Events 2-5. ....	53
Table 6. Most representative threshold values of initial (background) pressure head, pressure head at movement, and depth to elevation head (water table) for slow and fast slide movement. ....	54
Table 7. Time lag of major changes in pressure head between drill holes for rainfall events causing movement at all extensometers. ....	55
Table 8. Time lag of east-to-west propagation of peaks in pressure head from borehole to borehole, amount of extension or compression between boreholes prior to each movement event, and displacement during each event .....	55
Table 9. Trial calculations of rates of groundwater movement or hydraulic pressure transmission calculated assuming either lateral transmission (down the hydraulic gradient) between piezometers or vertical percolation of water through the vadose zone to the water table at each piezometer. ....	57
Table 10. Summary of material strength and density parameters.....	65
Table 11. Summary of Sensitivity Analyses .....	68
Table 12. Remediation option evaluation.....	74
Table 13. Threshold (minimum) values of movement, rainfall and piezometric head to be used in a possible landslide warning system. ....	83

## EXECUTIVE SUMMARY

This is an interim report summarizing geotechnical research on the Johnson Creek Landslide, located 0.5 km north of Newport on the Oregon coast. The five-year research project started in the fall of 2002 and is aimed at determining what makes the slide move and what are the most cost effective means of slowing or stopping it. The project is funded by the Oregon Department of Transportation (ODOT) Research Program, utilizing Federal Highway Administration (FHWA) support. ODOT and FHWA are interested in this slide, because it is representative of many large translational slides along the US west coast.

The Johnson Creek Landslide is a large translational slide in seaward-dipping siltstone and sandstone of the Tertiary Astoria Formation. Six boreholes were drilled at three sites in an east-west line approximately in the center of the slide; from west to east the sites are LT-1, LT-2, and LT-3. At each of the three sites an inclinometer hole was drilled to establish slide depth followed by a matching piezometer hole targeted at the slide plane. One piezometer was also installed below the slide plane. Rainfall was monitored by a rain gauge in a clear cut at the headwall of the slide. Movement during December 2003 deformed the inclinometer casing enough that standard inclinometer logging devices no longer passed by the slide plane. Cable-type extensometers were then installed in each borehole to track movement.

The central part of the landslide has a total displacement of ~28 m horizontal and 6 m vertical based on a balanced cross section developed through the drilling transect. Offset of the Old Coast Highway since its abandonment in 1943 for the new Highway 101 alignment is  $3.35 \pm 0.6$  m horizontal and  $0.91 \pm 0.05$  m vertical, or a mean rate of  $5.4 \pm 1$  cm/yr horizontal and  $\sim 1.5 \pm 0.08$  cm/yr vertical. The slide plane dips seaward, cutting through weak siltstone units and generally deflecting along the top of more competent sandstone and zeolitized tuff beds. In the northern 85 percent of the slide, the slide plane reaches below sea level and then curves upward at the toe of the slide, rotating the westernmost slide block backward and overriding slide talus on the beach. In the southern 15 percent of the slide the slide plane at the toe is relatively flat but still has a back-rotated slide block at the sea cliff.

During severe rainfall events, the slide can undergo movements that offset Highway 101 by tens of centimeters lateral and vertical over a period of only a few hours or days, posing serious risk to vehicular traffic and significant highway repair costs. Six slide movements were recorded by inclinometers or extensometers, all correlating with intense rainfall events that trigger large increases in piezometric head. The largest movement occurred at the end of January 2003. Only minor offset of the Highway 101 occurred at the northern slide margin during this event, but movement increased toward the southwest where the slide plane at the toe is flat rather than forming an east-inclined buttress like it does to the north. Vertical offset on the southernmost slide margin was so large that emergency gravel was dumped on Highway 101 to keep it open until it could be paved later in the year. Extensometer and resurvey data revealed that interior blocks within the slide apparently moved at different rates during this event, creating areas of extension, compression and lateral movement within the slide. This one large movement caused most of the maintenance cost in the two-year observation period. The other five movement events were all slow creeping movements each of <4 centimeters lateral (<1 cm vertical) that caused only minor highway damage. Marker nails monitored around the slide perimeter and data from extensometers in the center of the slide during the slow movement event in March 2003 revealed that the slide moved as a whole about equal amounts in the center and at the north, south and east margins. These data are consistent with two distinctive

styles of slide movement, slow and fast, with differential offset within the slide occurring principally during the fast movements. Only 1.5-2.7 m of head separates slow versus fast slide movement, so lowering of piezometric head by ~3 m would probably eliminate the most dangerous, highly damaging slide movements.

Based on borehole core and outcrops, a relatively impermeable silty gouge coats the slide plane, effectively isolating the fractured slide mass from the Astoria Formation below. Piezometric elevation head below the slide plane is 4-6 m lower than head at the slide plane, illustrating the lack of hydraulic communication across this gouge. The piezometer below the slide plane could only collect data until it was severed at the slide plane by the rapid movement event of February 1, 2003, an observation period of 24 days, but up to that time the elevation head steadily increased below the slide plane at a rate of about 4.5 cm/day. In contrast, water pressure above the slide plane underwent sharp rises in response to rainfall events but fell back to a fairly constant (background) value between events. Water wells in the slide produce water from Astoria Formation that is adequate for domestic well use, whereas those in Astoria Formation outside the slide have negligible flow rates in many cases, so the Astoria Formation, where not fractured by mass movement, is relatively impermeable. We conclude that intact Astoria Formation below the slide tends to store meteoric water during the wet months, building up water pressure gradually by regional scale groundwater flow, whereas groundwater drains away much faster in the shallow fractured Astoria Formation within the slide. During a wet year it might be possible by April or May for the pressure head below the slide to equal or exceed the background pressure at the slide plane, contributing to a decrease in forces resisting movement.

Hourly piezometer data reveal that spikes in pressure head occur progressively from east to west (down the hydraulic gradient) over a period of 30-44 hours in response to large rainfall events. About 90 mm of hourly head rise occurs for each millimeter of hourly rainfall at a piezometer located on the west margin of the headwall graben where the water table is relatively close to the surface. Walls of the piezometer hole at this locality are composed mostly of well-sorted (poorly graded) Pleistocene marine terrace sand that caps the Astoria Formation throughout much of the slide. The intergranular void space in the terrace sand is on the order of 40 percent, but the large rise in piezometric head (9 times the rainfall) can be accommodated only if the voids being filled comprise ~1.1 percent. Field estimates of fracture voids in a structural position within the slide identical to this drill site were also 1.1 percent. These data and field observations of the slide fracture system in other localities are consistent with pressure head “spikes” being caused by downward percolation of rain into ~1 percent fractures spaced ~0.3 m apart in the slide mass. A further implication of these observations is that water is seeping much more slowly into intergranular pores than into the fracture system, so piezometric head is representative of pressure in the fractures rather than the interiors of blocks of rock bounded by the fractures. Groundwater, unless drained away through the fracture system will, over time, saturate the intergranular pore spaces, effectively transmitting hydraulic pressure throughout the rock mass, so multiple, closely spaced rainfall events in the winter will gradually saturate the rock..

The one large, fast slide movement that occurred at the end of January 2003 was preceded by two intense rainfall events, one starting a few days before the movement and another about 6 weeks earlier. The fast movement event also had somewhat higher overall piezometric head (“background head”) prior to the triggering rainfall event and associated head “spike” than the other five movement events, all of which had small slow movements. These observations suggest that a long period of significant rainfall and high head in the fracture system may allow greater penetration of groundwater into intergranular pores and microfractures, thereby increasing the effectiveness of buoyant forces that promote large, fast slide movement when combined with lateral force of water in fractures.

Currently available limit equilibrium software is not designed to simulate buoyant forces associated with partial saturation of a slide mass or lateral forces from water in multiple fractures. Much additional work needs to be done to more accurately simulate these forces with numerical models.

Since movement is triggered by rainfall and correlative water pressure increases, dewatering should be an effective remediation option. A significant amount of the water in the slide is from direct rainfall percolating into well-connected, steeply dipping fractures that appear to effectively drain groundwater after each rainfall event, so dewatering schemes should be efficient. An array of horizontal drains emplaced by drilling from the toe of the slide only lowers the factor of safety by ~1 percent in the main central mass of the slide, owing to the geometry needed for gravity drainage (Landslide Technology, 2004; written communication, 2005). Horizontal drains are also vulnerable to rupture by the rotated block at the slide toe. If pumped vertical wells could keep the water table at normal winter levels, this would amount to a ~9 percent increase in the factor of safety during large rainfall events. Costs for vertical wells would be higher than horizontal drains and should be estimated in the final report. Modeling of slide forces revealed that dewatering fractures at the toe and slowing or eliminating toe erosion is particularly critical in achieving an increase in the factor of safety.

Buttressing the toe of the slide with basalt rip rap is higher in cost than dewatering by horizontal drains both in dollars and environmental impact but is simple to construct and much less likely to fail. Buttressing also eliminates erosion. The most cost effective approach, both in dollars and environmental impact, would be to buttress only the southern 30 percent of the slide where the most damaging movement has occurred and where a rip cell embayment focuses wave erosion. Minimum cost would be ~\$330,000, equivalent to about 16 years of road maintenance at ~\$20,000 per year. There would still be some small road maintenance cost in the northern part of the slide and periodic cost to maintain the buttress.

According to Landslide Technology (2004), remediation utilizing a tied-back shear pile wall or by unloading and draining the upper part of the slide with perforated pipes parallel to the headwall would also be effective, but are much higher in cost than dewatering by horizontal drains or buttressing. These options do not compare well with just maintaining the road under current conditions.

The analysis in this report is still incomplete without an accurate measure of wave erosion at the toe of the slide. Limit equilibrium analysis by Landslide Technology (2004) and outlined in Appendix J illustrates that erosion is a highly significant factor probably capable of triggering movement even if dewatering lowers water pressure in the slide. Erosion can, over time, make the slide more susceptible to rainfall events by gradually lowering the factor safety. Ground-based LIDAR surveys should be completed annually or semiannually to accurately track erosion. Monitoring wave activity from offshore buoy data will allow empirical relationships to be established between erosion and wave strike that will allow erosion prediction in the future from the buoy data alone. An analysis of erosion control utilizing a dynamic revetment in the southern part of the slide should be evaluated in the final report. A dynamic revetment composed of cobbles could offer a significant increase in the factor of safety by both controlling bluff loss and buttressing the slide, while minimizing environmental impact.

Additional investigation of the hydrology and geotechnical properties of the slide mass are needed in order to design the most cost effective remediation through a combination of dewatering, buttressing, and erosion control. This landslide offers an ideal natural laboratory for evaluation of innovative new approaches to modeling, instrumentation, and remediation of large translational landslides.

Movement, piezometric head, and rainfall data are all being collected on an hourly basis since the US Geological Survey upgraded the instrumentation November 20, 2004. These data will, for the first time, allow hourly movement to be correlated with the water pressure data. It is likely that the waves of water pressure that travel from the east to the west in response to rainfall events are accompanied by contemporaneous movement when threshold pressures are reached, but earlier extensometer data were not collected often enough to resolve these details.

The USGS reportedly plans to install cell phone links to the dataloggers in the future. This new instrumentation offers the opportunity to provide real-time warnings to ODOT of actual and impending slide movement. However, such warnings would be experimental at best, and should not be relied upon without other types of observations. A warning system based on the currently installed data collection system might give false alarms, or movement could still occur unexpectedly as a result of instrument failures, communications failures or other factors. The following are thresholds for warning of impending large (tens of centimeters) fast movement (more indicators = more certainty):

- Pressure head of 9 m, 12 m, and 6.5 m for piezometers, LT-1p, LT-2p, and LT-3p, respectively.
- Background pressure head of ~6.9 m, 9.4 m, and 4.6 m in LT-1p, LT-2p, and LT-3p, respectively.
- Antecedent rainfall of 118 mm for 48 hours and 717 mm in the previous 48.7 days.
- ~2 cm of movement over about 4 days.

## INTRODUCTION

This is a progress report for a five-year investigation by Oregon Department of Geology and Mineral Industries (DOGAMI) and Oregon Department of Transportation (ODOT) of the Johnson Creek Landslide, Lincoln County, Oregon (Figure 1). The project is sponsored by the ODOT Research Program and is aimed at understanding the driving forces behind large translational landslides that commonly occur in Tertiary sedimentary rocks on the west coast of the US. The slide is less than 0.5 km ( $\frac{1}{4}$  mile) south of Otter Rock, Oregon and impacts U.S. Highway 101, two private structures and local utilities. The site location is shown on Figure 1 and site features, including locations of boreholes and a rain gauge are shown on Figure 2. This report is an update on results from the 2002-2003 investigation summarized previously by Landslide Technology (2004), hence, much of the information given here from the fall of 2002 through spring of 2003 is duplicated in the Landslide Technology report and we have borrowed freely from that report.

This report summarizes the observations through November 20, 2004 and includes much of the data and many of the interpretations outlined by Landslide Technology (2004). New information is mainly centered on additional geologic observations, three new slide movement events from the winter of 2003-2004 and a more detailed analysis of the correlation between movement, changes of pressure head, and rainfall. These correlations provide insights into the critical role of hydrostatic forces in fractures versus intergranular pore spaces for factor of safety calculations. Also summarized in detail here are possible rainfall, water pressure and movement parameters for a potential landslide warning system.



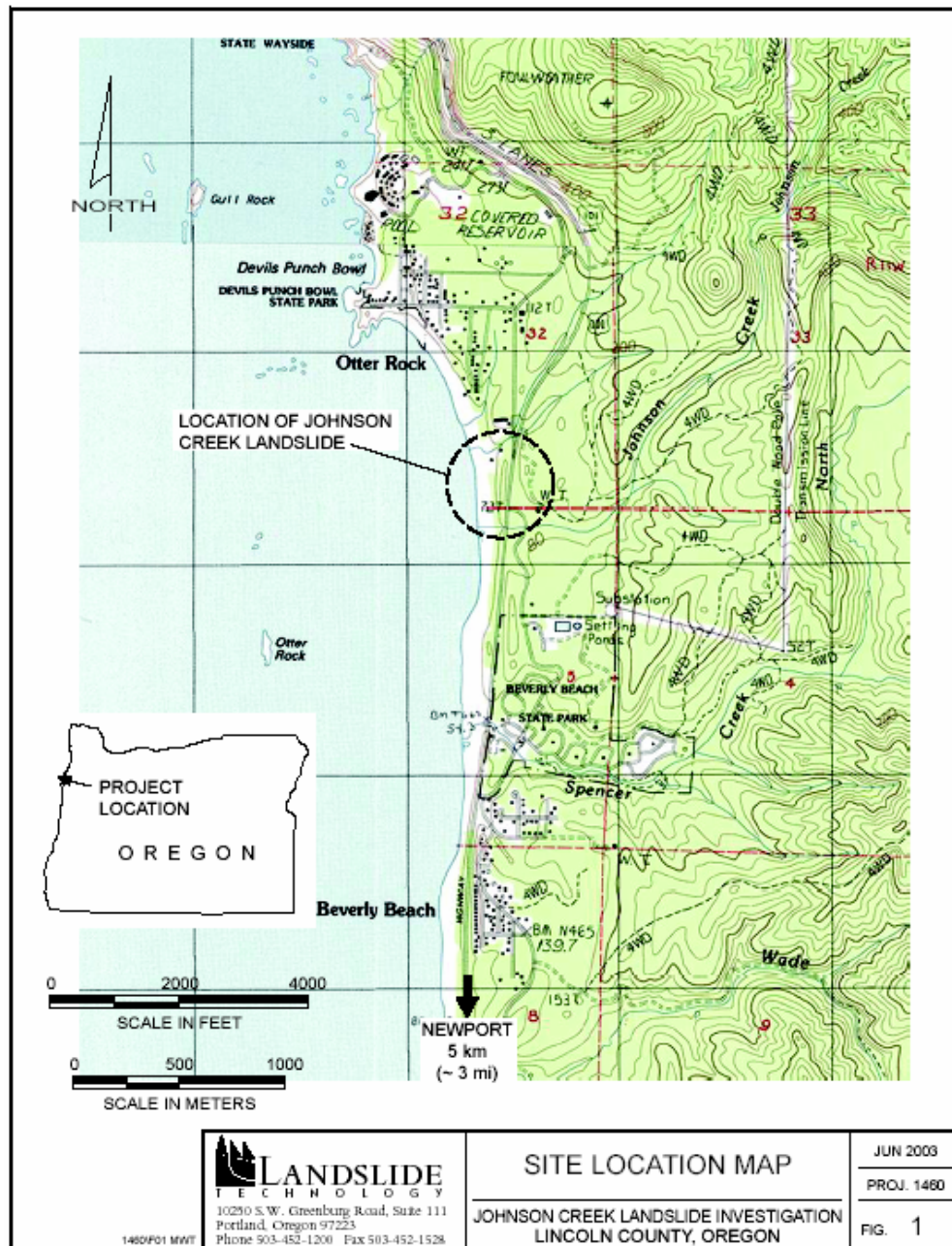
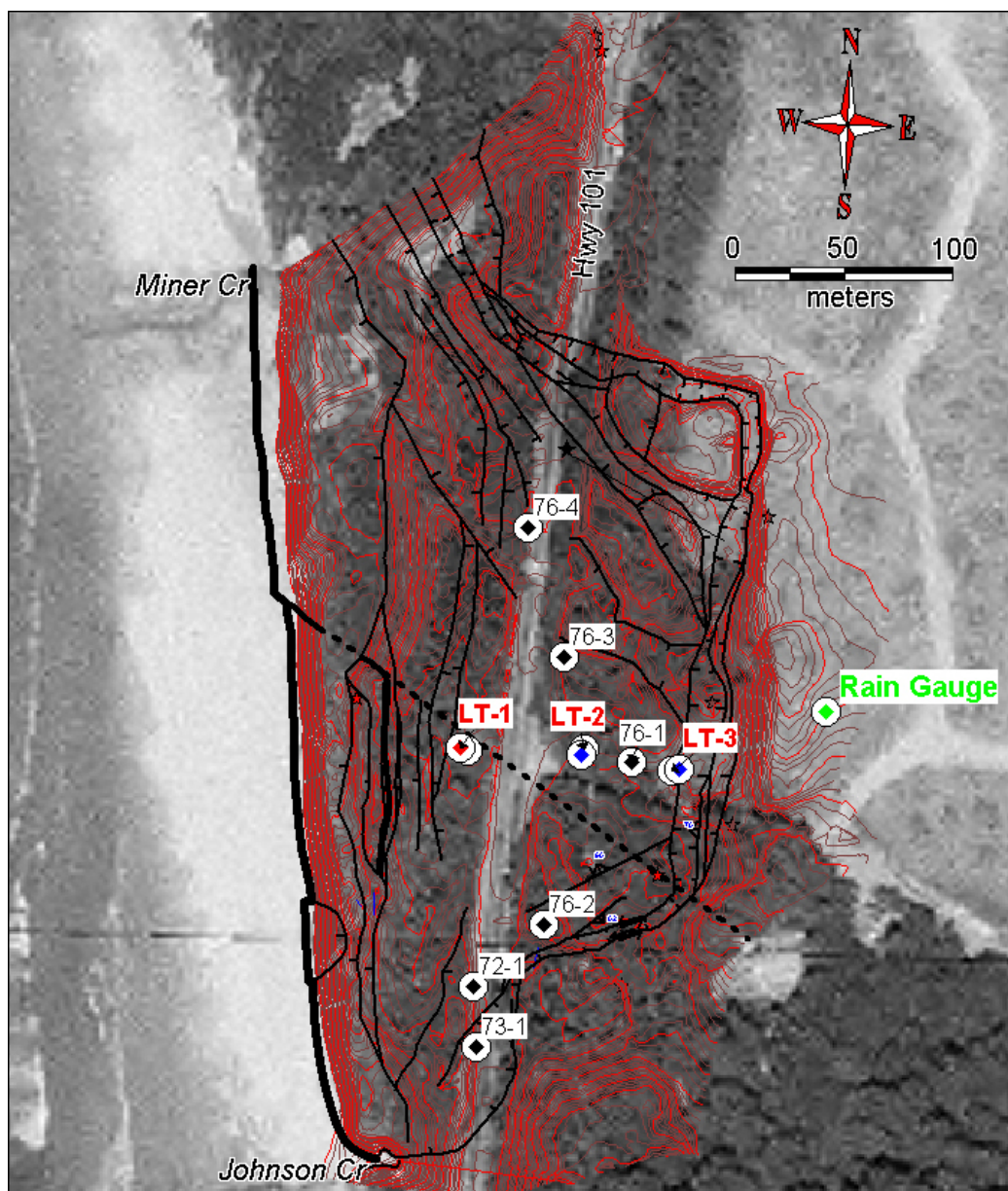


Figure 1. Location of the study area. Figure is taken from Landslide Technology (2004).



**Figure 2.** Site map of the Johnson Creek Landslide showing the drill sites, LT-1, 2, and 3 (red labels) plus location of 1970's boreholes (black diamonds with circles) and the rain gauge. Base map is a 2002 US Geological Survey digital orthophoto quadrangle (DOQ). Red lines are topographic contours at 2 m intervals; muted brown lines are contours at 0.5 m intervals; black lines are major slide block boundaries. Black teeth on slide boundaries point toward the down thrown side.

## **Purpose and Scope of Work**

The primary purpose of this study is to analyze the causative factors of slide movement, and to evaluate the effectiveness and cost of remediation alternatives. The objective is to develop information on Oregon's coastal translational landslides to enhance scientific understanding of their movement, and to provide information to ODOT on the scale and costs of mitigation and remediation. Landslide Technology (LT), a consulting firm in the Portland area, conducted the initial field investigation and analysis in the winter of 2002-2003. Their scope of work consisted of the following tasks:

- Collect and review available data
- Public meeting to present plan of investigation
- Permitting and utility locates
- Subsurface exploration, installation of geotechnical instrumentation, and instruction of DOGAMI personnel on instrument monitoring
- Laboratory testing
- Data and stability analyses
- Remedial options evaluation
- Technical Report (Landslide Technology, 2004)

DOGAMI was responsible for overall project management and field data collection, including monitoring of the slide over a five-year period. Their principal tasks include:

- Project management, including contracting, reporting and convening periodic meetings of a technical steering committee consisting of ODOT and DOGAMI personnel.
- Field data collection (geologic mapping, logging and stratigraphic interpretation of drill hole samples, collection of piezometer, rainfall, extensometer, and inclinometer data.)
- Geological and geotechnical interpretation of data.
- Publication of three reports, the LT report (Landslide Technology, 2004), an interim report after about two years (this report) and a final report in 2007 at the end of five years of data collection.

## **Background Information and Previous Investigation**

The Johnson Creek Landslide has a history of impacting U.S. Highway 101 and two private structures. The slide is clearly visible on 1939 aerial photos and appears to have affected the alignment of the Old Coast Highway since its construction some time in the early part of the 20<sup>th</sup> Century. The alignment of Highway 101, constructed ~1943 is similarly affected. In the 1970s ODOT performed a series of explorations to investigate the depth of the landslide and evaluate the potential costs of remediation. Six borings with inclinometers were installed between 1972 and 1976 (Figure 2). All of these inclinometers pinched off within a few years. Copies of the logs and inclinometer readings are included in the LT report (i.e., Landslide Technology, 2004). A brief report was prepared by ODOT in 1979 that summarized the results of the investigation and provided discussion of possible remedial options. LT conducted the initial geotechnical drilling for this project in winter 2002-2003 and produced a report in 2003 that was published by DOGAMI in 2004 (Landslide Technology, 2004). The LT report documented three movement events, including a large movement at the end of January 2003 that

sheared all of the inclinometers and caused serious damage to Highway 101. Movement since that time has been minor, consisting of three slow, creeping events that caused minimal damage to the highway during the winter of 2003-2004.

## GEOLOGY AND SURFACE CONDITIONS

Geologic mapping was conducted by George Priest with assistance from Alan Niem. The area is covered by dense vegetation and deep soil that hindered bedrock mapping. A 1-meter steel split tube punch coring device was utilized to penetrate the soils where bedrock was poorly exposed. Some areas had such dense brushy vegetation that they were virtually inaccessible. The most accurate geologic data were gathered at the sea cliff where waves have cleaned off vegetation, soil and talus.

### Surface Features

Johnson Creek Landslide is approximately 200 meters (660 feet) from the headscarp to the toe (east-west) and 360 meters (1180 feet) north-south. The slide is bounded by steep-sided ravines at Johnson Creek on the south and at a creek to the north called Miner Creek by local residents. Surface features within the slide area include: the headscarp, graben, the slide toe at the base of the shoreline bluff, the bluff, slumps in the bluff, and elongate ridges and depressions. Most of these features are outlined on the Site Plan, Figure 2.

**Headscarp.** The headscarp is up to 10 meters (33 feet) high around the east limit of the landslide. The headscarp has two generalized appearances: steep to the north and relatively gentle to the south. The northern scarp exposes terrace sand in a near vertical cliff, while the southern scarp is mostly covered with colluvium and vegetation. Considering the time that is necessary for erosion and development of colluvium, the difference in the condition along the scarp suggests that the northern area is a more youthful feature, while the southern portion of the scarp is older.

East of the headscarp the surface elevation varies from 33 to 40 meters (108 to 131 feet). Within the landslide the surface elevation rises from about 22 meters (72 feet) in the south to 34 meters (112 feet) in the north. The difference in elevation within the slide is interpreted to be due to older and more significant amounts of displacement in the southern portion of the slide.

**Graben.** The graben of this landslide changes from south to north. To the south the graben is very subtle with a 10-meter (33-foot) headscarp to the east and an irregular 1 to 2-meter (3- to 7-foot) back or reverse-facing scarp to the west. In this area the graben varies from about 10 to 20 meters (33 to 66 feet) wide. To the north the graben is well defined with prominent 10-meter (33-foot) headscarp and 5 to 10 meters (16 to 33 feet) width. At the northeast corner, the graben wraps around onto the northern side margin at approximately the same width (Figure 2), suggesting net extension toward the southwest on a vector bisecting the angle between the strike of the northern and eastern headscarps, ~S46°W.

**Northeast Area.** Northwest-trending ridges and depressions occur that are approximately perpendicular to the inferred S46°W extension direction inferred from the northeastern headscarp. In addition, a relatively intact slide block with fresh, near vertical sides appears isolated in the northeast corner of the



landslide. The northeast features are likely influenced by: stress relief southward into the older slide area, westward movement along the tilted bedding, and pre-existing northwest-trending tectonic fractures.

**Toe**. The toe of the landslide is at the base of the shoreline bluff (Figure 3). At the south where Johnson Creek flows onto the beach, in-place bedrock is exposed in the creek ravine. Sheared bedrock is exposed at the base of the cliff to the north during winter beach conditions (Figure 4).



**Figure 3.** Looking north at Tertiary Astoria Formation sandstone (smooth light tan unit) and sandy siltstone (overlying dark orange gray unit) at the toe of the Johnson Creek Landslide. Dark gray unit exposed in small patch below the sandstone is highly sheared sandy siltstone from the basal shear zone of the slide. Black 0.8 m long back pack is shown for scale.



**Figure 4. Highly sheared dark gray sandy siltstone unit at the toe of the Johnson Creek Landslide. Chuck Dennison of Dennison Surveying is pointing at the soft, highly deformed material.**

**Sea Cliff.** Exposures of landslide debris in the sea cliff above the toe include bedding that is tilted, fractured and sheared. Bedding that is relatively intact tends to dip between 15 and 45 degrees to the east (Figure 3). This “back-rotation” is likely due to upward movement of slide blocks and local slumping of the sea cliff. If the basal slide zone of a translational slide rises to the surface at its toe, a passive wedge is formed where material can rotate relative to the main slide mass. Local slumps can also result in back-rotation of slide blocks. Westward movement of the main slide mass oversteepens the bluff, which can locally slump over the low strength gouge. The scarp bounding the passive wedge on the east trends north-south consistent with westward movement.

**Central and Southern Area.** Elongate ridges and depressions characterize the ground surface within the central and southern part of the landslide. These features are visible in the relatively flat terrace, but due to the high amount of natural surface activity in this coastal environment, they are often relatively subtle and covered with dense vegetation. Shown on the Figure 2, these features appear to occur in two regions: along the bluff and in the northeast. Very long and narrow features characterize the ground surface along the bluff. These features are interpreted to be high angle tensional features that occur due to stress relief parallel to the bluff, possibly along pre-existing tectonic faults or joints and fractures within the bedrock. Most interior scarps within the southern half of the slide trend approximately north-south consistent with westward slide movement.



## Geology

**Rock Units.** The Johnson Creek Landslide is within mudstone, siltstone, fine- to medium-grained, poorly sorted sandstone, and hard, tuffaceous claystone of the Miocene Astoria Formation (Figures 3 and 4). The Astoria Formation is widespread on the Oregon Coast, with mapped exposures from Astoria to south of Newport. Numerous landslides occur within this formation, the largest in areas like this one where bedding dips toward the sea cliff. None of the Astoria Formation lithologies in this area appear to have sorting high enough to have high permeability.

The slide also cuts Pleistocene marine terrace sand deposits that lie on a nearly flat-lying Pleistocene wave cut terrace (Figures 4-8). These deposits are 3 to 6 meters (10 to 20 feet) thick and are comprised of well-sorted fine- to medium-grained quartz-feldspathic sand underlain by a basal cobble layer. In some places post-depositional erosion has removed or redistributed the original deposits. The deposits have much higher permeability than the finer grained, cemented and poorly sorted sedimentary rock of the underlying Astoria Formation. The Pleistocene sand is slightly cemented by thin films of poorly crystalline goethite (Johnson, 2003; <http://web.pdx.edu/~grathog/StudentWork/Catrina%20Johnson%20UG%20honors%20thesis%20SP03.pdf>) and/or allophane with some larger voids locally filled with gibbsite (Grathoff and others, 2001; Grathoff, 2005; [http://web.pdx.edu/%7Egrathog/CMS2003\\_files/frame.htm](http://web.pdx.edu/%7Egrathog/CMS2003_files/frame.htm); Johnson, 2003), but overall porosity is still quite high. As allophane dehydrates and shrinks, it loses its cementing qualities, causing the terrace sand to become highly friable where exposed (Grathoff, 2005), hence, most exposures of the terrace sand quickly become covered in talus unless the exposure is recent or talus is continuously removed by erosion. The best exposures are at the recently exposed portion of the northeast headscarp (cover page picture and Figure 5) and at the top of the sea cliff.



**Figure 5.** Pleistocene marine terrace sand exposed in the northeast headwall of the landslide. Jonathan Allan of DOGAMI is measuring the thickness of the unit. Note the nearly flat surface of the sand sheet. The contact with underlying Tertiary Astoria Formation is ~1 m below the base of the ladder.

According to the structural-stratigraphic analysis detailed in Appendix A, total downward displacement on the Pleistocene wave-cut platform at the toe of the slide is on the order of 21 m (70 ft), measured at the center of the slide (latitude of boreholes LT-1, -2, and -3). The lower contact of the Pleistocene sand deposit is at an elevation of ~29 m (95 ft) in the northern half of the headscarp to ~32 m (105 ft) in the southern half. The lower contact on the north appears to be a wave-cut platform, whereas the one on the south appears to be irregular with colluvial material at the contact consistent with deposition in a subaerial environment with intermittent runoff. If the Pleistocene marine terrace age and contemporaneous sea level can be determined from sea level curves, then tectonic uplift rate can be estimated. This rate would allow estimation of the ages of two higher terraces that are preserved east of the landslide at elevations of ~70 m and 120 m. Older (higher) marine terraces are apparent east of the headscarp; assuming that this rate is representative of uplift rate during the last million years or so, older terrace ages can probably be inferred from this rate and elevations of wave-cut platforms.

The terrace deposits overlie a 0.3- to 2-meter (1- to 6-foot) layer of orange, decomposed Astoria Formation, which in turn, overlies gray, unaltered Astoria Formation bedrock. The structural dip of the Astoria Formation at the site has been measured in nearby exposures at 15 to 20 degrees to the west. The Astoria Formation at the headwall of the landslide strikes  $N5^{\circ} \pm 2^{\circ}W$ ; and dips  $17^{\circ} \pm 1^{\circ} W$  (Figures 6-8). The coastline trends  $N4^{\circ} \pm 1^{\circ}W$ , so bedding dips directly toward the sea cliff. See Appendix A for a discussion of the detailed stratigraphy of the boreholes and the cliff face.

**Overview of Landslide Structure.** Within the landslide these formation materials are displaced, fractured and sheared but still retain fairly coherent structure within the large translational blocks that make up the slide (Figures 6-11; Appendix A). For example, single sandstone beds can be traced continuously along nearly the entire north-south exposure of the landslide toe (Figures 9 and 10). There is one offset of about 2 m down to the north on a northwest-striking fault or internal slide block (Figure 9). A tectonic fault (or faults) offset of similar amount and direction is needed between boreholes LT-1 and LT-2 to explain stratigraphic correlations between the holes, according to detailed work by Alan Niem (Appendix A). The southeast extension of the structure at the toe falls between these two boreholes, so the offset at the toe is probably the same fault and is depicted that way on the generalized cross section (Figure 7). See Appendix A for a complete balanced geologic cross section through the slide. Minor differences between the cross sections in Figure 7 and Appendix A result from field data gathered after Appendix A was produced and from some simplification of the cross section in Figure 7 relative to Appendix A.

The landslide is relatively shallow near its head, deepens toward the west, and then thins as the basal slide zone rises toward the surface (Figures 7 and 11). A deep landslide graben does not occur at the head of the main slide mass (i.e., it has a small driving wedge). Instead, the graben appears to be a remnant as the slide has moved laterally and down slope away from the headwall.

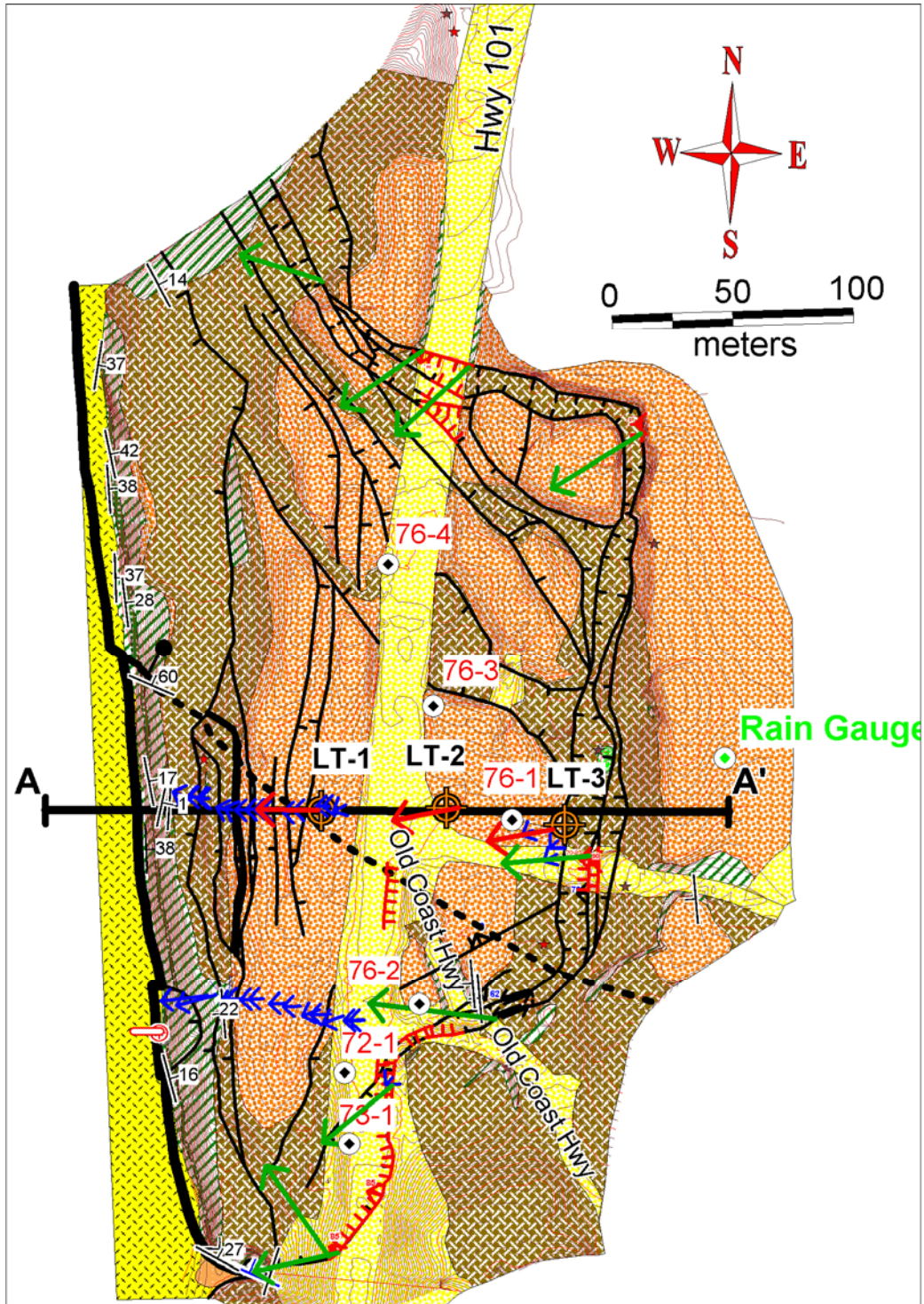


**Figure 6. Geologic map of the Johnson Creek Landslide.** Thin brown and red lines are elevation contours at intervals of 0.5 m. See Figure 7 for cross section and Figure 8 for explanation of patterns and symbols. Large green arrows are direction of movement determined from lateral displacement of marker nails on fresh slide scarps. The slide creates a left lateral offset of the Old Coast Highway at this locality (yellow fill unit trending northwest on the east side of borehole 76-2). Smaller red arrows are directions of slide movement from inclinometer data; blue arrows are direction of movement from re-survey of survey markers between 2002 and 2003 (see Appendix D).



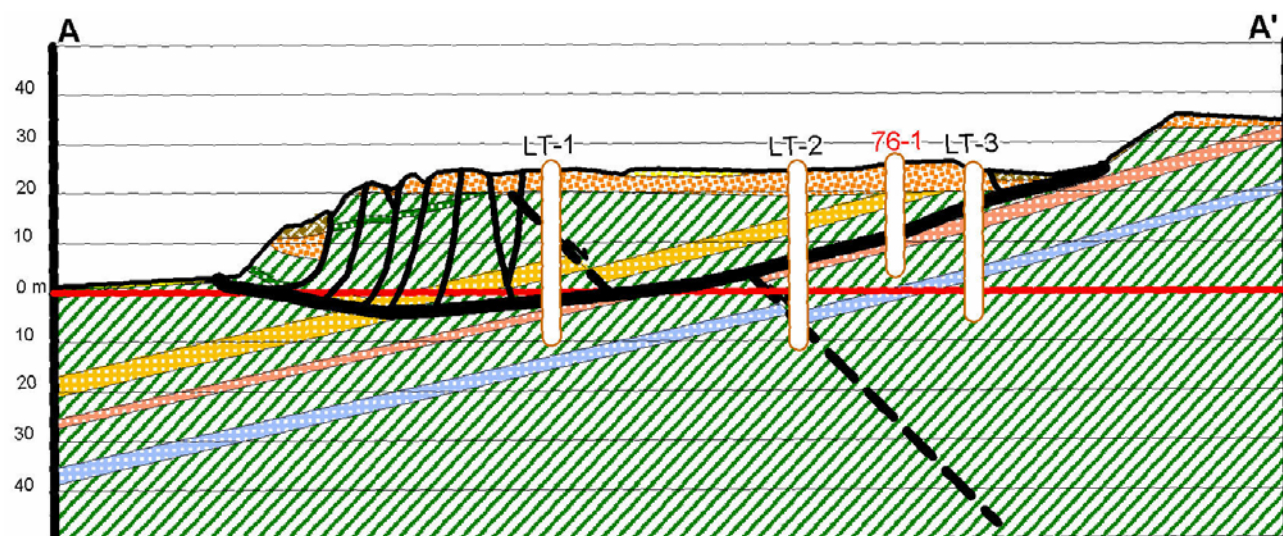


Figure 7. Simplified geologic cross section A-A'.

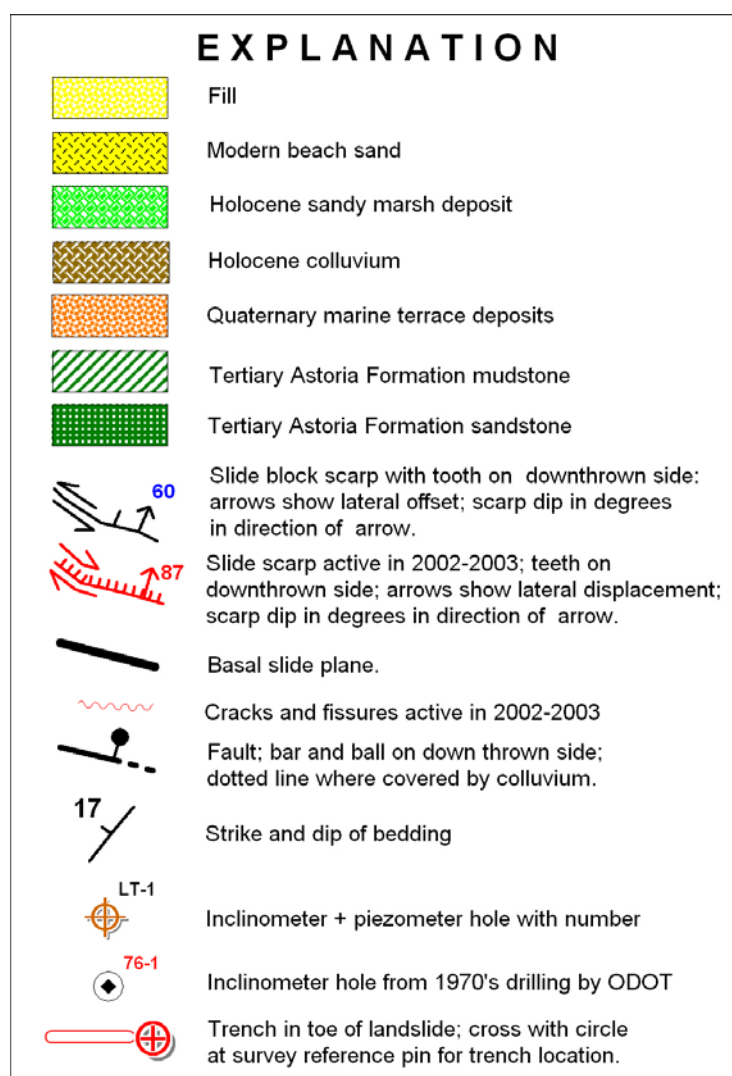
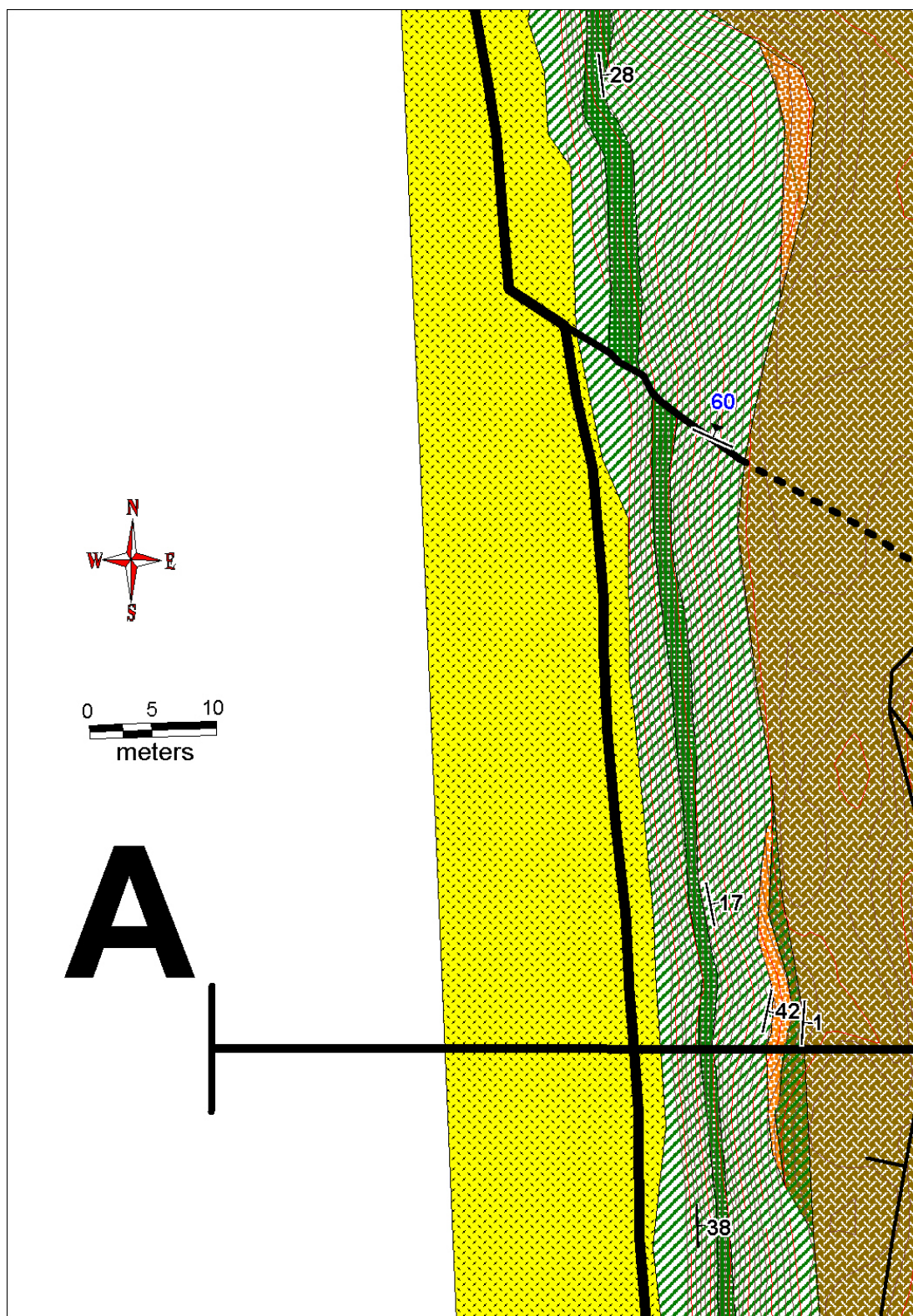


Figure 8. Map explanation for geologic map.



**Figure 9. Geologic map illustrating general continuity of bedding along the large block at the toe of the landslide. Note the cross cutting structure. This may be a tectonic fault now offset and possibly reactivated within the landslide (see discussion in the text).**





**Figure 10. View north at white marker bed that is easily traced for hundreds of feet along the toe of the Johnson Creek Landslide. This is the same general area as in Figure 9 above. The sandstone unit in green in Figure 9 is the cliff forming unit with the white marker bed at the lower contact.**

Johnson Creek Landslide is a complex, translational slide. Slide geometry and movement appear to be controlled by bedding in the Astoria Formation. In the middle of the slide at the latitude of the boreholes, the basal slide plane dips  $\sim 21\text{--}23^\circ$  west between boreholes LT-3 and 76-1,  $13\text{--}15^\circ$  west between boreholes 76-1 and LT-2, and  $10.5^\circ$  west between boreholes LT-2 and LT-1 (Figure 7). This gently curving slide surface appears to follow weak siltstone layers of the Astoria Formation (Figure 7). The Astoria Formation in outcrop and below the slide plane dips on average about  $17^\circ$  west but dips  $10\text{--}20^\circ$  in core below the slide plane (Appendix A). In the cross sections, both the simplified one of Figure 7 and the more complex one of Appendix A, the slide plane does not necessarily follow the stratigraphic dip but cuts across siltstone bedding. The slide plane appears to be bounded in some places by stronger sandstone and zeolitized tuff beds, deflecting along the top of these units (Figure 7; Appendix A). At borehole LT-1 the slide plane reaches below sea level and then must rise to reach its outcrop at  $\sim 3$  m elevation on the beach (Figure 7). A trench at the toe of the slide in the south central part (Figure 6) revealed slide gouge of dark gray siltstone overriding slide talus on a near horizontal surface at the westernmost edge but inclined  $\sim 30^\circ$  east 2 m to the east (Appendix C). In the southern part of the slide Johnson Creek exposes the slide plane lying at  $\sim 4\text{--}5$  m elevation on a nearly flat bedrock surface of much less fractured Astoria Formation sandstone (Figure 12). The exposure extends 16 m east to the Johnson Creek culvert (Figure 12). The slide surface crops out in the steep hillside above and east of the culvert rising to  $\sim 24$  m elevation at Highway 101 only 30 m to the east (Figure 12). While the west-central part of the slide east of borehole LT-1 must be relatively deep, reaching below sea level on some



sort of upward curving slide plane (Figure 7), the southern end is apparently much shallower (a few meters above sea level) and has a near horizontal dip near the toe (Figures 11 and 12).

**Offset and Age of the Slide.** According to the balanced cross section of Appendix A, total down dip slip on the central part of the slide at the latitude of the drilling transect is  $\sim 28.6$  m (94 ft). The horizontal and vertical components of slip are 28 m (92 ft) and 6 m (20 ft), respectively. At the southern margin of the slide east of Highway 101 offset of the Old Coast Highway since highway abandonment in  $\sim 1943$  (Len Saltekoff, ODOT, 2005 personal communication; Figure 6) is  $\sim 3.35 \pm 0.6$  m ( $11 \pm 2$  ft) left lateral and  $\sim 0.91 \pm 0.05$  m ( $3.0 \pm 0.17$  ft) vertical (tangent of the slide plane =  $\sim 0.3$ ; arctangent =  $\sim 15 \pm 2^\circ$  west) over a period of 62 years; hence, overall rate of movement in that interval was  $\sim 5.4 \pm 1$  cm/yr horizontal and  $\sim 1.5 \pm 0.08$  cm/yr vertical. These values are based on excavation (through colluvium) of the original gravel surface to its east margin inside and outside of the slide. Only a few centimeters of gravel are present, so it is likely that the road was only graveled once or twice before abandonment. The trend of the road embankments would seem to offer another datum for estimation of lateral offset, but there was apparently continual realignment of the road as the slide moved, creating a curving embankment that is now disrupted at the slide margin. Lateral offset since initial construction of the Old Coast Highway can be crudely estimated by assuming the road was originally straight, trending about  $N27^\circ W$  (north part in the slide) to  $N38^\circ W$  (south part outside the slide). Left lateral offset determined in this fashion is  $\sim 6.4 \pm 1.2$  m ( $21 \pm 4$  ft), or  $8.5 \pm 1.6$  cm/yr. Vertical offset since initial construction cannot be determined easily, since it is likely that the road was continuously graded as the slide moved. Age of the Old Coast Highway is not known for certain, but could be from construction known to have been widespread on the coast highway in 1927-1932 (Len Saltekoff, ODOT, 2005 personal communication). If this is correct, the average rate of lateral movement since that time would be  $\sim 8.5 \pm 1.6$  cm/yr, about 57 percent higher than the rate calculated from highway abandonment in 1943. There is more uncertainty in the 1927-1932 age of construction than the 1943 age of abandonment, so the  $\sim 5.4 \pm 1$  cm/yr horizontal and  $\sim 1.5 \pm 0.08$  cm/yr vertical rates are preferred. Interestingly, if these rates are used to predict age of construction based on the  $6.4 \pm 1.2$  m lateral offset since construction, construction could have occurred anytime between 1832 and 1924, based on combined measurement errors for offset since construction and the 1943-2005 rates. Accuracy of the rates is further diminished by the highly irregular (episodic) movement of the slide demonstrated during the observation period. Movement is as irregular as rainfall, which can vary widely.

The total age of the landslide cannot be accurately determined from the rate of movement based on the offset highway, because movement has been episodic and may not have been the same in the past as in the last 62 years. Initiation of slide movement could be from an unusual rainfall event or from an earthquake accompanied by large initial slip. Loss of strength through time may increase rate of movement, while loss of driving force as the slide reaches lower elevation may slow movement. Large-scale climate cycles will also cause non-linear movement over periods of decades by changing wave erosion and rainfall.

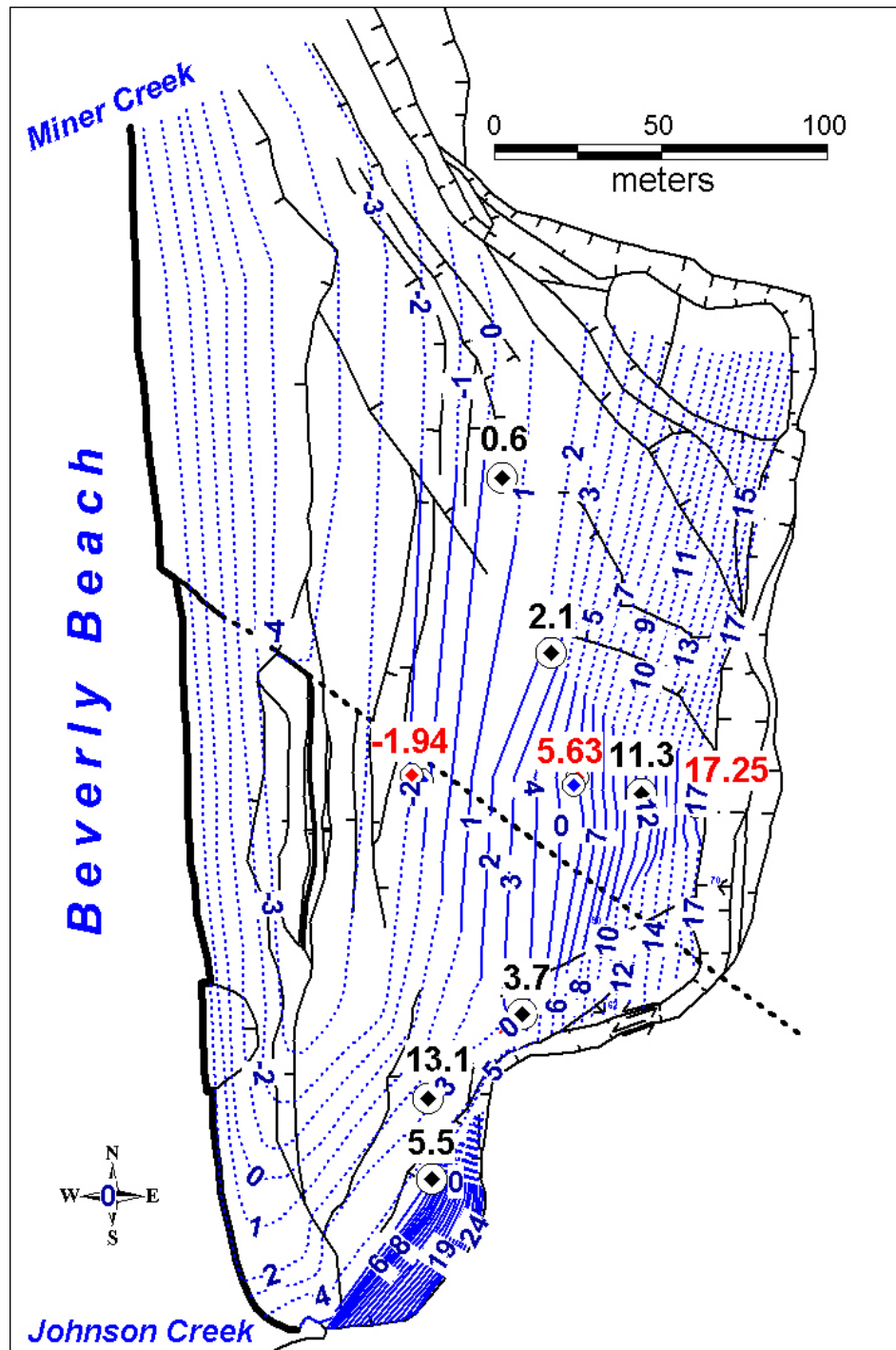


Figure 11. Blue lines are structure contours in meters of elevation (relative to geodetic mean sea level NAVD88) on the slide plane. Data for the contours consist of outcrops of the slide plane and the inclinometer holes from this project (large red elevation numbers) and previous work by ODOT in the 1970's (large black elevation numbers). Elevations for the 1970's boreholes should be considered minimum values according to Landslide Technology (2004). The zone of movement intercepted at 13.1 m elevation was ignored, since this is probably a fast moving, shallow part of the slide rather than the main slide plane at depth; note the much lower elevation intercepts immediately south and northeast of this point. Dashed lines are highly speculative, whereas solid lines are inferred (assuming linear change) between drill holes and outcrops. Contours are assumed to be roughly perpendicular to slide movement direction inferred from slide geometry and data from inclinometers and re-surveys.

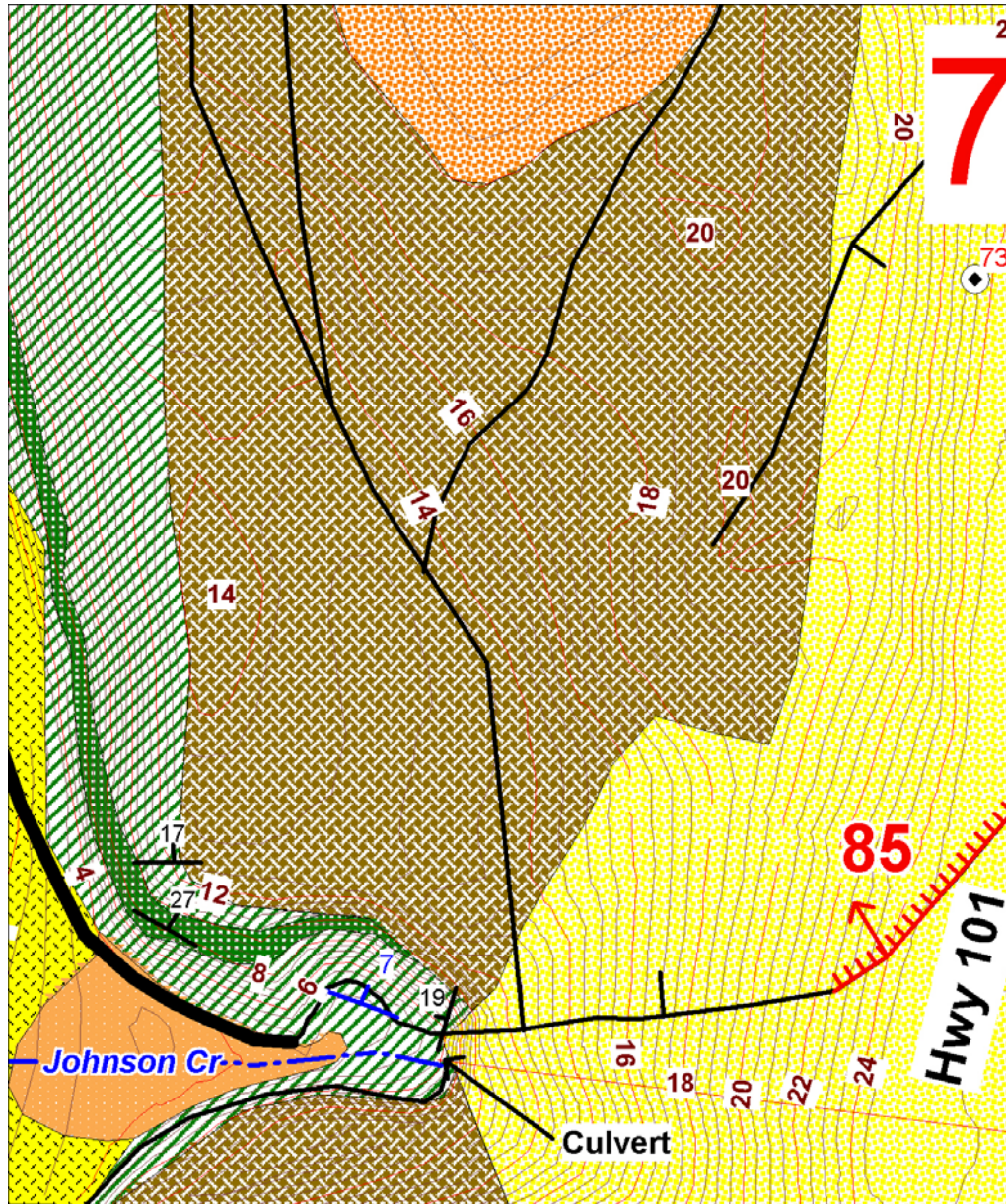


Figure 12. Detailed geologic map of the southwest end of the Johnson Creek Landslide. Brown numbers are elevations in meters above geodetic mean sea level (NAVD88); black numbers are bedding dip in Astoria Formation; red number is dip of recently active shear plane cutting highway fill, and the blue number is the dip of basal slide plane at Johnson Creek. Note that the prominent sandstone marker bed (green unit) has dips to the north and northeast at the sea cliff but crops out at similar or higher elevation to the east on the north side of Johnson Creek. The dip must therefore change to lower dip in the interior of the westernmost slide block, probably subparallel to the slide plane dip. The west dip of 19° on the east side of this exposure illustrates complete reversal of dip from that at the toe of the slide. These observations are consistent with a synclinal structure in this exposure.



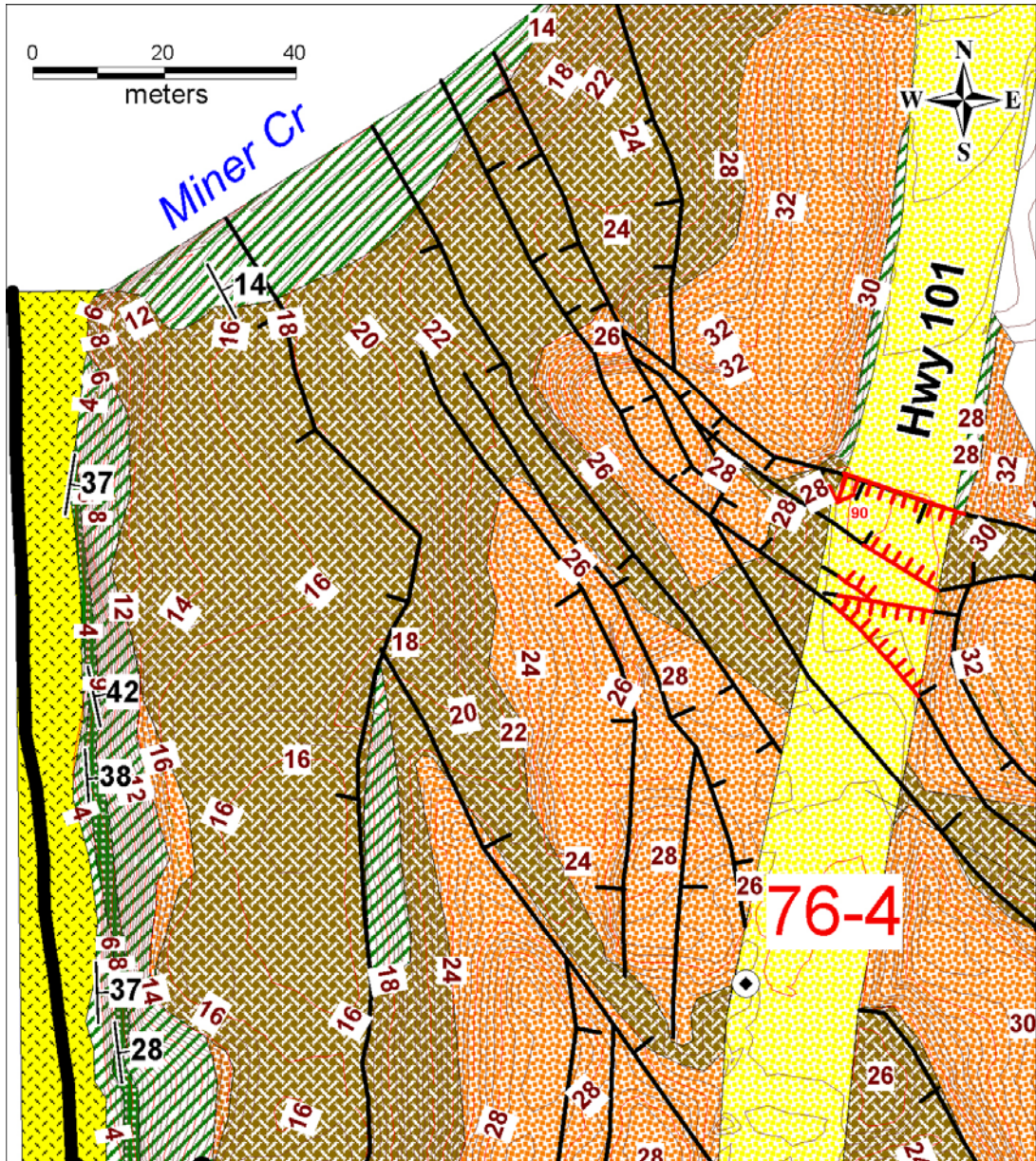


Figure 13. Detailed geologic map at northwest margin of the landslide at Miner Creek. Labeling is the same as previous figure. Note that the same sandstone marker bed from the previous figure (green unit) occurs in the sea cliff but disappears under the beach sand near Miner Creek.

**Back-Tilted Slide Block at the Toe.** The westernmost slide block on the Johnson Creek Landslide is tilted eastward, but the width of this rotated block narrows from 50 m on the north end at Miner Creek to 19 m at the south end at Johnson Creek (Figures 6 and 11). The style of deformation appears to change from north to south as well. The east-west exposure on the south end at Johnson Creek reveals a cross section of this back-tilted block (Figure 12). In that area no sharp slide block boundary can be identified where the dip of Astoria Formation changes from 27° northeast at the toe to 19° west on the east side of the exposure above the culvert (Figure 12). The dip change appears to occur gradually over an east-west distance of only 13 m along a series of closely spaced, complex sheared fractures with a

variety of dips and terminating downward on a near horizontal slide plane dipping  $\sim 7^\circ$  northeast near the center of the slide block (Figure 12). This dip change in the slide in Astoria Formation forms a syncline with opposing limbs dipping northeast and west and with an axis plunging  $7^\circ$  northeast. This folded slide block terminates east against a well-defined headscarp  $\sim 6$  m high (Figure 12). At the north end of the back-tilted slide block Astoria Formation changes from a dip of  $37^\circ$  east at the toe to  $14^\circ$  east at the back of the tilted block (Figure 13). The tilted block at the north end is backed by a headscarp up to 12 m high. The exposed cross section on the north end at Miner Creek reveals deeply penetrating fractures within the tilted block that are near vertical with an increasing tendency to be open toward the east side of the block. Openings on these fractures at the east boundary of the block were 0.4-1 cm. The modest change in dip on the north end of the tilted block from west to east appears to occur by slight drag folding of the strata on the large scarp at the back of the block with much of the deformation probably accommodated by sheared fractures. The north end is thus not a syncline but a discrete block rotated  $31$ - $44^\circ$  east from the original  $\sim 17^\circ$  west dip of the Astoria Formation. The difference in deformation between the north and south ends of the back tilted block probably reflects higher degree of curvature in the slide plane at the toe on the north. More curvature is probably accommodated by somewhat deeper penetration of the slide plane on the north relative to the south. Indeed, the LT-1 borehole crosses the slide plane below sea level, whereas the slide plane intercepted in all boreholes on the south end of the slide and the slide plane exposed at Johnson Creek are above sea level (Figures 6 and 11), so the slide plane does appear to plunge toward the north. The net result of this northward plunge of the slide plane is progressively greater buttressing of the slide toward the north by the upturned mass at the toe and the rampart of Astoria Formation and talus below the slide at the toe.

**Tectonic Joints and Fractures.** Tectonic joints are rare in the Pleistocene marine terrace deposits. Tectonic joints in the Astoria Formation are generally in two sets trending northwest and northeast. Within 100 m east of the landslide headscarp are two joint systems striking  $N10$ - $30^\circ$  W, dipping  $62$ - $88^\circ$  W crossing a less numerous set striking  $N70^\circ$ E to  $N88^\circ$ W and dipping  $63$ - $73^\circ$  N. A few vertical fractures striking  $N45$ - $52^\circ$  E occur locally. Tectonic joints below the landslide in exposures at Johnson Creek are also in two groups, one striking  $N17$ - $60^\circ$  W and dipping within about  $13$ - $17^\circ$  of vertical and a vertical set striking  $N54$ - $57^\circ$ E. Spacing of the joints below the side plane at the toe and east of the headscarp tends to be irregular with some areas nearly devoid of joints over distances of a few meters next to areas with sets of joints spaced at a few tenths of a meter.

**Joints and Fractures within the Slide.** Joints and fractures within the landslide are much more closely spaced than the tectonic joint systems and tend to strike subparallel to adjacent slide block boundaries and to northwest or northeast trending tectonic joints. For example, in an exposure at the sea cliff on the north side of Johnson Creek (southwest corner of the landslide) major fracture systems in the Astoria Formation were spaced at an average of 12 cm with many at only a few centimeters apart throughout the outcrop. The fractures were in three major sets,  $N47^\circ$ E, dipping  $88^\circ$  N,  $32$ - $42^\circ$ W, dipping  $72$ - $78^\circ$  E, and roughly parallel to the sea cliff (slide toe) at  $N7$ - $17^\circ$  E and dipping within  $17^\circ$  of vertical. As explained above, a more complex pattern of closely spaced fractures in a variety of directions occurs in this same exposure proceeding east into the back-tilted slide block at Johnson Creek. At the north end of the tilted block at Miner Creek the near vertical fractures within the back tilted block trend roughly parallel to the



sea cliff (toe of the slide). Slide blocks of Quaternary marine terrace sand freshly exposed in the northeast corner of the landslide in the east-facing scarp bounding the west side of the headwall graben have fractures and sheared surfaces at N7-55° W, dipping 78-90° W. The strike of most of these fractures is roughly parallel to the trend of the north-trending graben. Fresh sheared surfaces at the base of the north-south headscarp in the same area strike north-south and dip 87° west. Other freshly sheared surfaces cutting roads at the north, east, and south boundary of the landslide also strike parallel to the boundary and have inclinations toward the slide of 70-90°.

**Slide Plane Gouge.** The clayey siltstone gouge of the Astoria Formation exposed at the toe of the slide appears wet and malleable and probably has fairly low permeability. Similar wet sheared clayey siltstone occurred at the slide plane in the boreholes (Figure 14). A Shelby tube sample of the slide gouge had 24.5% clay, 74.6% silt and 0.9% sand and similar material forms the slide gouge at the toe of the slide (see detailed analyses by Alan Niem, Appendix A).

**Permeability of Rock Units and Structures.** It appears that the fractures within Astoria Formation in the slide blocks are to some extent following the same directions as the tectonic joints but are much more numerous, creating much higher permeability for the passage of ground water. Fresh sheared surfaces at the landslide boundary on the north, east and south sides are mostly near vertical and parallel to the slide margin. The slide plane itself is composed of fine-grained gouge that is probably a barrier to groundwater flow. Likewise, undisturbed Astoria Formation below the slide plane probably does not have high permeability, because it is poorly sorted and only discontinuously jointed. In contrast, the well-sorted Pleistocene marine terrace sand and colluvial fill of this same sand in the headwall graben probably have higher permeability. The heavy deposition of iron oxide in altered Astoria Formation at the terrace sand contact is probably evidence of groundwater flow in the relatively permeable terrace sand and basal gravel.



Figure 14. Soft wet silty gouge at slide plane in borehole LT-1 at 27.4 m (90 ft) depth.



## Surface Water and Groundwater

Surface water on the landslide locally ponds in the headwall graben, forming marshy areas. Creeks on the north and south margins of the slide flow all year long. Prominent wetland features are not readily evident over most of the landslide, probably due to the high permeability of the terrace deposits and fractured landslide debris. However, apparent wetland plants occur in scattered areas of flat terrain, indicating that temporarily perched groundwater probably occurs in local, less fractured slide blocks during prolonged periods of intense rainfall. One such area occurs several meters south of borehole LT-1.

Modest seeps and a few springs of groundwater emerge from fractured Astoria Formation along the base of the landslide at the sea cliff during the winter months. The toe of the slide was searched for springs and seeps on January 8, 2005 after an intense rainfall event. One spring with field-estimated flow at ~27 liters per minute (lpm) (~7 gallons per minute or gpm) issued from fractured Astoria Formation in the sea cliff 10 m south of north edge of the slide. No other significant seeps or springs were seen in this particular event, in part, because beach sand was covering the lower ~meter of the sea cliff where some slow seeps had been observed in the past. Nevertheless, even where no significant sand covered the lower part of the slide at the south end at Johnson Creek, no significant springs were observed in the fractured Astoria, so there may be a real difference in permeability from north to south at the toe of the slide.

Intermittent groundwater seeps have been observed in the uppermost part of the sea cliff in past winters, issuing from a perched aquifer in basal Pleistocene marine terrace sand and lag gravel where these deposits lie on less permeable Astoria Formation. It may be that altered, orange-stained Astoria Formation immediately below this contact is partly the result of chemical reactions attending groundwater passage. The orange stain probably indicates that at least one of these reactions is oxidation of soluble  $\text{Fe}^{+2}$  to insoluble forms of iron. The iron mineral precipitated in the Pleistocene marine terrace sand at the headwall is poorly crystalline goethite, which may have been precipitated by oxidation of soluble ferrihydrite (Johnson, 2003). Such oxidation is consistent with flow of perched aquifers through the vadose zone where abundant oxygen would be present.

According to well records from the Oregon Department of Water Resources (ODWR), two wells within the landslide at its north end yielded ~45-64 lpm (12-17 gpm) below a static water level of ~9 m (28-30 ft) depth (in Astoria Formation), while a well ~200 m south of the landslide in Astoria Formation bedrock had a yield of 2 lpm (0.5 gpm) below the static water level of 14.6 m (48 ft) depth. All of these data are for September-October water conditions. No wells from the ODWR database in this area appear shallow enough to be drawing water from the Pleistocene marine terrace sand.

We conclude from field observations and water well data that the Astoria Formation within the landslide is much more permeable to groundwater than intact Astoria Formation. Water appears to pond in the permeable Pleistocene marine terrace sand and colluvial sand fill in the headwall graben and fissure system. The silty clay gouge at the slide plane is probably a barrier to groundwater flow, so groundwater is likely ponded in the landslide mass with this gouge acting as a kind of impermeable liner. Baum and Reid (2000) concluded that persistent movement of large translational slides is related

to weak, low-permeability clays at basal and lateral shear zones that isolate the landslide mechanically and hydrologically from adjacent unfailed material. The requirements for this condition appear to be present at the Johnson Creek Landslide. Geotechnical data discussed below are consistent as well.

## **FIELD INVESTIGATION**

In addition to geologic mapping, the field investigation included topographic mapping, subsurface drilling and installation of inclinometers and piezometers, a rain gauge, and metal pins to track erosion and slide movement. Piezometer holes were drilled after slide movement was detected on inclinometers in order to target pressure transducers immediately above the basal slide plane. In one borehole (LT-2p) an additional transducer was installed below the slide plane.

### **Topography Survey**

Dennison Surveying of Newport, Oregon performed a survey of the topography. This information was used for surface geologic mapping, cross sections, and detection of ground movement. The survey resulted in topographic contours at 1-meter intervals. The morphology of the landslide was in general well represented by the survey except in some areas of dense vegetation and in one part of the headwall at the northern end of the slide where a small graben-fissure feature was overlooked.

There was some difficulty in adjusting the local survey datum to the regional geographic datum, so the geographic information files for the topographic contours will not be released in this interim report. They will be released in the final report after necessary corrections have been made.

### **Exploratory Drilling and Borehole Instrumentation**

**Drilling.** The exploratory drilling program consisted of six borings completed between November 18 and December 5, 2002 (first phase) and January 6 to January 10, 2003 (second phase). Borings completed as part of phase one are designated LT-1, LT-2, and LT-3 at the locations shown on the site map, Figure 2. Companion borings that were drilled in the second-phase installation of piezometers are designated LT-1p, LT-2p, and LT-3p.

Geo-Tech Explorations, Inc. of Tualatin, Oregon, performed the exploratory drilling using a track-mounted CME 850 drill rig. A combination of 15-cm (5<sup>7</sup>/<sub>8</sub>-inch) O.D. tricone mud-rotary, casing installation through overburden, and PQ3-wireline diamond core drilling techniques were used to drill the slope inclinometer borings to final depth. Hollow-stem auger techniques were utilized to drill the piezometer borings to final depth. An engineering geologist from LT was present throughout the field program to coordinate the drilling operations, log and sample the subsurface materials that were encountered, and assist with the installation of instrumentation. DOGAMI personnel and Alan Niem also examined soil and rock samples from the boreholes. Alan Niem was present throughout the drilling, logging lithologies and taking pictures of the samples.

Soil samples in the inclinometer borings (LT-1, LT-2, and LT-3) were obtained at approximately 0.76- or 1.52-meter (2.5- or 5-foot) intervals using a 7.6-cm (3-inch) O.D. split-spoon sample barrel driven by a 63.5-kg (140-lb) auto-trip hammer. The underlying bedrock was sampled by obtaining rock cores using 1.52-meter (5-foot) long, triple barrel coring techniques. The quality of the bedrock was recorded

using Rock Quality Designation (RQD) and core recovery indices. Samples were also collected in the piezometer borings in the zones of measured slide movement, using 7.6-cm (3-inch) diameter thin-walled Shelby tubes. In addition, select soil samples were obtained in Boring LT-3p using Standard Penetration Test (SPT) procedures. Drilling methods, sampling depths, total drill hole depths, and descriptions of the soil and rock materials encountered are shown on Summary Boring Logs in Appendix B.

**Instrumentation.** Slope inclinometer casings were installed in borings LT-1, LT-2, and LT-3. The inclinometers consist of 3.048-meter (10-foot) lengths of Slope Indicator Company 7.0-cm (2.75-inch) O.D. ABS casings with quick-connect couplings. The annular space between the casings and boring sidewalls was backfilled with cement bentonite grout, and each inclinometer was capped with a protective surface monument and concrete. Details of the inclinometer installations are included on the Summary Boring Logs, Appendix B. Coaxial cable was attached to the down slope exterior of the slope indicator casings. The RG59U coaxial cable is commonly used for home electronics. The cable can allow the use of Time Domain Reflectometry (TDR) technology for measurement of additional information on slide movement at depth after the casing has been sheared. Manual boring extensometers were installed within the slope inclinometer casings after the inclinometer probe was unable to pass the shear zone. A schematic of the extensometer is shown in Figure 15. The extensometers allow for continued slide monitoring, although at a reduced accuracy and with no directional information as compared to the inclinometer. The extensometer consisted in the original installation of a braided steel rope anchored with an attached chain in a 3-m (10-foot) long concrete and sand plug at the bottom of the casing. A 0.6-0.9 m (2- to 3-foot) section of steel rope extended from the top of the casing with a crimped ferrel attached near the end of the rope. The distance between the top of the casing and the bottom of the ferrel became the gauge length of the extensometer. Four vibrating wire pressure transducers, manufactured by Slope Indicator Company, were installed in companion borings LT-1p, LT-2p, and LT-3p. In each boring, the pressure transducers were installed within 2 meters (7 feet) above the slide plane. The sand pack around the transducer penetrated the slide plane. Therefore, continued slide movement would not damage the transducers, but would still measure pore water pressures at the slide zone. An additional pressure transducer was installed 5.1 meters (20 feet) below the slide zone in LT-2p. This transducer lost communication with the datalogger due to slide movement on February 1, 2003. Pore-water pressures were recorded every hour with single channel GEOKON dataloggers provided by ODOT. Table 1 summarizes depths and elevations of the slide plane, boreholes and piezometers.

**Table 1. Depths and elevations of boreholes, piezometers, and the slide plane at each hole. The slide plane depth is from inclinometer data at LT-1, LT-2, and LT-3. At LT-1p, LT-2p, and LT-3p the slide plane depth is estimated from a geologic cross section and location of the piezometer hole. All inferred depths and elevations are shown in parentheses.**

	LT-1	LT-1p	LT-2	LT-2p	LT-3	LT-3p
Elevation (m NAVD 88)	24.6	24.7	24.5	24.2	24.3	24.0
Total Depth (m)	33.8	26.8	34.7	25.0	28.7	7.0
Upper Piezometer Elevation (m)	—	-0.1	—	7.5	—	18.5
Lower Piezometer Elevation (m)	—	—	—	-0.5	—	—
Upper Piezometer Depth (m)	—	24.8	—	16.7	—	5.5
Lower Piezometer Depth (m)	—	—	—	24.7	—	—
Upper Piezometer tip distance above slide plane (m) <sup>1</sup>	(1.5) <sup>1</sup>	1.0	(1.31) <sup>1</sup>	1.3	(1.11) <sup>1</sup>	0.1
Slide Plane Depth (m)	26.3	(25.9)	18.0	(18.0)	6.6	(5.6)
Slide Plane Elevation (m)	-1.8	-1.2	6.5	6.2	17.7	18.4

The U.S. Geological Survey (USGS) on November 20, 2004 set up PsiTronix extension transducers (80-inch range) attached with a pulley and reel assembly to the braided wire in each of the three extensometer holes (Figure 16). They replaced the three GEOKON dataloggers with two Campbell Scientific CR10X dataloggers, one at the LT-1 site and one at the LT-3 site. Piezometer and extensometer data from LT-2 and LT-3 installations flow through wire to the datalogger at the LT-3 site. LT-1 piezometer and extensometer data flow to the logger at the LT-1 site. Both loggers are powered by rechargeable gel cell batteries that are hooked to solar panels. All data are recorded hourly. Extensometer data from this new system will thus be recorded hourly with rainfall and water pressure and will be much more accurate, since constant, equal tension is on the cables at all times. Even slight (mm) movements of the cable into the boreholes should be detectable. No data from this new set up will be reported in this paper, owing to time limitations and some minor inconsistencies between calibrations of the piezometer data in the old and new systems. These inconsistencies will be removed when the final report is produced in 2007. Movement has been negligible since November 20, 2004 in any case.

**Monitoring.** Landslide Technology measured initial readings of the inclinometers and piezometers. DOGAMI performed subsequent instrument monitoring. All geotechnical data in this report from the boreholes and rain gauge is current as of November 19-20, 2004, when the USGS installed the new dataloggers.

**Permits.** Permission to perform the drilling and instrumentation were acquired from:

- Oregon Department of Transportation (temporary access)
- Oregon Water Resources Department (geotechnical hole reports, tributary water use)
- Boise Cascade Building Solutions (temporary access)
- Johnson Creek Water Services Company (public water use)

<sup>1</sup> Distance that the piezometer would be above slide plane in inclinometer holes is projected based on piezometer depth in the adjacent piezometer hole and location of that hole relative to the fault plane and the inclinometer hole. No piezometer is actually in these inclinometer holes but the inferred depth of the piezometer is listed to aid in calculation of pressure head above the slide plane at the inclinometer holes.

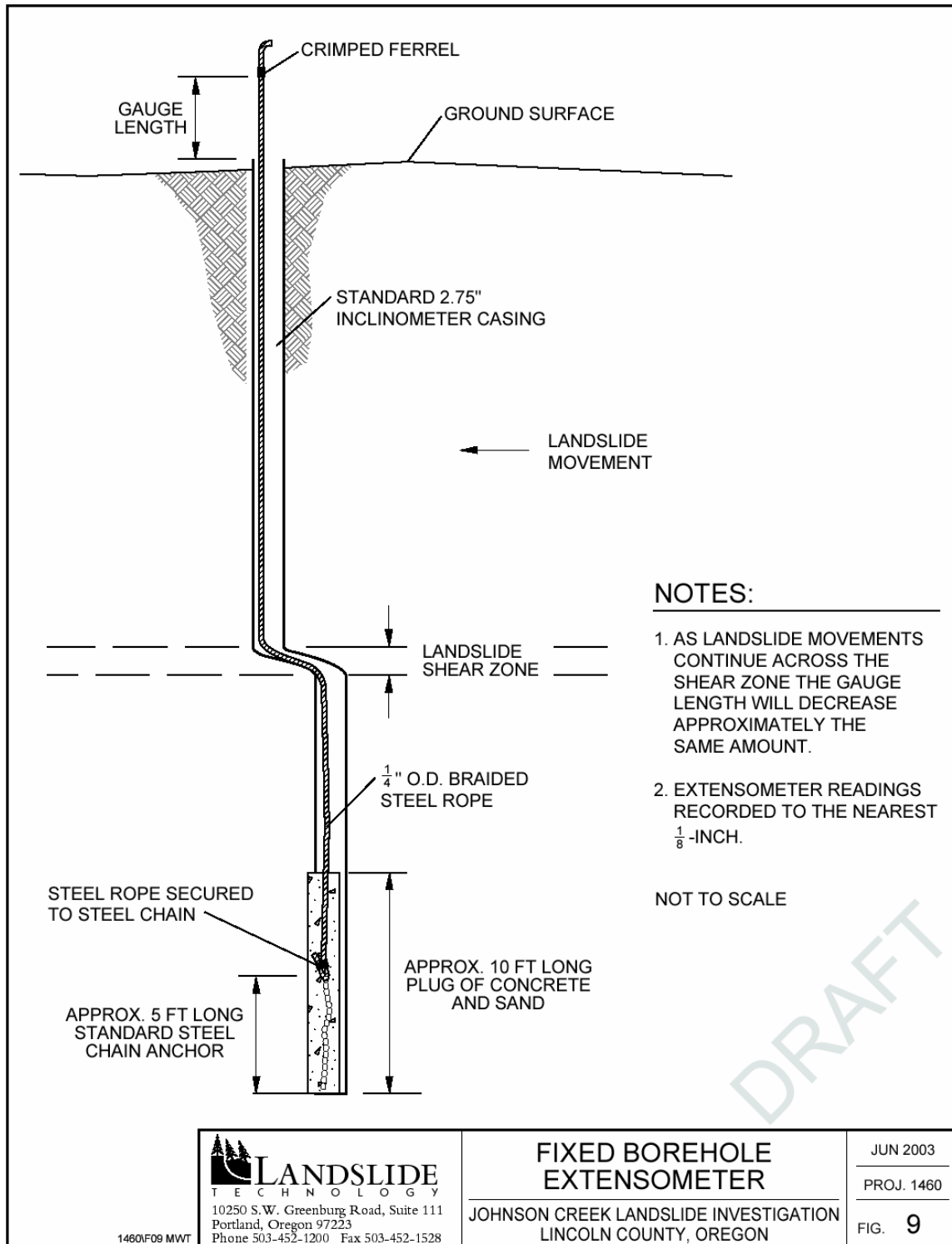


**Figure 15. Schematic diagram of extensometer construction in boreholes LT-1, LT-2, and LT-3. Taken from Landslide Technology (2004).**



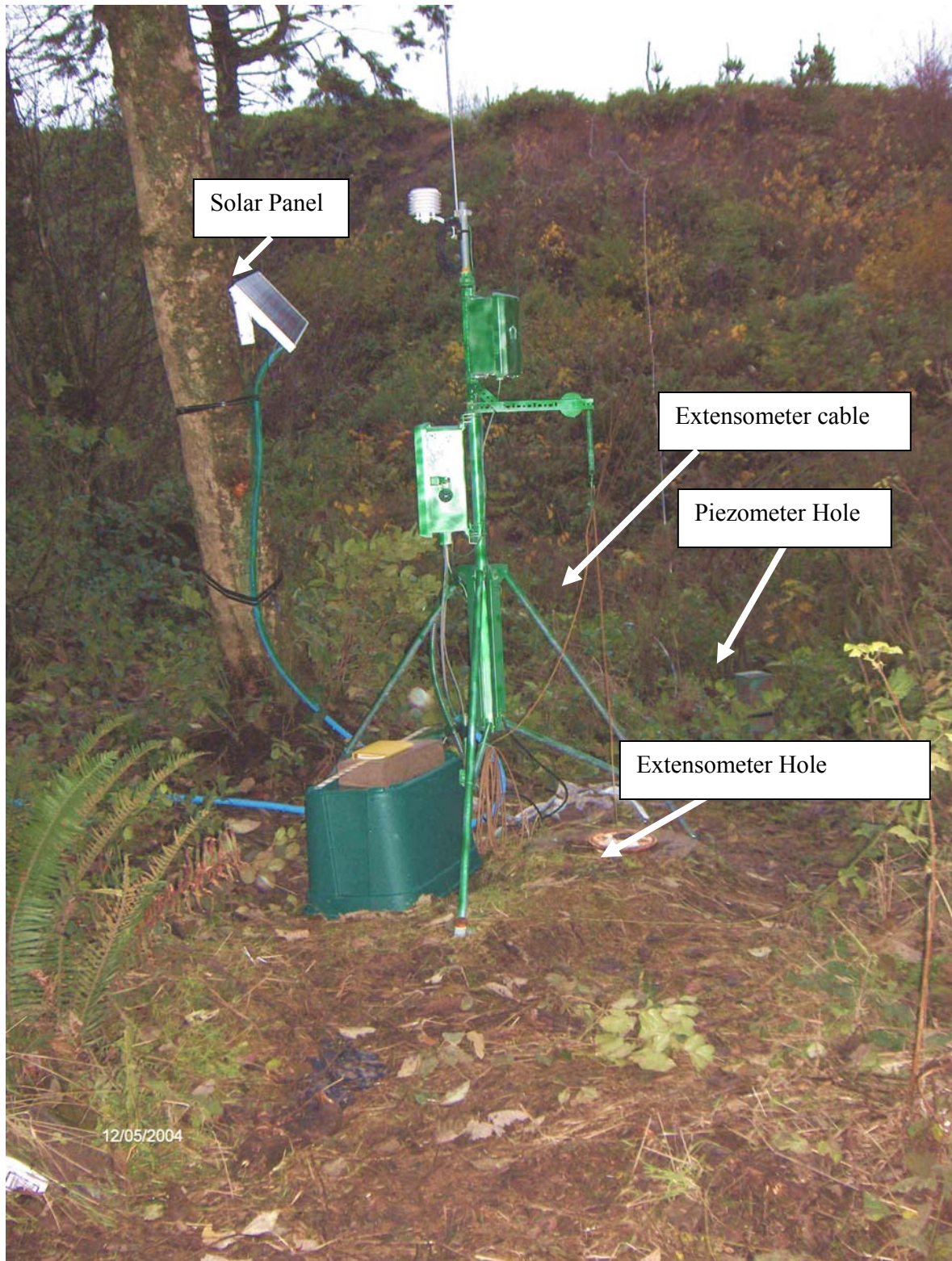


**Figure 16. Automated data collection system installed November 20, 2004. Photo is looking east at the site of the LT-3 borehole showing the cable and pulley system for the extensometer (center) and solar panel (left on tree) that recharges the batteries in the data logger (left mounted on tripod). Headwall of slide is in the background.**

## **Precipitation**

A rain gauge was installed above the headscarp at the location shown on Figure 1 about 80 m northeast of the LT-3 site. The rain gauge is a Global Water, Inc., RG200 tipping bucket rain gauge initially connected to a Global Water model GL400-1-1 pulse type datalogger. As of November 20, 2004 the new Scientific CR10X logger at the LT-3 site also receives data through a wire from the rain gauge. Both the current and former dataloggers were programmed to record rainfall amounts every hour.

Estimates of precipitation before installation of the rain gauge were compiled from the Hatfield Marine Science Center archives (<http://hmsc.oregonstate.edu/weather/archives/guinlib/>). The rain gauge for this data is located at Yaquina Bay ~11 km south of the landslide.

## **Test Pits**

Two exploratory test pits were excavated on March 24, 2003 on the beach near the toe of the bluff. A diagram depicting the subsurface materials encountered in the test pit is included in Appendix C.

## **Surface Ground Movement Survey**

Permanent hubs and line-of-sight surveys were used to monitor surface ground movement. Permanent survey hubs are established along three east-west lines as shown on maps in Appendix D.

A line-of-sight survey was established along U.S. Highway 101 at the location shown in Appendix E. The purpose of this survey line is to obtain measurements of lateral movement between pins and a north-south line that is fixed at points outside of the landslide.

In addition, a series of nails and heavy gauge wires were installed on freshly sheared surfaces of scarps and on the slide block below these scarps with the ends of the nails or wires touching. Movement amount and direction was determined from the separation of the ends of the sets of nails or wires during March and April 2003 (Appendix G).

## **Erosion**

Survey pins were installed into the face of the bluff by DOGAMI to measure the rate of erosion. Thirty-five, 298-mm (11<sup>7</sup>/<sub>8</sub> inch) long pins were inserted in six profiles up the face of the bluff. Since many of the pins were lost to erosion in the first season, steel stakes 77 cm (30 inches) long were driven into the base of the sea cliff in the spring of 2004 to obtain additional data. Locations and observation data for all pins and stakes are given in Appendix F.

A ground-based Light Detection and Ranging Data (LIDAR) survey of three segments of the sea cliff at the toe of the landslide was obtained May 14, 2004 to establish a baseline for measurement of erosion in the future; those data will be reported after a second measurement is completed to measure bluff retreat.

Airborne LIDAR surveys by USGS in 1997, 1998, and 2002 were examined for erosion information, but once the data were gridded and reduced to elevation contours, errors of a 1.2-2.4 meters (bluff accretion or exaggerated erosion) became apparent. These errors appear to be from smoothing of relatively sparse data on steep bluff slopes. It is also possible that slide movement may have affected the measurements. The much more detailed 2004 ground-based LIDAR survey appeared to represent the steep slopes much

more accurately than the airborne data and will serve as a better reference for future erosion determinations. The ground-based LIDAR is so detailed that individual trees at the top of the sea cliff can be tracked as an independent means of measuring slide movement at the toe of the slide where slide movement data is sparse or lacking altogether. Removing the effects of movement will be crucial for estimates of erosion by LIDAR.

### Sand Movement

Beach sand movement can affect the stability of the Johnson Creek Landslide. Measurements of beach sand levels were obtained using two methods: LIDAR and topographic survey. Results of the surveys are provided in Appendix H. Landslide Technology (2004) concluded that the modest amount of beach sand present is not a major factor in buttressing the slide, so field surveying of topographic profiles on beach sand was suspended after the spring of 2003. The currently available data is, however, of interest with respect to location of persistent embayments in the beach that might promote wave erosion. Such an embayment is apparent on the southern margin of the landslide (Figure 17).

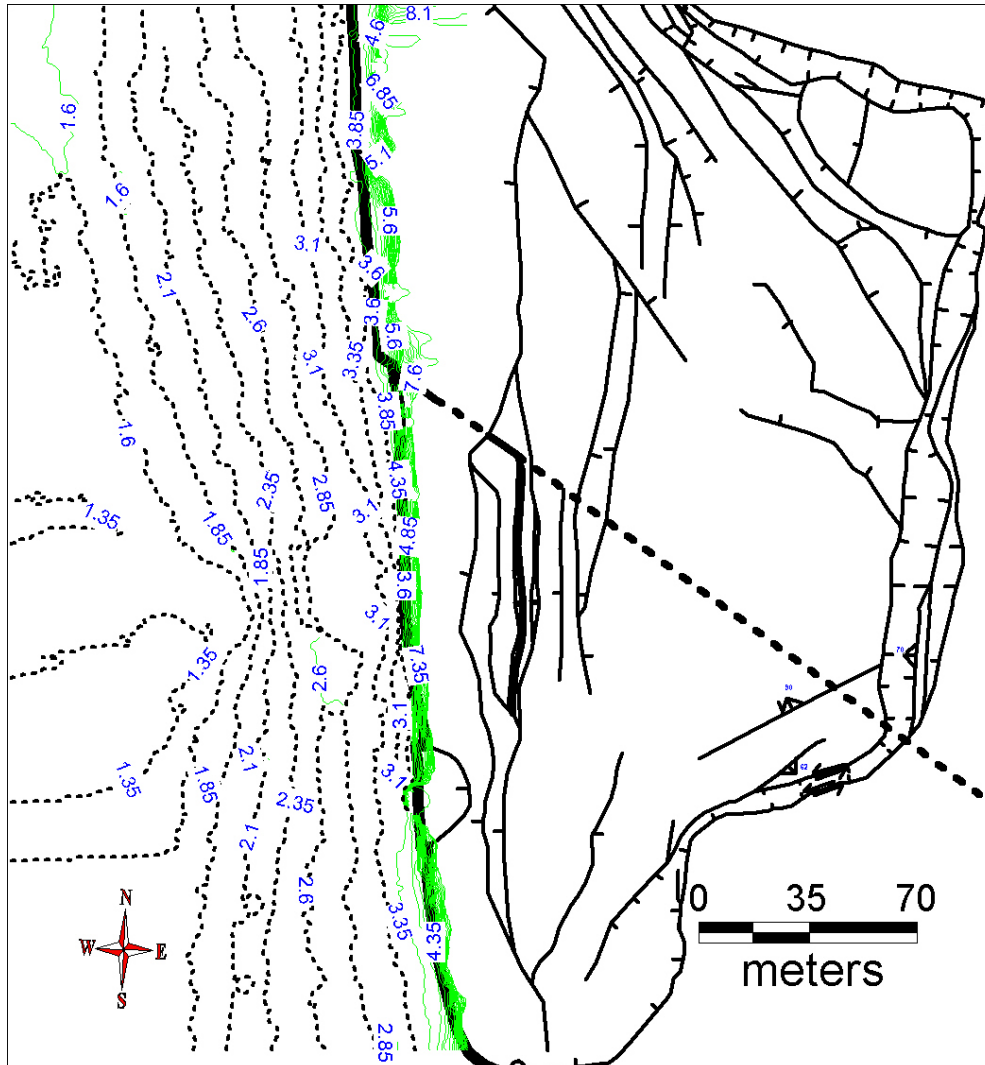


**Figure 17. Topographic contours at 0.25-m intervals on the beach west of the Johnson Creek Landslide. Heavy dark lines depict landslide scarps. Note the embayment in the beach at the south end of the slide; this is probably from rip current erosion.**



## LABORATORY TESTING

Laboratory testing was performed to determine soil index properties for correlation with engineering parameters and to aid with classification. All testing was performed at the Landslide Technology soil laboratory in Portland, Oregon. Tests were performed on selected samples collected during field explorations to verify field classifications and determine the following properties:

- Soil Classification
- Natural Moisture Content
- In-Place Density
- Residual Shear Strength

### Soil Classification

Soil and rock core samples obtained from the field exploration program were visually re-examined in the laboratory to confirm field classifications using ASTM D 2488. Together with the results of additional laboratory testing, final soil descriptions were prepared in general accordance with ASTM D 2487. Soil classifications and descriptions are presented on the Summary Boring Logs, Appendix B.

### Natural Moisture Content

Moisture contents were determined on all samples retrieved from the field explorations in general accordance with ASTM D 2216. The results of moisture content tests are shown on the Summary Boring Logs.

### In-Place Density

In-place density tests were performed on selected core samples obtained during field explorations. The tests were performed in general accordance with ASTM D 2937. The results of in-place density tests are summarized below (Table 2).

**Table 2. Summary of In-place density testing.**

Boring No.	Sample No.	Depth, m (feet)	Soil Description	Moist Unit Weight, kN/m <sup>3</sup> (pcf)	Moisture Content	Dry Unit Weight, kN/m <sup>3</sup> (pcf)
LT-1	R-4	10.5–10.8 (34.4–35.4)	SOFT (R2), gray, silty, fine SANDSTONE	21.3 (135.5)	21%	17.5 (111.8)
LT-2	R-10	18.8–19.0 (61.7–62.3)	VERY SOFT (R1), gray, fine silty SANDSTONE	21.5 (137.1)	18%	18.3 (116.5)



## Residual Shear Strength

Residual shear strength tests were performed on shear zone material obtained from a drill core sample. The specimen was obtained in boring LT-2 at a depth of 18.1 meters (59 feet). The zone of slide movement measured in inclinometer LT-2 is between depths of 17.4 to 18.6 meters (57 to 61 feet). The tested soil is soft, slightly clayey, sandy silt: no sand or gravel sized fragments were in the sample. This soft wet layer in the core appeared to be the gouge within the main slide plane (Figure 18).

The specimen was remolded by hand and placed into the ring-shear apparatus. The ring shear specimen is 0.20 inches thick and has a surface area of 6.2 square inches. Once the sample is placed in the ring shear apparatus it consolidates in a water bath for each load increment prior to shearing. The sample was tested at 490, 245 and 123 KPa (5.1, 2.6 and 1.3 tsf) confining pressure to simulate the range of in-situ effective confining stress along the shear zone. In-situ confining pressures at the shear zone within LT-1, LT-2 and LT-3 were estimated to be 380, 290 and 120 KPa (4.0, 3.0 and 1.3 tsf), respectively, using groundwater levels obtained from the vibrating wire piezometers. Following consolidation of the samples, shearing was commenced at a rate of 0.024 degrees per minute until reaching residual strength. The test was repeated for each of the three loads detailed above. A plot of the raw test data is included in Appendix I, Ring Shear Test Plot. Residual shear strength tests resulted in an effective residual phi angle of 13.1 degrees, with no cohesion. Results are shown graphically on Figure 19.

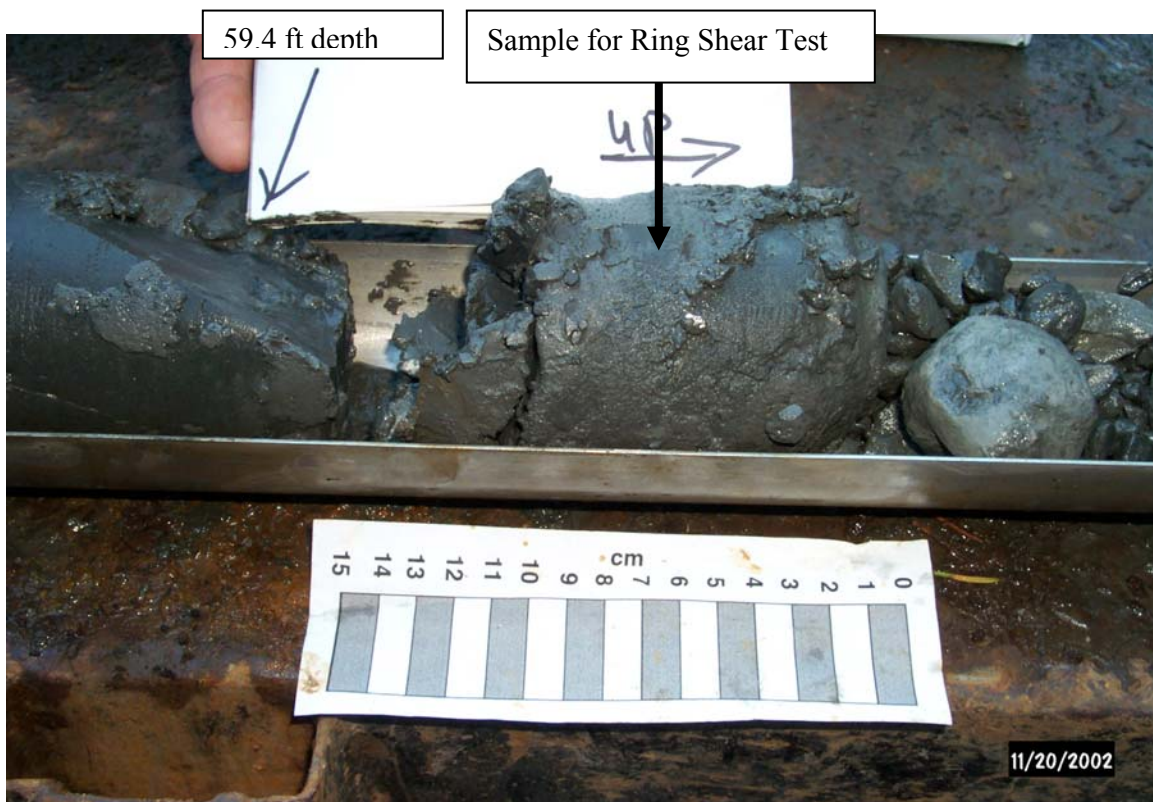


**Figure 18.** Sample used for ring shear test at a depth of 59 feet in borehole LT-2. Note that this brecciated material does not appear quite as soft and fine grained as the material in the slide plane in the LT-1 borehole (Figure 14), although such material may have been present but lost from the core barrel.

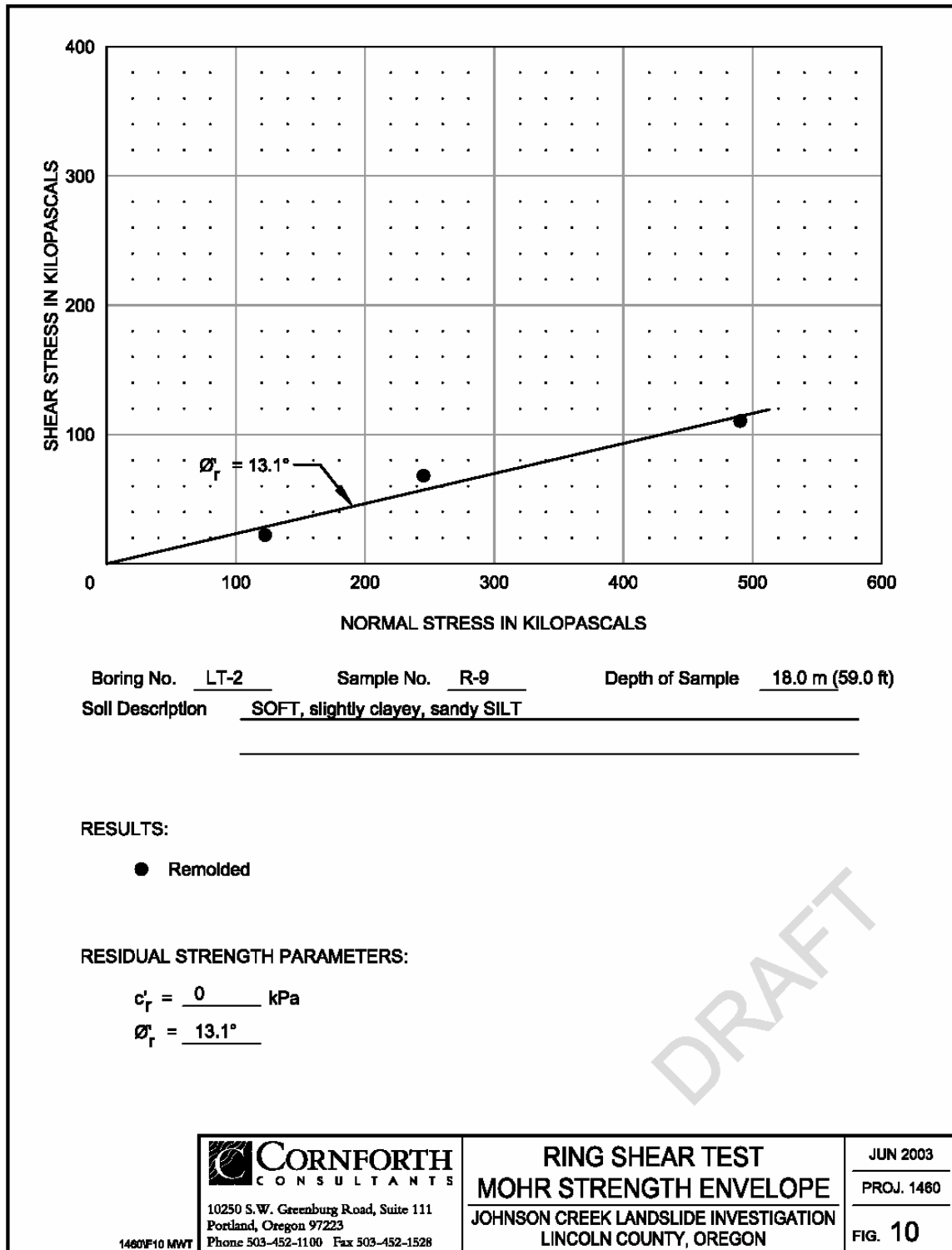


Figure 19. Results of ring shear test on sample from 59 ft depth in borehole LT-2.

## GEOTECHNICAL DATA

Geotechnical data collected for this investigation included subsurface materials, groundwater levels, precipitation, bluff erosion and movement of beach sand. Relevant impacts to landslide stability are summarized in the following paragraphs. Most of this information below is taken from Landslide Technology (2004) with updates for extensometer, piezometer, and rainfall data collected after that report was written.

### Subsurface Materials/Conditions

Exploratory borings encountered materials that are separated into three geotechnical engineering units identified as Pleistocene terrace sand overlying a thin layer of decomposed Astoria Formation, fractured Astoria Formation slide debris, and bedrock of Astoria Formation below the slide. Detailed descriptions of the subsurface materials are included on the Summary Boring Logs of Landslide Technology (2004) in Appendix B.

Pleistocene marine terrace sand and decomposed Astoria Formation was encountered to depths of 5.0 to 6.9 meters (16.4 to 22.6 feet). Pleistocene terrace deposits consist of loose to medium dense, silty sand. Decomposed Astoria lies immediately below the sand and is 1 to 2 meters (3 to 6 feet) of medium stiff, silty clay.

Astoria Formation slide debris consists generally of moderately to highly fractured sandstone, siltstone and tuffaceous mudstone. This fractured rock is typically very soft rock (R1) with lesser soft rock (R2). In-place Astoria Formation is typically a soft rock (R2). Due to drill and sample specifications for the drilling investigation, Standard Penetration Tests (SPT) were not taken in the drill holes, except to isolate the base of the terrace sand in Boring LT-3p.

Slickensides and apparent gouge zones were also encountered in both the slide debris and the in-place rock underlying the landslide. Slickenside orientations were typically near vertical. Vertical slickensides were also encountered on fracture surfaces in the in-place rock, which suggests that other tectonic-induced strain (faults) may be present in the slide area.

Gouge material encountered in the borings is classified as very soft, slightly clayey to clayey, sandy silt. Brecciated siltstone and sandstone was commonly encountered in the slide debris, and was not encountered in the in-place rock, except for a 0.15 m (0.5 ft) layer of wet, highly sheared siltstone dipping about 2° at 15.4 m (50.5 ft) depth in borehole LT-3. The gouge layer at 15.4 m depth is not noted on the Landslide Technology (2004) description (Appendix B) but was observed by the authors when the core was taken. The origin of this layer could be tectonic or from slide movement below the main slide plane in borehole LT-3. Available data is inadequate to distinguish between these two alternatives. All that is known is that no movement occurred at this point in the borehole during the time that inclinometer measurements could be made, December 13 through 31, 2002.

## Landslide Movements

Landslide movements were measured at the shear zone with inclinometers and extensometers, and on the ground surface with survey hubs.

Shear Zone Monitoring. Landslide movements have been detected in all three of the inclinometer casings. Inclinometer deflection plots are shown in Figures 20 to 22. Correlation of movement to rainfall, groundwater pressure and movement is shown on Figures 23 to 30. Shear movements were detected at depths of 26.5, 18.6 and 7.0 meters (87, 61 and 23 feet) below ground surface for LT-1, LT-2 and LT-3, respectively.

Initial readings were taken on the three casings on December 5, and November 25 and 27, 2002, respectively (horizontal movement  $> \sim 3.25$  cm). Shear movement was first detected in the casings on December 16, 2002. By December 26, inclinometers LT-1 and LT-2 could not be read due to the probe not being able to pass the distorted casing at the slide zone (horizontal movement  $> \sim 3.25$  cm). They were converted to fixed borehole extensometers at that time. By the first week of January 2003, LT-3 was no longer readable and was also converted to an extensometer. Movement continues to be recorded with the extensometers in each of the casings. It should be noted that ground movements obtained from the inclinometer system have a high precision (0.25-mm, 0.01-inch) compared to that of the extensometer (3-mm, 1/8-inch) prior to installation on November 20, 2004 by the USGS of the automated data collection system. The accuracy and precision of the new system is still being evaluated but should be much better than 3 mm, since the cable is under a constant degree of tension allowing even small movements to be detected by the digital logging device.

Inclinometers LT-1, LT-2 and LT-3 measured shear zone movement vectors in the directions 273, 258 and 247 degrees azimuth, respectively. Based on analysis of inclinometer data by Landslide Technology (2004), apparent shear movement near the bottom of inclinometer hole LT-2 is likely due to systematic error and is not related to actual shear movement.

The large displacement in LT-2 between January 31 and February 3, 2003 created  $\sim 10$  cm of compression between LT-1 and LT-2 and  $\sim 20$  cm of extension between LT-3 and LT-2 (Figure 31). Vertical offset on the southernmost slide margin was so large during this event that emergency gravel was dumped on Highway 101 to keep it open until it could be paved later in the year. Much smaller movements over the subsequent 2 years failed to significantly relieve this extension and compression. Note that overall displacement between boreholes LT-3 and LT-1 in this same time interval is about 11 cm of extension (Figure 32). The absolute compressional or extensional stress present after these differential movements is dependent on the previous history of differential movement, but the 2003 movement probably altered fracture porosity and the stress field within the slide.



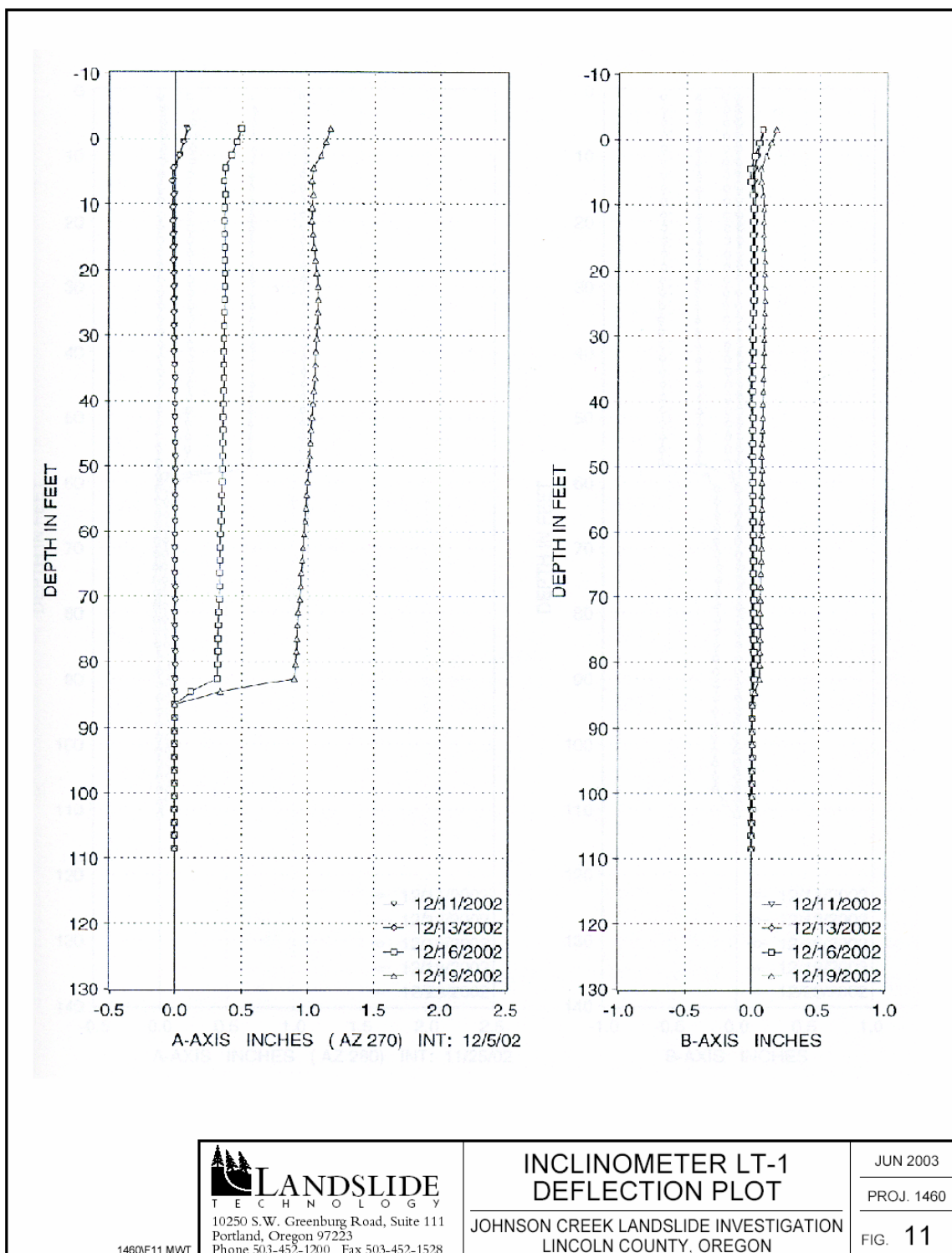


Figure 20. Inclinometer data for borehole LT-1.

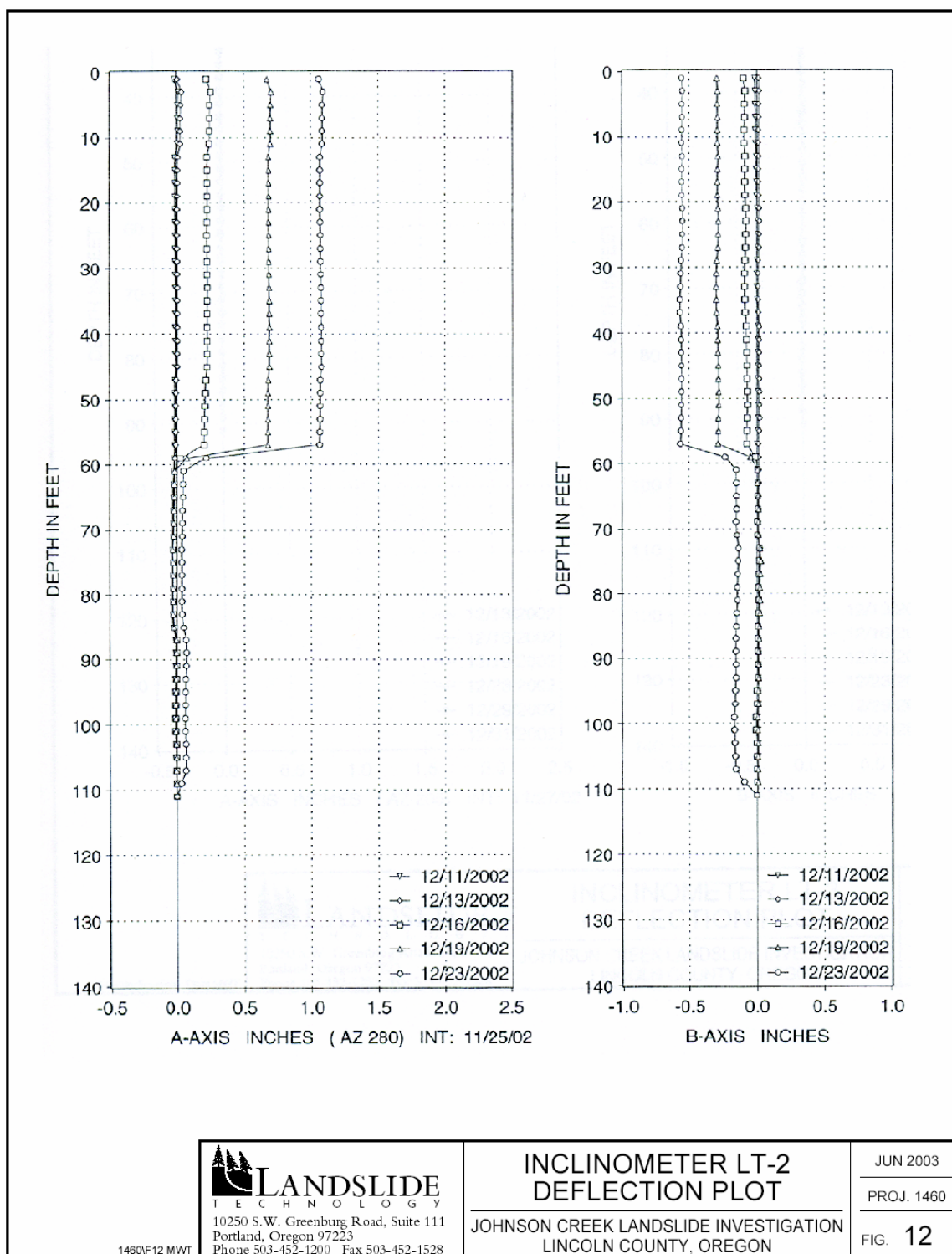


Figure 21. Inclinometer data for borehole LT-2.

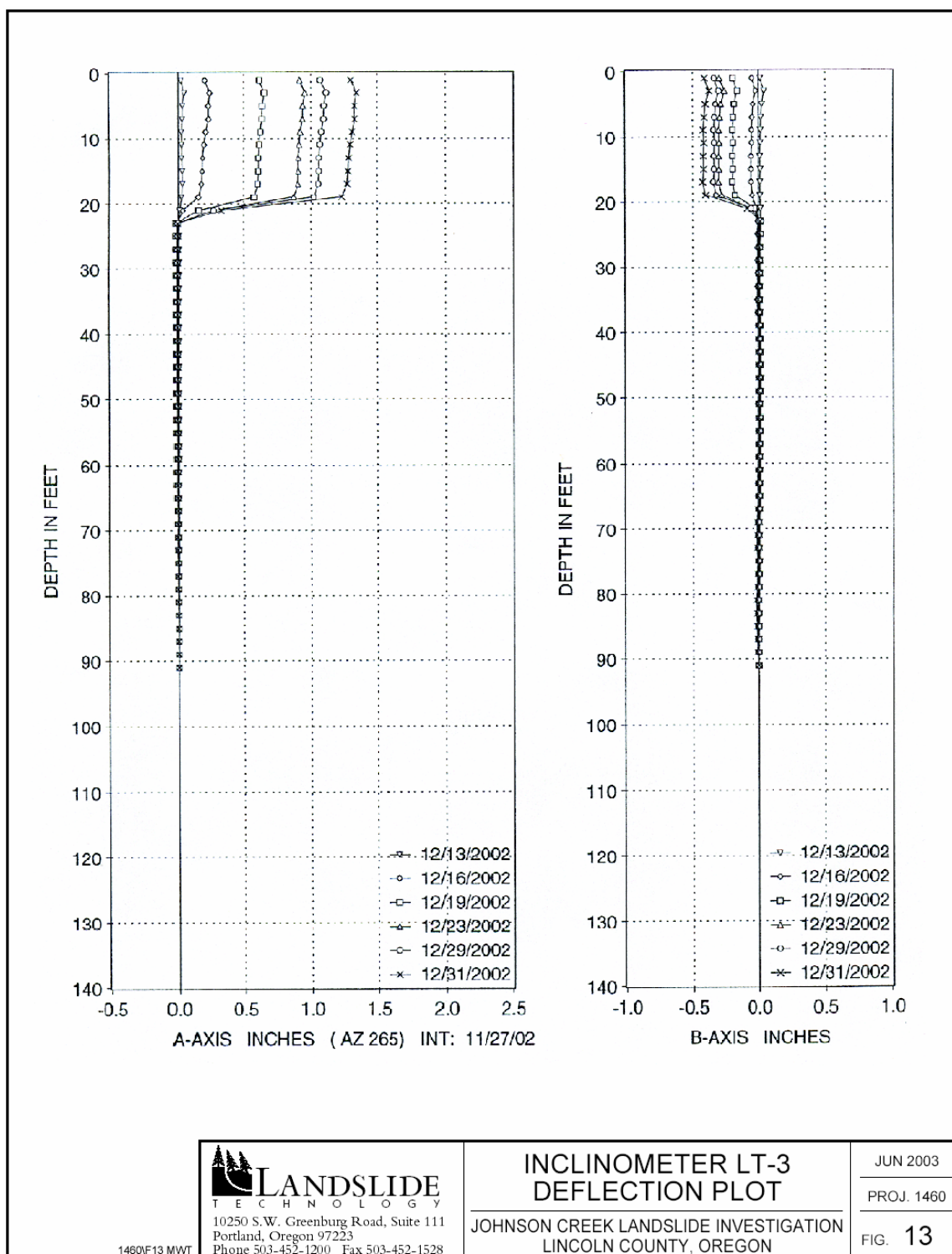
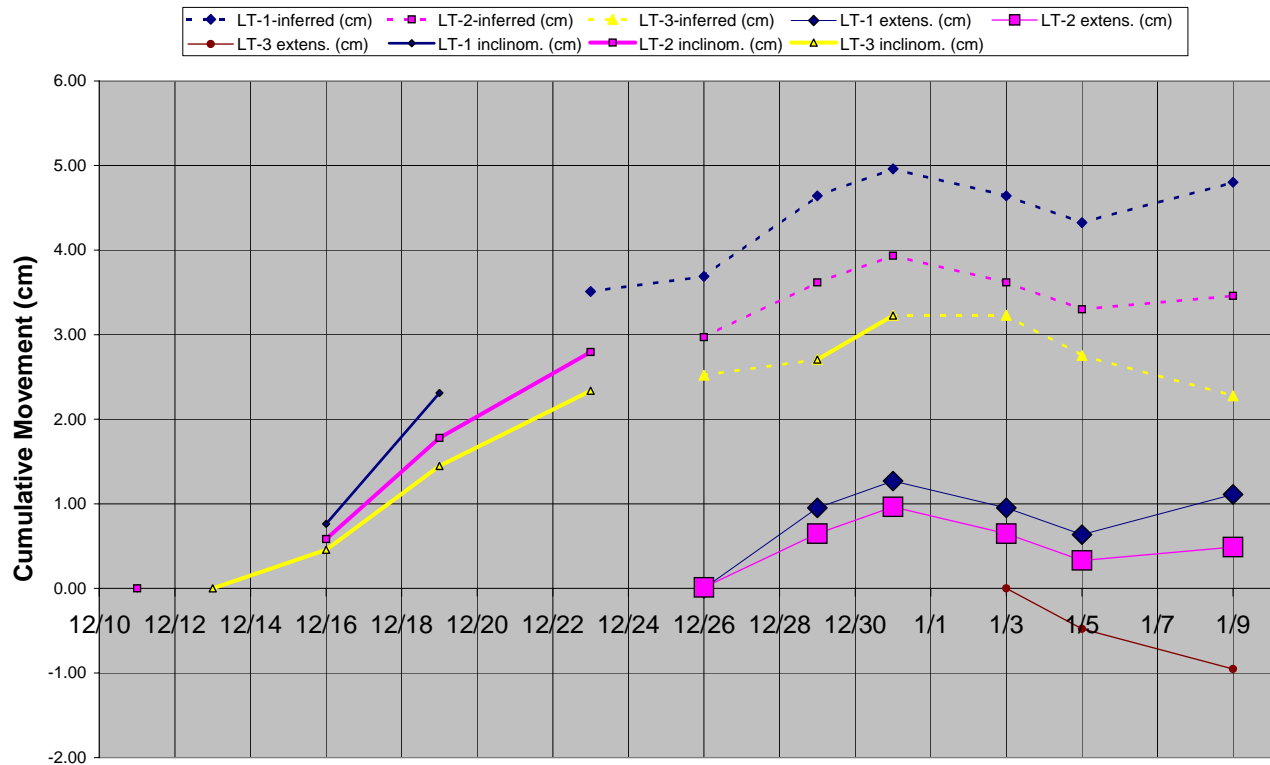
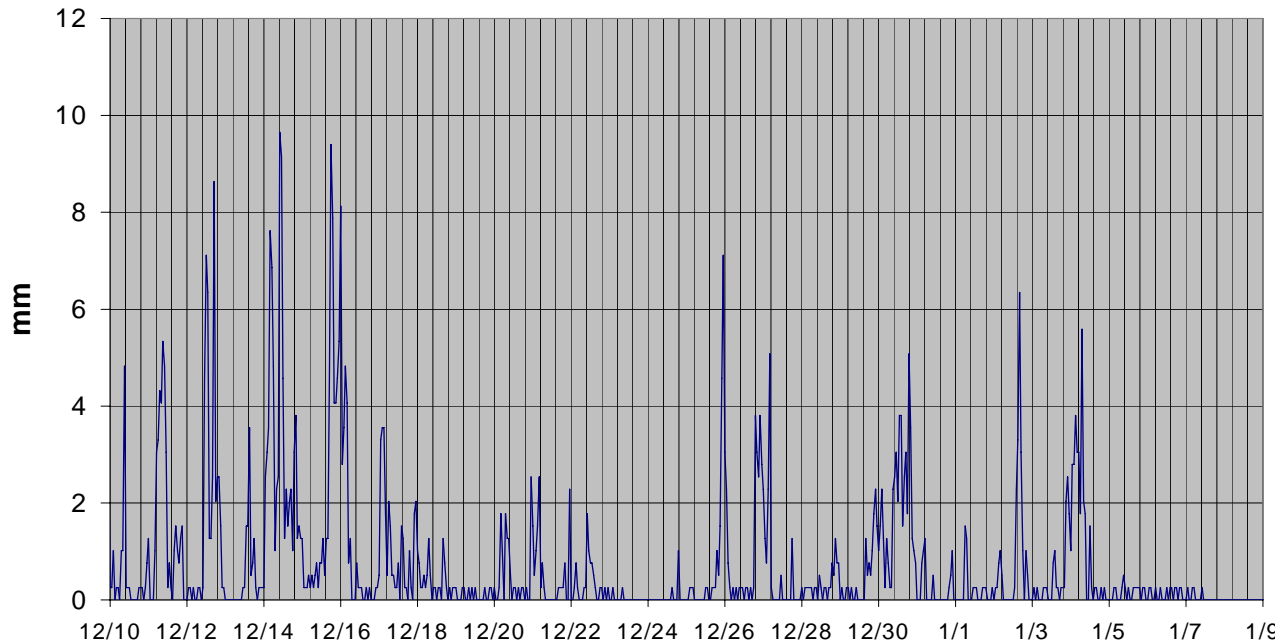


Figure 22. Inclinometer data for borehole LT-3.

### Extrapolation of Inclinometer Data to Extensometer Data



### 12-11-02 to 1-9-03 Rainfall



**Figure 23. Inclinometer, Extensometer, and rainfall data. Data was taken before installation of piezometers. Total slide movement from combined extensometer and inclinometer data is inferred (dashed lines) and forms the baseline for the movement data in Figure 24. Inference is based on relative values of LT-1, LT-2, and LT-3 from the inclinometer data.**



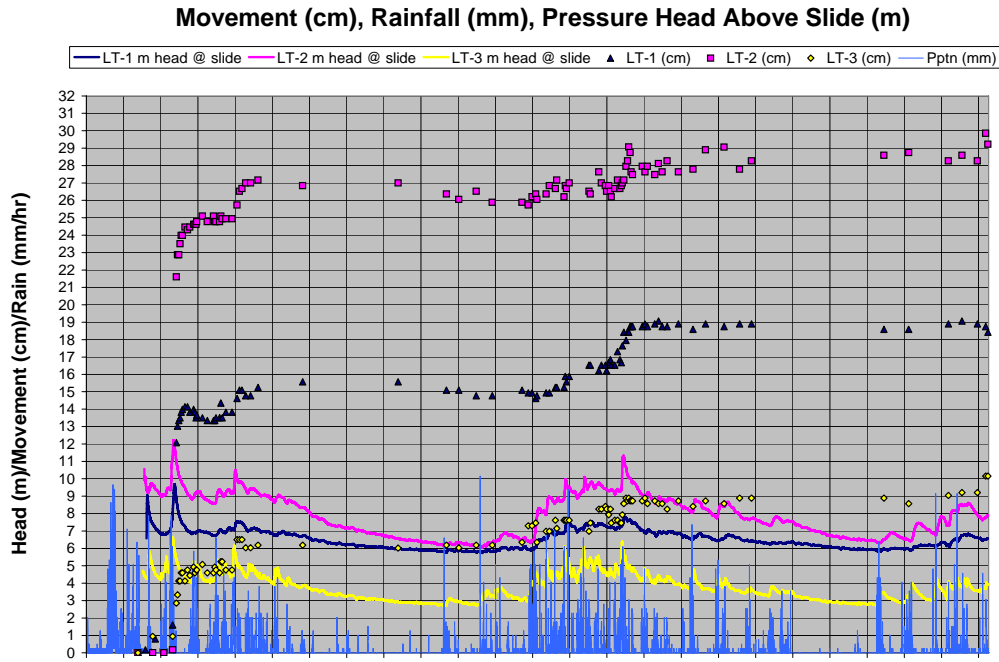


**Figure 24.** Total movement from combined inclinometer and extensometer data (cm) versus piezometer (pressure head in meters above the slide plane) data and rainfall (mm/hour).

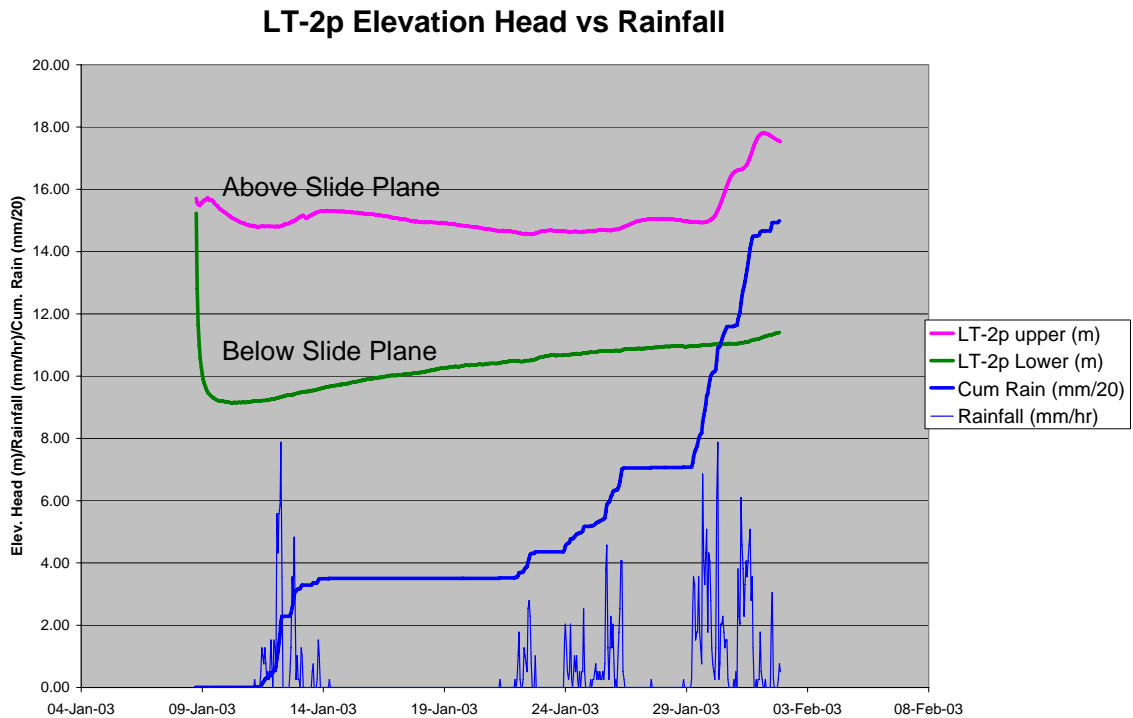


**Figure 25.** Piezometric head elevation above geodetic mean sea level (NAVD 88) at the LT-2p borehole, January 2003. Data for the piezometer below the slide plane ends when the piezometer cable was severed by slide movement at 9:00 PM on February 1, 2003. Cum. Rain = cumulative rainfall from 1-9-2003 to February 2003.

### February 2003 Movement Event

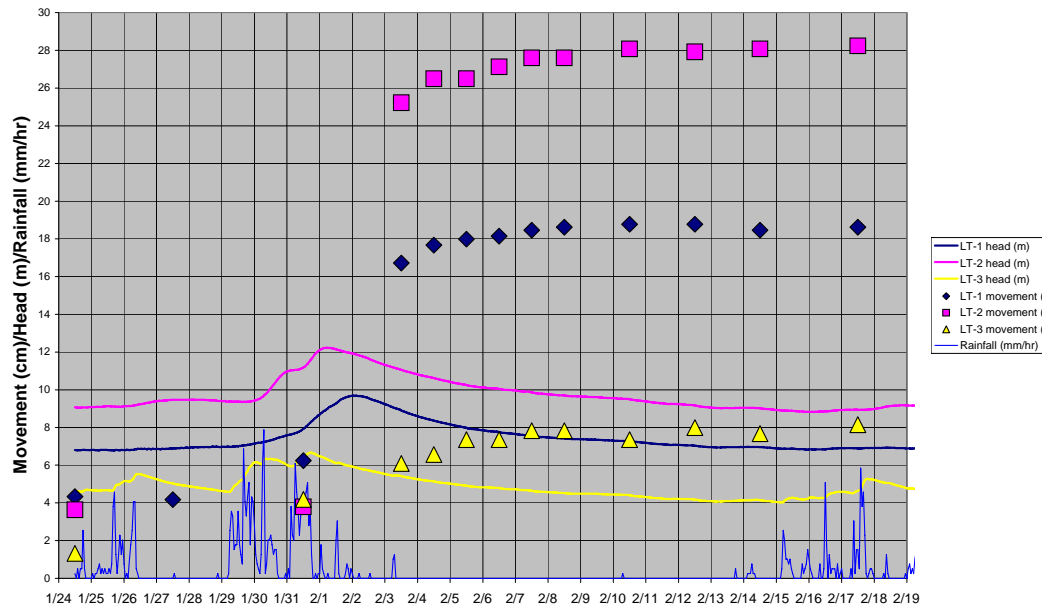


**Figure 26. January 31 to February 3, 2003 movement event versus head and rainfall. Note that the 21.4 cm of probable west (down slide dip) displacement in the LT-2 borehole is much larger than roughly synchronous movements at LT-3 to the east or LT-1 to the west and reverses the earlier pattern of LT-1 having slide movement greater than LT-2.**

### March 2003 Movement Event

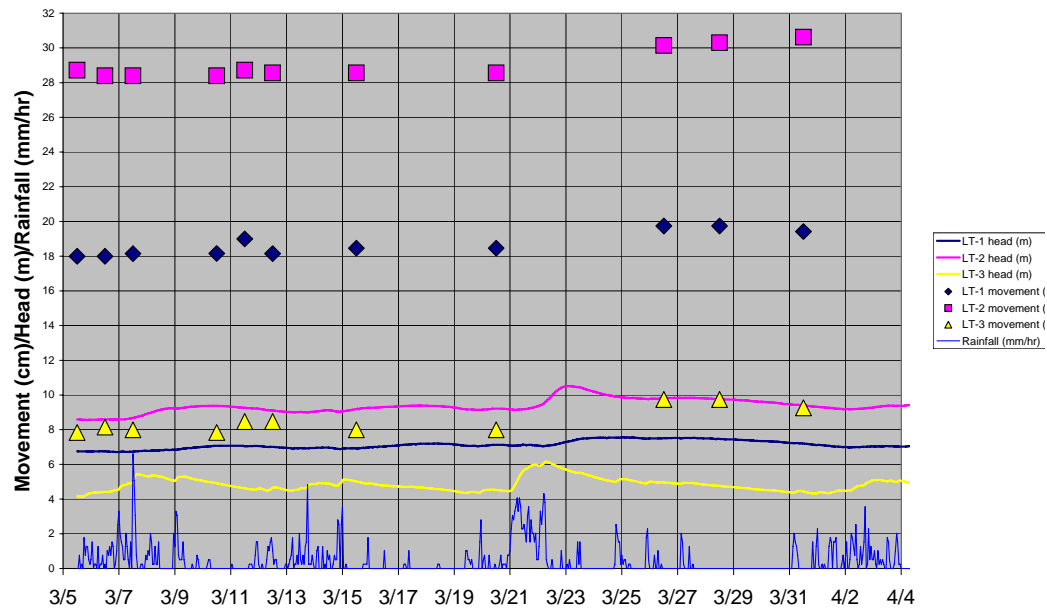


**Figure 27. March 2003 movement versus piezometer, and rainfall data.**

### 11-17-03 to 1-2-04 Rainfall vs Head and Movement

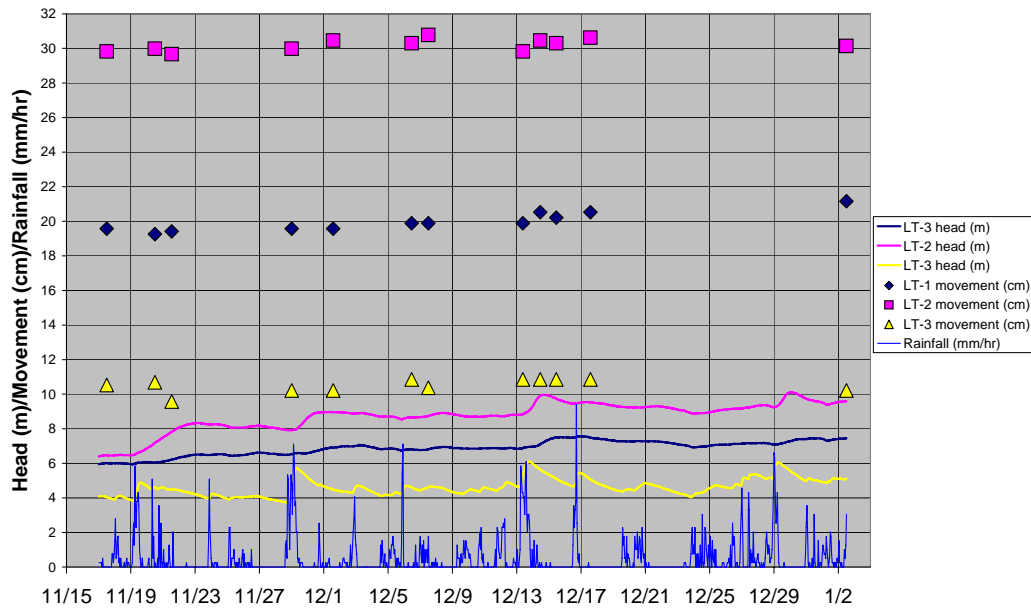


**Figure 28. November 17, 2003 to January 2, 2004 movement versus head and rainfall. In the interval December 14 to 15, 2003 peak pressure head above the slide plane was 7.48 m for LT-1p, 9.97 m for LT-2p, and 5.93 m for borehole LT-3p.**

### January 2004 Movement Event

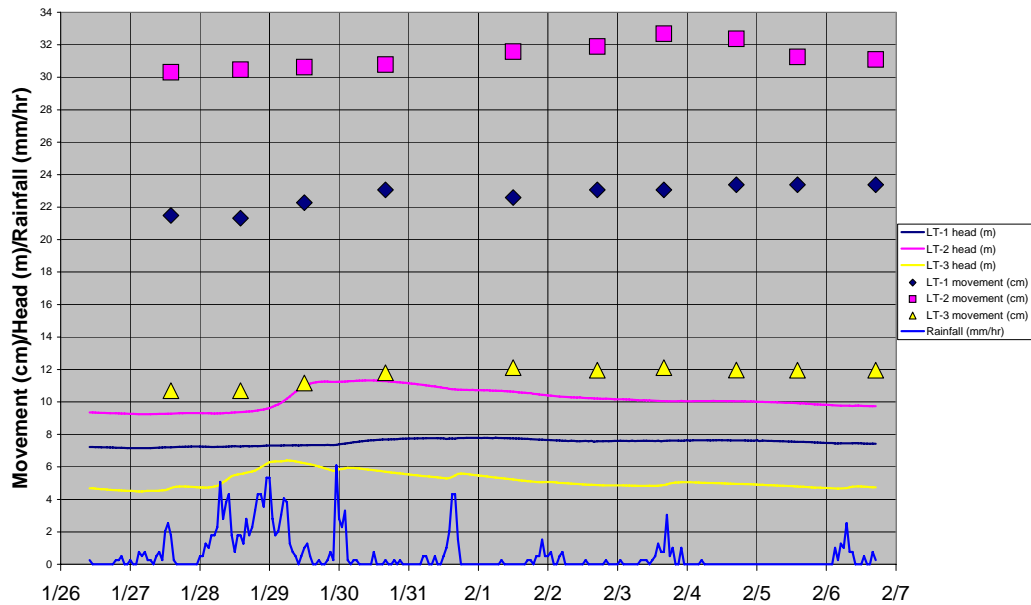


**Figure 29. January 27 to February 7, 2004 movement versus head and rainfall.**

### Correlation of Movement to Antecedent Rainfall

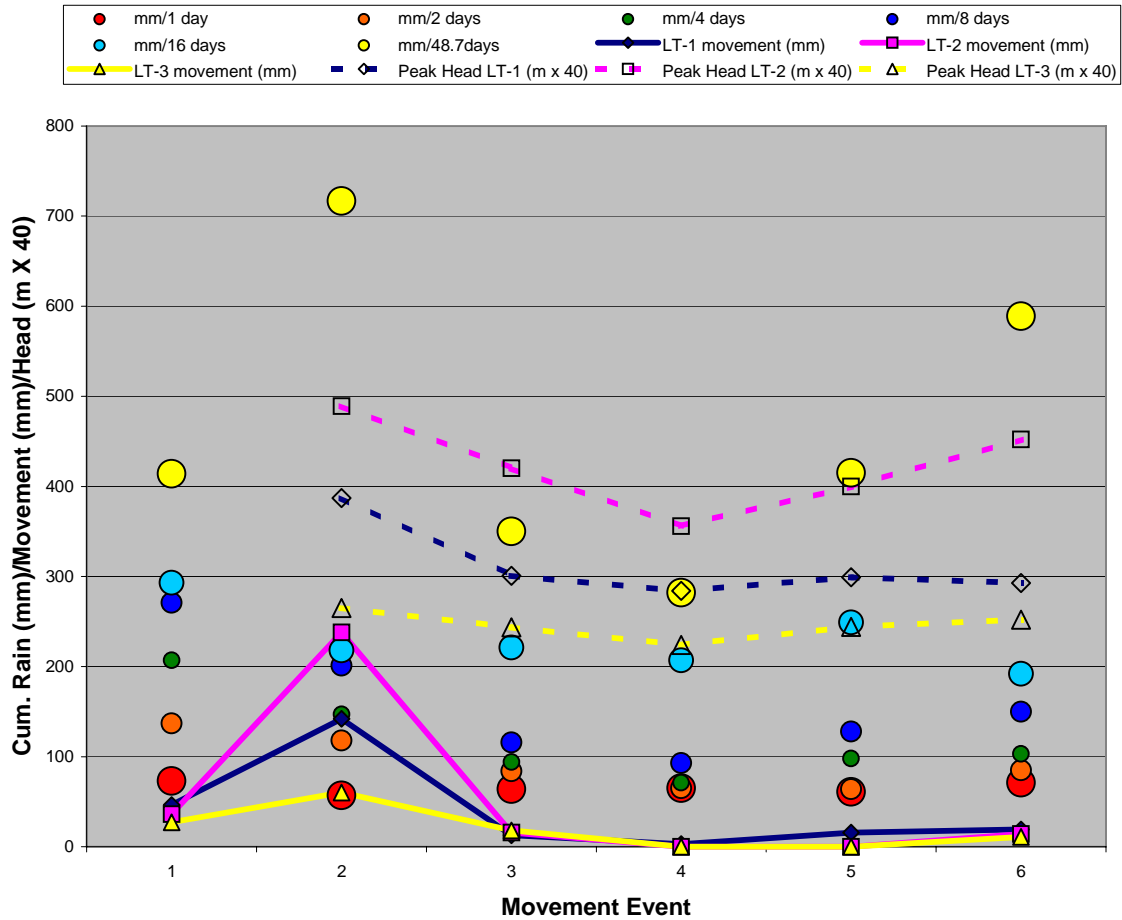
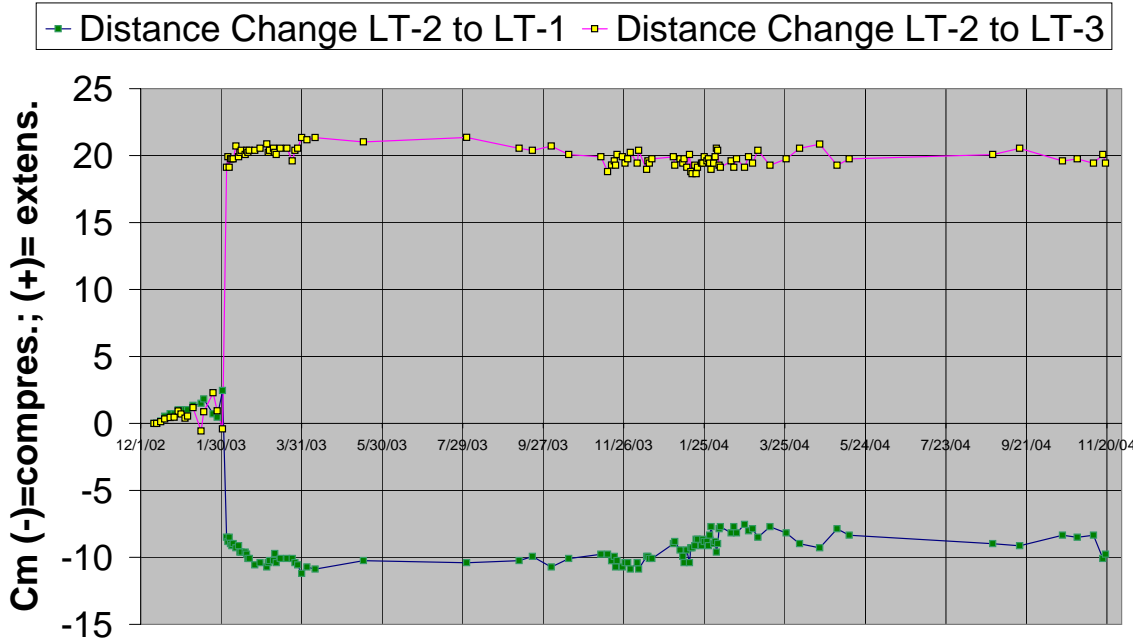


Figure 30 . Correlation of slide movement and pressure head above the slide plane in each movement event with cumulative antecedent rainfall 1, 2, 4, 8, 16, and 48.7 days before the event. Movement event 1 = December 13 to 16, 2002; 2 = January 27 to February 3, 2003; 3 = March 20 to 24, 2003; 4 = November 29, 2003; 5 = December 14 to 15, 2003; 6 = January 27 to 29, 2004.



## Distance Change Between Boreholes



**Figure 31. Compression (- values) and extension (+ values) between boreholes based on the 2002-2004 inclinometer and extensometer data. Note that the large movement at borehole LT-2 between January 31 to February 3, 2003 creates net extension east (between LT-2 and LT-3) and compression west (between LT-2 and LT-1) for the next 2 years.**

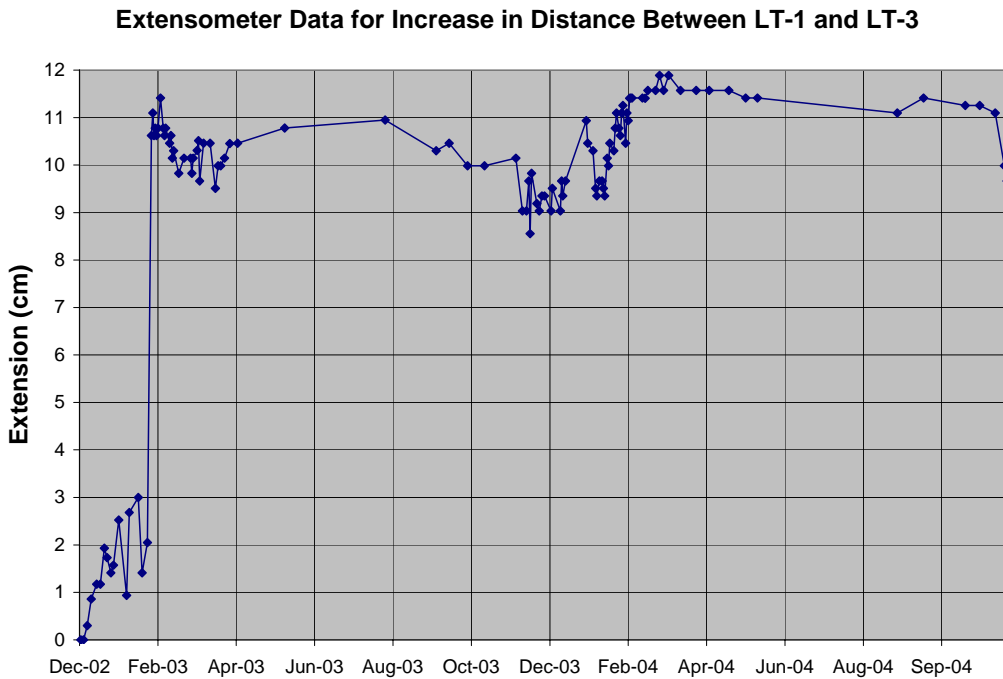


**Figure 32. Change of distance between boreholes LT-1 and LT-3.**

Previous Shear Zone Monitoring. Inclinator plots from six borings installed in Johnson Creek Landslide in the 1970s, along with accompanying boring logs, are included in Landslide Technology's (2004) report. These data provide additional information, but there are other variables to consider. According to Landslide Technology (2004) the vertical and horizontal datum is not included, and the measurement point for the "slope meter tubes" is unknown. The plots for three of the borings (76-2, 76-3 and 76-4) have similar appearances, which can be attributed to the depth of movement deeper than the casing. Therefore, the actual depth of movement in these borings is unknown. The plot for boring 76-1 appears reasonable; however, there is a high degree of uncertainty in the actual depth compared to the data from LT-1, LT-2 and LT-3. Nevertheless, we used the data from these boreholes to put crude constraints on the depth of the slide plane when constructing the structure contour map of the slide plane (Figure 11). We assumed that ground elevation at each borehole location was the datum from which depth was measured in each, so, if depth was actually measured from the top of casing not flush with the ground, depth could be over estimated somewhat from this factor. As movement may be slightly deeper than some of casings, it is possible that the two errors cancel out to some extent.

Ground Surface Monitoring. Survey points were established on the ground surface at three east-west sections across the slide (Appendix D). Two sets of readings were taken, one in October 2002 and one in April 2003. Based on readings taken upslope of the headwall graben in stable ground, the survey repeatability error appears to be relatively large, about 11 cm to 15 cm horizontal and 1 to 130 cm vertical (Table 3). There appears to be a slight positive correlation ( $R^2 = 0.5-0.6$ ) of degree of error and distance east of the landslide (Figure 33), possibly from the need to set up the surveying instrument multiple times instead of doing single line-of-sight shots. One point had an error of 130 cm vertical, probably from disturbance of the steel stake or calculation/transcription error. However, even with the relatively high error in the survey data, general trends emerge that are helpful in understanding the overall differences in ground movement across the slide during the large movement event that occurred at the end of January 2003 (Figures 34 and 35; Table 4; Appendix D). This event had movement large enough in the central and southern part of the slide to be detectable in spite of the measurement error.

**Table 3. Re-survey of steel stake markers at the headwall for error analysis (all horizontal and vertical values should be zero). Note some correlation of error with distance east of the active headscarp shear zone.**

Distance (m) East of Active Headscarp	Horizontal Error (cm)	Vertical Error (cm)	Area
3.2	0.0	2.2	NE headwall
6.0	10.9	0.9	NE headwall
93.0	10.9	9.2	NE headwall
3.6	0.0	0.3	Central headwall
4.4	0.0	1.1	Central headwall
21.0	10.9	2.9	Central headwall
37.5	10.9	129.9	Central headwall
72.8	15.4	5.5	Central headwall
101.6	10.9	2.8	Central headwall
18.5	0.0	1.4	SE headwall
Mean	7.0	15.6	All headwall sites
Std Dev	6.1	40.2	All headwall sites
Mean w/o 129.9 cm vertical error	6.5	2.9	All headwall sites but one
Std Dev. w/o 129.9 cm vertical error	6.4	2.8	All headwall sites but one
Mean w/o 129.9 cm plus 1 Std. Dev.	13	6	All headwall sites but one

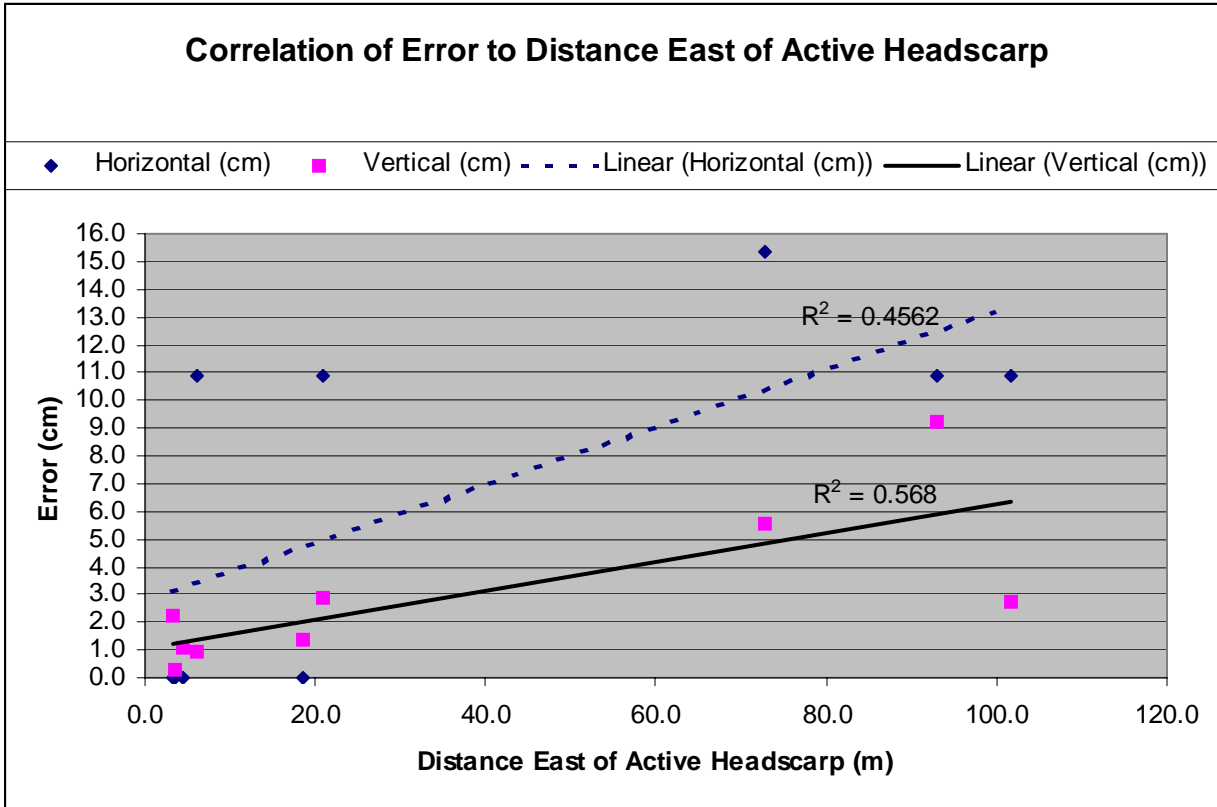


**Figure 33. Re-survey data for steel rods east of active slide movement for determination of error. Note how error tends to increase away from the active headscarp. Chart does not include one outlier with 129.9 cm of vertical error. See Table 1 for the entire data set.**

Ground movements within the landslide are generally faster toward the west and the south (Figures 34 and 35; Appendix D). The increase westward is expected, given the large topographic displacement of the slide toward the west (Figures 2 and 7), although the increase is really quite modest (well within the survey error) for the middle survey line along the east-west transect that includes the LT-1, LT-2 and LT-3 boreholes (Figure 35; Appendix D). Arctangents of the vertical over the horizontal movements agree well with dip of the slide plane between boreholes LT-3 and ODOT hole 76-1, but are significantly different from dip inferred from borehole data in other parts of the drilling transect (Table 4 compared to Figure 7). Differences in slide dip inferred from surveyed movement and that of the cross section are probably due to the relatively large survey errors and the role of complex movements of small interior slide blocks (tilted graben, etc.). Uncertainties in dip in the cross section are much less, since dip is measured in core and by stratigraphic correlation.

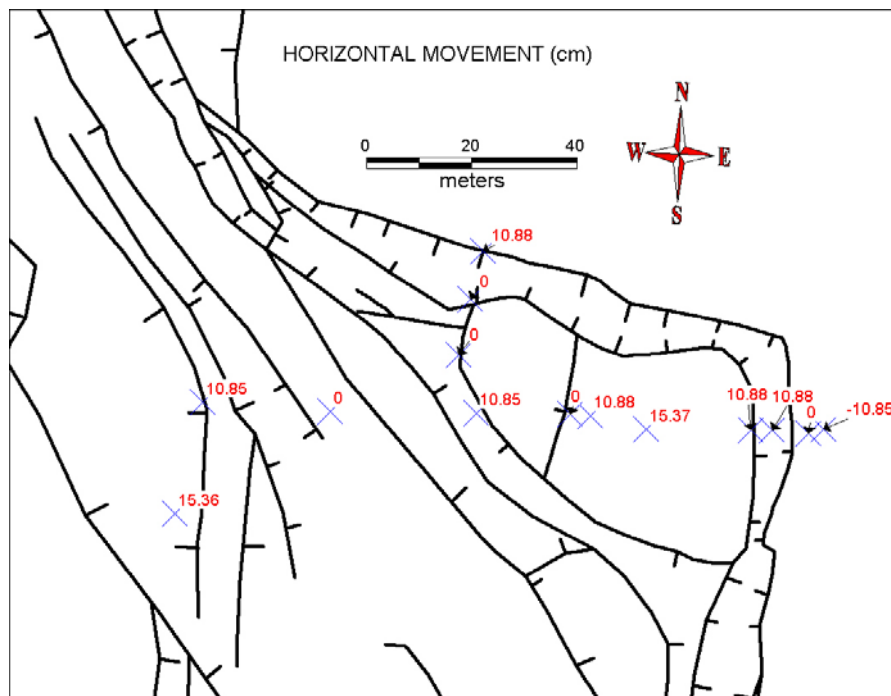


**Figure 34. Horizontal movement (cm) at steel stakes (blue crosses) in northern part of landslide between October 2002 and April 2003. Note that most movement is less than survey error of ~11-15 cm, so movement direction or amount could not be accurately estimated. Positive values are westerly movement; negative values are easterly movement. See Appendix D for vertical movement, movement vectors and a complete discussion of the data.**

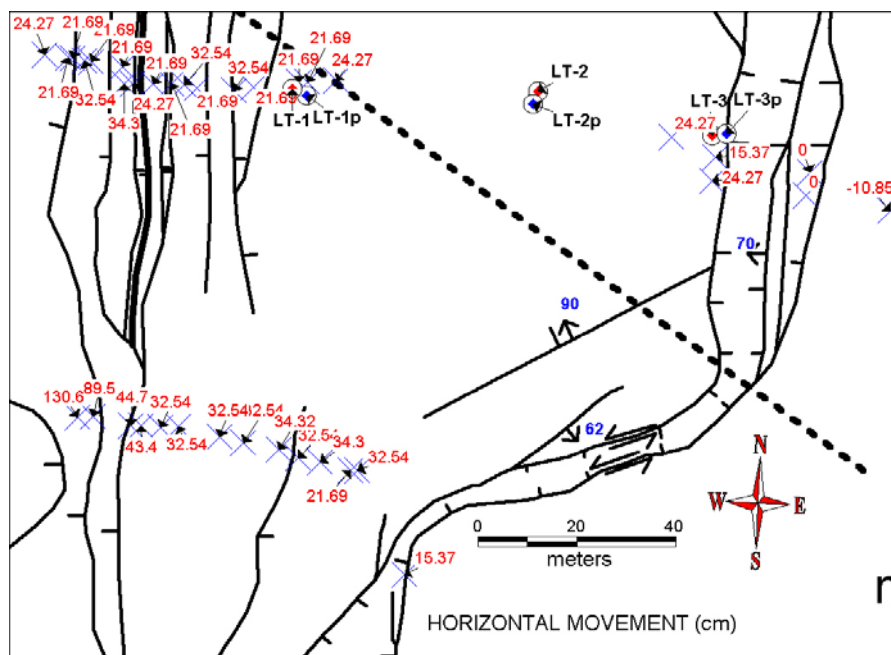


**Figure 35. Horizontal movement (cm) at steel stakes (blue crosses) landslide between October 2002 and April 2003 in southern part of landslide. Boreholes are also shown (circles with diamonds). Movement east of the headwall of -10.85 cm (eastward movement) is survey error, so this is the approximate error of the data. See Appendix D for vertical movement, movement vectors and a complete discussion of the data.**



**Table 4. Slide movement between October 2002 and April 2003 from re-survey of steel stakes. Error estimates are from Table 3 utilizing the mean error (without the 129.9 cm outlier) plus one standard deviation. Slide dips are estimated from geologic cross sections between drill holes and surface outcrop of the slide plane (Figure 7). Middle survey hubs are at the same latitude as the LT-1, LT-2, and LT-3 boreholes; no hubs were near the LT-2 borehole.**

Site	Horizontal (cm West)	Vertical (cm) (-) = Down to the West	Estimated Slide Dip from Resurvey (Arctangent of $\frac{\text{Vertical}}{\text{Horizontal}}$ )	Estimated Slide Dip from Boreholes Plus Outcrops (-) = East
North Survey Hubs	$< \pm 13$	$< \pm 6$	—	—
Middle Survey Hubs near LT-3 borehole (east of Hwy. 101)	$20 \pm 13$	$-8 \pm 6$	$22^\circ \pm 33^\circ$	$21\text{-}23^\circ$
Middle Survey Hubs near LT-1 borehole (west of Hwy. 101)	$22 \pm 13$	$-6 \pm 6$	$15^\circ \pm 33^\circ$	$\sim 10.5^\circ$
Middle Survey Hubs on back- tilted block at top of sea cliff.	$24 \pm 13$	$-6 \pm 6$	$14^\circ \pm 33^\circ$	$\sim 10^\circ$
South Survey Hubs east of Hwy. 101	$15 \pm 13$	$-22 \pm 6$	$56^\circ \pm 33^\circ$	no data
South Survey Hubs west of Hwy. 101	$33 \pm 13$	$-9 \pm 6$	$15^\circ \pm 33^\circ$	no data
South Survey Hubs on back- tilted block at top of sea cliff	$131 \pm 13$	$-70 \pm 6$	$28^\circ \pm 33^\circ$	no data

Vector movement azimuths and the raw data on movement at all points in the area are included in Appendix D. The middle and southern survey lines show similar direction of ground surface movement in the main part of the slide mass compared to direction measured by inclinometers at the shear zone -- west-southwest in the eastern part of the slide, and west in the western part.

A line-of-sight survey was established along Highway 101 and two sets of readings have been taken in January and February 2003 (Appendix E). These data also show that the southern area of the slide has moved faster than the northern area.

Additional line-of-sight data is being collected in 2004, but in the winter of 2003-2004 a new line-of-sight had to be established. Slide movement caused a sign to move across the field of view cutting off further observations. Additional data will be collected in the 2005 and 2006 to continue tracking slide movement, but based on extensometer data, too little movement had occurred at this writing to make such measurements worthwhile.

## Groundwater and Precipitation

Water pressures within the landslide were measured with vibrating-wire piezometers installed at the slide zone in Borings LT-1p, LT-2p and LT-3p, and in bedrock in Boring LT-2p. Water pressure above the slide plane (pressure head) and rainfall in millimeters per hour<sup>2</sup> is illustrated in Figures 23, 24, and 26 to 29. Piezometric elevation head at piezometers below and above the slide plane at borehole LT-2p is illustrated in Figure 25. Groundwater flow paths are shown schematically in Figure 36. Piezometric head elevations are shown on Figure 37 for the January-February 2003 maximum, summer minimum, and threshold levels for slide movement.

The shallowest piezometer, LT-3p, responds within about 2 hours to all rainfall events regardless of intensity or duration. Piezometers LT-1P and LT-2P show less obvious correlation to small rainfall events but do respond to events of larger intensity and duration (Figure 24). In general, the deeper the elevation head in the borehole, the less pressure response to small rainfall events, hence responsiveness (correlation) to rainfall events follows the pattern LT-3p>LT-2p>LT-1p (see elevation head depicted on Figure 38).

Figure 25 illustrates that below the slide plane in borehole LT-2p the piezometric elevation (elevation head) is about 4-6 m lower than piezometric head within and immediately above the slide plane, except at the first two days of data when drilling/installation effects were affecting the data. The piezometer below the slide plane recorded a steadily rising piezometric head of about 4.5 cm/day over the 24 days of observation (January 9 to February 2, 2003) with only small changes in rate that are hard to correlate with the rainfall data. During this same interval, piezometric head above the slide plane returned to ~15 m elevation after each “spike” in pressure from rainfall events. Below the slide plane groundwater storage appears to be continuously increasing during the wet season, building up water pressure, whereas above the slide plane groundwater is draining out rapidly enough after each rainfall event that pressure returns to about the same level as before the next event. Since Astoria Formation is the dominant rock above and below the slide plane, this dramatic difference in response is not likely due to a difference in rock type. The slide is known to be much more highly fractured than the underlying rock, so the difference in response to rainfall events is almost certainly due to higher fracture porosity and permeability in the slide. Based on these limited data, it appears that groundwater levels in the slide mass are strongly influenced by percolation of rainfall into the slide and that groundwater drains more freely out of the fractured slide material than it does below the slide plane. Piezometric head below the slide plane that is lower in elevation than head above the slide is consistent with poor hydraulic communication across the slide plane.

Pressure head below the slide plane could decrease resisting forces at the slide plane, if it rose high enough to exceed the pressure head at the slide plane. Based on the rate of increase in the 24 days of data, this could occur over a period of 77 days, assuming that the overall rate of pressure increase below

---

<sup>2</sup> The rainfall data were affected by wind gusts until a shield was installed on January 7, 2003. Prior to this date occasional false tipping occurred, usually no more than one tip per hour. Each tip equals 0.25 mm (0.01 inches) of rainfall.

the slide plane did not change. This observation leads to the conclusion that water pressure below the slide plane could become a factor in slide stability in April or May during relatively wet years. If this occurs, it would probably be manifested as slide movement during a peak in pressure head measured above the slide plane that is slightly lower than threshold values earlier in the year. No such event has occurred during the two-year observation time.

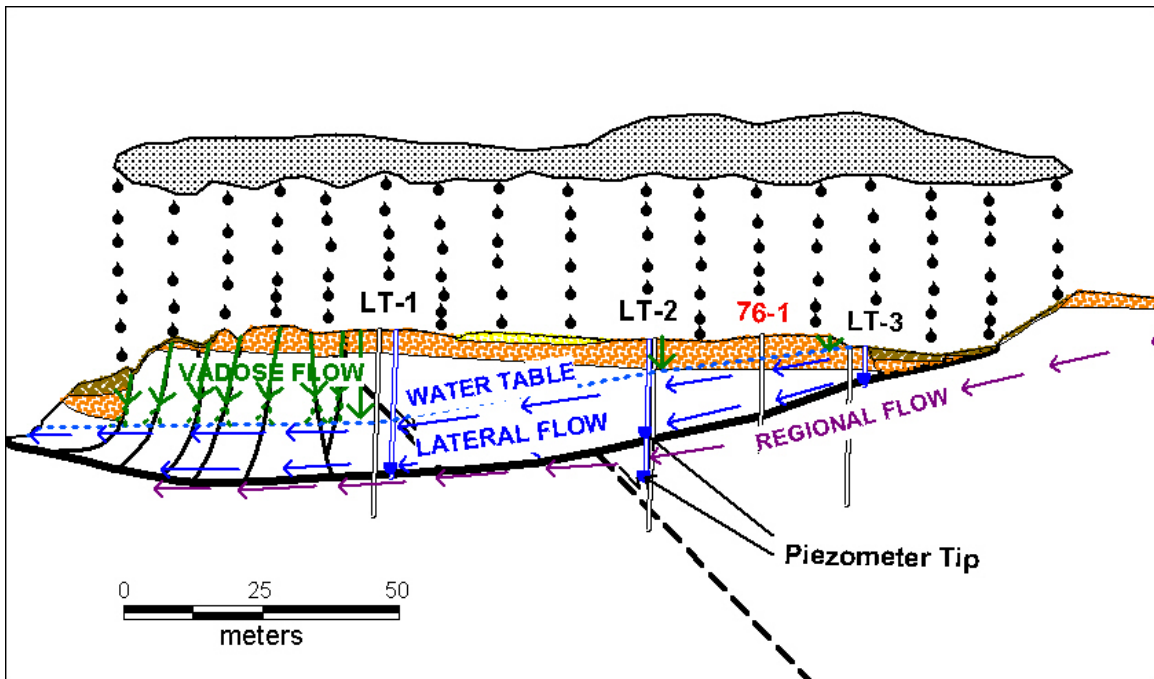


**Figure 36. Schematic illustration of groundwater circulation. Boreholes are shown; blue = piezometer holes; black = inclinometer/extensometer holes. Brown stippled unit is colluvium; orange stippled unit is Pleistocene marine terrace sand; uncolored unit is Astoria Formation.**

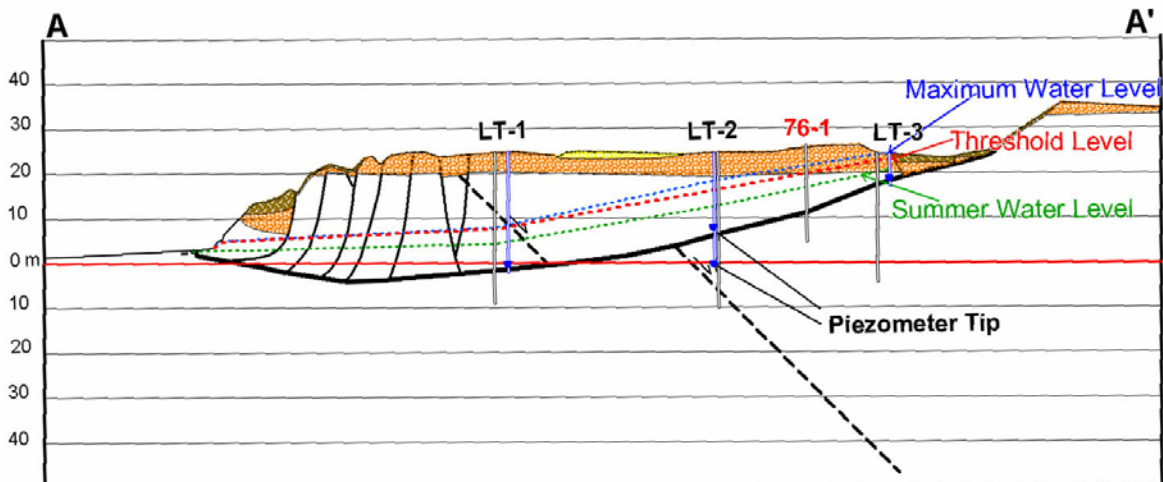


**Figure 37. Cross section illustrates inclinometer holes, piezometer holes, piezometer tip locations and the minimum water level (red dashed line) that initiates movement on the Johnson Creek slide relative to the February 1, 2003 maximum and summer minimum. Note that the slope of the water table between holes and from LT-1 to the sea cliff is highly uncertain. For example, the tectonic fault between LT-1 and LT-2 could be a hydraulic boundary that causes an abrupt change in water table elevation. Uncolored areas below the Pleistocene marine terrace sand (stippled tan unit) are Astoria Formation.**

There are no direct measurements of the phreatic water table, so it is not known with certainty whether elevation heads measured by the piezometers above the slide plane are equivalent to the phreatic elevation head. The abundance of steeply dipping fractures found in surface outcrops and drill core within the slide mass argue for good communication between the aquifers within the slide, so it is probable that the overall piezometric head measured above the slide plane is at least approximately equal to the phreatic head within the fracture system.

Data Correlation – Rainfall Versus Slide Movement and Head. Correlations between rainfall and ground movement were evaluated. Ground movement, piezometric head above the slide zone and precipitation are summarized in Figures 23-29. Five separate slide movement events were recorded as follows:

- Event 1: December 13 to 16, 2002
- Event 2: January 27 to February 3, 2003
- Event 3: March 20 to 24, 2003
- Event 4: November 29, 2003
- Event 5: December 14 to 15, 2003
- Event 6: January 27 to 29, 2004

Correlation was observed between piezometric head and slide movement during all movement events (Table 5). Threshold pressure heads above the slide plane and depths to water associated with slow and fast movement are summarized for each hole in Table 6. Note that even though peak pressure head values in excess of the threshold for slow movement (Table 6) were reached in November and December of 2003 in LT-2p and LT-3p (Events 4 and 5, Table 5), there was no measurable movement. The initial pressure head prior to the pressure head peak (the “background pressure head”) in these two cases was slightly lower in general than cases where movement occurred previously in the same holes (Table 5). There was barely measurable movement in LT-1 for the November event at the lowest initial pressure head and lowest peak head that caused movement there (Event 4, Table 5). We conclude that a minimum background pressure head of ~6.5 m, 9.2 m, and 4.5 m must be present at LT-1p, LT-2p, and LT-3p, respectively, before peaks of head listed in Table 6 can initiate movement.

**Table 5. Detailed correlation of piezometric head versus slide movement for Events 2-5. Ranges given are the piezometric head values at the time of extensometer measurements that bracket stop or start of slide movement.**

	Initial Head (m)	Head at First Movement (m)	Peak Head (m)	Head at Last Movement (m)	Movement (cm)
LT-1					
<i>Event 1</i>	No data	no data	no data	no data	4.6
<i>Event 2</i>	6.9	6.9-7.9	9.7	7.8	14.2
<i>Event 3</i>	7.1	7.1-7.5	7.5	7.1-7.5	1.3
<i>Event 4</i>	6.5	6.9-7.1	7.1	6.9-7.1	0.3
<i>Event 5</i>	6.9	6.9-7.1	7.5	6.9-7.1	1.6
<i>Event 6</i>	7.2-7.3	7.3	7.3	7.3-7.7	2.4
<b>Minimum</b>	<b>6.5</b>	<b>7.0</b>		<b>7.0</b>	
<b>Fast Movement</b>	<b>6.9</b>	<b>&gt;8.9; ≤9.7</b>			
<b>Total Movement</b>					<b>24.4</b>
LT-2					
<i>Event 1</i>	no data	no data	no data	no data	3.6
<i>Event 2</i>	9.4	11.2-12.2	12.2	9.7-9.9	23.8
<i>Event 3</i>	9.2	9.2-10.5	10.5	9.2-10.5	1.6
<i>Event 4</i>	8.0	no movement	8.9	no movement	0.0
<i>Event 5</i>	8.7-8.8	no movement	10.0	no movement	0.0
<i>Event 6</i>	9.3	9.4	11.3	<10.6; >9.9	1.0
<b>Minimum</b>	<b>9.2</b>	<b>9.4</b>		<b>9.8-10.6</b>	
<b>Fast Movement</b>	<b>9.4</b>	<b>&gt;11.2; ≤12.2</b>			
<b>Total Movement</b>					<b>30</b>
LT-3					
<i>Event 1</i>	no data	no data	no data	no data	2.7
<i>Event 2</i>	4.6	4.6-6.3	6.6	4.9-5.1	6.0
<i>Event 3</i>	4.5	4.5-6.1	6.1	4.5-6.1	1.8
<i>Event 4</i>	3.8	no movement	5.6	no movement	0.0
<i>Event 5</i>	4.2-4.6	no movement	6.1	no movement	0.0
<i>Event 6</i>	4.5-4.7	5.6-6.3	6.3	5.7-6.2	1.1
<b>Minimum</b>	<b>4.5</b>	<b>&gt;4.6; &lt;6.1</b>		<b>5.0</b>	
<b>Fast Movement</b>	<b>4.6</b>	<b>&gt;6.4; ≤6.6</b>			
<b>Total Movement</b>					<b>11.6</b>



**Table 6. Most representative threshold values of initial (background) pressure head, pressure head at movement, and depth to elevation head (water table) for slow and fast slide movement. Pressure head is in meters above the slide plane.**

Drill Site	Initial Pressure Head (m)		Pressure Head (m)		Depth to Elevation Head (m)	
	Slow Movement	Fast Movement	Slow Movement	Fast Movement	Slow Movement	Fast Movement
LT-1	6.5	6.9	7	~9.0–9.7	19.3	~16.6–17.3
LT-2	9.2	9.4	9.4	~12	8.6	~6
LT-3	4.5	4.6	~5.0	~6.5	~1.6	~0.1

Correlation was also noted between ground movement and antecedent rainfall and intensity. Figure 30 illustrates correlation between rainfall for 1, 2, 3, 4, 8, 16, and 48.7 days before a movement event versus movement and pressure head above the slide plane. Initiation of slide movement best correlates with two-day antecedent rainfall. Movement at borehole LT-1 west of Highway 101 starts when rainfall reaches ~64 mm in the previous two days whereas movement at sites LT-2 and LT-3 east of Highway 101 require at least 84 mm in the previous two days (Figure 30).

Note that none of the patterns of variation in antecedent rainfall for any of the time intervals duplicates the variation in slide movement (Figure 30). The large, fast movement in Event 2 apparently correlates with a combination of high antecedent rainfall (717 mm) during the previous 48.7 days plus intense rainfall over a period of 2 days (118 mm; Figure 30). The 48.7-day period was picked because it sums rainfall for Events 1 and 2.

Slide movement for Event 6 in response to a given head increase appears to be less in LT-2 and LT-3 relative to LT-1 (Figure 30; Table 5). The peak pressure head values for Event 6 in LT-2p and LT-3p are intermediate between peak values in the same holes for Events 2 and 3, but the Event 6 movement is less in these holes than in Events 2 and 3 (Table 5). LT-1 does not have this anomalously low movement during Event 6 relative to its response in Events 2 and 3 (Table 5). Either there is some change in resisting forces in local areas of the slide, or the extensometers are becoming less and less responsive to movement in LT-2 and LT-3 as inclinometer casing becomes more deformed. If the latter were true, then there should be a positive correlation between total cumulative movement (casing deformation) and failure to respond with movement to head changes. LT-3 has the least total movement but still has anomalously low movement, so the change in response appears to be real and probably indicates changing internal forces in the slide. It may be that the overall extension affecting the eastern part of the slide at the drilling transect after the large movement of January-February 2003 (Figure 31) decreased the driving forces.

**Table 7. Time lag of major changes in pressure head between drill holes for rainfall events causing movement at all extensometers. "No data" indicates that a sharp inflection of the head data could not be picked out.**

Head Rise	LT-3p	LT-2p	LT-1p	LT-3p to LT-2p (hr)	LT-2p to LT-1p(hr)	LT-3p to LT-1p (hr)
Start	1/29/03 7:00 AM	1/29/03 10:00 PM	no data	15	no data	no data
Peak	1/31/03 5:00 PM	2/1/03 6:00 AM	2/2/03 3:00 AM	13	21	34
Start	3/21/03 12:00 AM	3/21/03 8:00 AM	3/22/03 6:00 AM	8	22	30
Peak	3/22/03 7:00 AM	3/23/03 2:00 AM	3/23/03 8:00 PM	19	18	37
Start	1/28/04 4:00 AM	1/28/04 12:00 PM	1/29/04 11:00 PM	8	35	43
Peak	1/29/04 6:00 AM	1/30/04 10:00 AM	1/31/04 2:00 AM	28	16	44

**Table 8. Time lag of east-to-west propagation of peaks in pressure head from borehole to borehole, amount of extension or compression between boreholes prior to each movement event, and displacement during each event. Data are listed for rainfall events causing movement at all extensometers after installation of piezometers.**

Event	LT-3p to 2p (hr)	LT-3 to 2 Extension (cm)	LT-2p to 1p (hr)	LT-2 to 1 Extension (cm)	LT-3 Displacement (cm)	LT-2 Displacement (cm)	LT-1 Displacement (cm)
1/29/03 Peak	13.00	0.94	21.00	0.5	6.03	23.81	13.97
3/22/03 Peak	19.00	20.55	18.00	-10.09	1.75	1.58	1.27
12/13/03 Peak	24.00	20.39	22.00	-10.88	0.00	0.00	1.57
1/28/04 Peak	28.00	19.60	16.00	-8.82	1.11	0.79	1.75

Figures 26 to 29 and Tables 7 and 8 illustrate three fundamental characteristics of all of the pressure head data: (1) Pressure head above the slide plane tends to be highest at the LT-2p borehole relative to other boreholes; (2) boreholes with the shallowest water table (e.g. LT-3p) have sharp peaks in head that correlate well with rainfall events, but the deeper the water table in a borehole the less head increases can be correlated to rainfall events of small duration and intensity; and (3) there is a time lag between rainfall events and pressure head changes among the three piezometers at the slide plane (Figure 38). In every large rainfall event a wave of pressure head increases proceeds from east to west starting at LT-3p within 2 hours of the rainfall event, proceeding to LT-2p, within 15 to 30 hours, and to LT-1p within 36-46 hours.

It is likely that the waves of water pressure that travel from the east to the west in response to rainfall events are accompanied by contemporaneous movement when threshold pressures are reached, but the extensometer data were not collected often enough to resolve these details. Movement, piezometric head, and rainfall data are all being collected on an hourly since the US Geological Survey upgraded the instrumentation November 20, 2004. In the future hourly movement can be examined for correlation to hourly water pressure data.

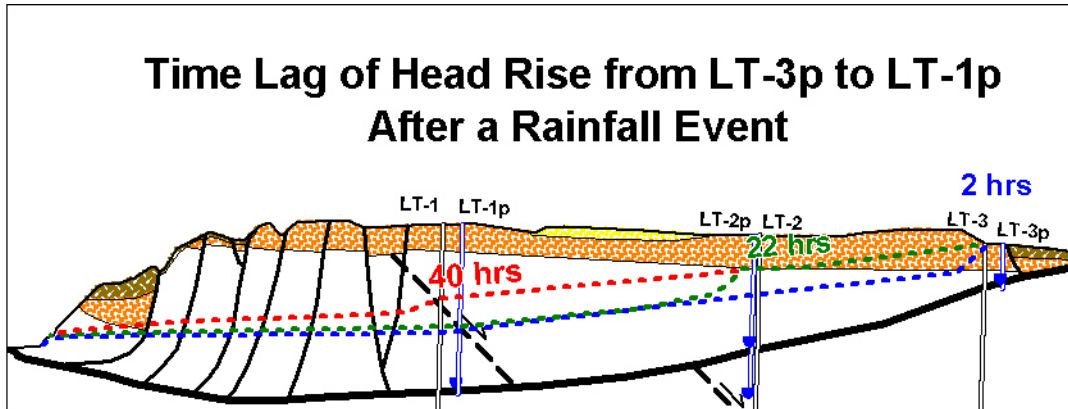


**Figure 38. Schematic illustration of progressive rise in piezometric head from east-to-west after a typical rainfall event. Elevation head is lower to the west, so rainfall must percolate further to reach the water table there. Lateral flow of water from east to west is another possible explanation for the east-to-west wave of pressure head increases that trigger movement at each borehole. Note the steep hydraulic gradient that must be present at the leading edge of the east-to-west wave of piezometric head rise.**

The time lag from hole to hole between peaks in pressure head are probably from some combination of differences in vertical distance traversed by downward percolating groundwater, groundwater flow down the west-sloping hydraulic gradient (Figure 36), and direct transmission of hydraulic pressure from higher head areas to the east to lower head regions to the west. Hydraulic pressure can also be transmitted by slide movement, however the same general pattern of east-to-west waves of head rise in response to rainfall events is observed even where there is no detectable movement.

Since fractured Astoria Formation dominates between all of the holes in the saturated part of the rock mass, it is unlikely that there are large differences in rock properties in the water table between holes. Lateral distance between boreholes divided by time lag between head peaks should therefore result in approximately constant rates (velocities), if lateral pressure transmission is dominant. Vertical flow paths in the vadose zone traverse similar amounts of marine terrace sand in all of the holes but progressively more Astoria Formation from east to west. If vertical percolation were the dominant process responsible for the time lags of head peaks and some percolation was through the intergranular pores, we would expect decreasing rates from LT-3p (vadose zone in terrace sand) to LT-1p (vadose zone dominated by Astoria Formation). If vertical percolation is mainly through the fracture system, and fracture density is more or less equal throughout the side mass, then vadose zone thickness divided by the time lag in each hole should yield a nearly constant velocity value for all.

Table 9 illustrates trial calculation of travel velocities assuming (1) that abrupt head rise is the result of rainfall percolating from the surface through the vadose zone distance estimated from the elevation head, and (2) that the time lag between head changes between drill holes is from lateral pressure transmission and/or water movement down the hydraulic gradient from east to west. The resolution of the time data is  $\pm$  one hour, so there is some difficulty in measuring a vertical rate for the LT-3p piezometer which responds in 1-2 hours to all rainfall events; this leads to large standard deviation for the mean vertical rate for LT-3p, so the slightly higher mean rate relative other cases is not very meaningful. One negative rate in Table 9 for vertical flow at the LT-3p borehole is at a peak

rainfall/head event that probably produced a near artesian flow, so there was no vadose zone present when head began to decline, excluding this value, the mean for all vertical flow rates is  $0.6 \pm 0.4$  m/hr. The rate calculations assuming flow or pressure transmission between boreholes average about  $2.5 \pm 1.1$  m/hr, about four times as high as the same calculation assuming only vertical percolation through the vadose zone. The high variability of the velocities for either the vertical or lateral transmission assumption does not offer a compelling means of distinguishing whether there is any tendency toward a constant or systematic rate change. The absolute velocities are quite different for the lateral versus vertical velocity calculations, but it is not known what velocities are reasonable for a fractured rock mass like this. The exhaustive search of the literature needed to assess absolute velocities is beyond the scope of this interim report; hence, these calculations of head rate change are inconclusive with respect to potential velocities of groundwater infiltration or lateral flow/pressure transmission. More insight can be gained by looking in detail at hourly head rise in response to hourly rainfall at a site like borehole LT-3p where the water table is so close to the surface that there is little opportunity for lateral flow or lateral pressure transmittal to be a factor in head rise.

**Table 9. Trial calculations of rates of groundwater movement or hydraulic pressure transmission calculated assuming either lateral transmission (down the hydraulic gradient) between piezometers or vertical percolation of water through the vadose zone to the water table at each piezometer. Three rainfall events were tested; in each case the upward inflection of head change at the start of the event and the downward inflection at the peak head value were used, yielding six measurements of rate. The entry “no data” indicates that there was no sharp inflection in head that could be used to track the rainfall event. For all vertical percolation rates the mean =  $0.6 \pm 0.4$  m/hr; for all lateral rates mean head transmission rate =  $2.5 \pm 1.1$  m/hr.**

	Rainfall Event			Vertical			Down Dip		
	LT-1p	LT-3p	LT-2p	LT-1p Rate (m/hr)	LT-2p Rate (m/hr)	LT-3p Rate (m/hr)	LT-1p – 2p Rate (m/hr)	LT-2p – 3p Rate (m/hr)	LT-1p – 3p Rate (m/hr)
Positive (start)	no data	1/29/03 7:00 AM	1/29/03 10:00 PM	no data	0.6	1.3	no data	2.4	no data
Negative (peak)	2/2/03 3:00 AM	1/31/03 5:00 PM	2/1/03 6:00 AM	0.3	0.4	-0.2	2.4	2.8	2.6
Positive (start)	3/22/03 6:00 AM	3/21/03 12:00 AM	3/21/03 8:00 AM	0.5	0.9	1.4	2.3	4.6	2.9
Negative (peak)	3/23/03 8:00 PM	3/22/03 7:00 AM	3/23/03 2:00 AM	0.3	0.4	0.8	2.8	1.9	2.3
Positive (start)	1/29/04 11:00 PM	1/28/04 4:00 AM	1/28/04 12:00 PM	0.4	0.9	1.2	1.4	4.6	2.0
Negative (peak)	1/31/04 2:00 AM	1/29/04 6:00 AM	1/30/04 10:00 AM	0.3	0.2	0.3	3.1	1.3	2.0
<b>Mean</b>				<b>0.4</b>	<b>0.6</b>	<b>0.8</b>	<b>2.4</b>	<b>2.9</b>	<b>2.4</b>
<b>Standard Deviation</b>				<b>0.1</b>	<b>0.3</b>	<b>0.6</b>	<b>0.6</b>	<b>1.4</b>	<b>0.4</b>

At borehole LT-3p five short duration (< 24 hours) rainfall events were analyzed for hourly correlation of rainfall to head change. Each event had little rainfall before or after, no detectable slide movement, and easily recognized pressure head responses. If hourly rainfall onto the headwall of the slide (at the rain gauge) is compared hour by hour to the head rise in borehole LT-3p, this should give some insight into the likely amount of interconnected void space that is filled during any given event. The LT-3p borehole penetrates into the west side of the headwall graben fracture system, so most of the groundwater affecting head changes there is probably from precipitation into the graben and the graben

fracture system. Ignoring evaporation, evapotranspiration, and runoff, and, if we can speculate from the crude data of Table 9 that lateral groundwater flow, lateral pressure transmission or downward percolation rate is on the order of 0.6-2.5 m/hr, then most of the rainfall affecting the LT-3p piezometer will be stored in the graben within ~14-60 m of the borehole during short intense rainfall events of less than 24 hours. Given that piezometric head in this borehole responds to rainfall events in 2 hours or less from the start of the event, flow or rises of head that transmit pressure to the site are probably from within about 2-5 m of the hole. Ignoring surface runoff is justified since there is no surface flow of water out of the graben, local slope at the drill site is low and no surface flow has been observed there during heavy rains, although some flow within the forest soil is possible. Ignoring evaporation is probably not a great source of error, since the rainfall events that are examined are in the winter rainy season when relative humidity is close to 100 percent. Ignoring evapotranspiration by trees is a source of error, since there are a few trees at the LT-3p site, so this error combined with the other assumptions makes any groundwater infiltration estimate a maximum value. Figure 39 shows some typical correlations of head rise for five rainfall events using contemporaneous (hourly) rainfall at piezometer hole LT-3p. The data pairs of rainfall and head rise are adjusted by shifting the hourly head data back two hours, to approximately adjust for the time lag between onset of rain and head response at the LT-3p site. Linear regressions through each dataset are shown with correlation coefficients (Figure 39). The mean slope of the regression lines is 0.09 m of head rise for each mm of rainfall per hour, or 90 mm of head rise per millimeter of rainfall. If all rainfall is assumed to percolate into the water table for these January-March 2003 data, then this corresponds to a crude estimate of maximum interconnected void space occupied by the water of about 1.1 percent of the rock volume at the LT-3p site. Porosity of the terrace sand was not measured but should be on the order of ~40 percent, consisting of well connected voids, based on its physical character from hand sample analysis: fine- to medium-grained sand; mostly ~0.25 mm, excellent sorting, and lack of significant cementing minerals (e.g. see porosities of Pettijohn, 1957, p. 86). The mismatch of the porosity estimates inferred from the head and rainfall data relative to the estimated intergranular porosity can be explained, if ground water flow is dominated by well-connected fractures comprising about 1 percent of the bedrock. In other words, this is a dual porosity system, consisting of intergranular and fracture porosity with vadose percolation dominated by fracture flow. One caveat on this reasoning is the unknown amount of residual intergranular water that could be present in the rock matrix wetted from previous rainfall events. Wet but unsaturated rock would be more quickly saturated than dry rock.

A freshly exposed slide scarp ~120 m north of the LT-3p site in an identical structural position on the west side of the headwall graben (see right-hand portion of cover photo) has nearly all fractures inclined near vertical, trending north-south to N55°W, and spaced about ~0.15-0.45 m, averaging about 0.3 m. Most of the fractures in the outcrop were open with openings of 0.3 to 3.8 cm., averaging 0.3 cm. If it is assumed that fracture spacing at LT-3p averages 0.3 m with openings of 0.3 cm (0.003 m), then fracture porosity should be 1.1 percent, the same as inferred from the rainfall and head data.



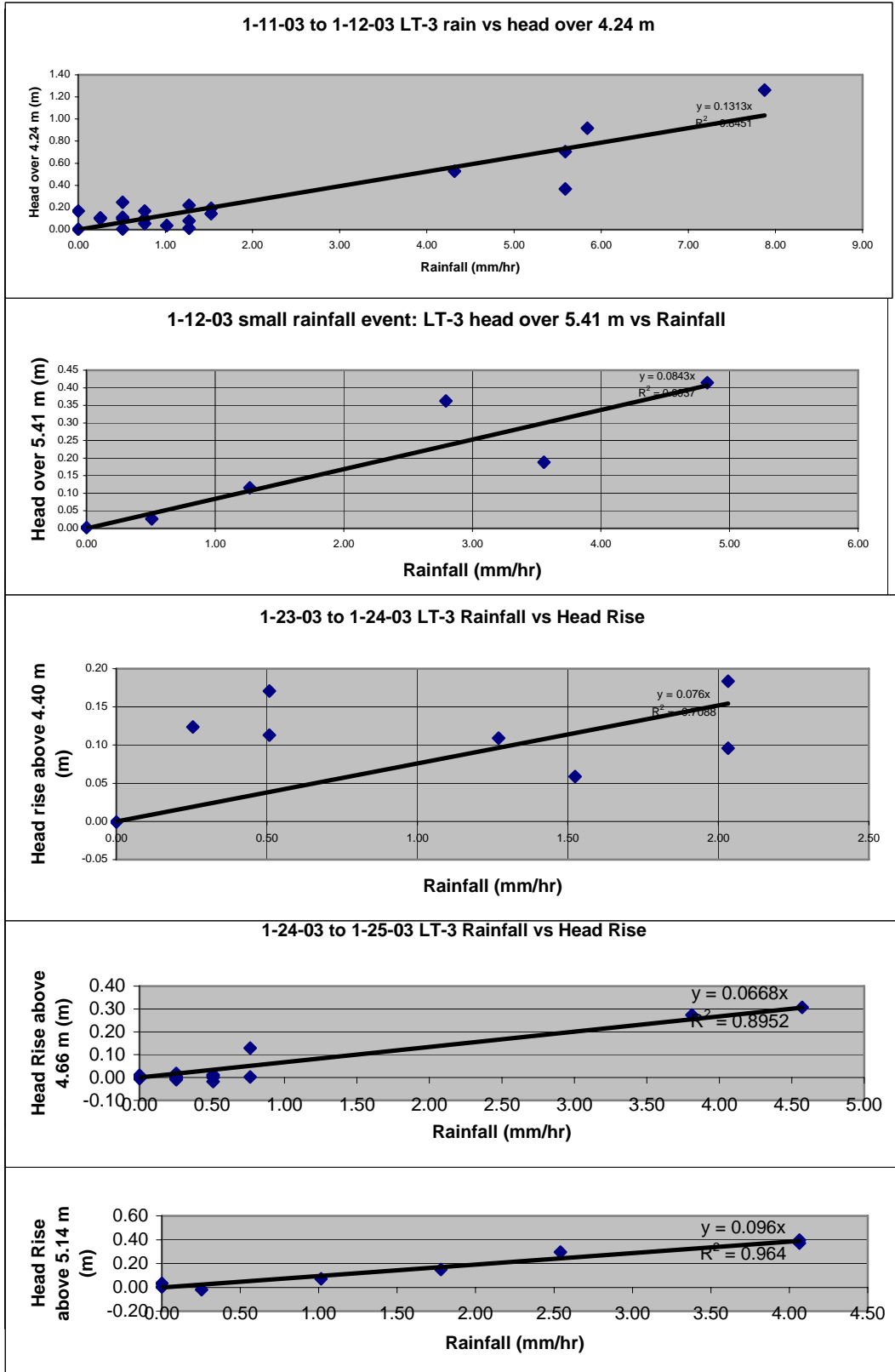


Figure 39. Positive correlation of hourly rainfall to same-hour pressure head rise for five 2003 rainfall events.

Whereas the smallest rainfall events do not produce obvious pressure head spikes in LT-2p and LT-1p, the largest rainfall event (Event 2, January-February, 2003) produced approximately equal head increases in all three piezometer holes. The duration of the increases was also approximately equal for all three holes. We conclude that the same processes are causing the head spikes in all three areas, probably vertical percolation of water in  $\sim 1$  percent fracture void space. The longer travel time through the vadose zone in the holes with deeper water table apparently “smears out” the high frequency signal of small, low intensity rainfall events. Small rainfall events have a harder time saturating longer flow paths through the vadose zone and lose a greater percentage of their water to local perched aquifers and to infiltration into the rock matrix, whereas large rainfall events saturate all of the flow paths and perched aquifers.

Additional insight into the role of fractures may be gleaned by comparing the amplitude of piezometric head spikes for large rainfall events in the boreholes before and after the occurrence of compression between boreholes LT-1p and LT-2p during the large movement of Event 2 (January- February 2003). The amplitude of the head change in LT-1p was subequal to that of LT2p and LT-3p during Event 2, but head change for large events decreased in LT-1p relative to the other two holes afterward (Figures 24-29). Fall off of each succeeding head spike in LT-1p after the Event 2 was quite slow compared to fall of the head during Event 2. Decreased head elevation and slow fall off of head after each spike may indicate more difficult water infiltration into and drainage out of the crack system owing to closure of fractures in the more compressed rock. Assuming that the  $\sim 10$  cm of compression between LT-1 and LT-2 (Figure 31) occurs from closure of the of a near-vertical fracture system between the two holes, then this amounts to a decrease in overall fracture voids by 0.2 % over the 50 m of distance separating the two boreholes. The same calculation for the  $\sim 20$  cm of extension between LT-2 and LT-3 (Figure 31) yields an increase of 0.6 % in the fracture voids. These numbers are consistent with field observations that, on the whole, the fracture system comprises about 1 % of the slide mass and can easily accommodate this amount of differential movement.

Persistently higher pressure head in the LT-2p hole may be the cause of faster movement at that location relative to LT-1 and LT-3 during Event 2. The reason for the higher pressure head at LT-2p and relatively high hydraulic gradient between LT-2p and LT-1p relative to LT-3p to LT-2p at all times of the year is not known. Possibilities are (1) poorer drainage of groundwater through fractures at this site because of its location in the center of a relatively coherent slide block (Figure 6); (2) an aquifer that is higher in elevation at this site; (3) depth of the slide plane relative to maximum possible elevation of the water table (i.e., the surface); and (4) some additional source of water. The rate of decline of water pressure at LT-2p after the major rainfall event of January-February 2003 (Event 2) was about the same in LT-1p, LT-2p, and LT-3p (Figure 26), so it is unlikely that there is a large difference in drainage efficiency or fracture porosity. A west-dipping sandstone bed of the Astoria Formation crosses the LT-2p and LT-1p boreholes near the elevation of the piezometric head for winter conditions (Figures 7 and 37) and could be an aquifer controlling background head at both sites. This same sandstone bed intersects the contact with the overlying marine terrace sand east of LT-2p (Figure 7) that (as previously explained) channels some perched water, offering another source of water to this potential aquifer. Astoria sandstone has relatively low permeability, but still higher than surrounding siltstone, so water

should be able to flow in the sandstone, given enough time. Since the sandstone is in contact with the perched aquifer at the marine terrace sand contact, there should be ample time for water to penetrate into the unit, effectively storing water. The sandstone is cut by a small-displacement fault before reaching the LT-1p site (Figure 7), but observations of the extension of this fault at the toe of the slide reveal increased fracture permeability around it, so there should be a good hydraulic connection across the small (~2 m) offset. Another possibility for higher head at site LT-2p is that a fault channels groundwater from bedrock below the slide plane. A fault is inferred near the LT-2p site in the geologic cross sections (Figure 7; Appendix A), but this fault is down the hydraulic gradient from the site and beneath the previously mentioned slide gouge that probably seals off water flow. It is also hard to reconcile the lower piezometric head below the slide plane at LT-2p, if a fault lies below (Figure 7) that is carrying large amounts of groundwater. The lower pressure head at LT-3p relative to LT-2p is probably caused in part by the shallow depth of the slide plane at site LT-3p, since any rise of water table to pressure head equivalent to the LT-2p site would cause artesian flow. The water table is so close to the surface at the LT-3p site that the ~1.5 m of topographic relief between the drill site and the graben to the east may promote eastward drainage of near-surface fractures during intense rainfall events. More efficient infiltration of water into the highly permeable terrace sand at the LT-3p site would also tend to keep water table somewhat lower. We conclude that the most likely reason for the higher pressure head at site LT-2p relative to site LT-3p is the larger depth of the slide plane at site LT-2p and better drainage of groundwater at the LT-3p site into intergranular pores of the marine terrace sand. The west-dipping Astoria Formation sandstone that intercepts site LT-1p deeper than at site LT-2p probably also has an influence on the head, if it is indeed an aquifer, but there is no data to test this hypothesis.

After a sudden rise of head in fractures from a rainfall event, pressure head at all of the drill sites decreases gradually, probably from infiltration into intergranular pores and lateral drainage through fractures that are not parallel to directions of equal piezometric head, but which is dominant? The sidewalls of the fractures in LT-3p are composed primarily of marine terrace sand with abundant intergranular pore space, while the sidewalls of the fractures in contact with the water table in the other two holes are composed of relatively impermeable Astoria Formation (Figure 37). If infiltration into intergranular pore spaces is an important factor controlling the rate of decrease in head, then borehole LT-3p should have the most rapid rate of decrease. Figures 24 and 26 illustrate that in general, head falls off in LT-3p at about the same rate as the other boreholes for the initial peak head on January 31, 2003 (Event 2). After that the fall off for large rainfall events is similar to that of LT-2p, but faster than at LT-1p (Figures 24 and 27-29). The previously mentioned compression at LT-1p (Figure 31), probably explains the slow fall off of piezometric head after Event 2. We conclude that, whereas infiltration into the rock matrix is undoubtedly occurring after each peak in the hydrostatic head, fracture flow probably continues to be the dominant process affecting the rate of decrease in head after each head peak or “spike.”

To summarize, rainfall and piezometer data are consistent with a dual porosity system of fractures and intergranular pores with both vadose infiltration of rain and lateral groundwater flow within the slide mass controlled principally by the fracture system. The rapid hydrostatic head changes in the slide mass at the LT-3p borehole in response to each rainfall event are consistent with downward percolating vadose water filling fractures faster than seepage into intergranular voids, even for the well sorted sand of the Pleistocene marine terrace deposits that occur at this borehole. Control of lateral drainage of groundwater through the fracture system is consistent with decline in water pressure after rainfall events at nearly the same rate as the increase due to vadose infiltration. In contrast, no such decline occurs in rock below the slide plane with little fracture permeability. Groundwater pressure below the slide gradually increases during the wet season, draining very slowly by intergranular flow and limited fracture flow. Elevation head is actually lower below the slide than within the slide in the fall and early winter, so the two are hydraulically isolated probably by the nearly impermeable slide plane gouge. We conclude that submersion forces due to saturation of intergranular pore space in the slide mass may be to some extent disconnected from lateral hydraulic forces in the steeply dipping fractures in this dual-porosity system (Figure 42). Head spikes at the piezometers in the slide immediately after rainfall events may therefore be good indications of head in fractures but not necessarily hydrostatic forces (submersion forces) related to saturation of the slide mass as a whole. Field observations suggest that fractures tend to be near vertical and sub-parallel to local slide block boundaries or to tectonic faulting mostly on northwest trends. Movement is initiated at threshold pressure heads above the slide plane of 7, 9.4, and 5 m at boreholes LT-1, LT-2, and LT-3, respectively. Movement abruptly accelerates when pressure head reaches 9.0-9.7, 12, and 6.5 m at sites LT-1, LT-2, and LT-3, respectively. In all cases head increases start at the easternmost borehole, LT-3 on the west side of the headwall graben and proceed progressively west to drill site LT-2 and then LT-1 over a period of 30 to 44 hours, taking the smallest time for the most intense rainfall event of January 31 to February 3, 2003, Event 2. Event 2 movement at borehole LT-2 was 10 cm less than at borehole to the west (LT-1) and 20 cm greater than the borehole to the east (LT-3), probably increasing fracture void space to the east by ~0.6 % of the rock mass and decreasing (compressing) void space in fractures to the west by 0.2 %. The more rapid movement at the LT-2p site may be caused by higher pressure head than the other two sites at all times of the year, albeit, elevation head is intermediate relative to the other two sites. Head peaks at site LT-1 in response to large rainfall events after Event 2 decreased in amplitude and took longer to decline after succeeding rainfall events, probably because of decreased permeability of the compressed fracture system at site LT-2. Movement at the LT-2 and LT-3 boreholes did not occur during a December 2003 piezometric head spike that rivaled values that caused the large, rapid movement in January-February, 2003, apparently correlating with lower overall (background) water pressure in the weeks before the event. Multiple sharp rises in head over an extended period of time should also increase partial saturation of rock above the water table leading to more rapid development of full saturation. Slide movement at sites LT-2 and LT-3 east of Highway 101 requires at least 84 mm of rain over a 48-hour interval, whereas only 64 mm of rain over 48 hours is required to initiate movement at the LT-1 site west of Highway 101. Rapid movement of the slide correlates with 48-hour rainfall of  $\geq 118$  mm and with rainfall  $\geq 717$  mm over 48.7 days; hence, the rain gauge alone can be used to predict start of slide movement and movement rapid enough to be dangerous to vehicular traffic.

**Data Correlation – Surface versus Subsurface Movement:** Since the west and east parts of the slide appear from the survey data to have moved at about the same rate, this is ostensibly in disagreement with the compression and extension inferred from the extensometer data (Figures 31 and 32). There is no obvious deflection of the inclinometer casings above the slide plane (Figures 20-22), so surface displacement should be similar to displacement on the slide plane. The re-survey data measures distance change between boreholes LT-3 and LT-1, not between these holes and borehole LT-2, since there are no steel stakes resurveyed near the LT-2 site. The extension between sites LT-1 and LT-3 from extensometer data is only ~11 cm during the observation period of the resurvey (Figure 32), well within the horizontal error in the survey measurements. Total westward movement of ~20 cm measured from the inclinometer/extensometer at LT-1 is in close agreement with the 22 cm of west movement measured in the same period by resurveying (Figure 32; Appendix D).

### **Erosion and Beach Sand Movement**

Bluff erosion data was collected using survey pins (Appendix F). Erosion was measured between December 9, 2002 and April 10, 2003. Measurements suggest that the sandstone and siltstone erode at different rates. Sixty-seven percent of the siltstone sites and twenty-two percent of the sandstone sites lost the 30-cm-long pins. Nineteen percent of the siltstone and twenty-two percent of the sandstone sites had no measurable erosion. The large scatter of erosion values does not allow an average bluff retreat to be calculated.

Landslide movement can affect the rate of erosion. Movement would increase the likelihood of mass wasting with the loss of blocks or slivers of slide debris during storm events. This may account for some of the lost monitoring pins.

Annual cyclic beach sand movement was measured with LIDAR and survey techniques (Appendix H). About 1.5 to 2 meters (5 to 7 feet) of sand moved off the beach between September 2002 and April 2003. At the toe of the slide about 1 meter of sand moved out during the same time period.

No correlation was recognized between erosion or beach sand movement and the ground movement measured with inclinometers and survey hubs. The erosion data are so sparse and hard to interpret that it is difficult to place much importance on this observation.

In the northern 85 percent of the north-south length of the slide, the westernmost part of the slide plane apparently dips eastward (Figure 11), so the toe of the slide forms essentially a buttress pushing east. The southern 15 percent of the slide has a nearly flat slide plane (Figure 11). Erosion of the toe in the northern 85 percent should therefore have a more profound effect on slide stability than equivalent erosion of the toe in the southern 15 percent.



## LANDSLIDE STABILITY EVALUATION

A slope stability evaluation of the landslide at the drilling transect for boreholes LT-1, LT-2, and LT-3 was performed by Landslide Technology (Landslide Technology, 2004) using data available in 2002 and spring of 2003, including: (1) borehole data; (2) depth of sliding and groundwater data from instrumentation; (3) geologic reconnaissance of the site; and (4) topographic map. The results of the stability analysis were used in evaluating potential slide treatment options, which are discussed in the section below entitled Remediation Option Analysis. Samuel R. Christie and Dr. Stephen E. Dickenson of Oregon State University reexamined the stability analysis of Landslide Technology (2004); their results are summarized in Appendix J and generally agree with the Landslide Technology analysis for the cross section through the boreholes. They obtained similar results for cross sections north and south of the boreholes.

The stability and remediation analysis from Landslide Technology (2004) are for convenience of the reader reproduced below unchanged from the original report, except for a quotation from an unpublished letter from Landslide Technology in response to review comments. The quotation is in regard to the effect on slide stability of water-filled fissures or cracks in the landslide. A discussion section has been added that integrates the analysis by Landslide Technology, a second analysis by Christie and Dickenson (Appendix J), and other observations of this paper.

### **Back Analysis (from Landslide Technology, 2004)**

The stability analyses were performed on Cross-Section A-A', Figure 40. This section was selected because it is near parallel to the direction of slide movement and passes through the three sets of instrumented borings. Analyses were performed using Spencer's Method in the computer program XSTABL. Soil parameters used for this study are discussed in more detail in the following sections.

The analyses were performed by back-calculating the required strength (angle of shearing resistance,  $\phi'$ ) along the shear zone for incipient failure conditions (i.e., for a factor of safety equal to 1.0). The improvements to the factor of safety (FS) were then checked for various treatment options using the back-calculated  $\phi_r'$ .

Shear Zone. The location of the shear zone is estimated based on the known depth of movement in inclinometers LT-1, LT-2 and LT-3, the location of cracks observed upslope from the instrumentation, interpreted topography, and observations from the test pit at the slide toe. The analyzed slip surface is shown in Figure 40.

Groundwater Levels. Groundwater levels used in the back analysis stability evaluation are based on piezometer measurements when a threshold level of 10.0 meters (32.8 feet) of head on the slide plane was reached in LT-2p. The depth of the groundwater measured below the ground surface at this time for LT-1p, LT-2p and LT-3p was 19.2 meters (Elev. 5.4 m), 8.6 meters (Elev. 15.7 m) and 0.7 meters (Elev. 23.3 m), respectively. This groundwater level was kept constant throughout the back analysis and is shown in Figure 40.

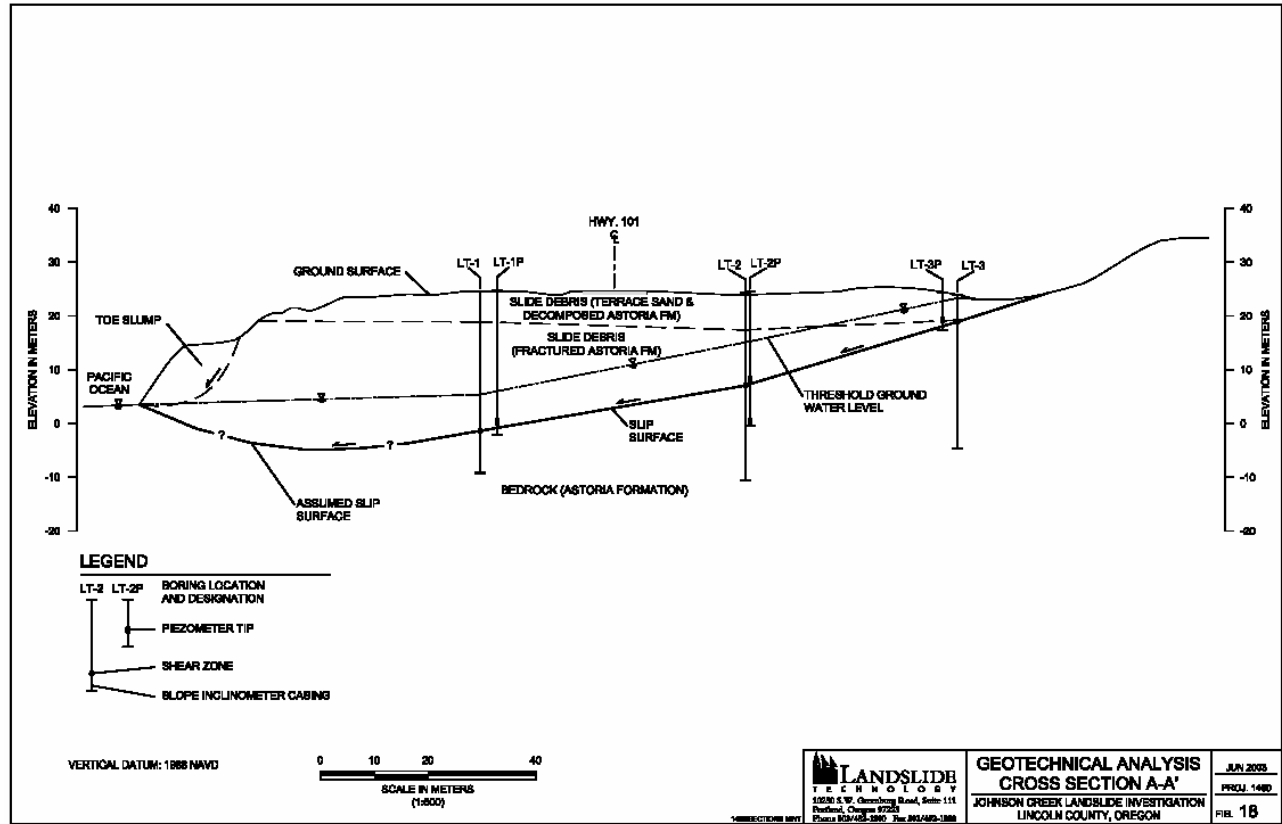


Figure 40. Generalized cross section used by Landslide Technology (2004) for stability analysis. Note that the locations of LT-3 and LT-3p are reversed from actual locations (i.e. Figure 31). This minor error should not materially affect the analysis. Location of the cross section is essentially the same as A-A' on Figure 6.

Material Parameters. Strength and density parameters of the soil and rock used in the analyses were estimated based on moisture content, material classification, and our experience with similar materials. Residual ring shear testing of the Astoria Formation material found in the shear zone resulted in an effective residual friction angle of  $\phi'_r = 13.1$  degrees. The strength and density parameters of the soil and rock used in the analysis are summarized in Table 10.

Table 10. Summary of material strength and density parameters.

Material	Unit Weight kN/m <sup>3</sup> (pcf)	Cohesion Intercept, c' Pa (psf)	Angle of Shearing Resistance, $\phi'$ (degrees)
Terrace Sand and Decomposed Astoria Formation	18.1 (115)	0	32
Astoria Formation	21.2 (135)	0	6.5*
Rock fill	18.1 (115)	0	42

\*Back calculated value from the geologic cross-section shown in Figure 40.

Analysis Results. The back-calculated residual strength ( $\phi_r'$ ) value for the slip surface analyzed in Cross Section A-A' (Figure 40) was determined to be 6.5 degrees. This single digit value is comparable with similar slides in the Astoria Formation and other large translational landslides in tuffaceous sediments and decomposed volcanic rocks, all of which have been investigated Landslide Technology. The difference between the back analyzed  $\phi_r'$  value and the value obtained from the ring shear testing (13.1 degrees) may be attributed to the fact that the sample tested may not be representative of the entire failure surface. The back-calculated  $\phi_r'$  value is an average value for the model.

### **Sensitivity Analysis**

A parametric investigation was performed to evaluate the sensitivity of landslide stability to the following parameters: precipitation, groundwater levels, erosion and beach sand level. Specific parameters were varied as discussed in the following sections.

Precipitation and Groundwater. An evaluation of the sensitivity of slide movement to precipitation and groundwater level was performed. As discussed in Section 5.3, a rainfall event which measures 55- to 60-mm of rainfall in a 24-hour period is likely to trigger landslide movement. Peak rainfall events cause groundwater to rise above threshold levels, further destabilizing the landslide. With the available piezometer data, groundwater levels for a “severe storm” were modeled by raising the highest measured levels in piezometers LT-1p, LT-2p and LT-3p by 1.5 meters (but not above the ground surface). Groundwater levels used for the theoretical “severe storm” analysis are elevation 9.0 meters, 19.0 meters and 24.1 meters at piezometer locations LT-1p, LT-2p and LT-3p, respectively. The results indicate that a rise in groundwater level of 1.5 meters above the back-analyzed level would decrease the FS of the slide mass by seven percent.

During the winter months groundwater levels appear to stay at reasonably stable levels, except during moderate to severe rainfall events. These “normal winter” levels were measured at average elevations of 5.0 meters, 14.6 meters and 21.4 meters in piezometers LT-1p, LT-2p and LT-3p, respectively. By varying only the groundwater level in the slide the results of the analysis indicate that decreasing the groundwater level to the theoretical “normal winter” results in an increase in the FS of the slide on the order of two percent higher than the back analysis.

Water-filled Cracks. Landslide Technology (2004) did not discuss the effect of water-filled cracks, but reviewers of the 2004 report did ask about this issue. Here is the response from Landslide Technology in their September 4, 2003 unpublished letter:

“Regarding the potential effect of water-filled tension cracks, Boring LT-3 is located near the head of the slide and any cracks downhill from LT-3, with or without water, would be modeled as an internal force in the stability analyses of the overall landslide and would have very minor effect on the friction angle (only the added weight of water in the tension crack). A water-filled crack uphill from LT-3 might have an effect on the back-calculated friction angle, and we tested this to see any difference. We placed an 18-foot high water filled crack east of LT-3, and the factor of safety against sliding increased slightly, and the resulting phi residual dropped from 6.5 to 6.45 degrees. We interpret that this difference is due to the removal of a small portion of the landslide’s driving wedge.”

Erosion and Beach Sand Movement. To evaluate the effect of ocean surf on the stability of the slide, both erosion of the cliff face at the toe of the slide and the seasonal deposition and removal of sand due to surf action were analyzed.

To evaluate the sensitivity of the slide to erosion of the bluff at the beach, stability analyses were performed and compared to the back-analysis results. The models were developed by offsetting the entire face of the bluff (up to an approximate elevation of 14.6 meters) 0.3 meters (1 foot), 1.5 meters (5 feet), and 3.0 meters (10 feet) to the east, respectively (Figure 42). To isolate the effect of the erosion, the geometry of the shear zone at the toe remained unchanged from the back analysis. To keep the groundwater conditions constant through the analyses, groundwater levels for the 3.0-meter erosion study were used. The only difference between this groundwater level and that used in the back analysis is a slight lowering of the water level west of LT-1P due to a change in the inflection point of the groundwater surface at the beach as a result of the changing location of the cliff face.

An additional study was performed to isolate and evaluate the effect of seasonal deposition and removal of sand from the beach relative to the stability of the slide. The model for this analysis consisted of adding approximately one meter of sand to the beach area, which isolated the effect of the sand by limiting variations to the model (i.e., the failure surface). For this analysis the groundwater level remained unchanged from the back analysis model. The geometry of the shear zone was modified only by extending the toe outward to the new ground surface.

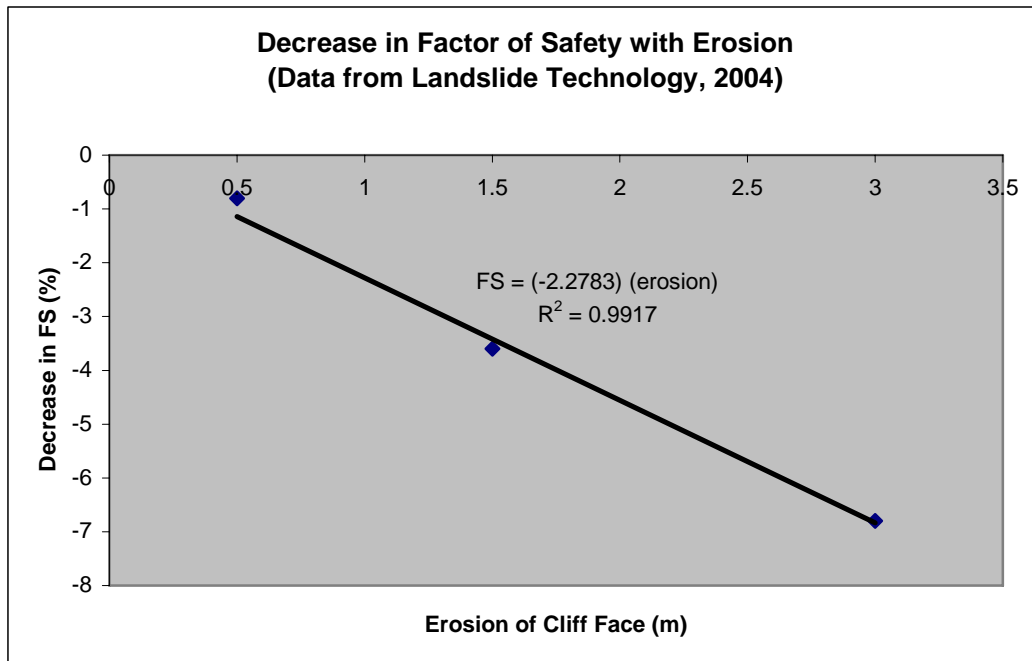


**Figure 41. Decrease of factor of safety at the Johnson Creek Landslide from erosion of the slide toe (sea cliff). Calculations for the three points were done by Landslide Technology (2004), but the present authors produced this figure to illustrate the linear relationship.**

Summary of Sensitivity Analysis. A parametric study has been performed to evaluate the sensitivity of the slide to three major parameters: (1) precipitation and groundwater, (2) erosion, and (3) the seasonal deposition and removal of sand on the beach. The back analysis model was used as the reference, and for each parameter incremental changes were made to determine the resulting percent change in FS. A summary of the analyses is provided in Table 11 below.

**Table 11. Summary of Sensitivity Analyses.**

<b>Parameter</b>	<b>Change in FS From Back-Analysis (- Decrease / + Increase)</b>
<b>Groundwater</b>	
“Normal” 2003 winter level	+2.0 %
“Severe Storm”	- 7.2 %
<b>Erosion of cliff face</b>	
0.5 meters (1 foot) of erosion	- 0.8 %
1.5 meters (5 feet) of erosion	- 3.6 %
3.0 meters (10 feet) of erosion	- 6.8 %
<b>Seasonal deposition/removal of sand</b>	
1.0 meter (3 feet) removal	- 0.3 %
1.0 meter (3 feet) deposition	+ 0.3 %

## CONCEPTUAL REMEDIATION OPTIONS

Landslide Technology (2004) evaluated several remedial options to increase landslide stability and minimize ground movement affecting the roadway; for convenience, their analysis is reproduced below. These options include (1) unloading near the headscarp, (2) toe buttress, (3) horizontal drains, (4) tied-back shear pile wall, and (5) maintenance. Each remediation option was designed to improve the factor of safety by at least 10 percent (FS=1.10) during the “severe storm” event.

A brief discussion of each option is presented, along with advantages and disadvantages. The cost estimate for each option is based on general and specialized construction costs, plus a 25 percent contingency to provide for the uncertainties of conceptual level design. The cost estimates do not include costs for environmental issues (e.g. permitting), final design, preparation of plans and specifications, contractor procurement, or construction control.

The northern and southern limits were estimated based on topographic interpretations and headscarp cracks observed in the highway and along the approximate northern and southern limits of the slide area (Figure 2). For the purpose of estimating costs of the treatment options, the slide is assumed to be 360 meters (1180 feet) north-south along the beach.



### **Option 1 – Unload Upper Slide**

This option entails unloading the head of the slide by excavating material east of the highway, and installing two French drains along the east side of the excavation. The excavation would extend approximately 160 meters (525 feet) north from the access road crossing the headscarp. The approximate limits of the excavation are shown on Figure 42. The elevation of the excavation floor would be approximately 18 meters (59 feet) (Figure 43).

French drains would minimize ponding during and after construction. A connector drain would be constructed to tie the two drains together at the southern end of the excavation, and a drainline would outlet into the drainage swale south of the slide and east of the highway, as shown on Figure 42.

This option provides a theoretical improvement in the factor of safety of 20 percent using back-analyzed groundwater levels, and a 12 percent improvement using the “severe storm” event.

#### Advantages:

- Relatively low construction cost
- No environmental impact to the beach area
- Good access for construction
- Simple construction techniques
- Minor long-term maintenance required
- Highway alignment not affected

#### Disadvantages:

- Provides no protection against continued toe erosion, which could eventually reactivate slide movement even with unloading implemented
- Short-term environmental impacts
- Requires disposal of excavated material
- Relocation of utilities
- Potential ponding in the excavation area

Conceptual Construction Cost: \$0.9 million

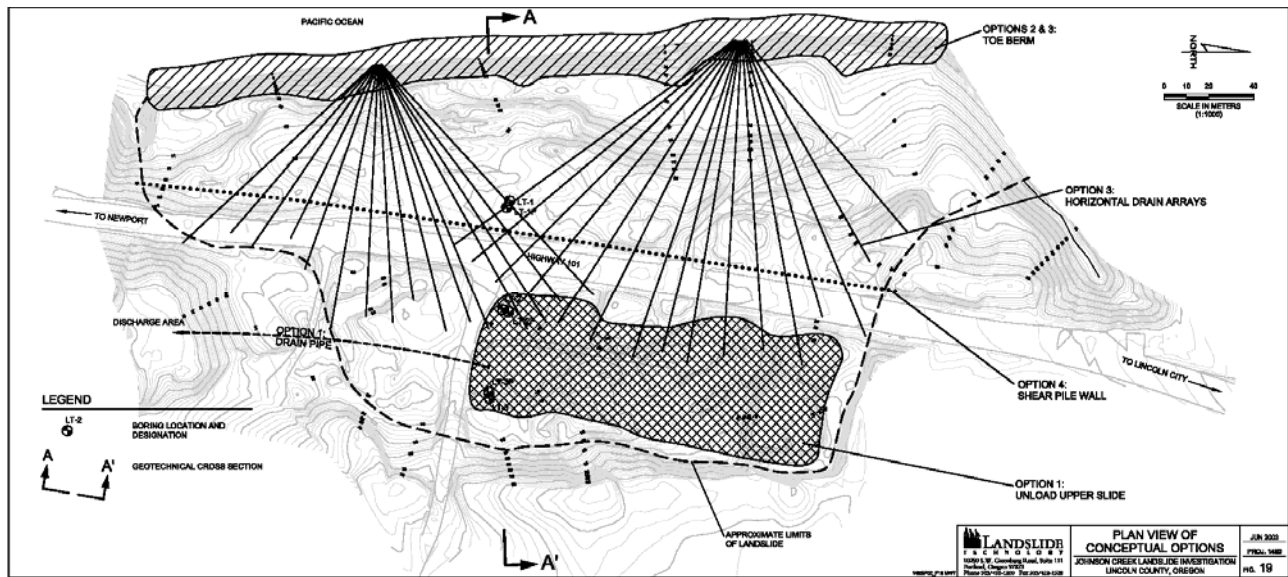


Figure 42. All remediation alternatives summarized by Landslide Technology (2003).

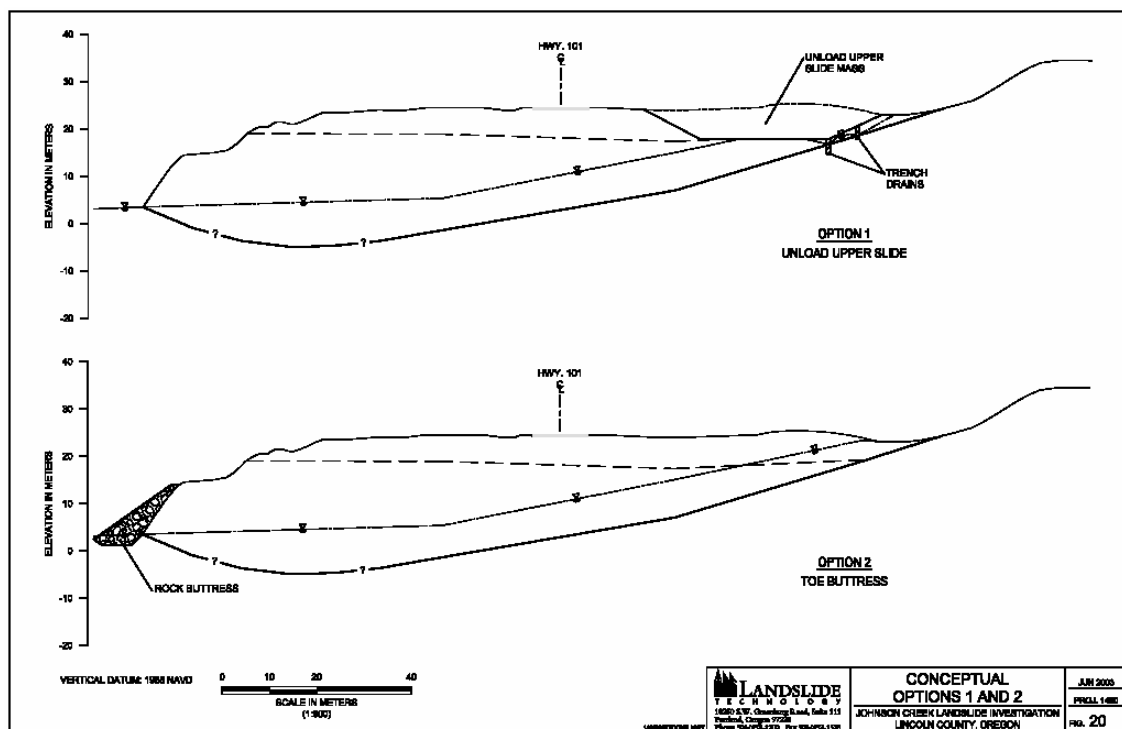


Figure 43. Remediation by unloading the head of the slide and buttressing the slide (taken from Landslide Technology, 2003).

## **Option 2 – Toe Buttress**

This option would involve building a buttress on the beach along the toe of the slide as shown in Figures 42 and 43. The buttress would consist of rockfill with a key extending approximately 2 meters (6 feet) below the beach, and riprap facing for erosion protection. The buttress would be 11 meters high (36 feet), extend approximately 8 meters (26 feet) onto the beach from the bluff, and have a 1V:1.5H slope face with the level top extending approximately 2 meters (6 feet) out from the existing slope face.

Construction would consist of excavating the key trench in sections, placing a geotextile fabric and then rockfill materials in lifts. The construction of the key trench would occur in 15-meter (50-foot) sections to prevent slide instability during construction. Once the length of key was fully constructed, rockfill and riprap would be placed in lifts along the length of the slide to the finished height.

This option provides a theoretical improvement in the factor of safety of 19 percent using back-analyzed groundwater levels, and a 12 percent improvement using the “severe storm” event.

### Advantages:

- High degree of confidence in stability improvement
- Relatively low construction cost
- Limits rate of bluff erosion
- Simple construction techniques
- Minimal long-term maintenance required
- Highway alignment not affected

### Disadvantages:

- High environmental impact (construction on beach)
- Limited access to site

Conceptual Construction Cost: \$1.1 million

### **Option 3 – Horizontal Drains**

This option would consist of installing horizontal drains through the slide mass from the toe of the slope (Figures 42 and 44). The drains would consist of slotted PVC pipe installed laterally into the slope face with a specialized drill rig. The horizontal drains would attempt to reduce the groundwater level during normal conditions and prevent the buildup of groundwater pressure during extreme rainstorm events.

Based on the stability analyses, improvement in the FS from horizontal drains is about 1% during the “severe storm” event. Also, the rotational failures at the toe of the larger slide are likely to shear the horizontal drains rendering them less effective or inoperable, which could also worsen the stability of the rotational failures.

Other options would be necessary to provide additional stability to the overall slide, such as a toe buttress. A riprap toe buttress could minimize erosion of the bluff and could provide stability to the rotational toe failures.

Based on the 1% improvement in FS during the “severe storm” and the potential for rotational failures at the slide toe, this option is not recommended for the Johnson Creek Landslide. Nevertheless, to provide comparison to other options, a conceptual design might include two drain arrays as shown in Figure 42. The cost estimate includes a total of 36 horizontal drains in two arrays for a total constructed length of 4270 meters (14,000 feet).

#### Advantages:

- Relatively low construction cost
- Simple construction techniques
- Highway alignment not affected
- Low long-term environmental impact
- Minor long-term maintenance

#### Disadvantages

- Stability improvement is low
- Limited design life of the drains with erosion and slide movement
- Limited access to site

Conceptual Construction Cost: \$0.5 million

### Option 4 – Tied-Back Shear Pile Wall

This option consists of constructing a row of large diameter, heavily reinforced concrete piles with tieback anchors to resist slide movement, installed just west of the highway as shown in Figures 42 and 44. Conceptual design consists of a 342-meter-long (1122-foot) wall of 1.4-meter (4 feet) diameter and 36 meter (120 feet) deep piles with a spacing of 3.0 meters (10 feet). A continuous, structural capping beam would be constructed at the top of the shear piles. Two rows of tiebacks would be installed through the capping beam (Figure 44). The tiebacks would decrease pile deflection and movements, and would result in less passive contact pressures in the sandstone below the shear zone. The wall and anchors could be covered and the site restored to a natural condition. This conceptual design provides a factor of safety of 1.3 during the “severe storm” event.

#### Advantages:

- High degree of confidence in stability improvement
- Low environmental impact (no construction on beach)
- Minimal long-term maintenance
- Highway alignment not affected

#### Disadvantages:

- Expensive
- Specialized construction technique
- Construction could impact highway traffic
- Lower slide area may continue to move due to continued bluff erosion

Conceptual Construction Cost: \$11 to 14 million

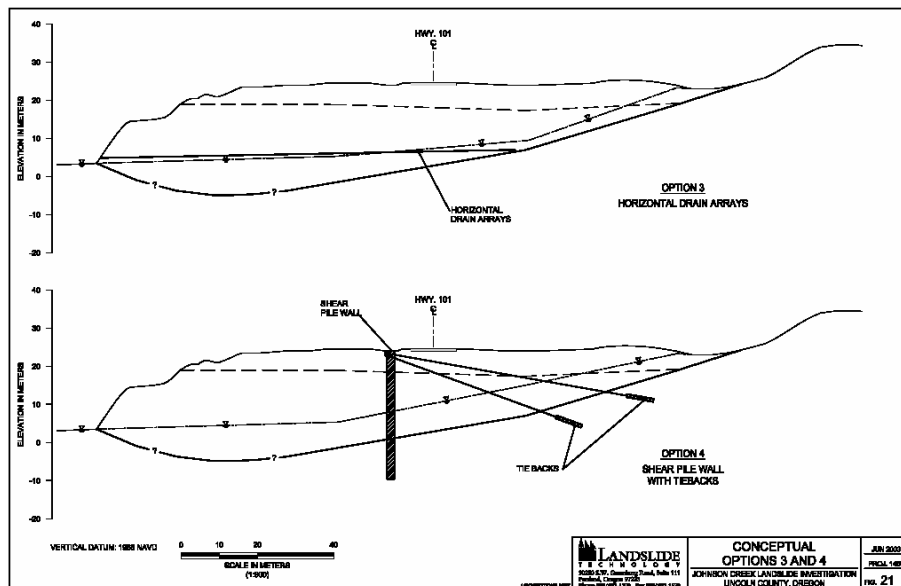


**Figure 44. Remediation by horizontal drains and shear pile wall with tiebacks (taken from Landslide Technology, 2003).**



### Option 5 – Road Maintenance

This option would consist of continued maintenance of the road. This option requires that the slide area continue to be inspected on a weekly basis and a daily basis during large storm events, and then quickly repaired when significant movements occur. ODOT records indicate that yearly costs for maintenance have been approximately \$15,000 per year prior to the late 1970s, and \$20,000 per year more recently.

#### Advantages:

- Inexpensive
- Low environmental impact

#### Disadvantages

- No effective stabilization
- Landslide will continue to move
- Continued risk to property and life safety
- Requires continual inspection and emergency repair as necessary

Cost: \$20,000 a year for basic maintenance (~\$400,000 for 20 years)

### Summary of Remediation Options

Remediation options that were evaluated for Johnson Creek Landslide include unloading, buttressing, draining, a tied-back shear pile wall, and maintenance. A summary of the construction options is provided in Table 12.

**Table 12. Remediation option evaluation.**

	Remediation Option				
	1 Unload	2 Buttress	3 Horizontal Drains	4 Tied-Back Shear Pile Wall	5 Maintain
Effectiveness	Moderate	High	Low	High	Low
Constructibility	Good	Good	Moderate	Difficult	n.a.
Engineering	Simple	Moderate	Moderate	Difficult	Simple
Environmental Long-Term Impact	Low	High	Low	Low	Low
Maintenance Long-Term	Low	Low	Moderate	Low	High
Construction Costs (\$ Million)	0.9	1.1	0.5	11–14	0.4 (20 yrs)

Unloading, buttressing and a tied-back shear pile wall are effective methods to remediate this landslide. Considering the large size of this landslide, unloading and buttressing are relatively low cost options. With stabilization and cost consideration, buttressing would be a preferential option; however, it has a significant environmental impact. A shear pile wall is extremely expensive primarily due to the depth of sliding. Draining groundwater from the landslide through horizontal drains would be ineffective. Groundwater levels within the slide mass are relatively low, and high groundwater levels following precipitation events rapidly drop or naturally drain from the fractured slide mass. Based on the conceptual costs for the construction of these remediation options, annual maintenance becomes a reasonable option. [*This is the end of the analysis by Landslide Technology (2004)*]

### **Discussion of Stability Analysis**

Buttressing is probably the most cost-effective remediation option, given the difficulty of placing horizontal drains and the added benefit of stopping erosion at the toe. Erosion left unchecked can by itself cause continued slide movement. It may be possible to buttress only the southern third of the slide where movement is largest and repair cost is highest.

Landslide Technology (2004) did not specifically evaluate pumped water wells as a remediation option. They discount drainage options in general because of (1) the calculated ~1 percent increase in factor safety that could be gained from horizontal drains, and (2) potential rupture of horizontal drains by rotation at the slide toe. The 1 percent increase in factor safety by horizontal drains was the result of lowering the normal winter water table by only about 3 feet, a value determined by limitations in the angle of the drains needed to maintain gravity flow. Near-vertical wells would get around both the drain angle and toe rupture problems. Christie and Dickenson (Appendix J) recommend maintaining a normal winter water table level, thereby eliminating the 9 percent decrease in factor safety caused by severe winter storms. A water well dewatering system may be able to achieve this, but thorough hydraulic testing of the slide would be necessary to evaluate the efficiency and design of such a system.

Disadvantages of wells are cost of electricity to run pumps, cost of hydraulic testing, cost of water discharge pipes, permitting issues for discharge of water, and cost of maintenance. Electricity use and pump maintenance could be minimized if wells were pumped only during the most intense rainfall events. If the slide continues to move after the well system is installed, wells could be damaged, leading to possible pump failure. This problem can be ameliorated by careful placement of the pumps above the slide plane and construction with large enough well diameter to prevent pump damage from small deformations of the borehole. Judging by how rapidly head peaks decline after a rainfall event, the fracture system may be relatively well connected, which might increase well efficiency and spacing, thereby decreasing cost. Nevertheless, dewatering systems must always overcome significant uncertainties in the hydrologic and geologic conditions that may be understood only after the system is installed and monitored.

The analysis of Christie and Dickenson (Appendix J) found that even a single water-filled crack at the toe of the slide could profoundly lower slide stability. We conclude that dewatering wells or drains should also target the toe of the slide, if possible. Well placement, inclination and design throughout the slide should be adjusted to maximize interception of as many high-angle fractures as possible, since rapid head changes are probably the result of infiltration into fractures.

## DISCUSSION

The Johnson Creek Landslide is a large translational slide with a slide plane that decreases in dip toward the west, reaching a near zero dip at the southwestern toe of the slide and an eastward dip in the central and probably the northern toe of the slide. Bedding along the entire toe of the slide is back-tilted to the east in a passive wedge. The slide plane follows weak siltstone units in the Astoria Formation and is coated in soft malleable clayey silt that is probably a groundwater barrier isolating the fractured slide mass from the nearly impermeable Astoria Formation below. The lower elevation head of the rock below the slide plane relative to the slide mass above demonstrates the lack of hydraulic communication across the slide plane. The slide may be pictured as a fractured bowl of rock with a weak, relatively impermeable liner isolating it from bedrock that itself has limited permeability to groundwater flow. Nevertheless, the bedrock below appears to gradually build up water pressure rather than draining away groundwater after each rainfall event as occurs within the slide itself; hence, it is possible that in an unusually wet year water pressure below the slide could build up enough in April or May to decrease the factor of safety. This might be manifested as slide movement at somewhat lower pressure head above the slide plane than would otherwise be expected. No such event has occurred in the two-year observation period.

Virtually every movement on this slide correlates with sharp rises in piezometric head after intense rainfall events; larger, more rapid movement correlates with rainfall of highest intensity and duration. Slow creeping movement of the slide begins west of Highway 101 at the LT-1 drill site after a minimum of 64 mm of rainfall during a 48-hour period. Equivalent movement east of Highway 101 at the LT-2 and LT-3 drill sites begins after a minimum of 84 mm of rainfall during a 48-hour period. Rapid movement of the slide correlates with 48-hour rainfall of  $\geq 118$  mm combined with rainfall  $\geq 717$  mm over 48.7 days; hence, the rain gauge data can be used to predict start of slide movement and potential for rapid movement that might pose a danger to vehicular traffic on Highway 101.

Movement of the slide at the LT-2 and LT-3 sites (east of Highway 101) in response to piezometric head increases in 2004 was less than for nearly identical head increases in 2003. In contrast, the LT-1 site west of Highway 101 moved in a fairly uniform way in response to all of the big rainfall events of 2003-2004. One difference between site LT-1 and the other two sites is the apparent compression developed between LT-1 and LT-2 during the large, rapid slide movement that occurred near the beginning of observations in January-February of 2003. After this large movement event, head increases from rainfall events also persist longer at site LT-1 relative to sites LT-2 and LT-3, so groundwater is not draining away as quickly at this site as east of the highway. Is it possible that the compression creates a lateral force that makes the western part of the slide more likely to move when hydraulic pressure is added? Is the extension east of LT-2 decreasing lateral forces on the slide, making it, at least temporarily somewhat more stable there? If lateral force from water in cracks is a major driving force, would this in some way make the slide more sensitive to small differences in compression and extension? Does the slower decay of elevated head at site LT-1 allow more time for penetration of groundwater into intergranular pores of rock bounding the fracture system? Does this greater saturation

of the matrix increase buoyant forces at LT-1 promoting more responsive movement there than at the other sites? Do water-filled cracks at the toe of the slide create larger movement there as suggested by the analysis of Christie and Dickenson (Appendix J)? Could these movements at the toe decrease buttressing forces, initiating and then prolonging movement at LT-1 to the east? Whatever the cause, it is clear that at present less rainfall is needed to trigger movement at the LT-1 site than at the sites east of Highway 101.

Based on resurvey of steel stakes and on extensometer data for the January-February 2003 movement (Event 2), rapid movements of tens of centimeters affect the slide unequally in different parts of the slide. The largest movement was in the southwestern part of the slide where the slide plane at the toe is flat rather than forming an east-inclined buttress like it does to the north. During this rapid movement some internal blocks moved faster than others, creating zones of compression, extension, and translational (lateral) motion. The zones of compression and extension complicate factor of safety calculations by creating internal forces that may be transient as the slide adjusts through time.

Based on inclinometer data and on monitoring of marker nails during the March 2003 movement event (Event 3) at localities around the slide perimeter, slow creeping movements of a centimeter or two appear to affect the entire slide more or less equally, in sharp contrast to the fast movement of January-February 2003. Movement during March 2003 was concentrated at the slide plane and slide perimeter with insignificant differential movement between the inclinometer holes in interior blocks. Why does creeping movement not produce differential movement within the slide as occurs during rapid, larger movement events? Are the lateral connections within the slide so much stronger than lateral connections at the slide perimeter that the buttressing effect of the slide toe on the north relative to the south is overcome? Would a 3-D numerical simulation of the slide forces resolve this issue?

The slow creeping motions are a manageable maintenance issue for Highway 101, whereas the rapid differential motions require more expensive maintenance and pose a significant hazard to vehicular traffic. Remediation of rare rapid movements should therefore be the highest priority.

The pressure head difference between rapid and slow creeping movement is 7 m versus ~9.0-9.7 m (difference of 1.3-2 m) for site LT-1, 9.4 m versus ~12 m (difference of 2.6 m) for site LT-2, and ~5.0 versus ~6.5 m (difference of 1.5 m) for site LT-3; hence, lowering pressure head 1.5-2.6 m should eliminate rapid movements. Since these rapid movements only appear to affect the slide in the central and southern part, lowering of the head by ~3 m in this portion of the slide should be adequate to eliminate the rapid movement events.

The stability analysis by Landslide Technology (2004) identified that piezometric head peaks caused movement and are good measurements of the submersion forces acting on the landslide. Rapid increases in piezometric head following rainfall events at this slide are consistent with vertical percolation of groundwater to a water table that fills a system of cracks comprising about 1% of the slide mass. These rapid increases in head are not consistent with complete groundwater saturation of intergranular pore spaces of the sedimentary rock in the fracture walls, even where the walls consist of well sorted, loosely consolidated Pleistocene marine terrace sand. The 90 mm of head rise per millimeter of rainfall observed at piezometer LT-3p is simply too large to allow for saturation of intergranular pore spaces, unless they are already nearly saturated with water. The physical situation

that must pertain immediately after a rainstorm is a mass of fractures filled with water lying against rock pore spaces filled at least partially with air (Figure 45). Presumably at some depth in this system of fractures the water-filled cracks lie against rock with water-saturated intergranular pore spaces or rock with only a thin envelope of partially saturated pores surrounding saturated rock. Some insight into the amount of piezometric head that might represent the saturated intergranular pores can be gleaned from the observation that minimum background pressure heads of ~6.5 m, 9.2 m, and 4.5 m must be present at LT-1p, LT-2p, and LT-3p, respectively, before the rapid pressure head peaks can cause movement. Are these background head values representative of minimum submersion forces that must be present before movement can occur? Likewise, large, rapid movement of the slide appears to require not only intense rainfall over ~48 hours but also an intense rainfall event about six weeks prior to the fast movement (Figure 30). Is this the time needed for thorough saturation of intergranular void space in these rocks? Given that mean vertical fracture spacing in the slide (based on outcrop data) is on the order of 0.3 m, this would imply lateral flow rates of only ~4 mm/day through intergranular pathways. Such low flow rates are probably not unreasonable in the relatively impermeable Astoria Formation that composes the walls of most fractures below water table in this slide (Figure 37).

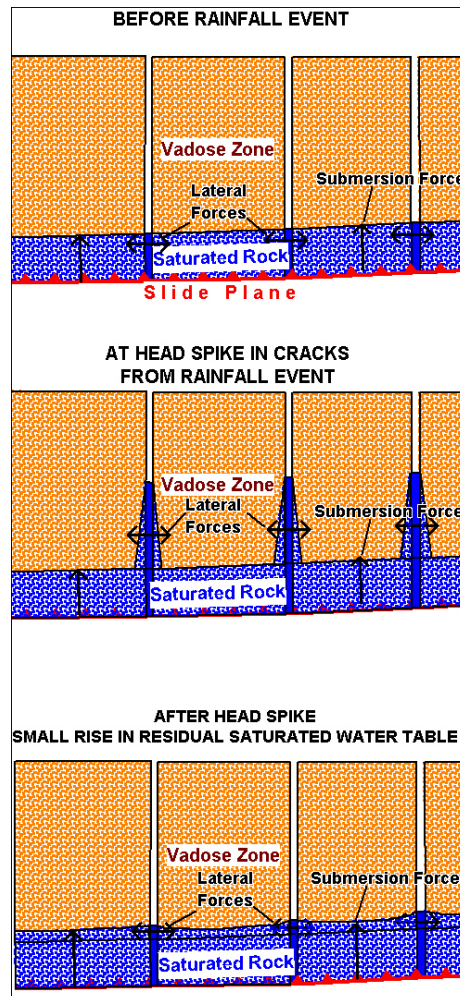


**Figure 45. Schematic illustration of probable water level changes in the landslide fracture system before, at, and after a sharp rise in pressure head from a rainfall event.**

Higher pressure head above the slide plane at the LT-2p site relative to the LT-3p site is best explained by the shallow depth of the slide plane at site LT-3p relative to site LT-2p (i.e. the head elevation cannot exceed the surface of the earth) and possibly by greater drainage into the highly permeable terrace sand at site LT-3p. While lateral forces from rapidly filling fractures may be as high at the LT-2p site as the other two drill sites, submersion forces from background levels of hydraulic pressure in Astoria sandstone aquifer may be higher at site LT-2p relative to the other two drill sites. These higher submersion forces may contribute to faster movement at this site during high rainfall, high displacement events. While pressure head is lower at LT-1p than at the LT-2p site, the same Astoria sandstone bed appears to be near the top of the water table there. Does this sandstone bed act as an aquifer and exert some control over head and efficiency of submersion forces at both sites?

These observations bring into question whether standard limit equilibrium stability analyses typically used on these types of slides accurately depict the real forces operating upon them. If they do not, what is the significance of the back-calculated  $\phi$  values derived from these analyses? Are submersion forces overstated? Are lateral forces from the weight of water in the landslide cracks understated? Standard limit equilibrium software is not able to simulate the forces from multiple water-filled cracks. What experiment would provide answers to these questions and what are the implications for remediation? We do not know all of the answers, but it seems obvious that drainage of the fracture system is a key means of stopping or slowing slide movement. We do not question that standard limit equilibrium methods provide a useful means of estimating relative feasibility of remediation options, but it is clear that the methods need refinement.

How efficient are horizontal drains and dewatering wells likely to be? Fractures exposed on the inner scarp of the northeast headwall graben and at the toe of the slide appear to be open, well connected over tens of meters, near vertical, and sub-parallel to slide block boundaries. If the side mass is hydraulically isolated by the impermeable slide plane, then the only source of water is direct rainfall into these well-connected fractures and lateral drainage within the slide down the hydraulic gradient. Piezometric head spikes in response to rainfall events appear to decay nearly as rapidly as they increase, consistent with drainage through a well-connected system of fractures. Any horizontal drain system would be drilled east from the toe of the slide. Numerous fractures probably strike perpendicular to the westerly movement vector at the drilling transect, since tens of centimeters of differential movement observed between the boreholes during rapid movements creates compression and extension that is most likely accommodated by such fractures. Since only about 2-3 meters of piezometric head separates slow creeping movement from fast movement (Table 6), modest drainage of the fractures could greatly decrease maintenance costs. Limiting such drilling to the central and southern part of the slide would be a cost-effective remediation option to explore. Targeting large fracture systems near the toe is particularly critical (see the analysis water-filled cracks in Appendix J).

The main difficulty with horizontal drains is the necessity to cross the back-tilted slide block at the toe. If the drains fail and then drain into the rotated block, that block could have accelerated movement, possibly destabilizing upslope areas. The stability analysis in Appendix J graphically demonstrates how



even one water-filled fracture at the toe can greatly decrease the factor of safety. Are there innovative drain designs that could overcome this problem?

The Landslide Technology (2004) sensitivity analysis clearly demonstrates that erosion of the landslide toe can significantly decrease the factor of safety. The more responsive movement of the LT-1 site west of Highway 101 to piezometric head increases could also be caused by erosion, progressively unloading the toe of the slide and thus setting up the conditions for movement. Error in estimation of erosion using marker pins or 1997, 1998, and 2002 LIDAR topographic data was too high to estimate erosion, so evaluation of erosion forcing was not possible. Mean erosion rates for Astoria Formation in the Beverly Beach littoral cell are on the order of -0.15 m/year (-0.5 ft/yr) and landslide masses of Astoria and Nye Mudstone fully exposed to winter wave action at Newport can erode at rates of  $\sim$ 0.9 m/yr (-3 ft/yr) (Priest and Allan, 2004), so it is likely that overall rates lie somewhere between these values. We would therefore expect that, averaged over the whole length of the slide toe, no more than about 1.8 m of the bluff face has been eroded over the last 2 years. Using the rate of decrease in the factor of safety (FOS) from erosion listed by Landslide Technology (2004) (Figure 41), the decrease in FOS during the observation period should be  $\leq 4\%$  at the latitude of the drilling transect. This is a significant decrease, so it deserves further study and serious consideration when weighing remediation alternatives.

## RECOMMENDATIONS

The Johnson Creek Landslide is subject to dangerous rapid movements that can offset Highway 101 by tens of centimeters lateral and vertical in the southern 60 percent of the slide. These movements can occur over a period of only a few hours or days, posing serious risk to vehicular traffic and significant highway repair costs. One of these events occurred during the 2 years of observation in this investigation and caused much of the repair cost in this period. Five other movement events were slow creeping movements of  $<4$  centimeters lateral ( $<1$  cm vertical)<sup>3</sup> that caused only minor damage to the highway where it crosses the slide perimeter. The rapid movements and slow, creeping movements correlate with rainfall events that trigger rapid increases in piezometric head; hence, both types of movement can probably be eliminated or greatly reduced by dewatering. While there would be significant cost for this remediation, avoidance of road maintenance costs, vehicle accidents and associated liability lawsuits would probably justify the expense.

A significant amount of groundwater in the slide is apparently from direct rainfall percolating into well-connected steeply dipping fractures comprising only about 1 percent of the slide. Dewatering of this small amount of water from well-connected fractures should be efficient from either pumped wells or horizontal drains. A cost estimate for installation of wells was not given by Landslide Technology (2004) but should be included in the final report. Horizontal drains are vulnerable to rupture by the rotated block at the slide toe, but, if this problem can be overcome through innovative design, this option would be cost effective. Using the array of horizontal drains recommended by Landslide Technology

---

<sup>3</sup> Vertical displacement estimated from a slide dip of  $\sim 15^\circ$  inferred from arctangent of vertical and horizontal offset of the Old Coast Highway at the southern slide margin east of Highway 101.

(2004) as an approximate indicator of cost, dewatering of the whole slide would cost ~\$500,000. Minimum costs (ignoring mobilization costs) for the southern 60 percent would be on the order of \$300,000, and the southern third ~\$167,000, equivalent, respectively, to ~15 and 8 years of road maintenance at the average of ~\$20,000 per year.

Ideally, one would do complete hydraulic testing of the slide, evaluating hydraulic parameters and at the same time testing water wells as a remediation alternative; however, estimated costs for such experiments are roughly the same as the array of horizontal drains covering 60 percent of the slide (~\$300,000).<sup>4</sup> A project of this kind could only be justified from a research perspective, since it would yield a wealth of useful data applicable to other translational landslides in sedimentary rock. Measurement of porosity and permeability of rocks and installation of additional inclinometers and piezometers, including innovative wireless piezometers below the slide plane, would be an important first step in such an analysis (see detailed recommendations in Appendix J). A cheaper option would be to install a series of water wells without hydrologic testing; then monitor effectiveness at slowing or stopping movement. Design of this array of wells would be a challenge without test data, but it is clear from the stability analysis of Appendix J that the toe of the slide should not be neglected when setting up the well array.

Buttressing the slide with basalt rip rap is higher in cost both in dollars and environmental impact than dewatering but is much less likely to fail. Buttressing has the added benefit of eliminating erosion that can by itself trigger further movement. The main environmental impacts are: (1) creating an unnatural feature at the shoreline; (2) causing loss of dry sand beach from scour and by fixing the shoreline in the face of rising sea level; and (3) cutting off sand supply from bluff erosion. There is little sand content in the current sea cliff (Appendix A), so loss of sand supply would be minimal. The other two impacts can only be mitigated by making the revetment as small as possible. The most cost effective and environmentally benign option would be to buttress only the southern 30 percent of the slide where the largest, most damaging movement has occurred and where a rip embayment focuses wave erosion. Based on the \$1.1 million cost estimate by Landslide Technology (2004) to buttress the entire slide, minimum cost (ignoring mobilization costs and economies of scale) for 30 percent would be ~\$330,000, equivalent to about 16 years of road maintenance. There would still be some small road maintenance cost and periodic cost to maintain the structure itself. Deformation of Highway 101 would probably be concentrated at the northern margin of buttress as creeping movements and some larger movements proceeded in response to rainfall events. Whether these movements would be decreased by the southern buttress is unknown but certainly possible.

Remediation utilizing a tied-back shear pile wall or by unloading and draining the upper part of the slide would also be effective, according to the analysis of Landslide Technology (2004), but both are much higher in cost than dewatering or buttressing. These options do not compare well with just maintaining the road under current conditions.

---

<sup>4</sup> Cost estimate based on a proposal prepared by the senior author and submitted to ODOT Research last year. The proposal was not funded primarily due to high cost.

The analysis in this report is still incomplete without an accurate measure of wave erosion at the toe of the slide. Limit equilibrium analysis by Landslide Technology (2004) and in Appendix J illustrates that toe erosion is a highly significant factor. Erosion might well trigger movement, even if dewatering lowers water pressure effectively (see analysis of Appendix J and Landslide Technology, 2004). Erosion is probably fastest in the southern half of the slide where there is the least beach sand to break wave energy; hence, this is the area where remediation will be most cost effective. Ground-based LIDAR surveys should be completed annually or semiannually to accurately track erosion so this variable can be properly evaluated. Monitoring wave activity from offshore buoy data will allow empirical relationships to be established between erosion and wave strike that will allow erosion prediction in the future from the buoy data alone.

It may be that innovative erosion-control such as a dynamic revetment can offer a significant increase in the factor of safety at reasonable cost and with low environmental impact. A revetment composed of cobbles would also help to buttress the landslide, possibly increasing the factor of safety significantly. The final report should provide an evaluation of this option, incorporating the findings of current ODOT-supported research on dynamic revetments.

Until remediation is implemented, the current data stream of hourly rain gauge, piezometer, and extensometer data should be used to warn ODOT of impending slide movement. This would require maintaining the current instrumentation and installing telecommunications links to the two dataloggers. The USGS reportedly plans to install dial-up cellular phone links to these dataloggers at some point, so that will offer an opportunity to test the effectiveness of such a warning system. Costs to the State of Oregon will be minimal for the next few years while USGS is maintaining the instrumentation, limited to personnel time from ODOT. Costs would rise slightly if and when USGS ceases their maintenance. Possible protocols for such a system are summarized in Table 13. The extensometer data could be used alone but would be more accurate if used in conjunction with the other data sets, the certainty of the prediction going up the more threshold values that are exceeded. ODOT should keep in mind that such warnings would be experimental at best, and should not be relied upon without other types of observations. A warning system based on this data collection system might give false alarms, or movement could still occur unexpectedly as a result of instrument failures, communications failures or other factors.

**Table 13. Threshold (minimum) values of movement, rainfall and piezometric head to be used in a possible landslide warning system. Exceedence of more of these values increases the likelihood of slow (a few cm over a few days) or fast (tens of centimeters over a few days) slide movement. Background pressure head is the average value over several days prior to a major change in pressure (head “spike”) from a rainfall event.**

<b>Warning Parameter</b>	<b>Impending Slow Slide Movement</b>	<b>Impending Fast Slide Movement</b>
Extensometer Movement (cm)	Any measurable movement	2 over 4 days <sup>5</sup>
LT-1p Pressure Head (m)	7	9.0
LT-2p Pressure Head (m)	9.4	12
LT-3p Pressure Head (m)	5	6.5
LT-1p Background Pressure Head (m)	6.5	6.9
LT-2p Background Pressure Head (m)	9.2	9.4
LT-3p Background Pressure Head (m)	4.5	4.6
Cumulative Rainfall (mm/48 hours)	64	118
Cumulative Rainfall (mm/48.7 days)	Not clearly correlated	717

Finally, we recommend that fundamental research be conducted on the physics of water in fractured slide masses. Emphasis should be on development of numerical models that adequately simulate both the lateral and buoyant (submersion) forces operating during transient pressure head spikes in networks of steeply dipping fractures. Models should be able to handle differing degrees of saturation of intergranular pore space in the slide mass independently from saturation in fracture systems while still taking into account the amount of time that water in fractures has the opportunity to infiltrate intergranular pores. Experiments should be designed to measure fracture and intergranular permeability as inputs into the new numerical models. This landslide offers an ideal natural laboratory for such detailed research.

<sup>5</sup> This value is minimum displacement taken from the two closest spaced (in time) extensometer measurements before the large movement of January-February 2003. Values are from the LT-1 extensometer/inclinometer hole.

## ACKNOWLEDGEMENTS

This project was funded as ODOT Miscellaneous Contract and Agreement, Project Name: *Detailed Geotechnical Analysis of Large Translational Landslides in Seaward-Dipping Sedimentary Rocks*. Funding for the project was provided to ODOT by the Federal Highway Administration.

In addition to providing overall technical guidance to the project ODOT loaned GeoKon LC-1 dataloggers and a Slope Indicator inclinometer cable, probe and Datamate to the project plus enough additional funding to do a ground LIDAR survey of the sea cliff in 2004. Len Saltekoff of ODOT provided estimates of the age of the Old Coast Highway. Jerry Stokes of ODOT provided estimates of average annual maintenance costs where the slide cuts Highway 101.

Technical advisory committee (TAC) reviewers are Michael T. Long, Steve Narkiewicz, Bernie Kleutsch and Matthew Mabey of ODOT, and Yumei Wang of DOGAMI. Numerous discussions with the TAC in meetings, by phone and through e-mail were invaluable. Mike Long also encouraged us in the early stages before the project was funded and kindly arranged for acquisition of a baseline scan of the slide toe using ground-based LIDAR. The scan was completed by David Wellman of D. Wellman Surveying L.L.C., Eugene, Oregon.

Len Saltekoff of ODOT provided valuable information on estimated age of Highway 101 and the Old Coast Highway construction.

Marshall Gannet of the US Geological Survey provided an invaluable review of the hydrologic interpretations. His discussions about the difference between lateral flow and lateral transmission of hydraulic pressure in causing head change were particularly useful.

Steve Dickenson and Samuel R. Christie of Oregon State University provided a useful review of the stability analysis by Landslide Technology and added some significant new insights into the forces governing movement. Their help is greatly appreciated.

Landslide Technology's team of geotechnical engineers and engineering geologists on the project included: Charles M. Hammond, CEG; Andrew Vessely, CEG, PE; Jonathan Harris, PE; Erica Meyer, EIT; and Darren Beckstrand, GIT. Mr. Hammond was the geotechnical study project manager and a reviewer of this paper. Mr. Vessely provided senior oversight, managed the engineering analyses, and reviewed this paper. Mr. Harris managed the instrumentation and data analysis, installed dataloggers and the rain gauge, and assisted with the engineering analyses. Ms. Meyer performed the engineering analyses. Mr. Beckstrand performed the field inspection and assisted with data analysis.

Geo-Tech Explorations, Inc., of Tualatin, Oregon performed the geotechnical drilling, and installed slope inclinometer casing and vibrating-wire piezometers under the direction of Landslide Technology. Slope Inclinometer Company supplied slope inclinometer casing and vibrating wire piezometers.

Wendy Niem did all of the graphical work for the detailed geologic interpretation of stratigraphy by Alan Niem in Appendix A. She also assisted in editing the paper.

Dennison Surveying Inc. of Newport, Oregon was retained under separate DOGAMI contract to survey the landslide topography and to establish permanent survey hubs for long-term monitoring. Dennison performed two surveys of these hubs, one in October of 2002 and one in April of 2003. These surveys provided invaluable information on overall slide movement. Dennison will complete an additional resurvey in the spring of 2005 or 2006, depending on the amount of movement that occurs in the winter of 2004-2005.

Rex Baum and William L. Ellis of the US Geological Survey, Menlo Park, California in November of 2004 installed more refined monitoring devices for the extensometers and piezometers. These devices will greatly increase the accuracy and ease of collecting data from the boreholes, particularly for the extensometers. They also offered useful technical review of the paper.

## REFERENCES

- Baum, R. L., and Reid, M. E., 2000, Ground water isolation by low-permeability clays in landslide shear zones, in Bromhead, E., Dixon, N., and Ibsen, M-L, eds., Landslides in research, theory and practice, Volume 1: Proceedings of the 8th International Symposium on Landslides held in Cardiff on 26-30 June 2000: Thomas Telford, London, p.138-144.
- Grathoff, G. H., 2005, Weathering mineralogy in dunal soils near Newport, Oregon: Oregon Society of Soil Scientists February 1, 18, 2005 Annual Meeting, oral presentation.
- Grathoff, G. H., Peterson, C. D., Beckstrand, D. L., 2001. Coastal dune soils in Oregon, USA, forming allophane and gibbsite. 12th International Clay Minerals conference, Bahía Blanca. Argentina July 22 –28, 2001.
- Johnson, C. M., 2003, Iron mineralogy in the Newport dune sheet: Portland State University Bachelor of Science thesis, 33 p; web link:  
<http://web.pdx.edu/~grathog/StudentWork/Catrina%20Johnson%20UG%20honors%20thesis%20OSP03.pdf>.
- Landslide Technology, 2004, Geotechnical investigation Johnson Creek Landslide, Lincoln County, Oregon: Oregon Department of Geology and Mineral Industries Open-File Report O-04-05, 115 p, published on CD.
- Pettijohn, F. J., 1957, Sedimentary rocks: New York, N.Y., Harper and Row Publishers, 718 p.
- Priest, G. R., and Allan, J. C., 2004, Evaluation of coastal erosion hazard zones along dune and bluff backed shorelines in Lincoln County, Oregon: Cascade Head to Seal Rock: Oregon Department of Geology and Mineral Industries Open-File Report O-04-09, on CD.



**APPENDIX A:**  
**Preliminary Borehole to Sea Cliff Correlations, X-ray Diffraction  
and SEM Analysis of Slip Plane, and Grain Size Study  
of Sedimentary Units of the Johnson Creek Landslide  
on US 101, Central Coast of Oregon,  
North of Newport**

by  
Alan R. Niem  
Professor Emeritus of Geology  
Oregon State University  
Oregon Registered Geologist #G659

submitted to DOGAMI on April 9, 2003  
revised June 25, 2003

**EXECUTIVE SUMMARY**

**and**

**RECOMMENDATIONS**

Dr. Alan Niem was contracted by DOGAMI to provide information to DOGAMI, ODOT, and Landslide Technology on the geologic nature and controls of the Johnson Creek landslide on the central Oregon coast north of Newport. This preliminary report consists of (1) a detailed discussion of east-west lithologic correlation of boreholes LT-1, LT-2, and LT-3 to a sea cliff section at the toe of the landslide; (2) XRD study of the mineralogical and microscopic (e.g., SEM) causes of slope failure; and (3) statistical grain size and thin section analysis of the stratigraphic section with emphasis on the lower and middle Miocene Astoria Formation exposed in the sea cliff at the toe of the landslide to determine the potential of these strata to contribute to the modern littoral sand budget.

**Results**

**(1) Borehole and Sea Cliff Correlation**

The Pleistocene terrace deposit in the upper part of the three boreholes consists of densely packed, well-sorted, reddish yellow iron oxide-stained, friable, fine to medium sand, 11 to 20 ft thick, a local paleosol (in LT-1), and a rounded siltstone cobble at the base of the deposit (in LT-2) (Plate I correlation diagram). Some sediment in the base of the terrace deposit is compositionally and texturally similar to the paleo-surge channel-fill quartzo-feldspathic-lithic (mainly Astoria mudstone clasts) terrace sand and gravel which overlie the angular unconformity on the Astoria Formation exposed a short distance east of the headscarp on the Boise Cascade logging road. Pleistocene terrace beach sands in the sea cliffs and headscarp consist of locally case-hardened, well-sorted, fine and some medium beach sand (mainly subrounded grains of quartz, feldspar, and lithics (volcanic)) and a fluvial sandy gravel channel fill with framework-supported, rounded, white

gibbsite, quartz, and Columbia River Basalt pebbles. These gravel lenses are overlain by a gray paleosol with gley or E-horizon and a dark, organic-rich A horizon. The Pleistocene deposits and the Miocene Astoria Formation are locally overlain and partly covered by thin to thick, surficial, Holocene landslide toe colluvium composed of mostly poorly sorted angular clasts of Astoria Formation siltstone in a reworked Pleistocene terrace sand matrix (see Middle sea cliff section on Plate I). The maximum vertical displacement by landsliding of the angular unconformity between the Quaternary terrace deposit and the underlying lower and middle Miocene Astoria Formation is calculated to be 70 feet on a 1:1 scale cross section between its position just east of the headscarp through the three boreholes to its position in the sea cliffs at the toe of the landslide (Plate I, cross section B).

Composite thickness of the Astoria Formation correlated in the three boreholes and exposed in the sea cliff is 140-ft. These 140 feet of strata include four stratigraphic sequences of shallow-marine (inner to middle shelf), fossil mollusk-bearing, very fine- to fine-grained, bioturbated sandstone (informally called sandstone sequences A, B, C, and D; see correlation diagram, Plate I). The sandstone sequences range from 5 ft to 31 ft thick. Sandstone sequences A, B, C, and D are separated by four units of massive, finely micaceous, medium gray siltstone (informally called units 1 through 4 from base to top; Plate I). In thin sections, the very fine- to fine-grained quartzofeldspathic-lithic (volcanic) mica-bearing Astoria sandstones are moderately well-indurated due to extensive sparry calcite and clay rim cement and some detrital clay. In contrast, the darker gray deeper marine (outer shelf and upper slope?), foram-bearing, micro-micaceous siltstone units are composed of expandable iron-rich smectite clay (see XRD analysis section, Figures. 3A, 3B, and 3C) and silt-sized angular quartz, plagioclase feldspar, pyrite, carbonized wood, and mica and are relatively less indurated (less strong). Siltstone unit 2 contains the active basal slip plane (based on inclinometer data) in boreholes LT-1, LT-2, and LT-3, suggesting some stratigraphic control on the landslide (Plate I).

Sandstone sequences A, B, C, and D and siltstone units 1, 2, and 3 are correlated on a 3.63:1 scale correlation diagram (Plate I) between the boreholes by stratigraphic position, regional strike and westward dip, similar fossils, internal stratigraphy, distinctive fragments of calcite-replaced pumice in a fine-grained bioturbated sandstone sequence, and adjacent altered glass shard-bearing tuff marker beds. In addition, the yellowish brown, 10- to 11-ft thick very fine- to fine-grained, shallow-marine, calcite-cemented sandstone D with large fossil scallops (*Patinopecten*) at the base of the sea cliff sections can be traced laterally and mapped (e.g., G. Priest, Figure. 2) north-south along the Johnson Creek landslide sea cliff. This sandstone sequence occurs with blocky jointed, thin tuffs at the top and base and an underlying distinctive, thin, buff, concretionary, foram-rich rib-forming bed in the underlying siltstone unit 3 (Plate I Middle sea cliff section). Sandstone sequence D, the underlying *Dentalium*- (tusk shell) bearing siltstone unit 3, and the overlying thick massive siltstone (unit 4) with horizons of calcareous concretions overlain by Pleistocene terrace/Holocene sand colluvium are in separate, back-rotated eastward dipping landslide blocks as shown in an east-west cross section (Plate I). These borehole and outcrop data were used in reconstructing two small east-west cross sections (A and B) of the Johnson Creek translational slide (before sliding - A and after sliding - B).

In cross section B on Plate I (no vertical exaggeration), correlation lines connecting Astoria sandstone sequence C and siltstone units 2 and 3 dip 17° westward above the active basal slip plane. Correlated sandstone sequences A and B and siltstone unit 1 (a more confident correlation between boreholes) also dip 17 to 20° west below the active slip plane. The dip of these correlation lines and calculated dips closely match the regional dips measured with a Brunton compass in an Astoria Formation wave-cut bench 150 feet west of the Johnson Creek landslide sea cliff by Alan Niem and

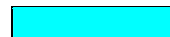
just east of the headscarp mapped by George Priest (Figure. 2) range from 17° to 20° west. Dips measured on rare bedding in the cores of the three boreholes during drilling (measured by Beckstrand, Niem, and Priest) averages 17° but ranges from 10° to 20° (Plate I). The lower dip amounts measured below the slip plane could be explained by (a) drag or displacement of different blocks of Astoria Formation by three postulated normal or oblique-slip faults (drawn to make a balanced cross section) or (b) inaccuracy of correlation or drafting or variation (plus or minus a few degrees) of measuring field and core attitudes (i.e., strikes and dips).

(2) X-Ray Diffraction Study of the Mineralogical and Microscopic (i.e., SEM) Causes of Slope Failure

The active basal slip plane in the boreholes consists of a thin sheared gouge of wet, soft, medium gray, sheared clayey siltstone. This wet sticky gouge could be easily rolled and molded into long threads between the thumb and index finger, suggesting a moderate clay content. Due to the soft wet nature of the slide plane gouge, recovery was usually poor. A Shelby tube sample of the slide plane gouge (from LT-2P at 59-60 ft) from Landslide Technology underwent XRD analysis but not hydrometer or sieve size analysis. However, a sample of the nearby host clayey siltstone (core sample N03-XX at 54 ft in LT-2) has the same mineralogy (see later XRD discussion) and contains 24.5% clay, 74.6% silt and 0.9% sand (Table 1).

Table 1. Size statistics data.

Sample No.	% Sand	%Silt	% Clay
GR03-00	0.6	93.1	6.3
GR03-1	12.8	74.5	12.7
GR03-5	0.3	79.4	20.3
GR03-6	13	66	21
GR03-7	37.5	55.8	6.7
GR03-8	71	24.6	4.4
GR03-9	5.6	87.7	6.7
GR03-10	5.7	76.9	17.4
GR03-13	31	57	12
N03-32	67.1	32.4	0.5
N03-53	79	20.5	0.5
N03-XX (LT-2 @ 54 ft)	0.9	74.6	24.5
Pin03-2	76	17.5	6.5
Pin03-4a	51.7	32.6	15.7

 siltstone sample; including slip plane gouge sample (GR03-00) at base of Southern sea cliff section

 sandstone sample

Based upon inclinometer depths to the basal slip plane and construction of a 1:1 cross section (on Plate I), the slip plane dips 17° westward between boreholes LT-3 and LT-2 and flattens to 8° westward between LT-2 and LT-1 (cross section B, Plate I). The slip plane is just below sea

level (NAVD 1983) and then curves up to the surface at the beach, cutting across sandstone sequences C and D and siltstone units 3 and 4 and forming a low bench which is seasonally covered by beach sand. A backhoe excavation of the slip plane near where it emerges on the beach (supervised by George Priest) and winter field observations of the low wave-cut bench that contains the slip plane at the base of the sea cliff suggest the slip plane is nearly horizontal at the surface and then dips 35° eastward thrusting out over 3 to 4.5 feet of modern winter beach heavy mineral sand, sandstone boulder talus, and a basal shelly basalt gravel and underlying intact siltstone unit 4 (bedrock). The basal slip plane gouge, which was temporarily exposed in February 2003 on the wave-cut platform below the Southern sea cliff measured section, was sampled (sample GR03-00) and underwent XRD and hydrometer/sieve size analysis. It consists of 6.3 wt % clay size grains, 93.1 wt % silt, and 0.6 wt % sand (Table 1; Figure. 4). It was surprising that the wet, plastic (i.e., moderate plasticity) siltstone gouge sample did not have more clay than indicated by the hydrometer grain size analysis because it felt sticky and easily rolled into a ball and thread (see further discussion in section on grain size analysis of siltstones).

Overlying the thin basal slip plane shear gouge (soft, micro-slickensided wet clayey silt) is 10 or more feet of landslide toe breccia, consisting of very poorly sorted, angular broken blocks of *Dentalium*-bearing siltstone unit 3 (the host rock) in a sheared clayey(?) silt matrix. The breccia is locally overlain by intact (nearly unfractured) siltstone unit 3 that occurs just below sandstone sequence D in the Southern sea cliff measured section. The sample of host rock siltstone unit 3 (sample GR03-1) consists of 12.7% clay, 74.5% silt, and 12.89% sand (Table 1). Landslide breccia also appears as a 16-ft thick section of subhorizontal landslide breccia zones (composed of angular mudstone clasts and chips in clayey silty gouge) and intervening intact siltstone unit 2 in the lower part of borehole LT-1 (Plate I). The active basal slip plane in LT-1, based upon inclinometer data, lies in the middle of this brecciated zone and includes many overlying and underlying high-angle, slickensided, open (or clay or iron oxide filled) planar extensional fractures that could act as permeable avenues for groundwater flow. Similar extensional high-angle fractures with normal listric-slip of a few to several meters occur above the basal slip plane gouge and landslide breccia zone in the sea cliffs at the toe of the landslide (i.e., west end of cross section B).

XRD analysis of the clay mineralogy of the basal slip plane clay-silt gouge in LT-2 (sample LT-2P Shelby tube at 59-60 feet, siltstone unit 2, in Figure. 3A) and in the sea cliff outcrop (siltstone unit 3; sample GR03-00) shows that the clay-sized fraction (<2 microns) in this gouge is composed mainly of expandable iron-rich smectite (clay mineral) with minor amounts of detrital illite (muscovite), chlorite (altered biotite?), and perhaps some kaolinite (kaolin) clay minerals (see XRD pattern Figure. 3A). Similarly, XRD analysis reveals that the silt-sized fraction (>2 microns) of the gouge contains detrital quartz, calcic plagioclase (i.e., anorthite Na, Ca), pyrite, muscovite, chlorite (clinochlore; altered biotite?), nontronite (Fe-smectite), and calcite (see XRD pattern Figure. 3B). X-ray diffraction and thin section study show that these clay mineral types and other minerals are identical to the minerals in samples (e.g., outcrop sample GR03-1 and core sample N03-XX from 54 ft in LT-2) of the adjacent foram-bearing host rock siltstone (units 3 and 2) (see XRD pattern of host rock sample GR03-1 and N03-XX; Figures. 3A and 3B). SEM photomicrographs of the sheared gouge show that the expandable iron-rich smectite clay (nontronite?) has been crudely aligned parallel to the slip planes and contains micro-slickensides and sheared and broken foram microfossil tests as a result of this slippage (Figures. 5A, 5B, and 5C) suggesting a preferred zone or plane of weakness and residual strength. Thin section and SEM photomicrographs also show that many intersecting micro-dehydration cracks can develop in the expandable smectite-rich gouge as a result of sample preparation (drying and dehydration; Figure. 6). It is suggested that these micro-fractures could also form naturally and could represent avenues

for groundwater flow which could further weather the gouge and weaken the cohesion and residual strength by chemical reactions (e.g., dehydration and rehydration of expandable smectite clay in the gouge zone due to seasonal fluctuations of the groundwater table related to rainfall). Groundwater access to such confined microfracture porosity in the slip plane could reduce frictional resistance force and increase the upward normal pressure on the overlying less permeable intact host clayey siltstone in the slide block overlying the basal slip plane.

### (3) Grain Size Analysis of Sedimentary Units in Johnson Creek Landslide and their Potential Contribution to the Modern Littoral Budget

Sieve and hydrometer grain size analysis was conducted on 12 Astoria Formation sandstone and siltstone samples (Tables 1 and 2). Most samples are from the Southern sea cliff measured section at the toe of the Johnson Creek landslide (i.e., sandstone sequence D and siltstone units 2, 3, and 4), but some came from the borehole cores, including siltstone unit 2 (Figures. 1 and 2). Three samples of modern (Holocene) beach and dune sands also were sieved (Table 2). Comparison of the grain size distribution and size statistics of these samples (modern sands and bedrock) allowed preliminary conclusions about how much sand from the Astoria Formation strata in the Johnson Creek sea cliffs contributes to the modern littoral sand budget (Task 3 of the contract). The slip plane siltstone gouge and siltstone unit samples\*<sup>1</sup> plot on a triangular sediment classification diagram (Figure. 4) as siltstone or sandy siltstone (% clay ranges from 6.3% to 24.5%, av. 14.3%), but we believe these rocks may contain more clay and less silt by weight than shown by the hydrometer settling tube analysis, perhaps due to incomplete disaggregation or some flocculation of clay-size grains as silt-sized flocs even though a deflocculating agent (sodium phosphate) was used. Initial visual thin section estimates suggest that these rocks should be classified as clayey siltstone or sandy clayey siltstone.

Binocular microscope study and grain size statistics of siltstone units 3 and 4 which comprise the dominant Astoria lithology in the Johnson Creek landslide sea cliffs (Figure. 2) suggest the minor sand fraction (<10%) of samples from siltstone units 3 and 4 is too fine-grained (i.e., mainly very fine sand) and partly the wrong mineral composition to contribute much to the coarser grained (i.e., largely fine and some medium sand) modern winter beach sands (Table 2 and Figures. 7 and 8). The very fine sand fraction of the Astoria siltstone units, for example, is rich in grains of muscovite, biotite, chlorite, quartz, feldspar, and pyrite. In contrast, the very fine sand size fraction of some modern winter beach sands (e.g., at the base of the Johnson Creek landslide sea

---

\*<sup>1</sup> Civil engineers and engineering geologists generally use the ASTM classification of sediments (e.g., used by ODOT; Bernie Kleutsch, 2003, personal communication) in which mud (i.e., mudstone) includes both silt-sized (siltstone) and clay-sized (claystone) sediment grains for geotechnical purposes. Muds (mudstones) are further differentiated in the Wentworth and National Research Council classifications used by many geologists. Figure 9 is a comparison of these scales used by engineers and geologists. We prefer to use the term siltstone in this preliminary report to agree with our hydrometer grain size analysis, with the sediment classification of Folk (Figure. 4), and with the definition of the Astoria Formation by Snavely and others (1976, 1964) as sandstone, siltstone, and tuff on their regional geologic maps and reports in the Newport area.

sea cliffs; Sample GRO, Table 2) is a largely different mineralogy. The very fine sand-size fraction is composed mainly of dark-colored heavy minerals magnetite/ilmenite, garnet, pyroxene, zircon, tourmaline, hypersthene and other heavies and some very fine sand-sized grains of quartz and feldspar.

Some very fine- to fine-grained poorly sorted, bioturbated, shallow-marine Astoria silty sandstones, such as the 10- to 11-ft thick sandstone sequence D in the lower sea cliff at the toe of the landslide, could contribute 60 to 70% of its weight and volume (visually estimated in thin section) as compositionally similar fine\*<sup>2</sup> sand-sized grains to the fine sand fraction of the quartz- and feldspar-rich modern beach sand. However, a large proportion (estimated 30 to 40 wt. %) of the sieved Astoria sandstone samples, in statistical plots of mean size, standard deviation (a measure of sorting), and median size, is generally finer grained and more poorly sorted than the modern beach sands (Figures. 10, 11, 12, and 13). Modern beach and Astoria sandstone bedrock and core samples generally overlap in skewness (a measure of the asymmetry of the grain size distribution). Quartz and feldspar grains in the Astoria Formation also are more angular than in the modern sand. A modern beach sand sample from near Otter Rock also contains, in addition to fine sand-sized quartz, feldspar, and very fine sand-sized dark-colored heavy minerals, well-rounded very coarse to medium sand-sized fragments of middle Miocene Columbia River Basalt derived from nearby basalt headlands and sea stacks (such as Cape Foulweather). This younger basalt unit overlies and invasively intruded (as dikes and sills) the older Astoria Formation. In contrast, the Miocene Astoria strata in thin section contain fine- and some medium sand-sized fragments of andesite/basalt lava derived from the western Cascades volcanic arc and texturally distinct basalt clasts eroded from older Coast Range Eocene basalts, very coarse sand-sized grains of calcite-replaced pumice, metamorphic rock fragments, micas, green hornblende, pyrite, and carbonized wood as well as silt-sized quartz and feldspar and clay-sized grains which form a visually estimated 30 to 40% of the total volume. These types of mineral and lithic (rock fragment) grains do not contribute to the modern littoral quartz-feldspar-heavy mineral-rich sand budget because they are either different in composition (Table 2) and/or some of the Astoria quartz and feldspar framework grains are too fine-grained (i.e., silt-sized to very fine sand-sized) to supply grain sizes that comprise the modern, largely fine (and some medium), quartz-feldspar-heavy mineral beach sand (Figure. 10). Thus, a large proportion of the 10- to 11-ft thick sandstone sequence D in the sea cliff at the toe of the landslide probably contributes an estimated only 60 to 70 percent of compositionally similar grain sizes (i.e., quartz, feldspar and heavy minerals) to the modern beach sand. This sandstone sequence also comprises an estimated less than 25% of the total stratigraphic section exposed in the sea cliffs at the toe of the Johnson Creek landslide that includes mainly siltstone units 3 and 4, Pleistocene terrace deposit, and Holocene colluvium (see Middle sea cliff section on Plate I and Figure. 2).

Ongoing grain size, thin section, and binocular microscope study of some Pleistocene terrace sand samples from the Johnson Creek landslide suggest these friable, fine to medium sands may contribute much more compositionally similar (i.e., rounded quartz and feldspar and similar heavy minerals) grain sizes to the littoral sand budget than the Astoria Formation sandstone and siltstone. However, some fine to coarse beach/fluviol terrace sand and gravels in the Johnson Creek landslide are lithic (rock fragments)-rich (mudstone, volcanics, quartz, agate) and contribute little compositionally to the modern littoral quartz- and feldspar-rich sands. Alternatively, much of the modern fine beach sand (quartz, feldspar, and heavy minerals) could have been recycled from other

---

\*<sup>2</sup> Note: the ASTM engineer's verbal and quantitative limits for sieved sand sizes are slightly different than the geologist's Wentworth scale and National Research Council scale. In this report, we use the Wentworth's scale, National Research Council scale, and phi scale (see Figure. 9 for comparison).

sources, such as from major rivers like the Umpqua and Columbia during sea level lowstands during Pleistocene glacial stages. These sands were transported northward and southward along an ancient shoreline now on the middle shelf. As sea level rose, eroding and drowning the coastline, that shoreline sand that prograded landward by waves subsequently became trapped with winter

beach gravels (basalts) in littoral cells between Miocene basalt headlands. In addition, within the Yaquina Head/Cape Foulweather littoral cell that includes the Johnson Creek landslide, small modern streams (e.g., Wade, Schooner, Johnson, Spencer creeks) have drainage basins headed in older formations (such as the 2000-ft thick sandstone-rich deltaic Yaquina Formation or widespread older Pleistocene terrace deposits; mapped by Snavely and others, 1976) on older terraced uplands. These small drainage basins could also supply some sand of comparable grain sizes and mineral composition to the modern littoral sand budget.

### **Recommendations**

- (1) Some additional hydrometer grain size, XRD, thin section and SEM study of the basal slip plane and Astoria siltstone units in outcrop and core would help define better the mineralogical and micro-textural causes (e.g., % clay vs silt) of this landslide which should then be further related to geotechnical engineering properties. A rapid sediment analyzer (sedigraph) could be used to obtain quantitatively more meaningful grain size analysis of % clay and silt than obtained with a hydrometer. Point counts of % silt and sand vs clay in thin section would give better quantitative volumetric results than visual estimation.
- (2) In order to draw a better balanced east-west cross section, a section of the westward-dipping Astoria strata along the Boise Cascade Johnson Creek logging road a short distance east of the headscarp should be measured, described, and projected (i.e., correlate sandstone, tuff and siltstone units) into the east-west correlation diagram to borehole LT-3 (Plate I, Figures. 1 and 2). This east of the headscarp section, unaffected by the Johnson Creek landslide, would help to show the relative movement that has occurred since the slide was initiated. (Time and funds prevent this from being done in this preliminary report.)
- (3) Additional sieving, pebble counts of gravels, measuring sections at the headscarp and augering the Pleistocene terrace deposit exposed in the headscarp should be conducted to define the geometry of this deposit, the topographic relief on the Pleistocene/Astoria unconformity (e.g., incised paleovalley fill? or wave-cut bench? with surge channels or older landslide or faults). Some additional measured sections along the north-south sea cliff could be measured. Fracture analysis of joints and slip planes in those sections could be done to measure quantitatively the percentage of vertical porosity and permeability. Two north-south geologic cross sections across the Johnson Creek landslide could then be constructed and units correlated to augment the east-west cross section. One section at the headscarp at the eastern end of the Johnson Creek landslide and the other section along the beach sea cliffs. A 3-dimensional fence diagram could then be constructed.
- (4) The contribution of sand-sized sediment from modern streams draining the Astoria and Yaquina formations and Pleistocene terrace and other sea cliff exposures of Astoria sandstones in the Yaquina Head-Cape Foulweather littoral cell should be studied by sieving, thin section (i.e., point counting) and field examination in order to determine the potential of these units to contribute similar size sediment to the littoral sand budget and to calculate the volume of sediment shed from these units. Such studies would provide better quantitative information with the sea cliff erosion studies being conducted by Jon Allan. The Astoria Formation samples from the Johnson Creek landslide study represent only 140 ft of the entire 1,000-ft plus Astoria section; this small sampling may not be representative of the potential grain size contribution of the entire sea cliff section in this cell.



### References

- Cooper, D. M., 1981, Sedimentation, stratigraphy, and facies variation of the lower to middle Miocene Astoria Formation in Oregon: Corvallis, Oregon, Oregon State University PhD dissertation, 524 p.
- Folk, R. L., 1974, Petrology of sedimentary rocks: Hemphill, Austin, TX, 182 p.
- Friedman, G. M., 1962, Comparison of moment measures for sieving and thin section data in sedimentary and petrological studies: *Journal of Sedimentary Petrology*, v. 32, p. 15-25.
- Snively, P. D., Jr., Rau, W. W., and Wagner, H. C., 1964, Miocene stratigraphy of the Yaquina Bay area, Newport, Oregon: *The Ore Bin*, v. 26, no. 8, p. 133-151.
- Snively, P. D., Jr., MacLeod, N.S., Wagner, H.C., and Rau, W. W., 1976, Geologic map of the Cape Foulweather and Euchre Mountain quadrangles, Lincoln County, Oregon: US Geological Survey Misc. Inv. Series Map I-868, scale 1:62,500.
- Welton, J. E., 1984, SEM Petrology Atlas: American Association of Petroleum Geologists, Methods in Exploration Series, no. 4, 237 p.
- Wentworth, C. K., 1922, A scale of grade and class terms for clastic sediments: *Journal of Geology*, v. 30, p. 377-392.

## FIGURES

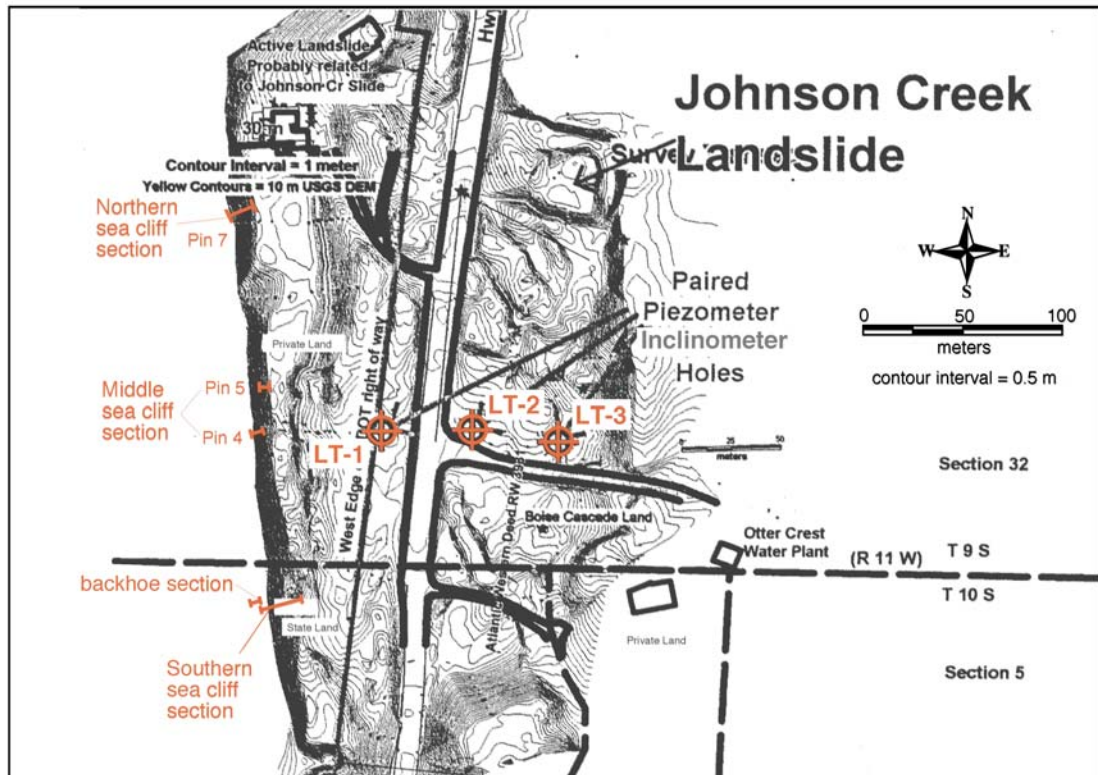


Figure 1. Index map of study area, showing line of cross section (Plate I).

Geologic Map - Johnson Creek Landslide  
updated 1-3-04 (Niem & Niem)

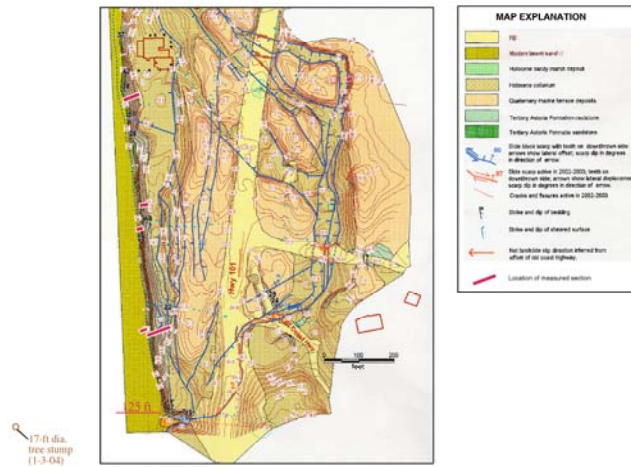


Figure 2. Geologic map of the Johnson Creek landslide study area by George Priest.

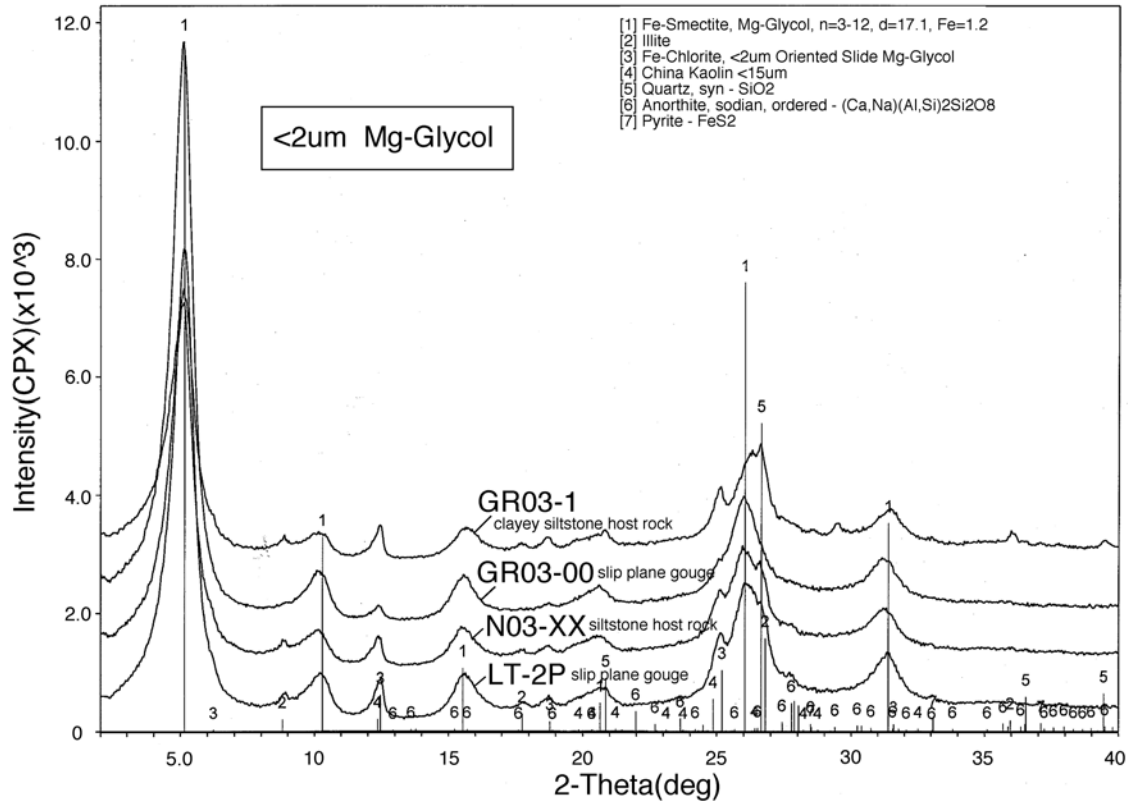


Figure 3A. Comparison of the X-ray diffraction patterns of clay-sized fraction (<2 microns) of four samples: Mg-saturated glycolated host rock in sea cliff (GR03-1), gouge in basal slip plane at the sea cliff (GR03-00, siltstone unit 3), core sample of host rock clayey siltstone (siltstone unit 2) at 54 ft (N03-XX), and clay-silt gouge in basal slip plane at 58.1 ft (borehole LT-1). All four samples contain mainly expandable Fe-smectite clay matrix (large peak labeled 1) with minor (smaller peaks) detrital illite, Fe-chlorite, possible kaolinite, quartz, anorthite, and diagenetic pyrite. The similarity of peaks suggests the host rock siltstone is the parent rock for the slip plane gouge.

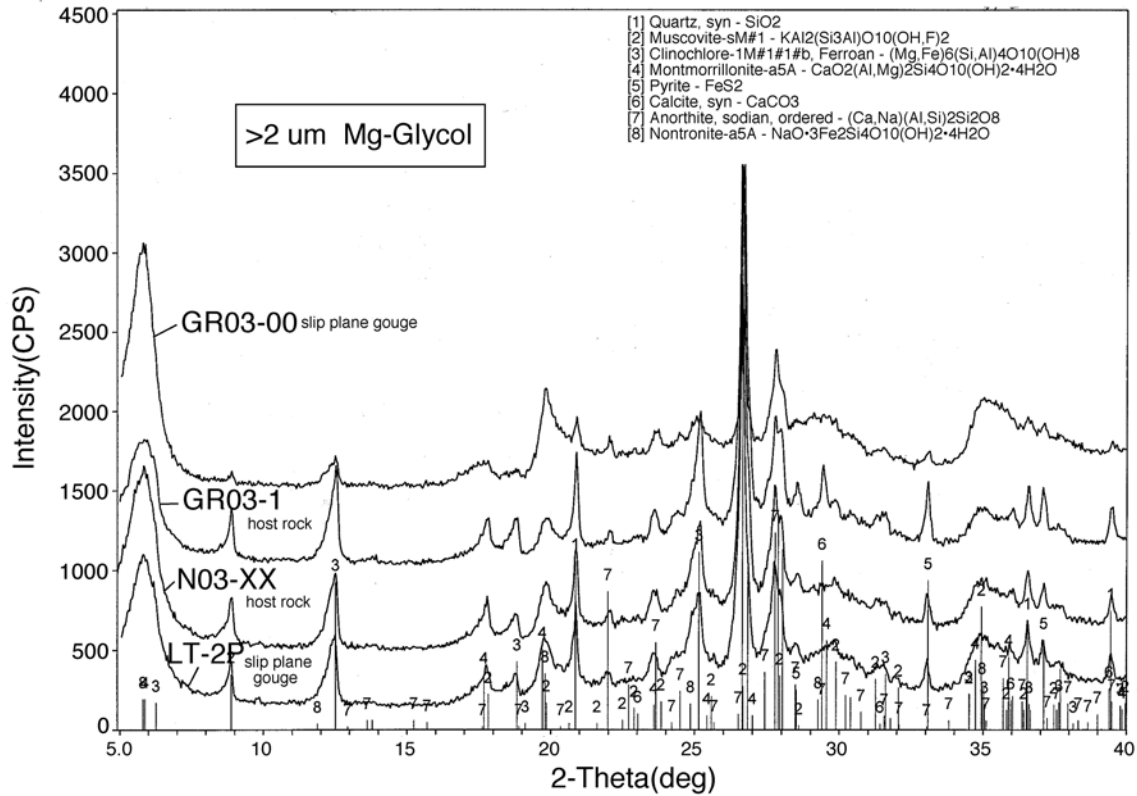


Figure 3B. X-ray diffraction patterns of the silt-sized fraction (>2 microns) of the clay-silt gouge of the basal slip plane show that the gouge contains detrital quartz, calcic plagioclase (i.e., anorthite Na, Ca), pyrite, muscovite, chlorite, nontronite (Fe-smectite), and calcite.

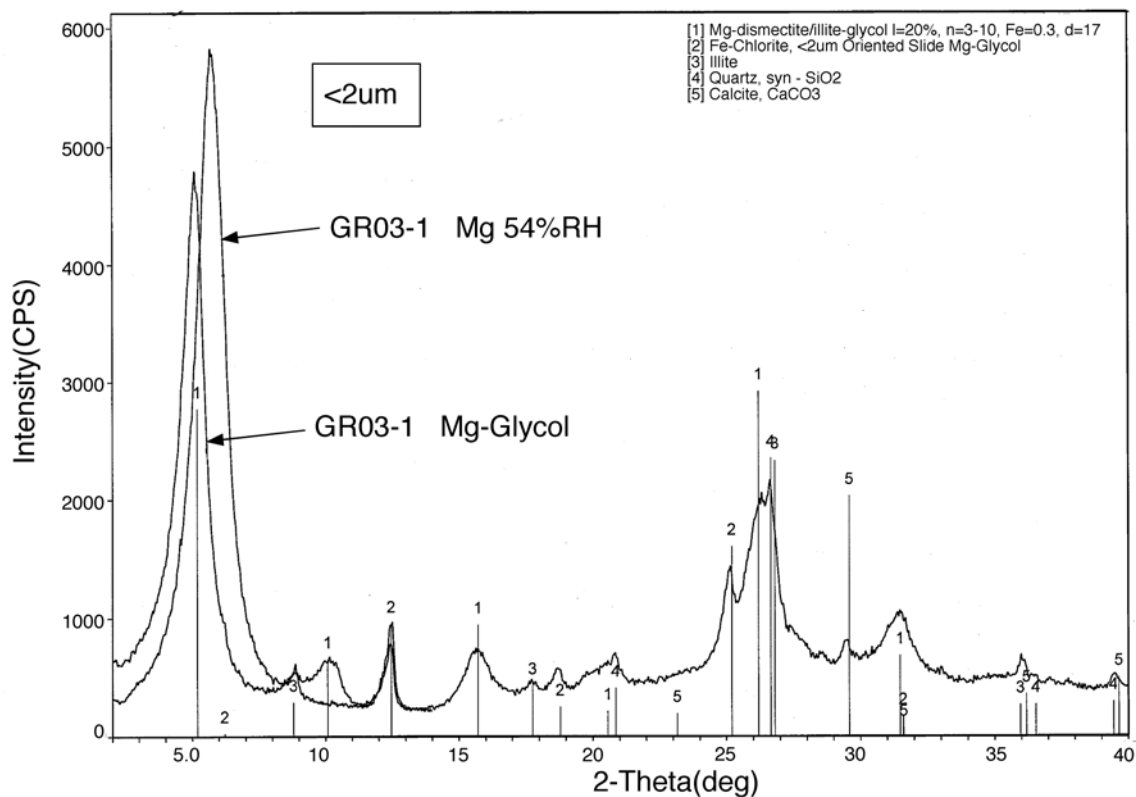


Figure 3C. X-ray diffraction pattern of the clay-sized fraction (<2 microns) of the host rock siltstone (siltstone unit 3) that contains the active slip plane at the base of the sea cliff outcrop. Note the shift to lower 2-theta value of the smectite peak upon glycolation. Other clay-sized components include detrital Fe-chlorite, illite, quartz, and calcite.

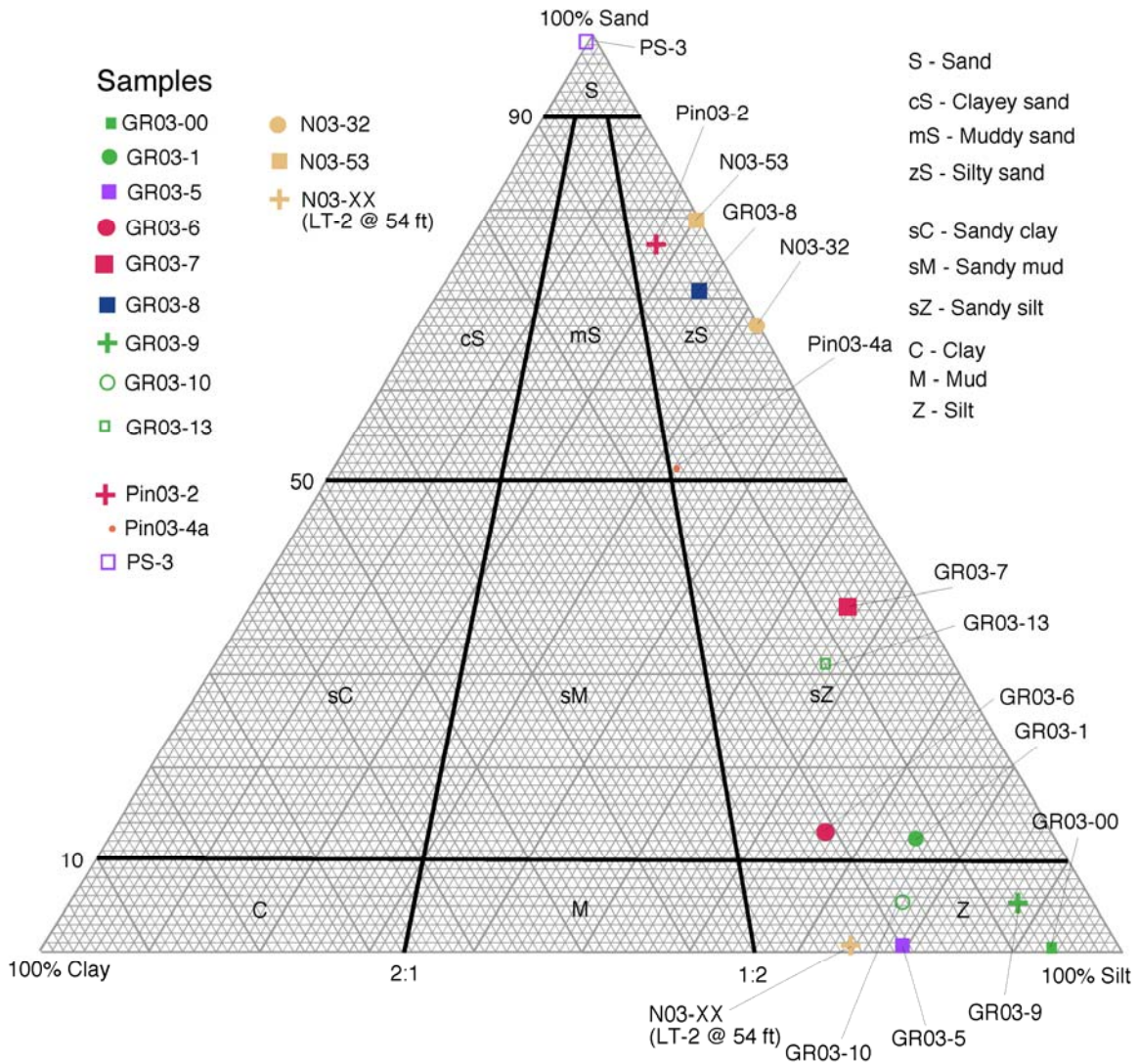


Figure 4. Grain size classification of disaggregated lower and middle Miocene Astoria Formation sandstones and siltstones from sea cliffs at the toe of the Johnson Creek landslide and from cored boreholes LT-1, LT-2, and LT-3. Grain sizes from sieve and hydrometer analysis. Triangular classification diagram of sediments by Folk (1974).



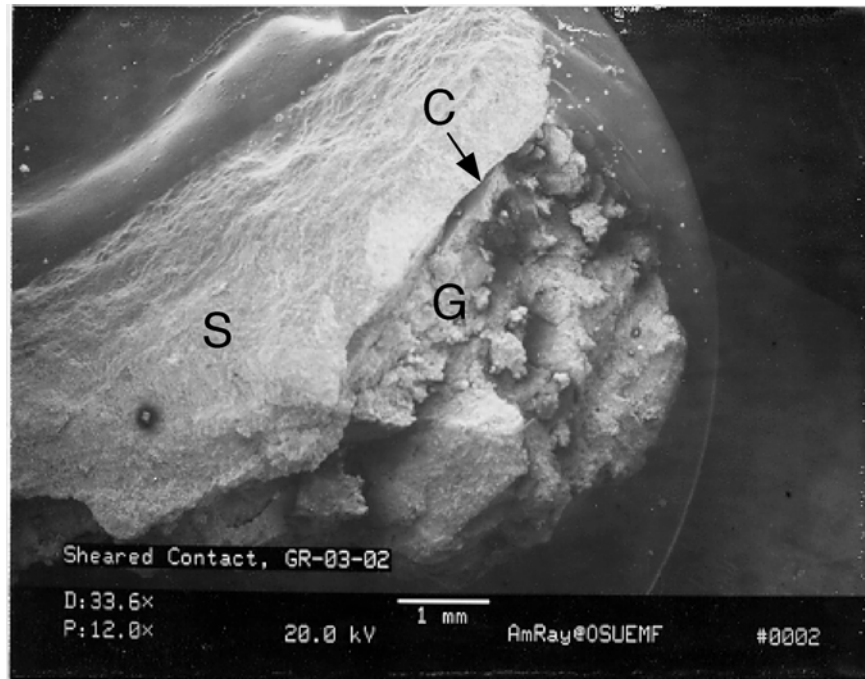


Figure 5A. SEM photomicrograph of sheared contact (Sample GR03-02) shows the contact of the undeformed host siltstone (labeled S) with broken fragmented clay-silt gouge (note angular broken siltstone fragments labeled G). The dark crack (labeled C) is the sharp 2 mm thick contact. Note 1 mm bar scale in bottom margin of photo.



Figure 5B. SEM photomicrograph at low magnification (12.5X) shows a sharp smooth shear plane (labeled Fr) which appears to step across the specimen. The specimen was mounted upside-down which places the shear gouge (g) in the upper NW half of the photograph and the unsheared siltstone (s) in the lower SE half of the photograph. The sheared gouge appears as a jumbled mass of largely subparallel (imbricated) smectite clay particles or packets. In the gouge, multiple fractures (dark lines), along which slippage has occurred, subparallel the main shear boundary.

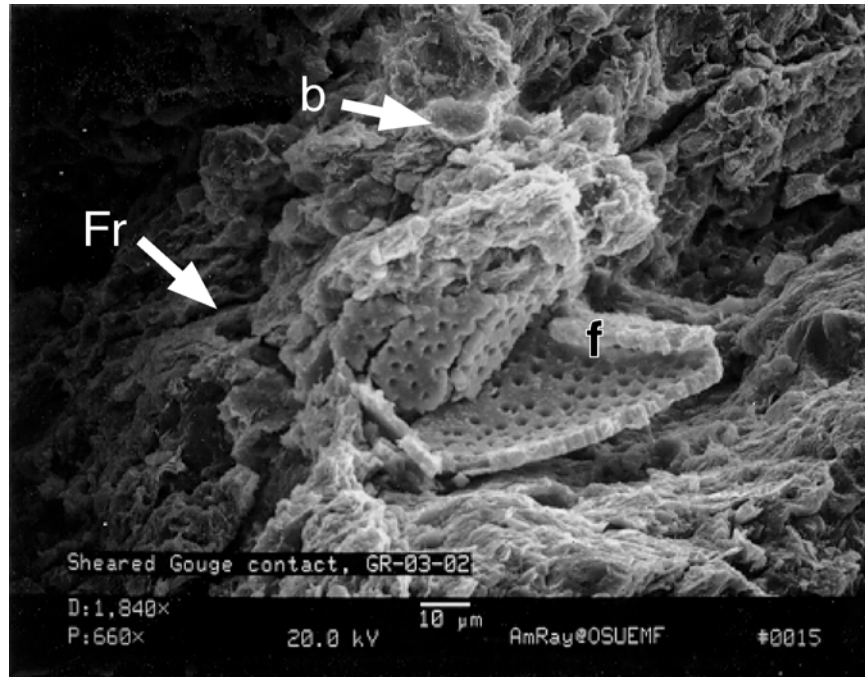


Figure 5C. SEM photomicrograph of bent and broken test (shell) of benthonic foraminifer (f) along a fracture (Fr). Flake of biotite (mica) is labeled b.

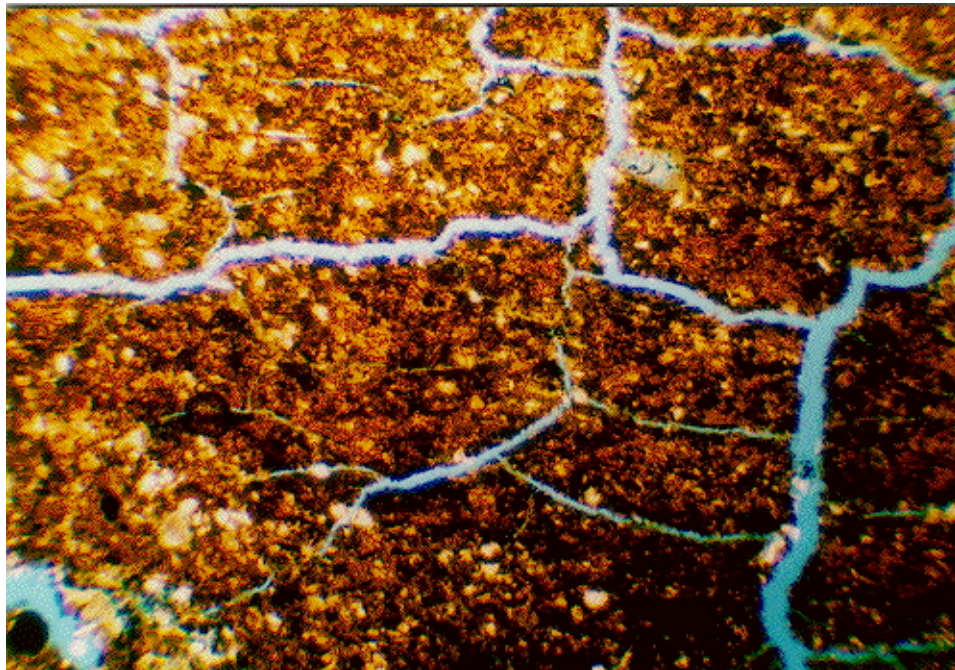


Figure 6. Photomicrograph of dessication microfractures in siltstone sample N03-XX (borehole LT-2 at 54 ft). Microfractures were created as the sample was dried and heated in the process of preparing the thin section. Blue-dyed epoxy fills the microfractures (3.5X, plane-polarized light).

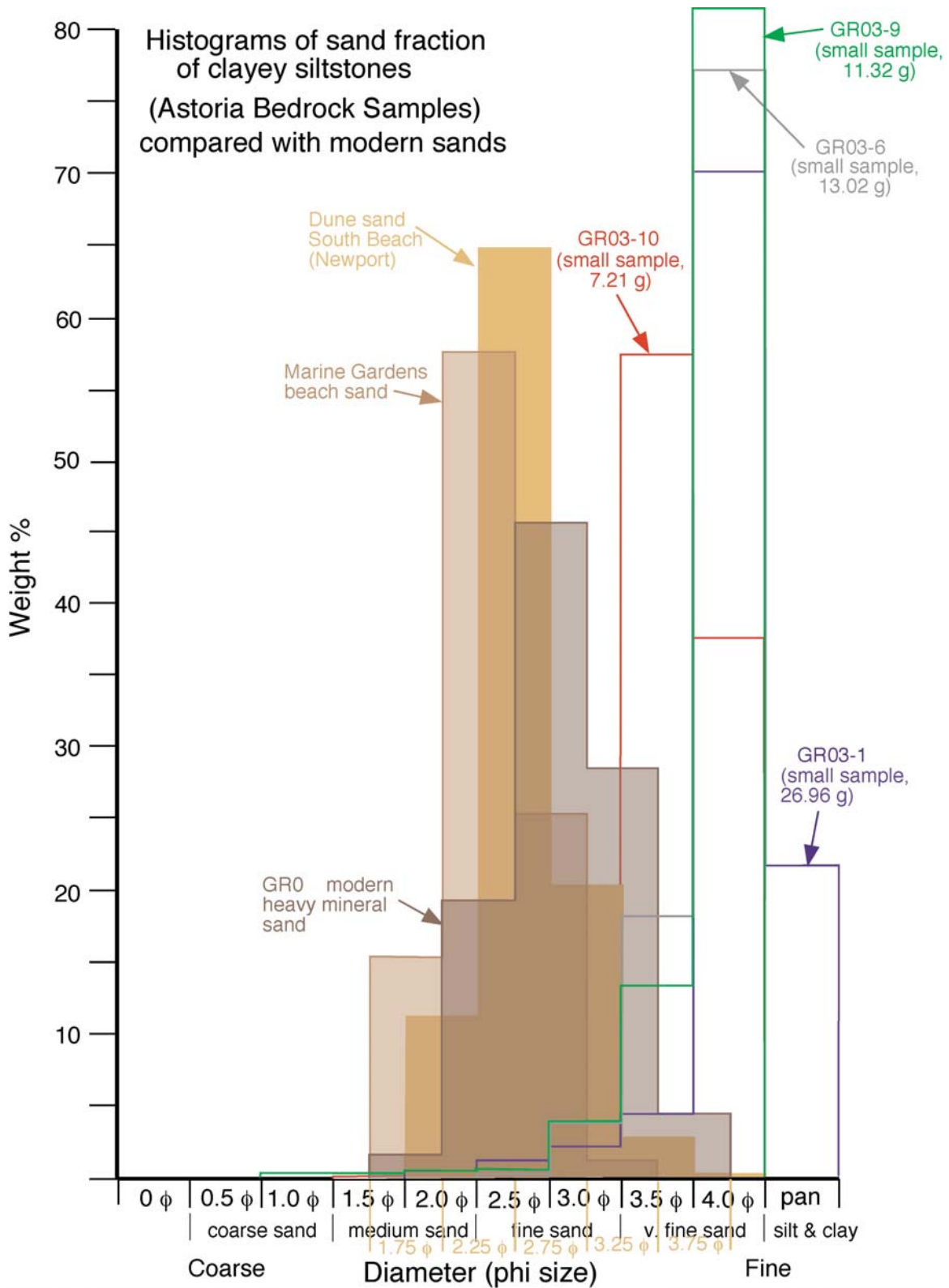


Figure 7. Histograms of sand fraction of Astoria Formation clayey siltstones and siltstones compared with modern sands.

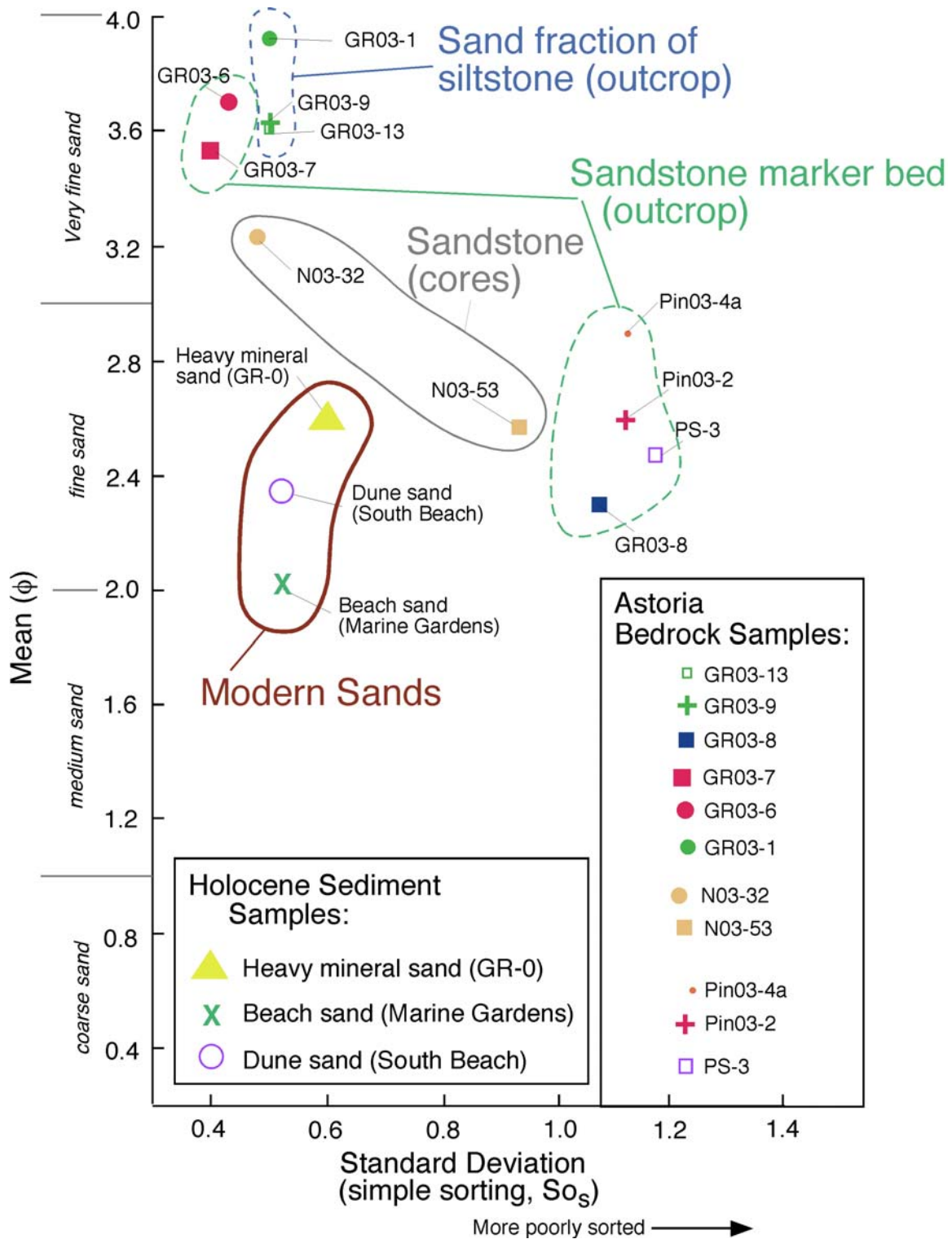


Figure 8. Binary plot of mean size versus standard deviation compares grain sizes of modern beach sands with grain sizes of bedrock. After Friedman (1962).



## Comparison of Size Scales \* \*

U.S. Std. Sieve No.	ASTM ODOT	Phi	mm	Wentworth (1922)	National Research Council
		-12	4096		VL boulders
		-11	2048		
		-10	1024	Boulder	L boulders
		-9	512	gravel	M boulders
					S boulders
12" (300 mm)	Boulders	-8	256		
		-7	128	Cobble	L cobbles
				gravel	S cobbles
3" (75 mm)	Cobbles	-6	64		
		-5	32		VC gravel
		-4	16	Pebble	C gravel
3/4" (19 mm)	C. gravel	-3	8	gravel	M gravel
		-2	4		F gravel
5/16	F. gravel	-1	2	Granule gravel	VF gravel
4/5	C sand	0	1	VC sand	VC sand
10		1	1/2	C sand	C sand
18	M sand	2	1/4	M sand	M sand
30		3	1/8	F sand	F sand
40		4	1/16	VF sand	VF sand
60	F sand	5	1/32		C silt
120		6	1/64	Silt	M silt
200		7	1/128		F silt
230		8	1/256		VF silt
		9	1/512		C clay-size
		10	1/1024	Clay	M clay-size
		11	1/2048		F clay-size
		12	1/4096		VF clay-size

\* Wentworth and Nat'l. Research Council scales used in this report.

Figure 9. Comparison of grain size scales used by geologists and by engineers.

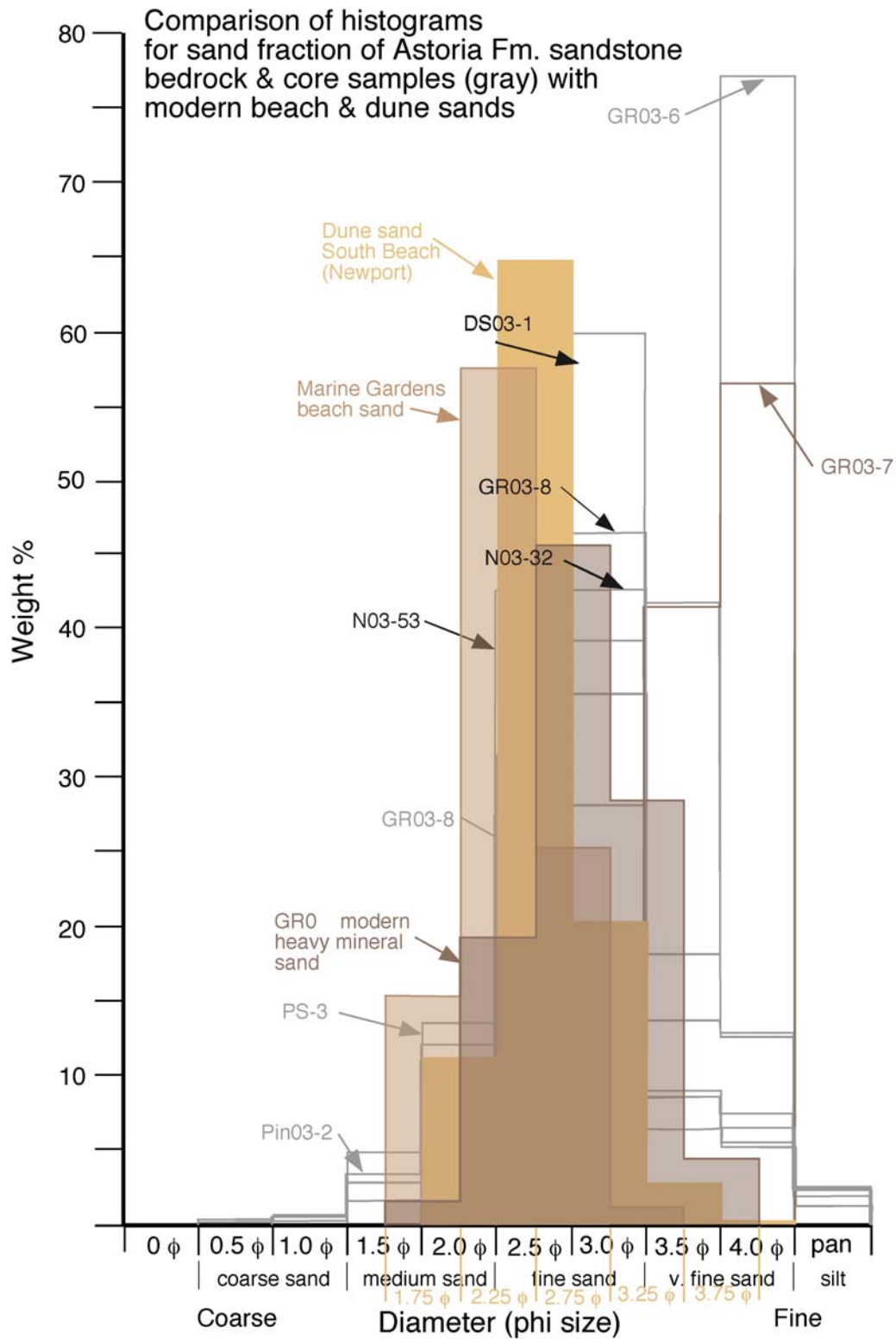


Figure 10. Comparison of histograms for sand fraction of Astoria Formation sandstone bedrock and core samples (gray) with modern beach sands and dune sands. The modern sands are distinctly coarser grained than the sand fraction in the bedrock.



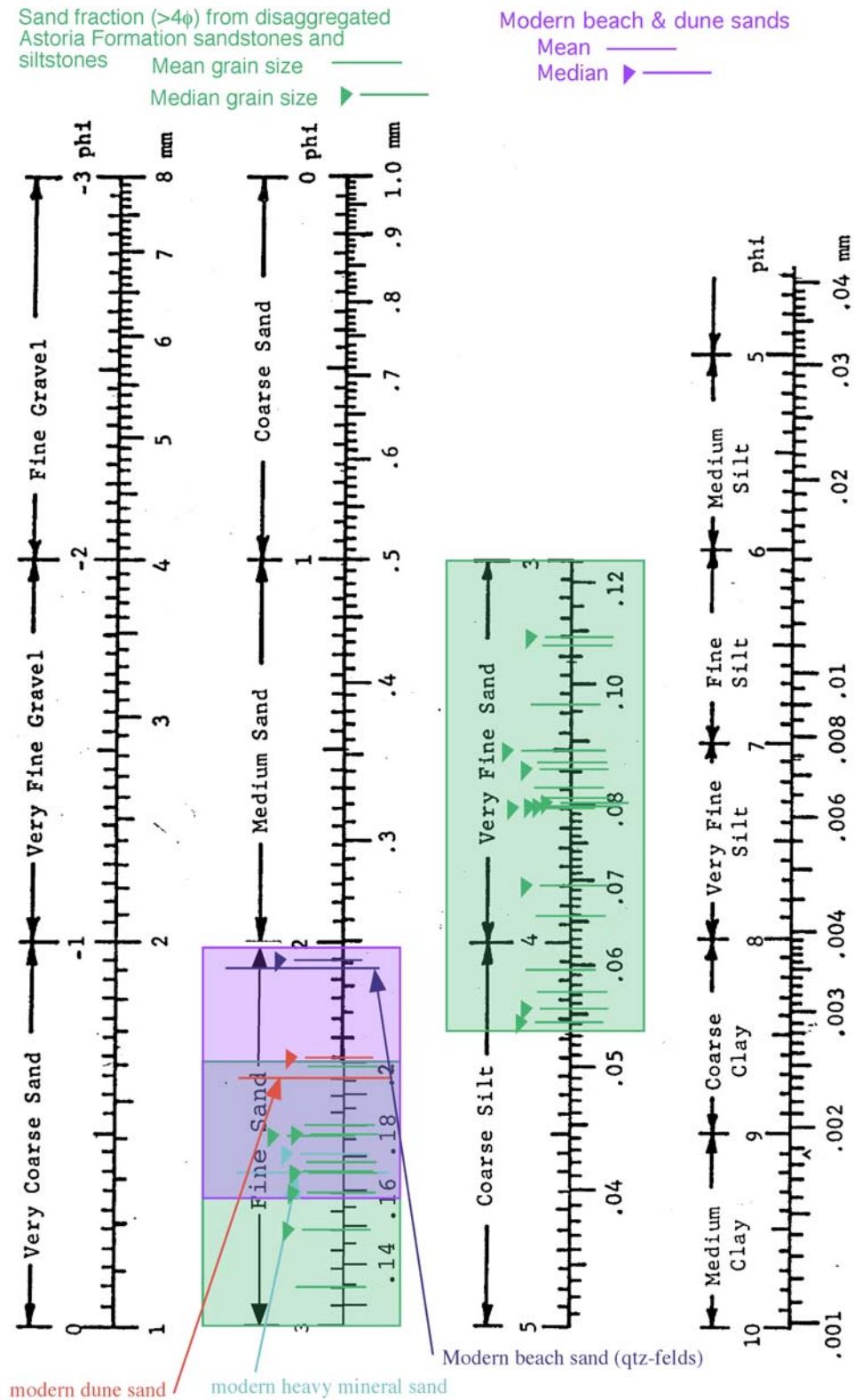


Fig. GMD

Figure 11. Nomogram with ranges of mean and median grain sizes of Astoria Formation (bedrock) samples and modern beach samples.

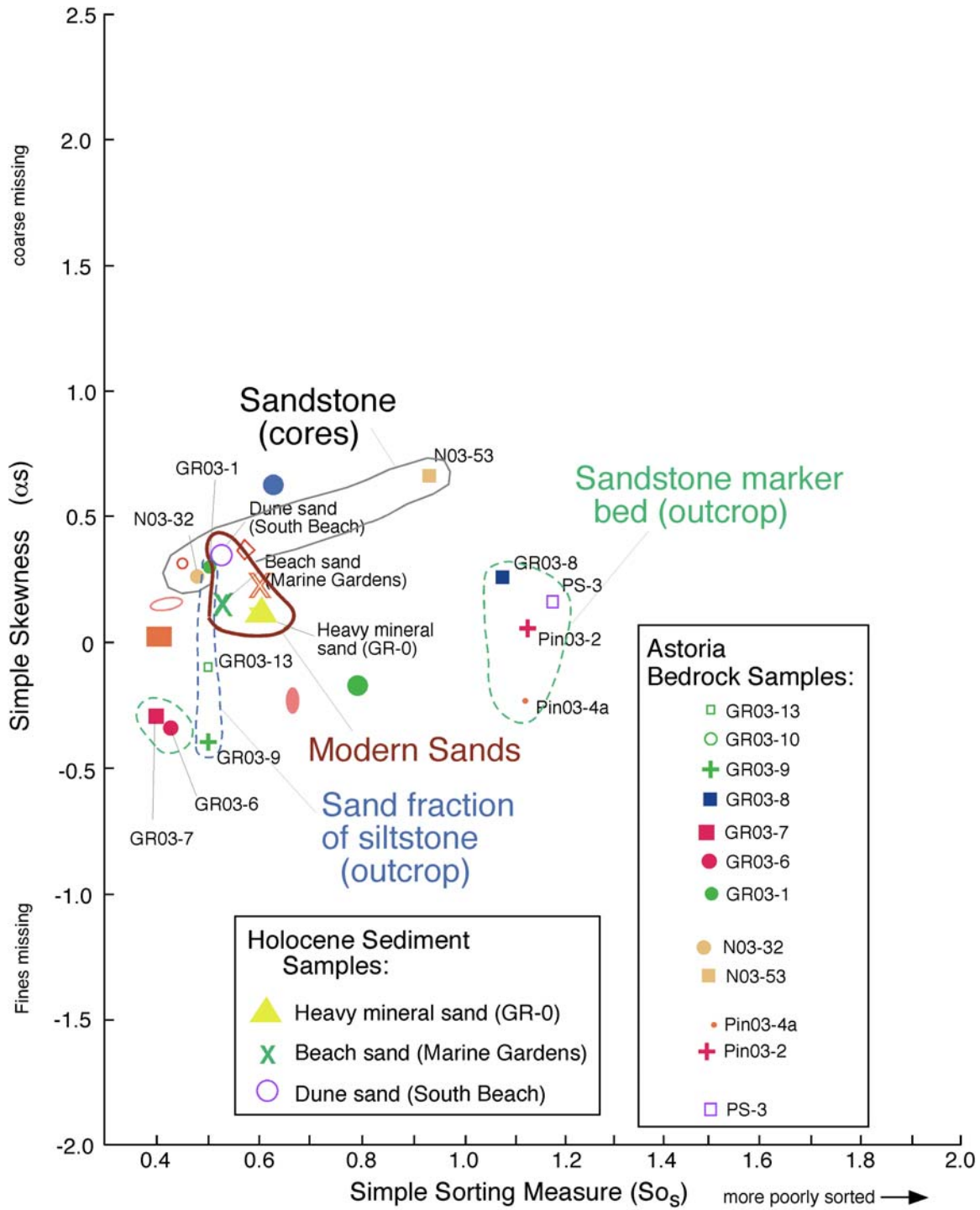


Figure 12. Binary plot of simple skewness versus simple sorting compares sand-sized fraction of Astoria Formation (bedrock) samples with modern sands (beach and dune). After Friedman (1962).

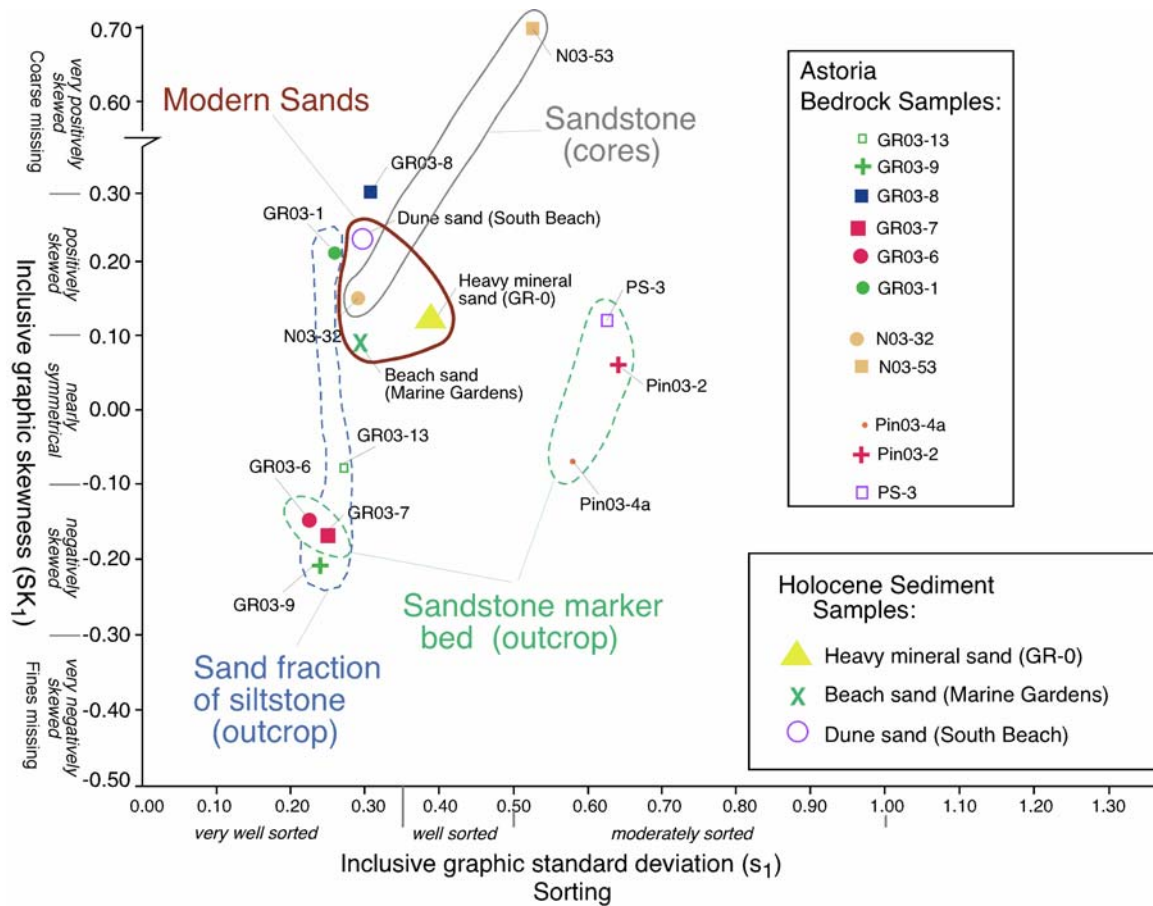


Figure 13. Binary plot of inclusive graphic standard deviation (representing sorting) versus inclusive graphic skewness for sand-sized fraction of Astoria Formation (bedrock) samples compared to modern sand samples (beach and dune). After Friedman (1962).

Table 2. Percentage sand, silt, and clay in samples.

Easting	North- ing	Elev. (m) relative to NAVD 1983	Sample No. **	Location Descrip- tion	Lithology or sediment class.	Principal Minerals	Sample Wt. (g)	Mean (nu- merical) □	Mean (verbal)	Median (nu- merical) □	Median (verbal)	Standard Deviation (s1) □	Simple Sorting (nu- merical) □	Sorting (verbal)	Skewness (numerical) (Sk1) □	Skewness (verbal)	Simple skew- ness (alpha s)	Kurtosis (numerical)	Kurtosis (verbal)
2,218,3 52.78	125,4 94.11		5.55 Pin03-4a	Northern sea cliff section	friable fine to medium grained sandstone	quartz (70-80%), feldspar (5-10%) mica (muscovite) (<3%), heavy minerals (green pyroxenes & opaques) (<6%)	110.09	2.9	fine sand	2.75	fine sand	0.5784	1.13	moderat- ely sorted	-0.07	nearly symmetric- al	-0.25	1.84	very leptokurtic
2,218.3 67.4	125,2 77.24		2.35 GR03-00	Southern sea cliff section	basal gouge	quartz, white & black micas, forams, quartz, translucent heavy minerals	2.74	4.18	coarse silt	4.21	coarse silt	0.3773	0.75	well sorted	-0.55	very negatively skewed		1.81	very leptokurtic
2,218.3 67.4	125,2 77.24		3.1 GR03-1	Southern sea cliff section	Dentalium (fossil scaphopod) -bearing clayey siltstone at base of section	quartz (50%), feldspar (15%), biotite/chlorite (20%), muscovite (10%), opaque heavy minerals (5%), forams (5%)	26.96 (without forams & shell fragments)	3.93	very fine sand	3.85	very fine sand	0.264	0.5	very well sorted	0.21	positively skewed	0.3	4.1	extremely leptokurtic
2,218.3 67.4	125,2 77.24		3.7 GR03-5	Southern sea cliff section	tuffaceous claystone	quartz, white & black micas, feldspar	1	4.07	coarse silt	4.17	coarse silt	0.3442	0.58	very well sorted	-0.37	very negatively skewed		1.57	very leptokurtic
2,218.3 67.4	125,2 77.24		3.85 GR03-6	Southern sea cliff section	fine-gr. calcite- cemented sandstone		13.02	3.65	very fine sand	3.65	very fine sand	0.2288	0.43	very well sorted	-0.15	slightly negatively skewed	-0.35	1.39	leptokurtic
2,218.3 67.4	125,2 77.24		4.6 GR03-7	Southern sea cliff section	Patinopecten sandstone	quartz (50%) feldspar (40%) white mica + biotite/chlorite (<2%), translucent heavy minerals (<2%), opaque heavy minerals (ilmenite/magnetite) (<3%), carbonized wood (3%)	57.3	3.53	very fine sand	3.6	very fine sand	0.2462	0.4	very well sorted	-0.17	slightly negatively skewed	-0.3	1.09	mesokurtic

(table continued)

Table 2 (continued). Percentage sand, silt, and clay in samples.

East	North	Elev. (m) relative to NAVD 1983	Sample No. **	Location Descrip- tion	Lithology or sediment class.	Principal Minerals	Sample Wt.	Mean (nu- merical)	Mean (verbal)	Median (nu- merical)	Median (verbal)	Standard Deviation (s1)	Simple Sorting (nu- merical)	Sorting (verbal)	Skewness (numerical) (Sk1)	Skewness (verbal)	Simple skew- ness (alpha s)	Kurtosis (numerical)	Kurtosis (verbal)
2,218.3 67.4	125.2 77.24	5.25	GR03-8	Southern sea cliff section	shallow marine fine-gr sandstone	quartz (70%), lithics (24%), feldspars (5%)	128.03	2.3	fine sand	2.65	fine sand	0.3133	1.075	very well sorted	0.3	positively skewed	0.25	1.47	leptokurtic
2,218.3 67.4	125.2 77.24	6.75	GR03-9	Southern sea cliff section	clayey sandy siltstone - 8" above 10-11 ft yellow sandstone marker bed	quartz (60%), feldspar (10-15%), biotite (5%), white mica (15%), opaque heavy minerals (5%)	11.32	3.63	very fine sand	3.65	very fine sand	0.239	0.5	very well sorted	-0.21	negatively skewed	-0.4	2.05	very leptokurtic
2,218.3 67.4	125.2 77.24	8.28	GR03-10	Southern sea cliff section	clayey sandy siltstone 3 to 5 ft below top of sea cliff	quartz (50%), feldspar (20%), mica (10%) opaques (5%), shell fragments (<3%)	7.21	3.5	very fine sand	3.5	very fine sand	0.2538	0.43	very well sorted	-0.06	nearly symmetrical		1.16	leptokurtic
2,218.3 67.4	125.2 77.24	14.83	GR03-13	Southern sea cliff section	weathered clayey sandy siltstone at 8 ft below top of section	quartz (60%), feldspar (30%), micas (5%), opaque heavy minerals (3%), translucent heavy minerals (2%)	41.65	3.6	very fine sand	3.65	very fine sand	0.264	0.5	very well sorted	-0.08	nearly symmetrical	-0.1	1.37	leptokurtic
2,218.4 30.39	125.3 83.68	3.7	N03-32	LT-3 @ 68.4 ft	pumice-bearing fine- to medium-gr. fossiliferous sandstone		54.53	3.23	very fine sand	3.2	very fine sand	0.2939	0.48	very well sorted	0.15	slightly positively skewed	0.25	0.87	platykurtic
2,218.5 15.77	125.3 74.33	6.3	N03-53	LT-1 @ 58.8 ft	medium-gr. sandstone	quartz (75%) lithics (25%)	92.78	2.57	fine sand	2.5	fine sand	0.5303	0.93	moderately sorted	0.7	very positively skewed	0.65	1.26	leptokurtic
2,218.4 80.36	125.3 83.12	8.1	N03-XX	LT-2 @ 54 ft	clayey siltstone	quartz, feldspar, white mica, black mica, pyrite, forams	2.94	3.38	very fine sand	3.64	very fine sand	0.6563	1.09	moderately sorted	-1.38	very negatively skewed		0.95	mesokurtic
2,218.3 52.78	125.4 94.11	4.35	Pin03-2	Northern sea cliff section	calcite-cemented fine- to medium-gr silty sandstone	quartz (70%), feldspar (20%) green translucent lithic (5%), opaque heavy minerals (2%), mica (<1%)	103.6	2.6	fine sand	2.6	fine sand	0.6409	1.125	moderately sorted	0.06	nearly symmetrical	0.05	1.42	leptokurtic

(table continued)

Table 2 (continued). Percentage sand, silt, and clay in samples.

Easting	North- ing	Elev. (m) relative to NAVD 1983	Sample No. **	Location Descrip- tion	Lithology or sediment class.	Principal Minerals	Sample Wt.	Mean (nu- merical)	Mean (verbal)	Median (nu- merical)	Median (verbal)	Standard Deviation (s1)	Simple Sorting (nu- merical)	Sorting (verbal)	Skewness (numerical) (Sk1)	Skewness (verbal)	Simple skew- ness (alpha s)	Kurtosis (numerical)	Kurtosis (verbal)
2,218,3 57.08	125,3 92.03	4.86	PS-3	Middle sea cliff section	calcite- cemented fine- to medium-gr sandstone	quartz (70%) lithics (30%)	195.88	2.47	fine sand	2.5	fine sand	0.63	1.175	moderat- ely sorted	0.12	slightly positively skewed	0.15	1.48	leptokurtic
		6(?)	Holocene Dune	South Beach State Park (Newpor- t)	dune sand	quartz (55%), feldspar (30%), translucent heavy minerals (pyroxene, garnet, hornblende, and others) (8%), opaque heavy minerals (7%)	202.48	2.35	fine sand	2.3	fine sand	0.2966	0.525	very well sorted	0.23	positively skewed	0.35	1.43	leptokurtic
		2(?)	Marine Gardens beach sand	Marine Gardens , Otter Rock	winter beach sand		173.11	2.07	fine sand	2.05	fine sand	0.2966	0.525	very well sorted	0.09	nearly symmetric al	0.15	1.08	mesokurtic
2,218,3 64	125,2 77	2.2	GR0 Heavy mineral beach sand	modern beach, Southern sea cliff section	winter beach sand		181.6	2.6	fine sand	2.55	fine sand	0.3943	0.6	well sorted	0.12	positively skewed	0.1	0.89	platykurtic
															Positive skewness = coarse fraction missing				Leptokurtic = very tall peak
															Negative skewness = fine fraction missing				Mesokurtic = close to normal curve
																			Platykurtic = flat curve

\*\* All samples for size analysis, thin section, SEM, and XRD from the Middle and Northern sea cliff sections were rock fall collected on the public beach (sand) and correlated to the adjacent sea cliff sections. These sections were measured from the public beach by visually estimating thickness of units using a 3-m pole tilted perpendicular to the angle of dip of the strata in the sea cliff. Samples from the Southern sea cliff section, which was described and measured with a Jacobs staff and Abney level, were collected directly from the coastal sea cliff which is on State of Oregon.



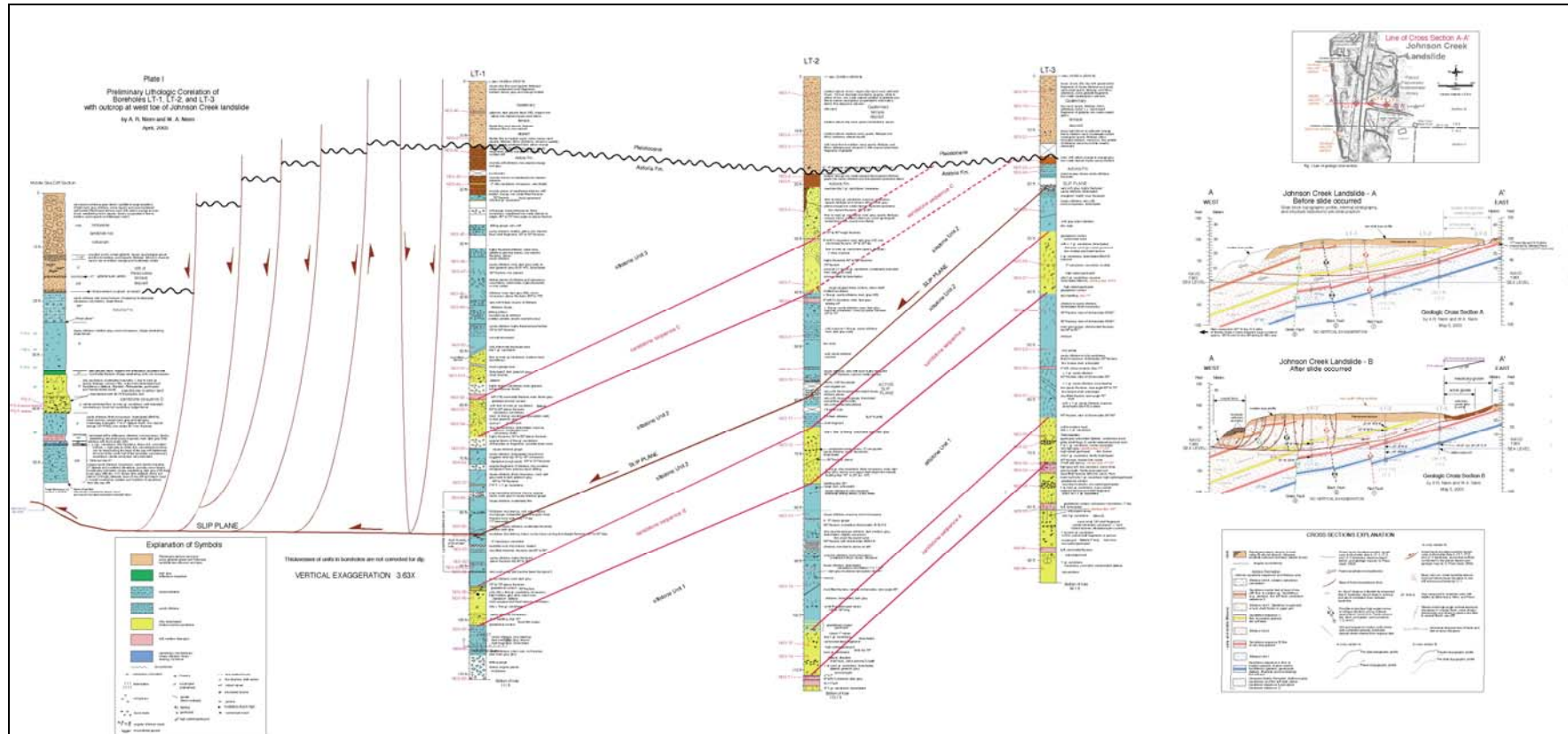


Plate I. East-west correlation diagram of LT-1, LT-2, and LT-3 Boreholes with Middle Sea Cliff Measured Section. Plate is best viewed at zoom level of ~400 percent.

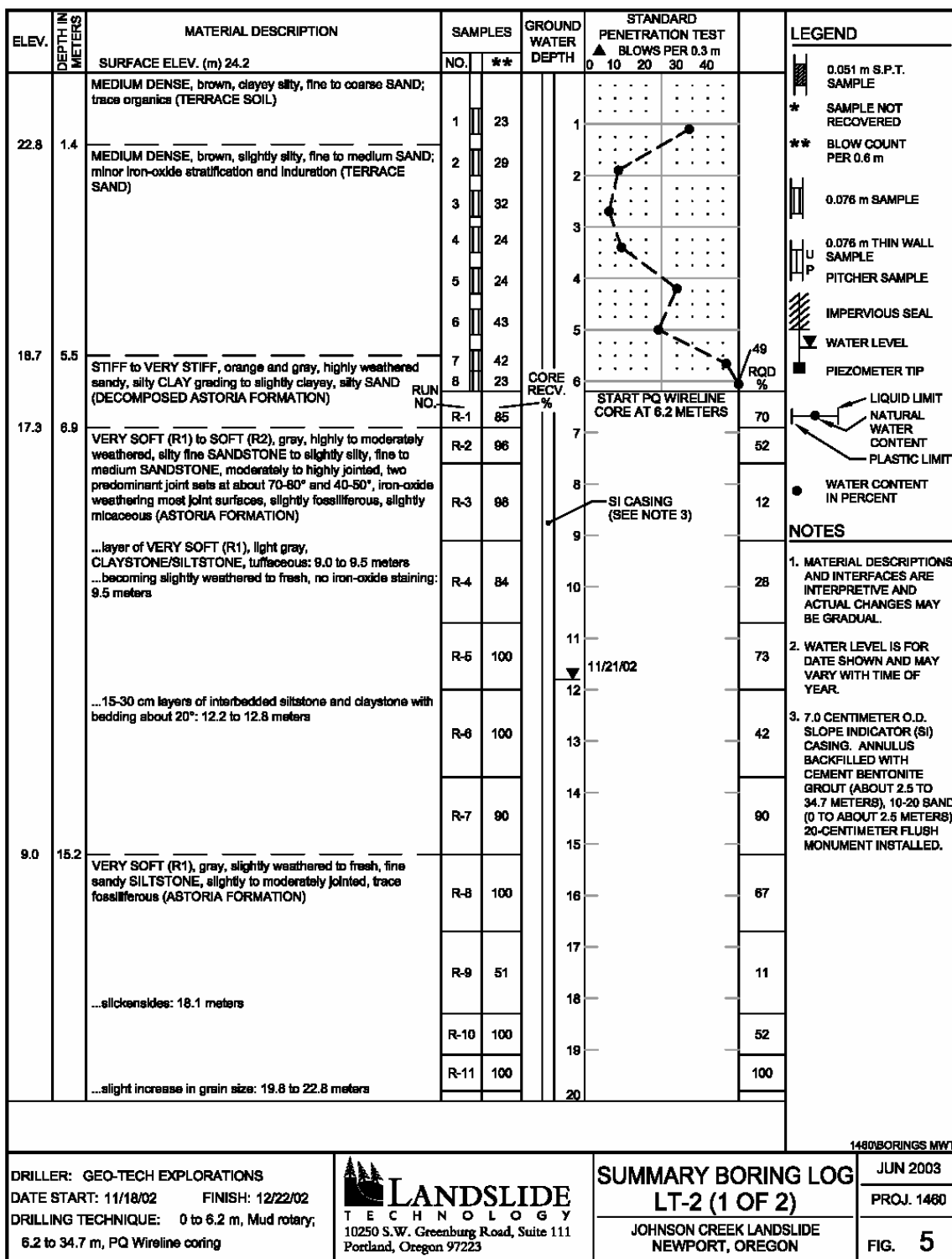


[illegible]

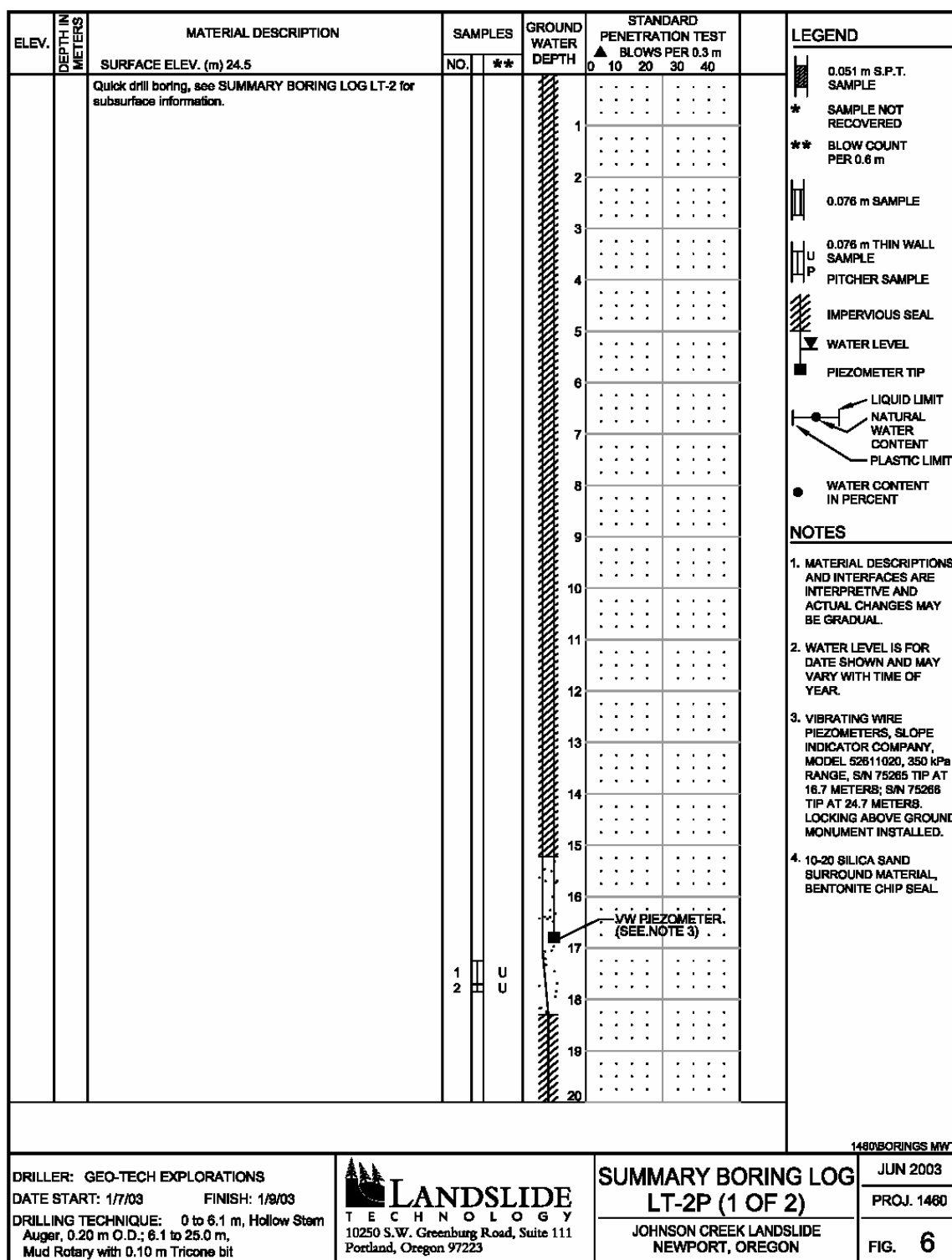
[illegible]



ELEV.	DEPTH IN METERS	MATERIAL DESCRIPTION	SAMPLES		GROUND WATER DEPTH	STANDARD PENETRATION TEST					LEGEND
			NO.	**		BLOWS PER 0.3 m					
		SURFACE ELEV. (m) 24.7				0	10	20	30	40	
		(continued from previous page)									



ELEV.	DEPTH IN METERS	MATERIAL DESCRIPTION	RUN NO.	CORE RECV. %	GROUND WATER DEPTH	STANDARD PENETRATION TEST BLOWS PER 0.3 m	RQD %	LEGEND
		SURFACE ELEV. (m) 24.2				0 10 20 30 40		0.051 m S.P.T. SAMPLE SAMPLE NOT RECOVERED BLOW COUNT PER 0.6 m 0.076 m SAMPLE 0.076 m THIN WALL SAMPLE PITCHER SAMPLE IMPERVIOUS SEAL WATER LEVEL PIEZOMETER TIP LIQUID LIMIT NATURAL WATER CONTENT PLASTIC LIMIT WATER CONTENT IN PERCENT
0.7	23.5	(continued from previous page)  ...bedding dipping 15-20°: 21.5 meters	R-12	96	21		96	0.051 m S.P.T. SAMPLE SAMPLE NOT RECOVERED BLOW COUNT PER 0.6 m 0.076 m SAMPLE 0.076 m THIN WALL SAMPLE PITCHER SAMPLE IMPERVIOUS SEAL WATER LEVEL PIEZOMETER TIP LIQUID LIMIT NATURAL WATER CONTENT PLASTIC LIMIT WATER CONTENT IN PERCENT <b>NOTES</b> 1. MATERIAL DESCRIPTIONS AND INTERFACES ARE INTERPRETIVE AND ACTUAL CHANGES MAY BE GRADUAL. 2. WATER LEVEL IS FOR DATE SHOWN AND MAY VARY WITH TIME OF YEAR. 3. 7.0 CENTIMETER O.D. SLOPE INDICATOR (SI) CASING. ANNULUS BACKFILLED WITH CEMENT BENTONITE GROUT (ABOUT 2.5 TO 34.7 METERS), 10-20 SAND (0 TO ABOUT 2.5 METERS). 20-CENTIMETER FLUSH MONUMENT INSTALLED.
			R-13	100	22		100	
			R-14	70	23		54	
		VERY SOFT (R1), gray, slightly weathered to fresh, clayey SILTSTONE, moderately to highly jointed, predominantly at 45 to 65°, trace fossiliferous, trace micaceous (ASTORIA FORMATION) ...occasional slickensides with 80-90° rake: 24.7 to 29.0 meters	R-15	24	24		0	
			R-16	100	25		100	
			R-17	67	26		67	
			R-18	80	27		80	
			R-19	100	28		100	
			R-20	100	29		100	
			R-21	100	30		100	
-7.5	31.7	SOFT (R2), gray, slightly weathered to fresh, silty fine SANDSTONE, slightly fractured to massive, fossiliferous, micaceous (ASTORIA FORMATION)			31		100	0.051 m S.P.T. SAMPLE SAMPLE NOT RECOVERED BLOW COUNT PER 0.6 m 0.076 m SAMPLE 0.076 m THIN WALL SAMPLE PITCHER SAMPLE IMPERVIOUS SEAL WATER LEVEL PIEZOMETER TIP LIQUID LIMIT NATURAL WATER CONTENT PLASTIC LIMIT WATER CONTENT IN PERCENT <b>NOTES</b> 1. MATERIAL DESCRIPTIONS AND INTERFACES ARE INTERPRETIVE AND ACTUAL CHANGES MAY BE GRADUAL. 2. WATER LEVEL IS FOR DATE SHOWN AND MAY VARY WITH TIME OF YEAR. 3. 7.0 CENTIMETER O.D. SLOPE INDICATOR (SI) CASING. ANNULUS BACKFILLED WITH CEMENT BENTONITE GROUT (ABOUT 2.5 TO 34.7 METERS), 10-20 SAND (0 TO ABOUT 2.5 METERS). 20-CENTIMETER FLUSH MONUMENT INSTALLED.
			R-22	58	32		58	
			R-23	100	33		100	
-10.5	34.7	...SOFT (R2) to MEDIUM HARD (R3), light gray, CLAYSTONE, tuffaceous: 33.8 to 34.4 meters Bottom of boring: 34.7 meters			34		100	0.051 m S.P.T. SAMPLE SAMPLE NOT RECOVERED BLOW COUNT PER 0.6 m 0.076 m SAMPLE 0.076 m THIN WALL SAMPLE PITCHER SAMPLE IMPERVIOUS SEAL WATER LEVEL PIEZOMETER TIP LIQUID LIMIT NATURAL WATER CONTENT PLASTIC LIMIT WATER CONTENT IN PERCENT <b>NOTES</b> 1. MATERIAL DESCRIPTIONS AND INTERFACES ARE INTERPRETIVE AND ACTUAL CHANGES MAY BE GRADUAL. 2. WATER LEVEL IS FOR DATE SHOWN AND MAY VARY WITH TIME OF YEAR. 3. 7.0 CENTIMETER O.D. SLOPE INDICATOR (SI) CASING. ANNULUS BACKFILLED WITH CEMENT BENTONITE GROUT (ABOUT 2.5 TO 34.7 METERS), 10-20 SAND (0 TO ABOUT 2.5 METERS). 20-CENTIMETER FLUSH MONUMENT INSTALLED.
					35			
								1480 BORINGS MWT
DRILLER: GEO-TECH EXPLORATIONS DATE START: 11/18/02      FINISH: 12/22/02 DRILLING TECHNIQUE: 0 to 6.2 m, Mud rotary; 6.2 to 34.7 m, PQ Wireline coring			<b>LANDSLIDE TECHNOLOGY</b> 10250 S.W. Greenburg Road, Suite 111 Portland, Oregon 97223			<b>SUMMARY BORING LOG</b> <b>LT-2 (2 OF 2)</b> JOHNSON CREEK LANDSLIDE NEWPORT, OREGON		JUN 2003 PROJ. 1480 FIG. <b>5</b>

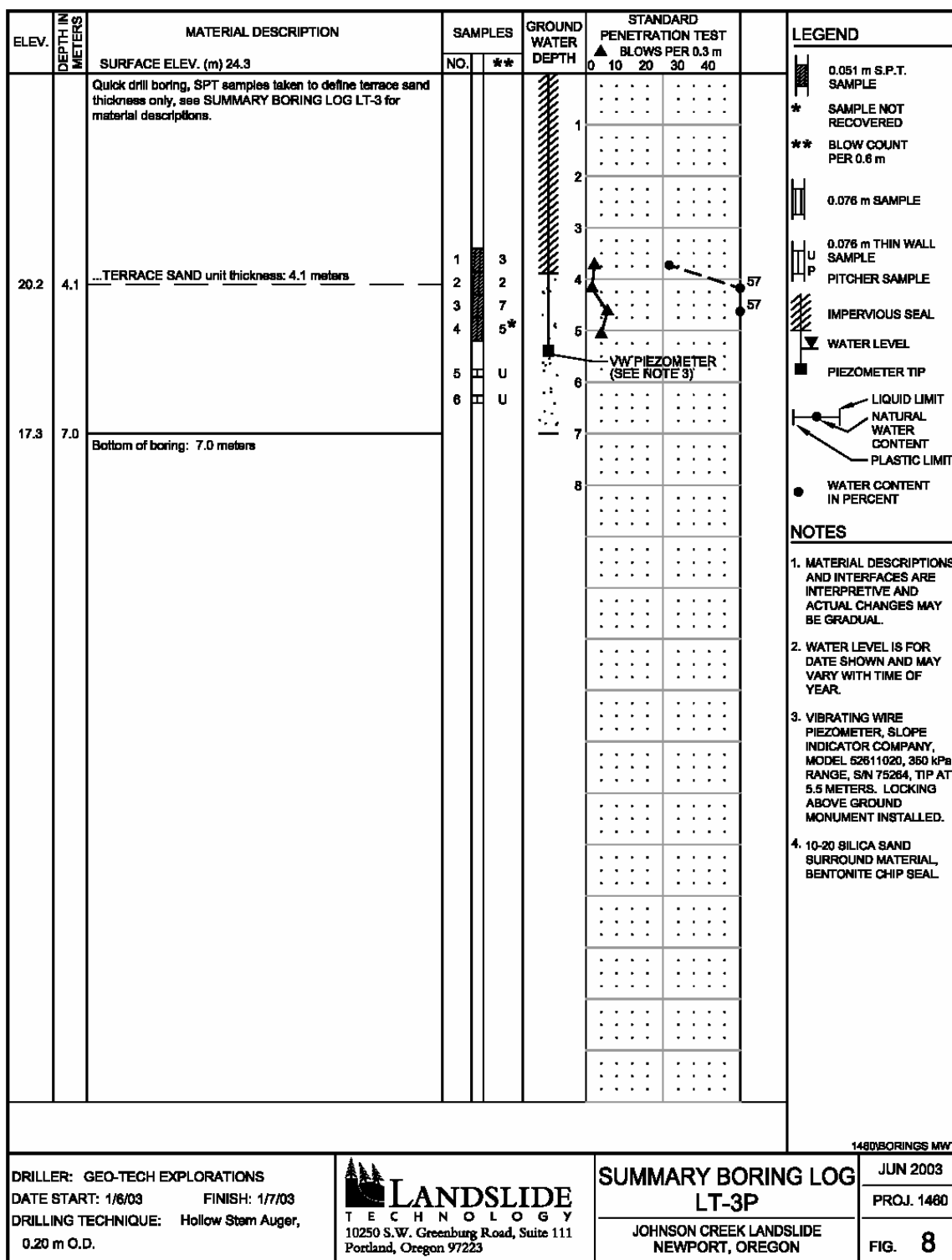




[illegible]

ELEV.	DEPTH IN METERS	MATERIAL DESCRIPTION	SAMPLES		GROUND WATER DEPTH	STANDARD PENETRATION TEST ▲ BLOWS PER 0.3 m	LEGEND	
			NO.	**				
		SURFACE ELEV. (m) 24.0						
22.7	1.3	LOOSE, brown, clayey, silty, fine SAND; high organic content, rootlets, wood (FILL)	1	4	1		0.051 m S.P.T. SAMPLE	
			2	4	2		* SAMPLE NOT RECOVERED	
			3	3	3		** BLOW COUNT PER 0.6 m	
			4	6	4		0.076 m SAMPLE	
			5	9	5		0.076 m THIN WALL SAMPLE	
19.0	5.0	...increase in fines: 4.5 meters					PITCHER SAMPLE	
		VERY SOFT (R1) to SOFT (R2), gray, moderately to highly weathered, sandy SILTSTONE; moderately to highly jointed, trace iron-oxide staining, trace fossiliferous (ASTORIA FORMATION)	6	20	6		IMPERVIOUS SEAL	
		...becoming slightly weathered to fresh, no iron-oxide staining: 6.4 meters	R-1	26	6		WATER LEVEL	
			R-2	100	7		PIEZOMETER TIP	
			R-3	98	8		LIQUID LIMIT	
15.0	9.0	SOFT (R2), gray, slightly weathered to fresh, silty fine SANDSTONE; moderately jointed, predominantly 50-70°, slickensides at 11.3 meters, fossiliferous, micaceous (ASTORIA FORMATION)	R-4	94	9		NATURAL WATER CONTENT	
			R-5	100	10		PLASTIC LIMIT	
			R-6	94	11		WATER CONTENT IN PERCENT	
			R-7	100	12		NOTES	
			R-8	92	13		1. MATERIAL DESCRIPTIONS AND INTERFACES ARE INTERPRETIVE AND ACTUAL CHANGES MAY BE GRADUAL.	
11.6	12.4	VERY SOFT (R1) to SOFT (R2), gray, fresh, slightly sandy SILTSTONE; moderately to highly jointed, occasional slickensides with 80-90° rake, brecciated at 14.5 meters (ASTORIA FORMATION)	R-9	98	14		2. WATER LEVEL IS FOR DATE SHOWN AND MAY VARY WITH TIME OF YEAR.	
			R-10	100	15		3. 7.0 CENTIMETER O.D. SLOPE INDICATOR (SI) CASING. ANNULUS BACKFILLED WITH CEMENT BENTONITE GROUT (3.8 TO 28.7 METERS) AND 10-20 SAND (0 TO 3.8 METERS). 20-CENTIMETER FLUSH MONUMENT INSTALLED.	
			R-11	100	16			
					17			
					18			
7.8	16.2	SOFT (R2), gray, slightly weathered to fresh, silty fine SANDSTONE; moderately to highly jointed, predominantly at 60-70°, occasional slickensides with 80-90° rake, bedding about 15-17°, fossiliferous, micaceous (ASTORIA FORMATION)			19			
		...becomes slightly fractured to massive: 19.4 meters			20			
1480 BORINGS MWT								
DRILLER: GEO-TECH EXPLORATIONS					SUMMARY BORING LOG LT-3 (1 OF 2) JOHNSON CREEK LANDSLIDE NEWPORT, OREGON			JUN 2003
DATE START: 11/22/02 FINISH: 11/27/02								PROJ. 1480
DRILLING TECHNIQUE: 0 to 5.3 m, Mud rotary;								FIG. 7
5.3 to 28.7 m, PQ Wireline coring								





**APPENDIX C:**  
**TEST PITS AT THE TOE OF THE JOHNSON CREEK LANDSLIDE**

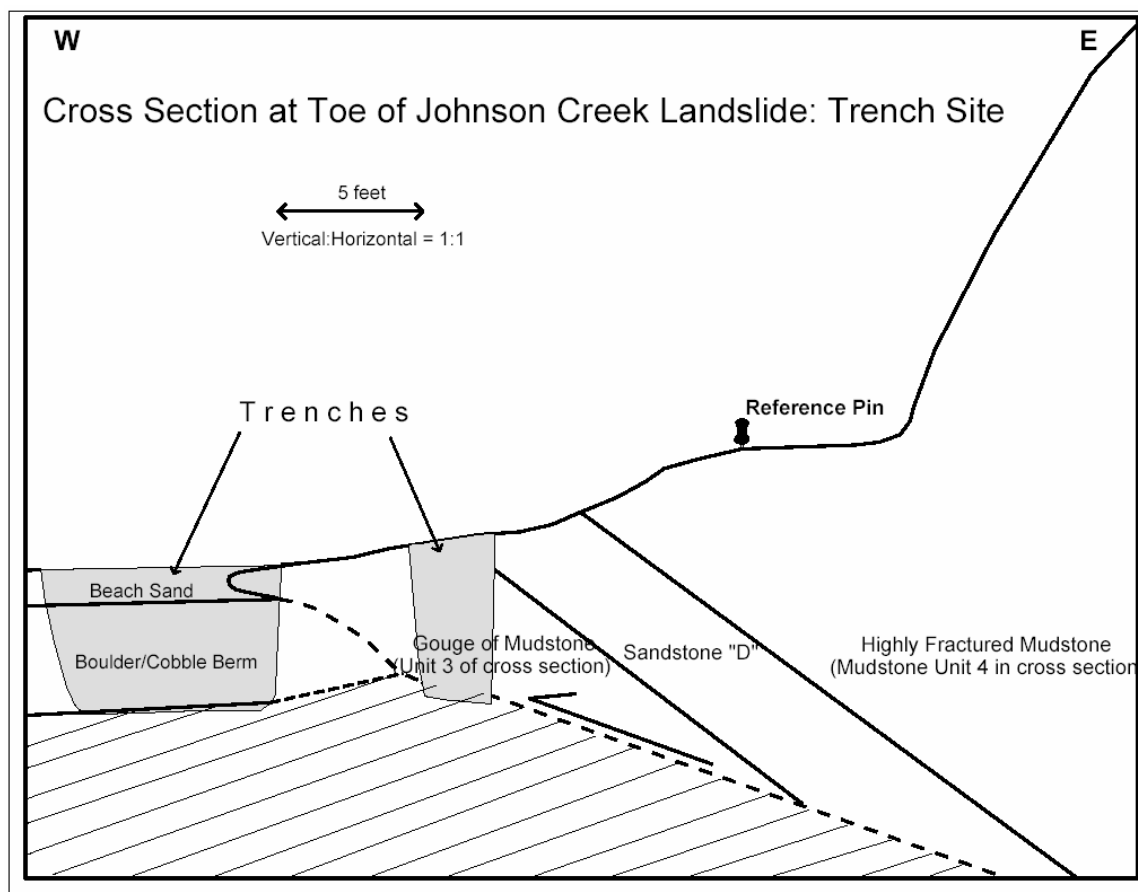


Figure 1. Cross section showing Astoria Formation mudstone and sandstone of the Johnson Creek Landslide overriding an apron of beach cobbles at the toe of the landslide. Slanted line pattern indicates west-dipping, undisturbed Astoria Formation below the landslide. Location of cross section is shown in Figure 6 of the main text.

**APPENDIX D:**  
**SLIDE MOVEMENT FROM SURVEYS OF IRON MARKER PINS**  
**OCTOBER 24, 2002 AND APRIL 17, 2003**

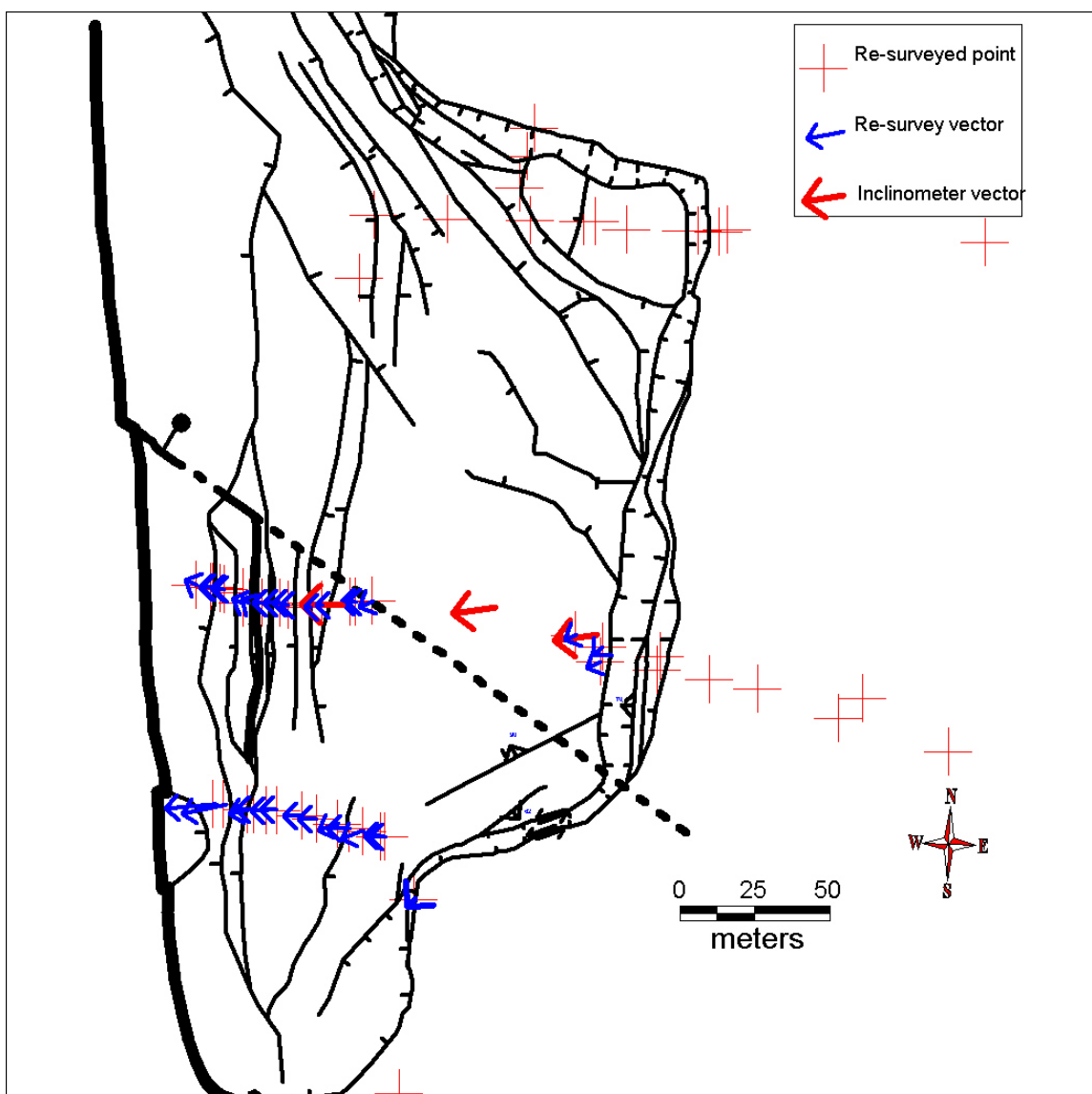


Figure 1. Qualitative vectors drawn in direction of slide movement for steel stakes surveyed October 24, 2002 and April 17, 2003 (blue arrows) and for inclinometer data (red arrows). Relative lengths of blue arrows correspond roughly to relative amount of movement. Red crosses without arrows are points where slide movement between surveys was less than the error in the measurement.

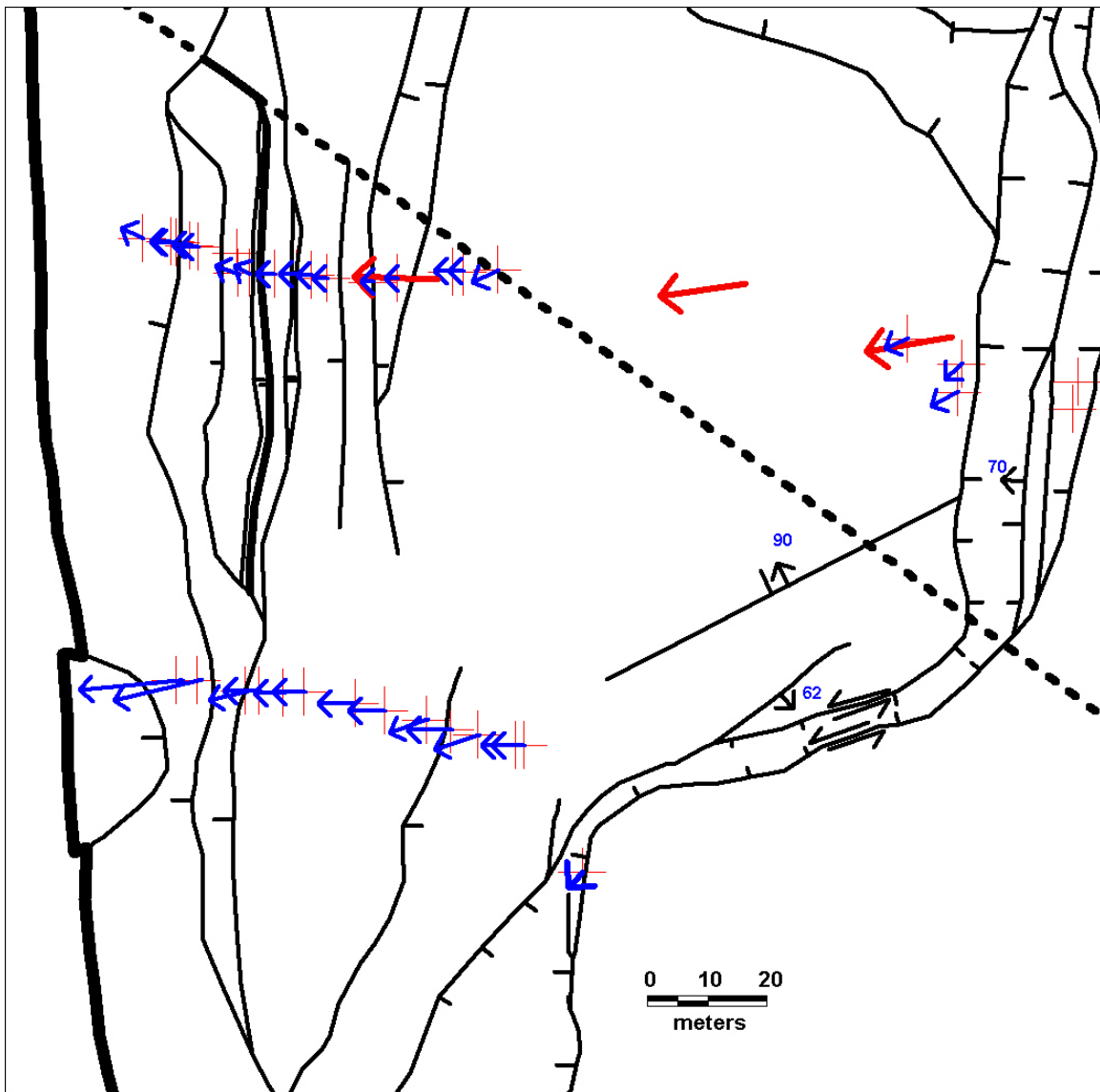


Figure 2. Close-up of southern part of Figure 1.



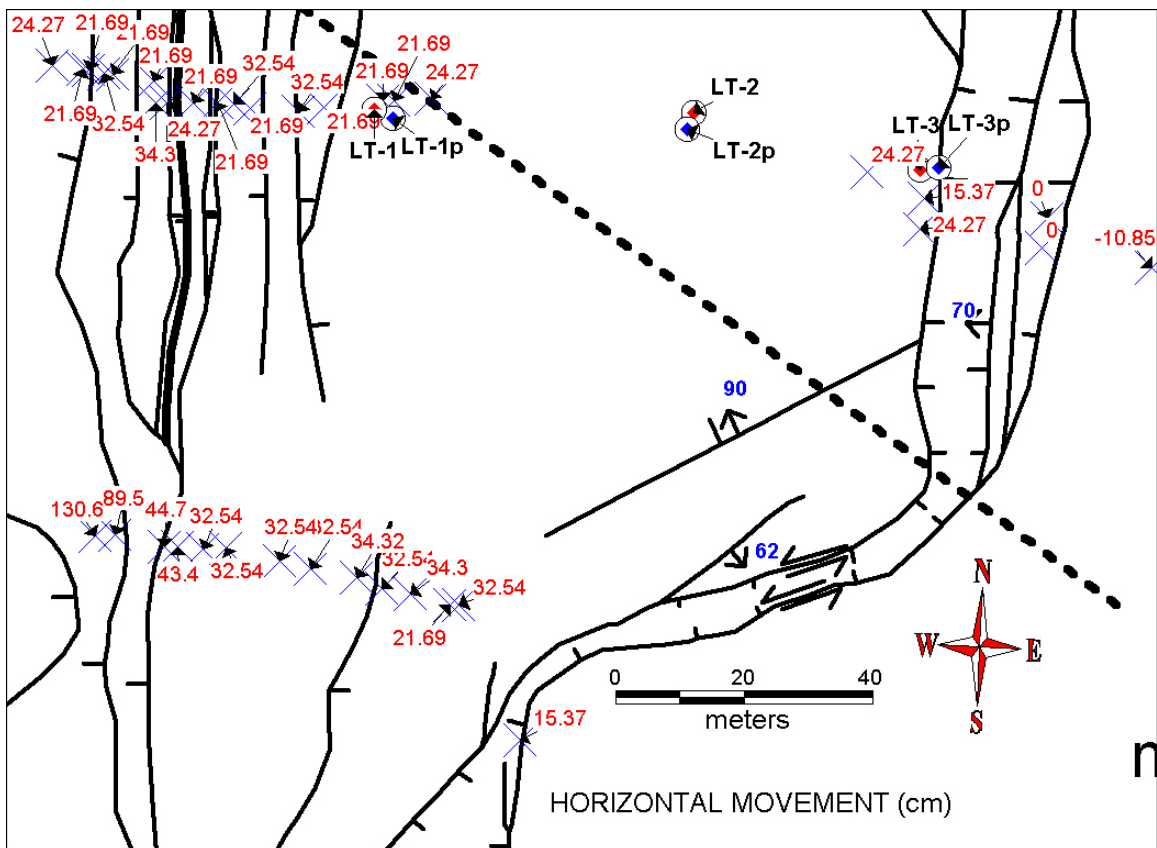


Figure 3. Horizontal movement (cm) at steel stakes (blue crosses) in southern part of landslide. Boreholes are also shown (circles with diamonds). Movement east of the headwall of -10.85 cm (eastward movement) is survey error, so this is the approximate error of the data.

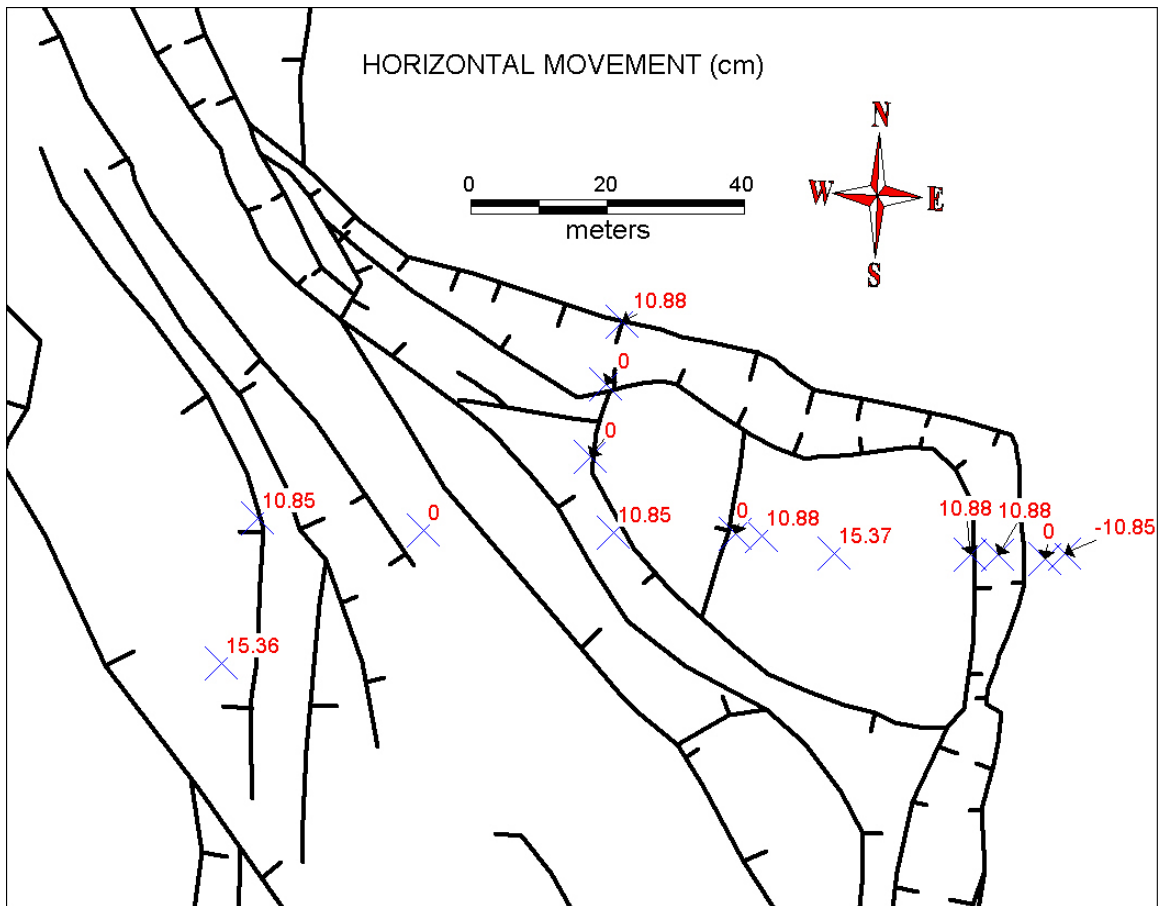


Figure 4. Horizontal movement (cm) at steel stakes (blue crosses) in northern part of landslide. Note that most movement less than survey error.

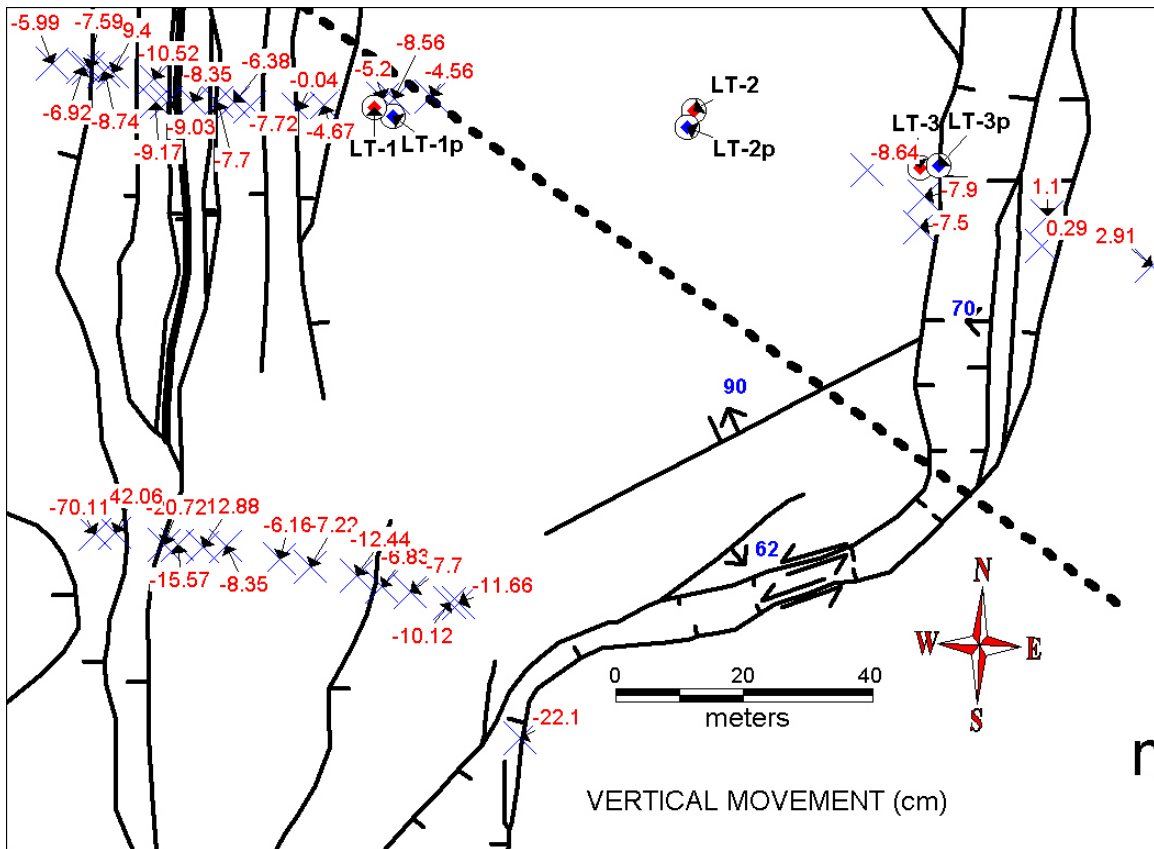


Figure 5. Vertical movement (cm) at steel stakes (blue crosses) in southern part of landslide. Movement east of the headwall of +2.91 to +5.51cm (upward) is survey error, so this is the approximate error of the data. There is one survey stake east of the headwall with an error of -129.88 cm, but this is probably a local anomaly caused by tampering with the steel stake or transcription error by the surveyor.

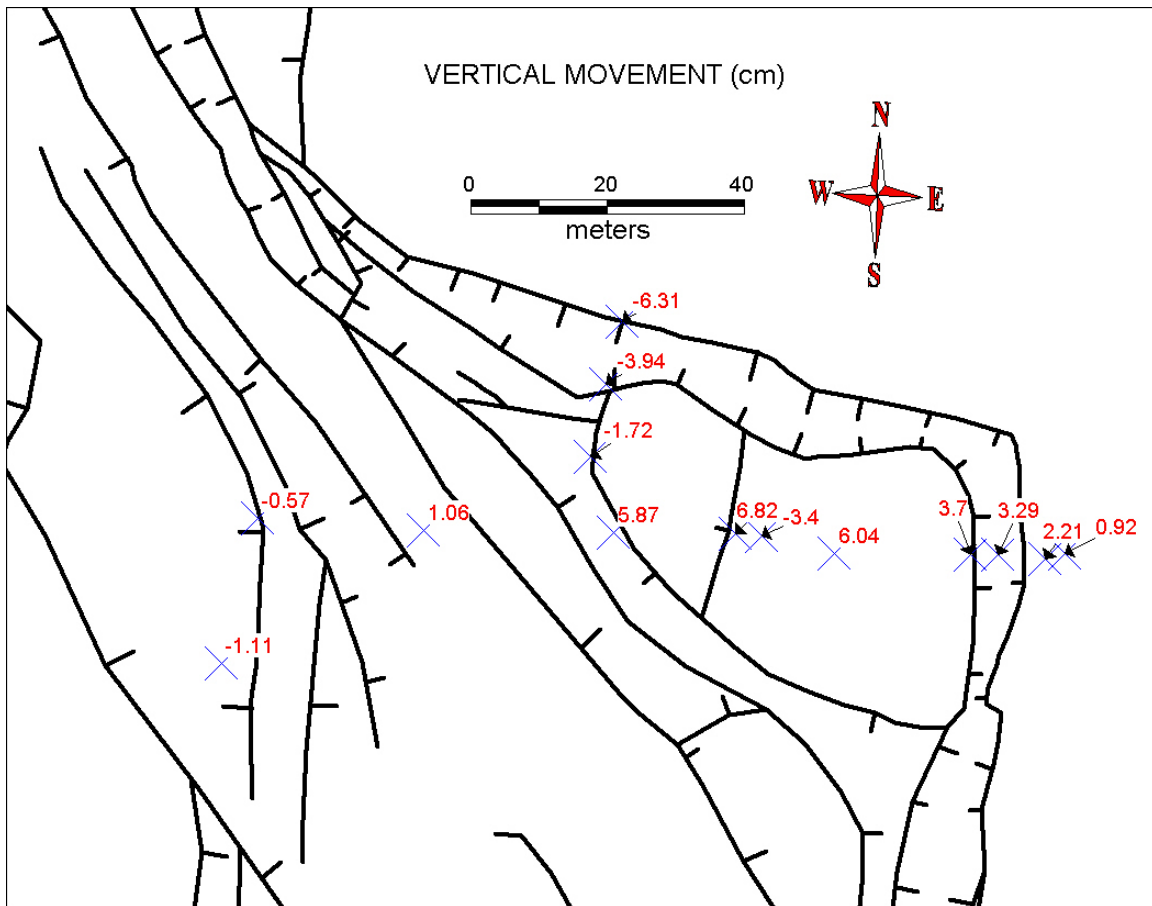


Figure 6. Vertical movement (cm) at steel stakes (blue crosses) in northern part of landslide. Note that all values are below survey error.

## APPENDIX E: LINE-OF-SIGHT SURVEYS ON HIGHWAY 101

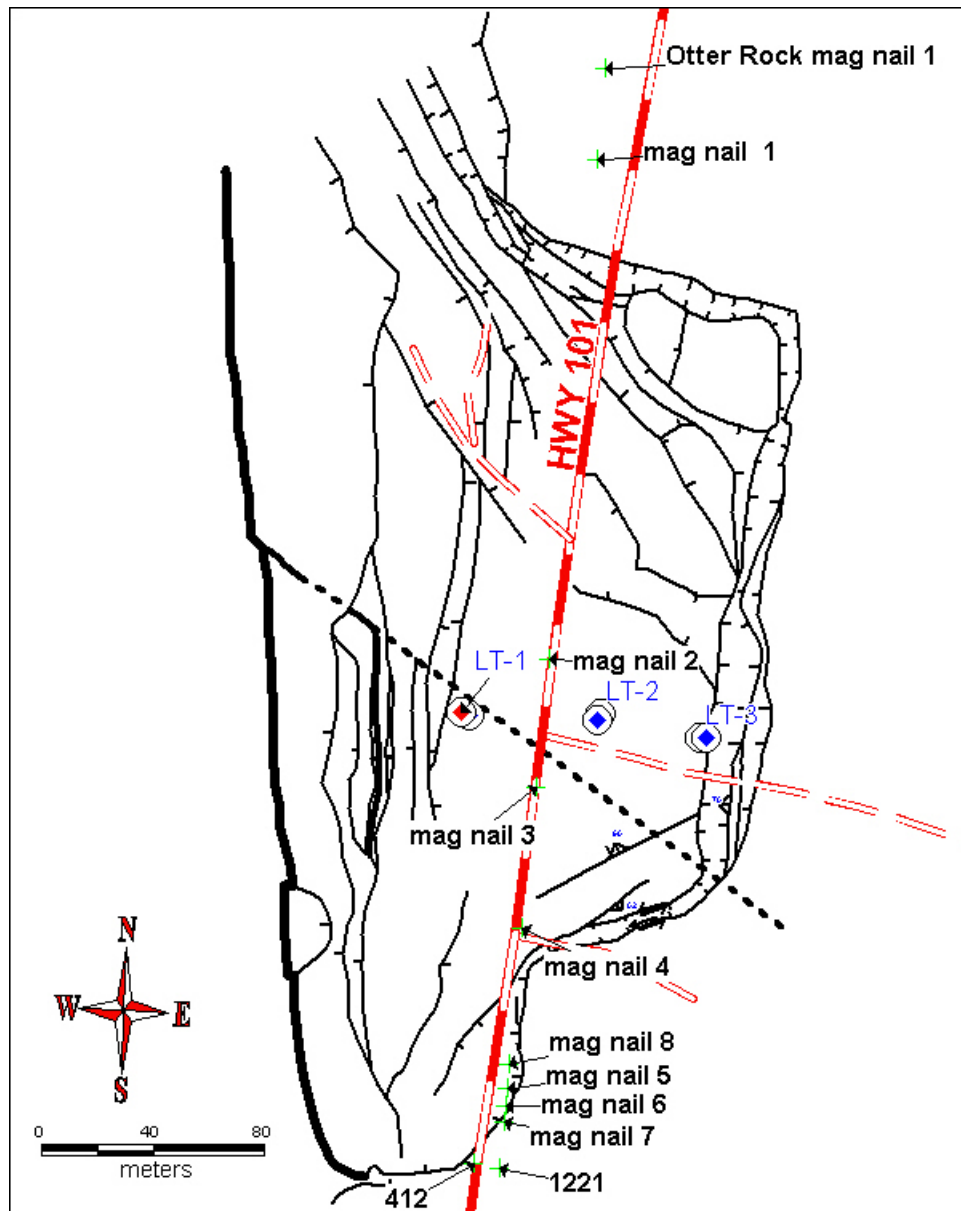


Figure 1. Location of line-of-sight survey pins. All surveys were done with a total station to sub-centimeter accuracies.

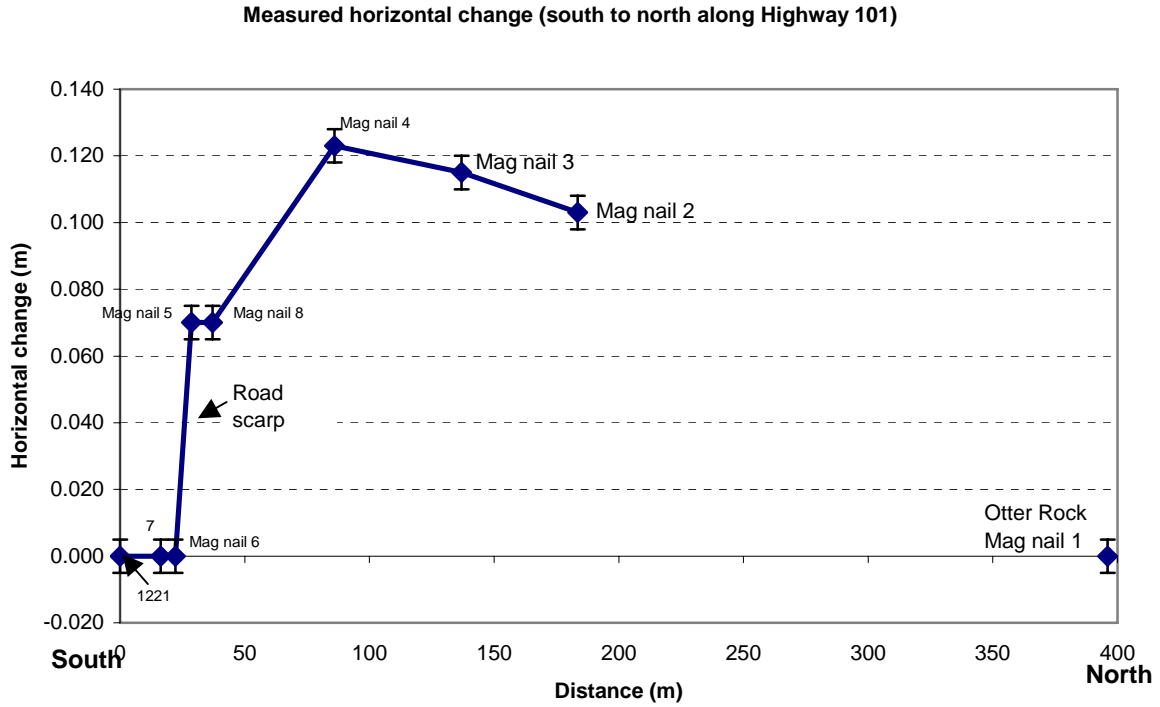


Figure 2. Horizontal change along Highway 101 January 16, 2003 to February 4, 2003;  
(+) = westward movement; (-) = eastward movement.

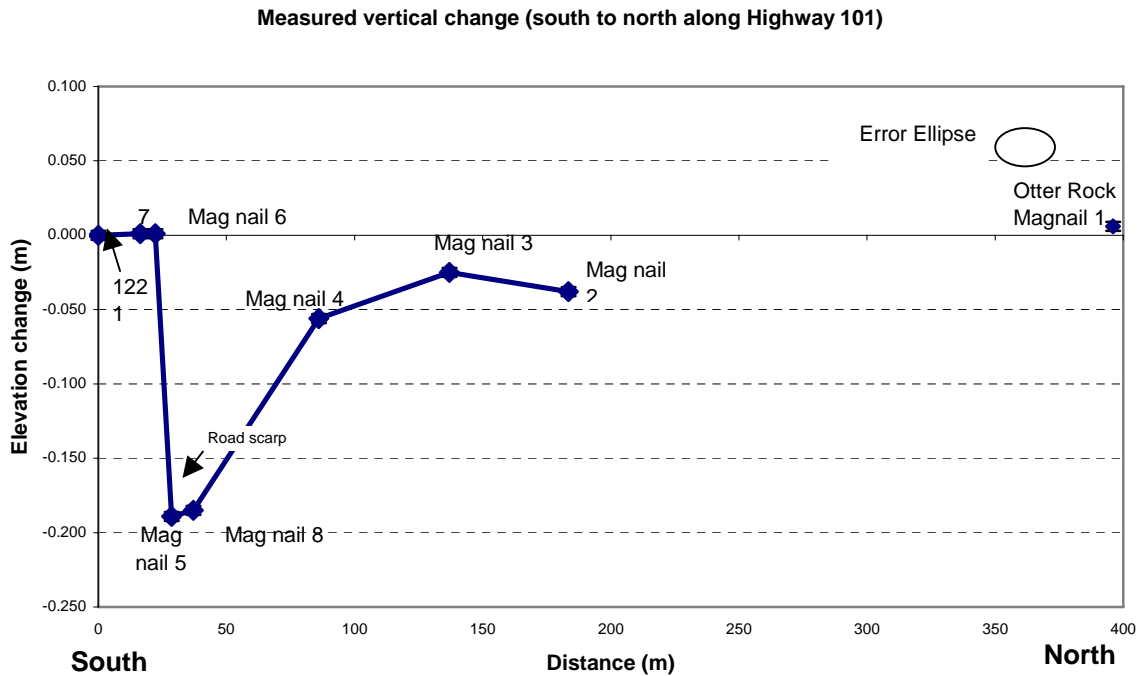


Figure 3. Vertical change along Highway 101 January 16, 2003 to February 4, 2003;  
(-) = down; (+) = up.

## APPENDIX F: EROSION PIN DATA AT THE SEA CLIFF

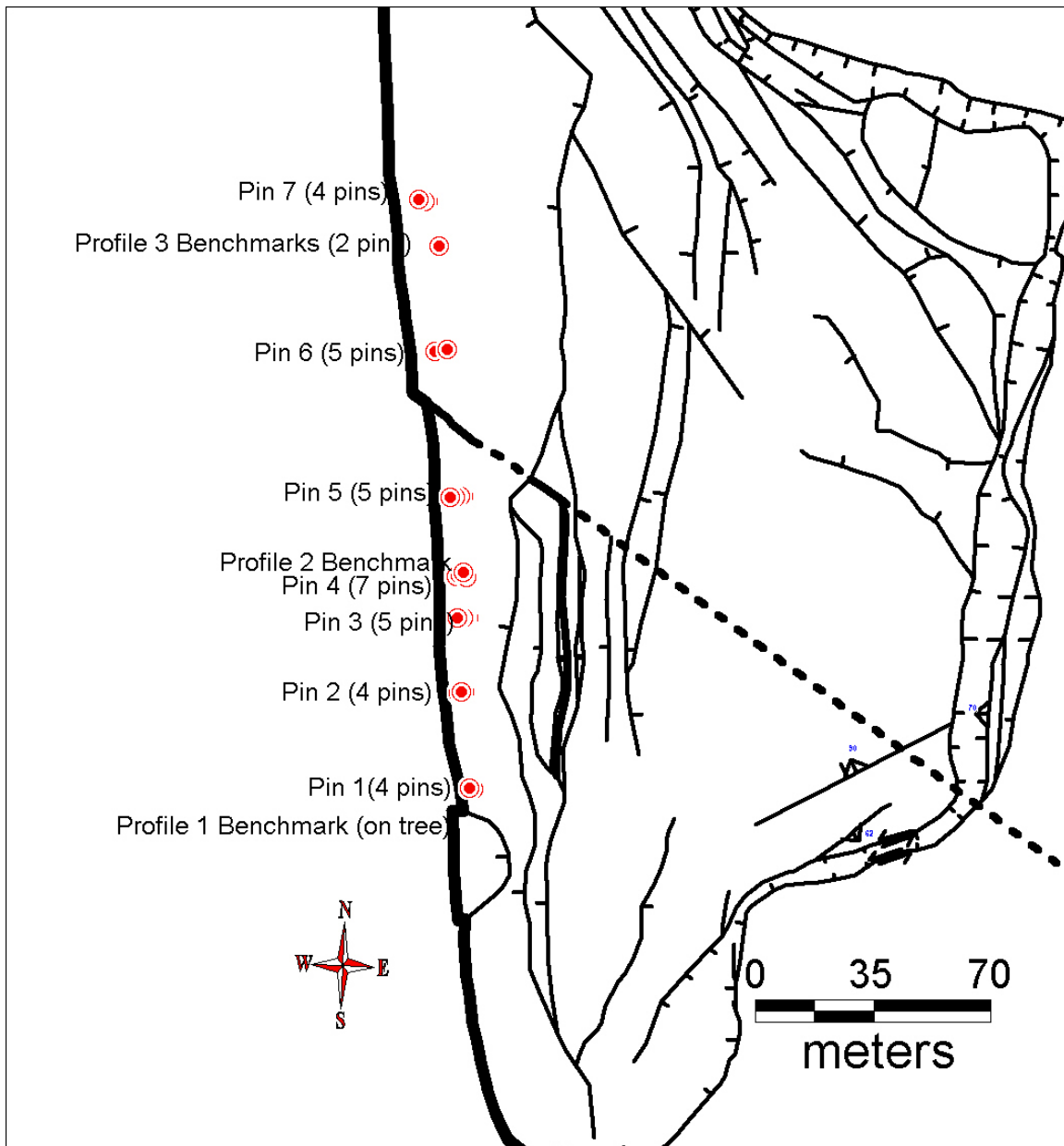
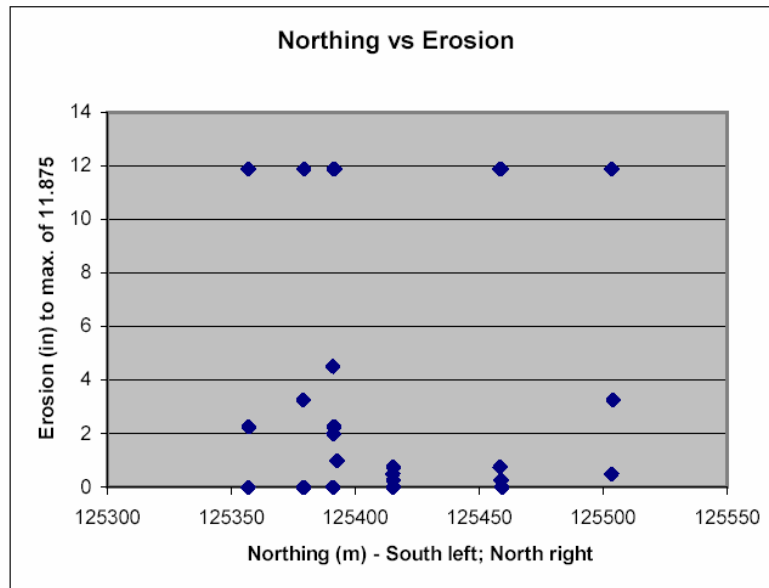
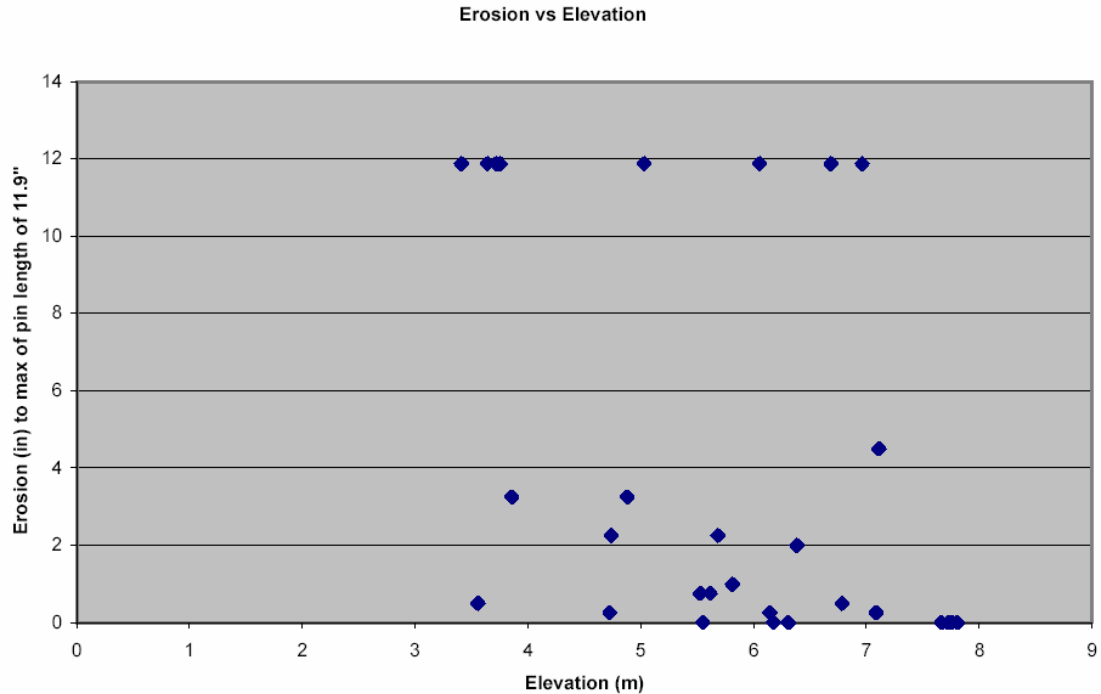


Figure 1. Location of erosion monitoring pins at the toe of the Johnson Creek Landslide (black lines are slide scarps; dotted line is buried tectonic fault).





## **APPENDIX G: MOVEMENT DATA FROM REFERENCE NAILS ON FRESH LANDSLIDE SCARPS**

### **MEASUREMENT METHOD**

Measurements were done in the field by first pounding 10 cm galvanized nails and/or galvanized wires into slide scarps around the margins of the slide such that the nail heads on the scarp and on the soil below the scarp touched. Several nails and/or wires were installed at each site. Wires were only used where it was difficult to seat the nails close enough together to get a measurement. Movement was measured using a plastic scale ruled in tenths and 20ths of an inch. Measurement error on the scale is  $\sim \pm 0.05$  inches, although the human eye can detect 0.01 inches of displacement between to linear objects. Thus movement less than 0.05 inches was detected when heads of nails or heavy gauge wires were displaced, but the exact amount below 0.05 inches is unknown. Values for multiple nails were averaged to obtain a representative value of movement. Some data were discarded where nails were obviously disturbed by roadwork, human activity, or instabilities in the soil itself (e.g. nails or wires gradually rotating because of loose soil). Data from the galvanized wires were generally not used because it was very difficult to seat them well enough to prevent shifting of the wires from wind.



Figure 1. A typical site with 6-inch ruler used for measurements. This is site JC-23.

**DATA**

<b>Station</b>	<b>Date</b>	<b>Lateral (cm)</b>	<b>Perpen- dicular (cm)</b>	<b>Vertical (cm)</b>	<b>Net Horiz. (cm)</b>	<b>Net Slip (cm)</b>	<b>Scarp Strike (°)</b>	<b>Scarp Dip (°)</b>	<b>Vector Bearing (°)</b>	<b>Vector Plunge (°)</b>
JC-14	4/11/2003	0.3	0.4	0.9	0.5	1.0	N80W	89-90 S	S47W	61 SW
JC-15	4/11/2003	0.6	0.6	0.3	0.9	0.9	N80W	89-90 S	S55W	16 SW
JC-17	3/24/2003	-0.1	0.0	0.2	0.1	0.2	N26E	89-90 W	S26W	58 SW
JC-18	4/11/2003	0.0	0.5	0.6	0.5	0.8	N4E	70-83 W	N86W	51 NW
JC-19	4/11/2003	0.0	0.0	0.0	no data	no data	N65E	89-90 NW	no data	no data
JC-20	4/11/2003	-0.4	0.3	0.1	0.5	0.5	N60E	85 N	N83W	14 NW
JC-21	3/24/2003	-0.2	0.2	0.0	0.2	0.2	N6E	87-90 W	S51W	51 SW
JC-22	3/24/2003	-0.6	0.5	1.0	0.8	1.2	N40E	85 NW	S80W	51 SW
JC-22b	4/11/2003	-0.1	0.9	1.3	0.9	1.6	N66E	85 NW	N36W	55 NW
JC-23	4/11/2003	0.0	0.3	0.0	0.3	0.3	N19W	89-90 NW	N71W	0 NW
JC-24	4/11/2003	-0.2	0.3	0.7	0.4	0.8	N2W	87 NW	S58W	62 SW

The table lists mean displacements between nail heads from best field data at last field measurement after installation on March 12, 2003. Negative lateral displacements are left lateral; positive lateral displacements are right lateral; positive perpendicular displacements are opening (dilation) perpendicular to the escarpment; positive vertical displacements are downward on the lower block of the scarp. Strike and dip of the fresh slide scarp are listed.

Most sites were destroyed by roadwork or other disturbances (burial by talus) after April of 2003 at which time monitoring ceased. If no April 11, 2003 data are listed, this means that the site was destroyed before April. See maps below for locations and geology of each site.

## LOCATION MAPS

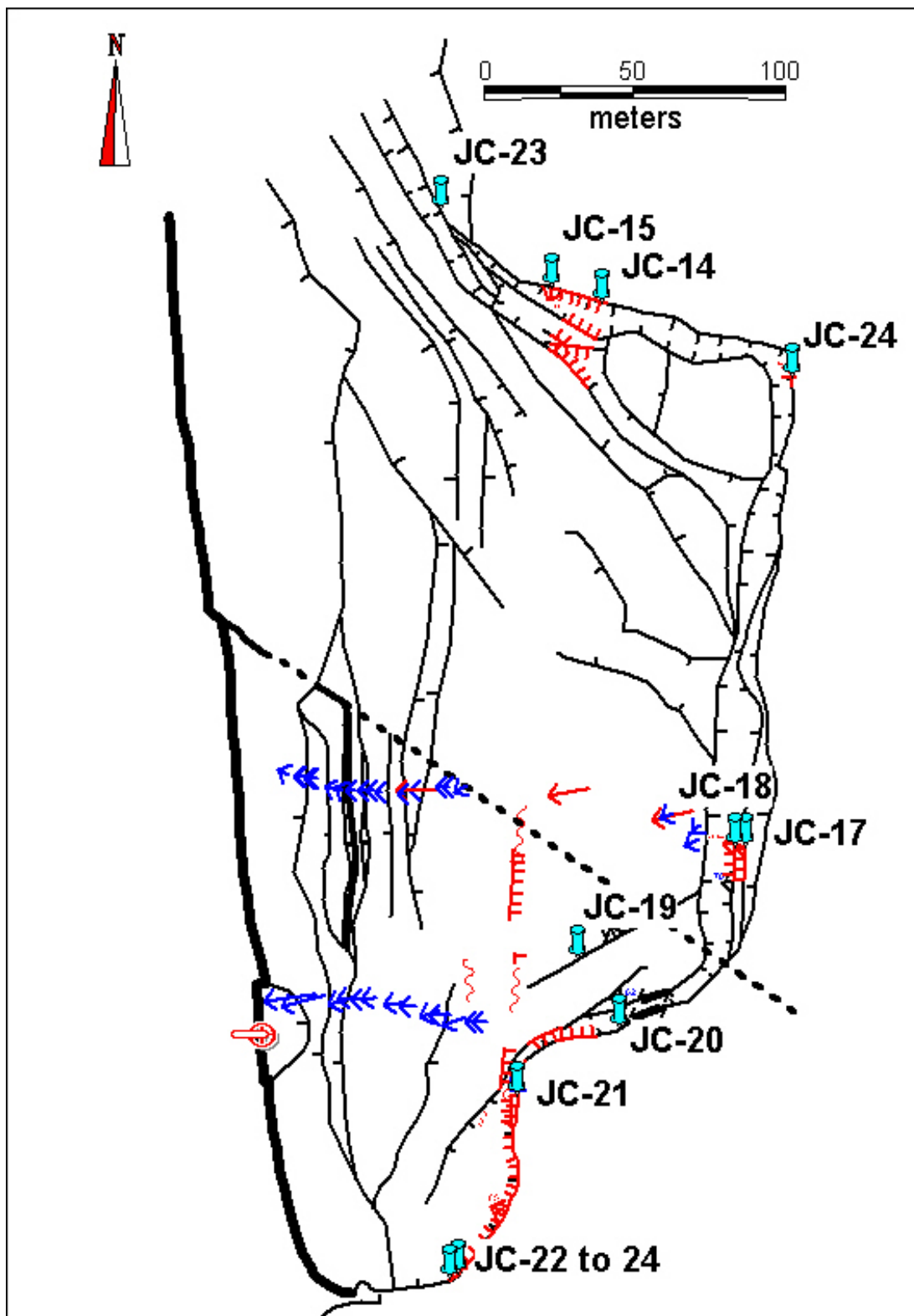


Figure 2. Overview of locations (blue push pin symbols) where marker nails were monitored for movement on fresh slide scarps. Red arrows are direction of movement from inclinometer data; blue arrows are directions from re-survey of steel stakes. Black lines are mapped slide block boundaries.



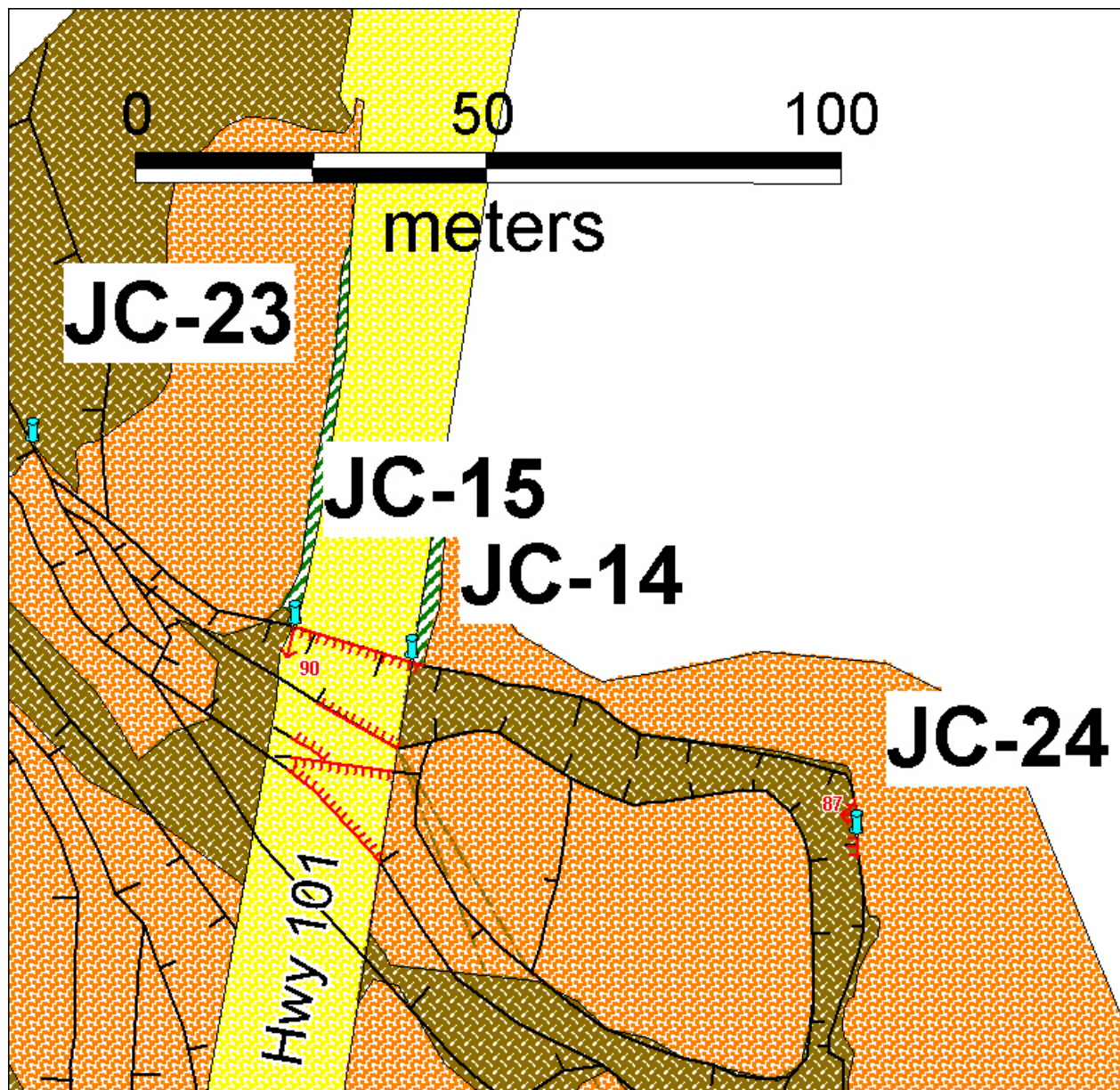


Figure 3. Locations in north part of slide. See geologic map legend in main text for explanation of geologic map units. Small red arrow indicates direction of dip of recently active slide scarp (red line with teeth in direction of scarp inclination).

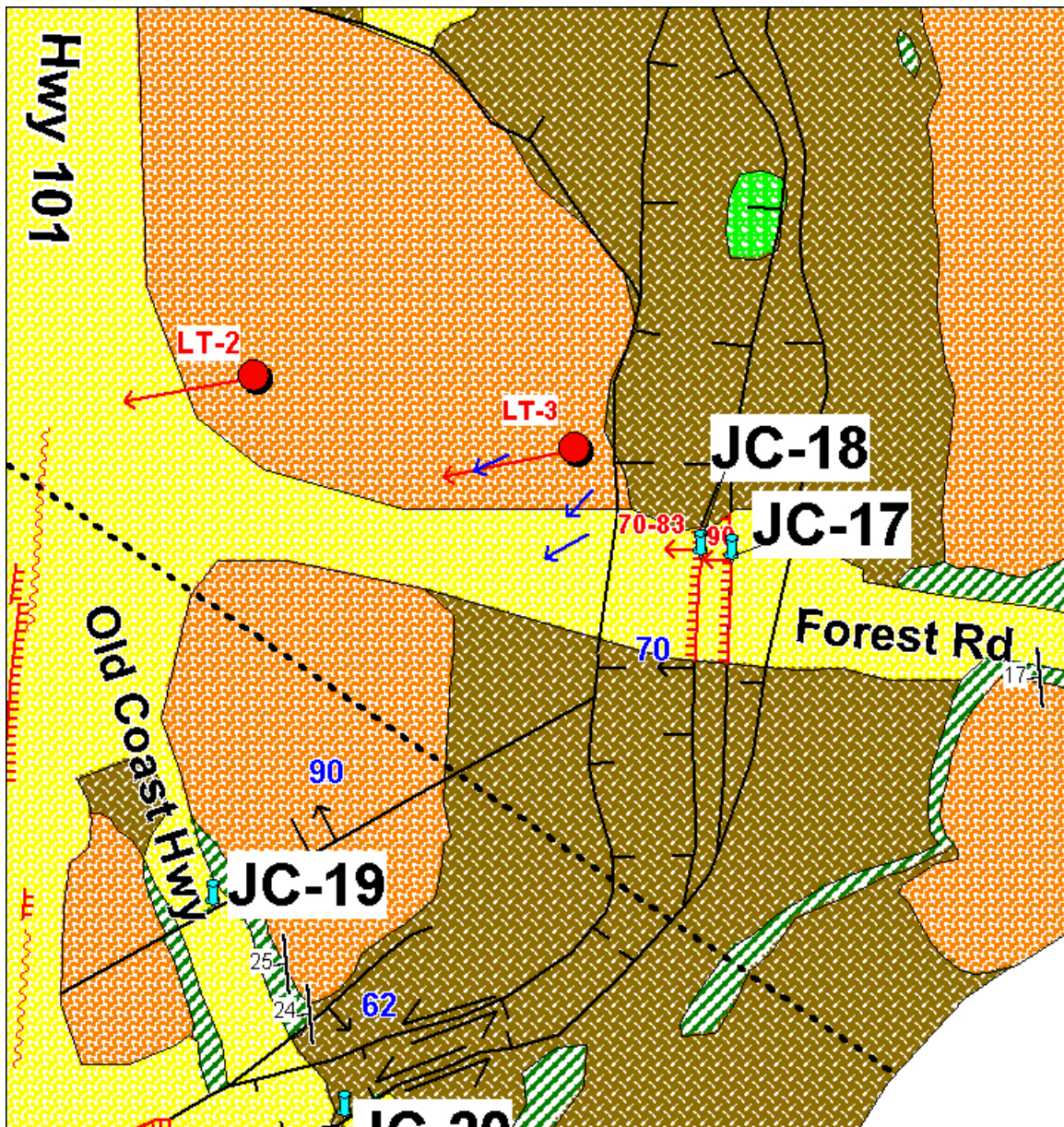


Figure 4. Locations in the central part of the slide. Red circles with arrows are inclinometer locations with movement vectors from inclinometer data; other symbols as in figures above.



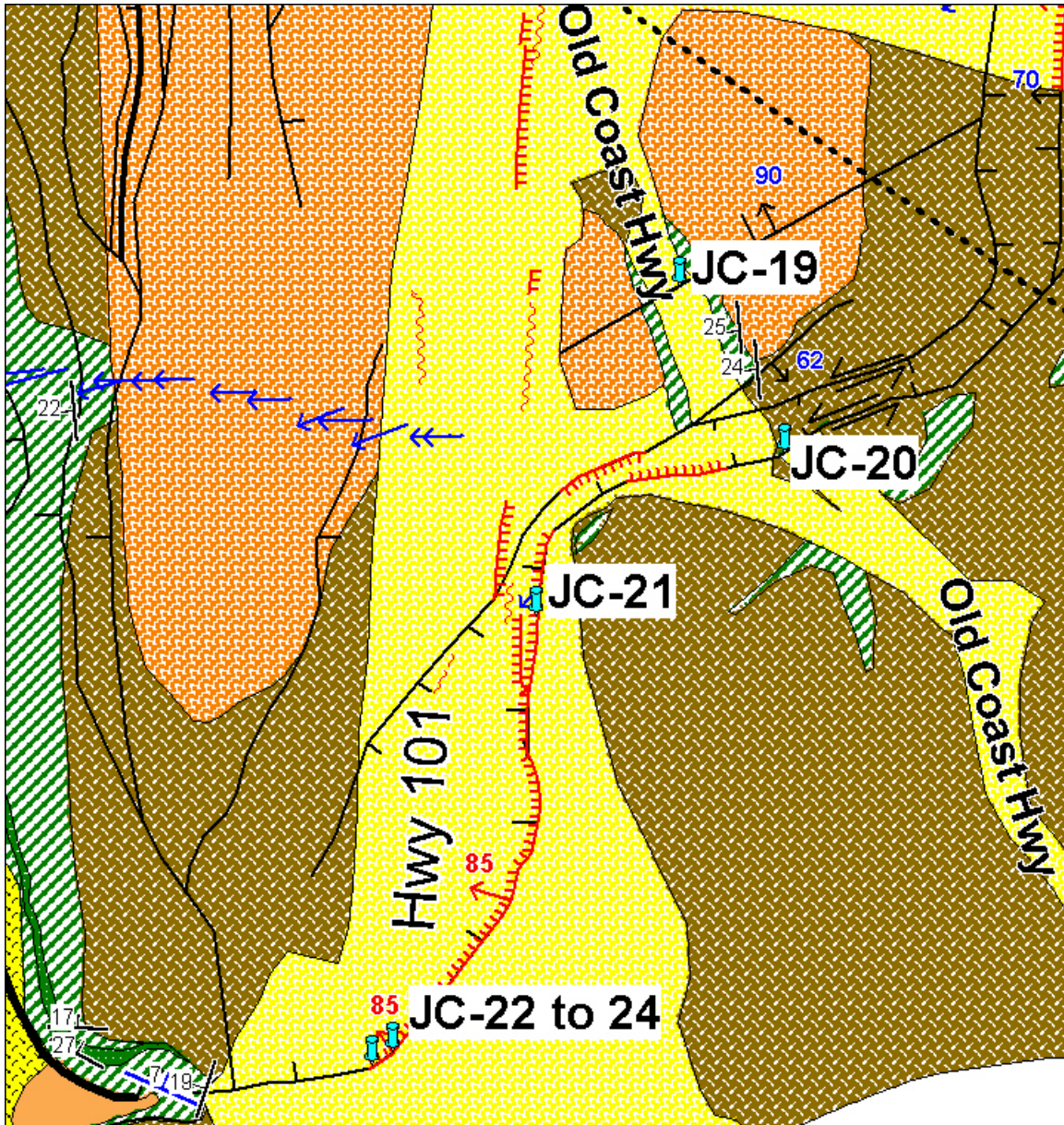


Figure 5. Locations in southern part of landslide; symbols as in figures above.

## DISCUSSION

All movement directions correlate in general with the vector movements measured by re-survey (blue arrows on the maps above) and by inclinometers. Lateral movement is left lateral in all southern slide margins where strike is subparallel to overall slide movement direction and right lateral in equivalent areas on the north margin. Measurements at the headscarp show extension and downward displacement but no significant lateral movement.

Point JC-17 had barely discernable movement, much less than movement on the adjacent headscarp to the west, point JC-18. Movement on JC-18 preceded the beginning of movement on the scarp at JC-17, so it appears that downward displacement at JC-18 destabilized the area to the east and triggered movement there.



Point JC-19 had no detectable movement during the observation period even though significant movement occurred during the same period at the slide plane (extensometer data) and the slide margins. The JC-19 slide scarp has ~40 cm of down-to-the north displacement over a period of ~64 years since the Old Coast Highway was abandoned, so significant movement has occurred in the past. A check of this sheltered site in November of 2004 revealed no movement had occurred to that time, so there is apparently no significant internal deformation in the landslide occurring along this northeast-trending slide scarp.

Movement at the extensometer in borehole LT-3 during the March 20-26, 2003 movement event is  $\sim 0.5 \pm 0.3$  cm. This is the same as the opening (dilation) measured on the fissure at the JC-18 site between March 12 and April 11, 2003 ( $0.5 \pm 0.1$  cm). We infer that this opening probably coincided with the March 20-26 movement at the LT-3 site, which lies only 18 m to the northwest of the JC-18 site.

The nails at the northern margin at Highway 101 recorded right lateral movement of  $0.3-0.6 \pm 0.1$  cm (sites JC-14 and -15). Nails at the northeast headscarp (Site JC-24) recorded  $0.3 \pm 0.1$  cm of dilation perpendicular to the scarp. Nails at the southern margin at the Old Coast Highway (Site JC-20) recorded left lateral movement of  $-0.4 \pm 0.1$  cm, while nails in the southernmost margin (sites JC-22-23) had left lateral movements of 0 to  $-0.6 \pm 0.1$  cm at three sites. We conclude that movement in the northern, central, and southern part of the slide at and east of Highway 101 was similar during the March 20-26 movement event. This movement was not translated to the northernmost site west of Highway 101 (Site JC-23).

Net horizontal movement at Site JC-20 on the southern margin of the slide where it cuts the Old Coast Highway is 0.4 cm left lateral and 0.3 cm perpendicular to the scarp striking N60°E. This corresponds to a net horizontal slip of 0.5 cm toward N83°W. This is probably a reasonably good estimate of the net horizontal slip vector for this part of the Johnson Creek Landslide, since it matches well with net direction of slip estimated independently from horizontal offset of the Old Coast Highway (see discussion in text). Since most of the slip is subparallel to the slide margin, a narrow graben would be expected. This is one of the narrowest graben at the slide margin.

Net horizontal movement at Sites JC-14 and JC-15 is 0.3 to 0.6 cm right lateral and 0.4 to 0.6 cm perpendicular to the scarp striking N80°W on the northern margin of the slide where it cuts the Highway 101. This corresponds to a net horizontal slip of 0.5-0.8 cm toward S47-55°W, 67-75° southwest of the scarp strike. Since a large part of the slip is perpendicular to the slide margin, a significant graben would be expected, and such is the case. The graben at sites JC-14 and JC-15 is 8-13 m wide, narrower than the 17-20 m graben at the central headwall where all movement is perpendicular to the margin, but wider than the 4-6 m graben at the southern margin (site JC-20) where most movement is subparallel to the margin.

## **SITE PHOTOS**

Available photos of individual monitoring sites are given below:



Figure 6. JC-17 site with displaced steel survey marker at headscarp, looking east.  
This stake was not used in the resurvey.





Figure 7. JC-17 site showing nail locations next to forest road, looking east southeast.  
The scarp is in gravel fill from the forest road.





Figure 8. JC-18 site, looking southeast. The scarp is in gravel fill from the forest road. Exposed portions of the two vertical nails is on the right~1.2 cm long. Note that fresh gravel dumped on the road has disturbed the nails on the right, so that measurement was not used.





Figure 9. JC-19 location looking south. Yellow field book is ~19 cm long. Note that all nail heads are still touching in this April photograph, so no significant movement occurred. Scarp is in relatively fresh Astoria Formation siltstone and sandstone with a thin covering of gravel from the Old Coast Highway.





Figure 10. .JC-20 site looking south. Yellow field book is ~19 cm long. Scarp cuts Old Coast Highway. The scarp is in weathered Astoria Formation colluvium below the Old Coast Highway and some gravel fill from the adjacent private driveway.





Figure 11. JC-20 site looking south. Yellow field book is ~19 cm long.





Figure 12. JC-21 site looking southeast. Yellow field book is ~19 cm long.  
The scarp is in gravel fill from the Highway 101.





Figure 13. Sites JC-22 (near red highway cone at top of highway embankment) to JC-24 (to the right of the yellow field book) looking northeast parallel to the strike of the fresh headscarp (red orange fill of excavated Astoria Formation). Yellow field book is ~19 cm long. Near vertical portion of scarp is ~1.2 m high.





Figure 14. JC-22 site looking southeast on west side of Highway 101. Scarp is asphalt and gravel.





Figure 15. JC-23 site with both wires and nails, looking south southeast. Scarp is in red orange fill of excavated Astoria Formation overlain by gravel and asphalt. Near vertical portion of scarp is ~1.2 m high.





Figure 16. JC-23 site on north margin of the landslide looking east southeast.  
Yellow field book is ~19 cm long.



Figure 17. JC-24 site looking southeast. This is the northeast headwall of the landslide. The tan unit in the near vertical escarpment is Pleistocene marine terrace sand.  
Talus lies along the base of the slope.



## **APPENDIX H: BEACH SAND MOVEMENT**

### **Beach Profile Data**

Beach profile information have been derived from analyses of Light Detection and Ranging Data (LIDAR) measured by the US Geological Survey, and from topographic surveys undertaken at the end of the winter season (April 2003). Some beach surveys were also carried out during the winter. However, storms between December 2002 and January 2003 eroded the benchmarks. As a result, we have been unable to reoccupy the study sites.

Figure 1 presents a location map that identifies the position of the beach profile sites studied. Figure 2 presents a three-dimensional image of the beach, while Figure 3 presents the cross-section information. It is worth noting that at the time of the LIDAR light in September 2002, a large rip embayment had become established in front of the landslide. The rip embayment has remained throughout the winter months and has probably contributed to localized erosion along the central portion of the bluff face over the winter months.

Total volumetric change in the amount of sand in front of the landslide is estimated to be 47,700 m<sup>3</sup> of sand (i.e. erosion of this amount over the duration of the winter, September 2002 to April 2003).

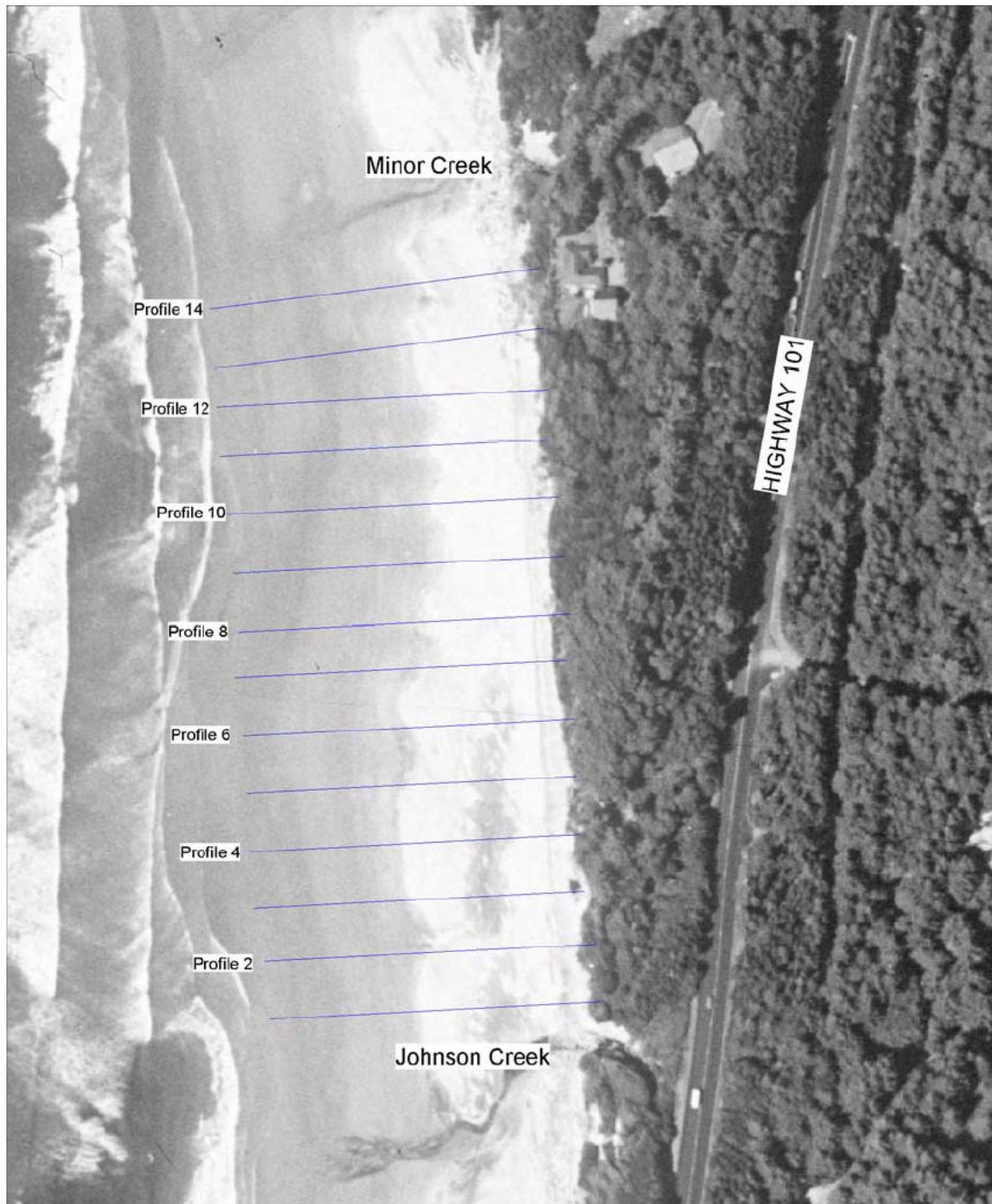


Figure 1. Location map of beach profiles.

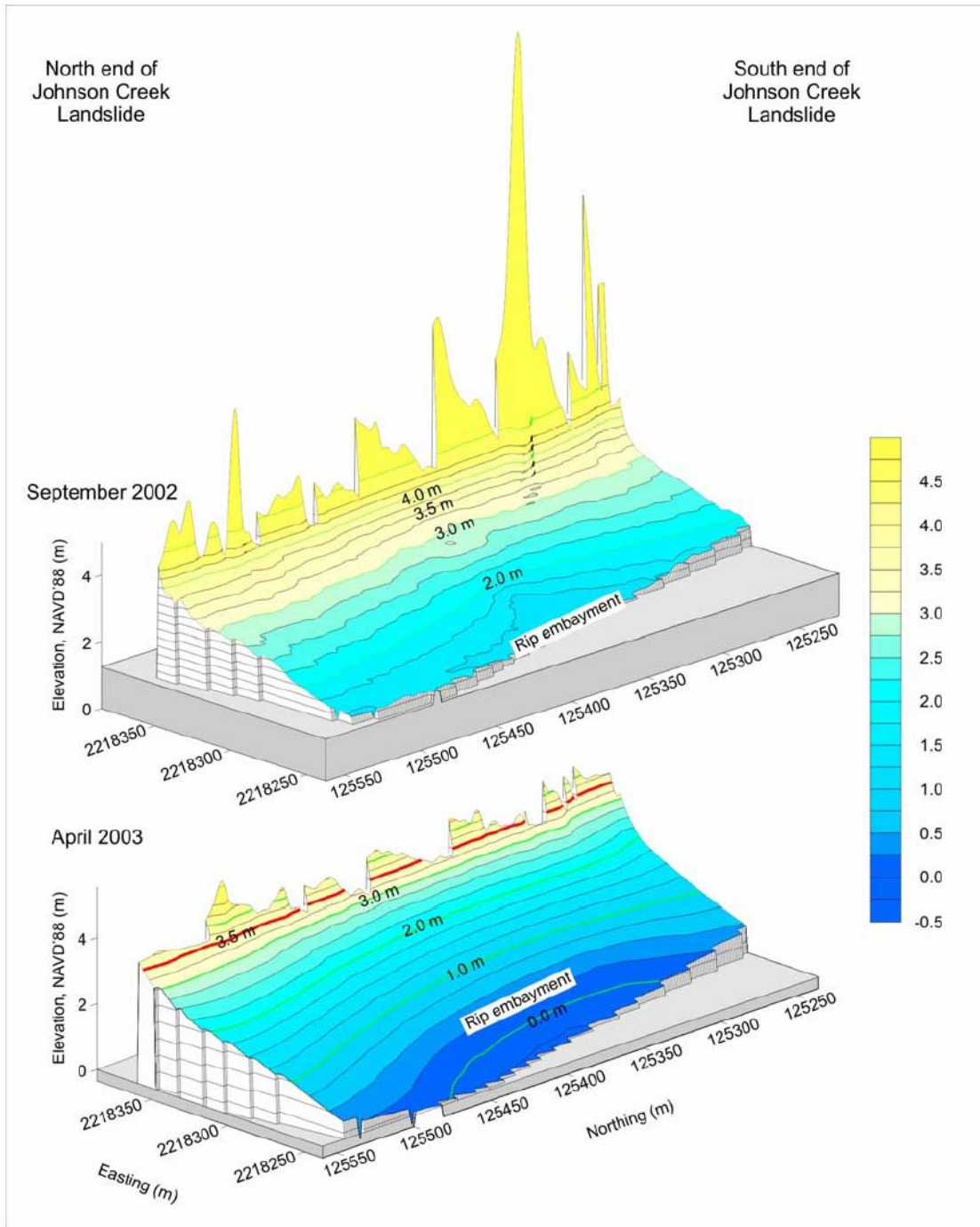


Figure 2. 3-D perspective overlooking the beach in front of the Johnson Creek landslide. View is toward the southeast. Contour elevations are 0.25 m, with 1.0 m contours delineated by the green line. The red line denotes the approximate location of the mudstone/beach contact in April 2003. The beach experienced a vertical drop of 1–2 m over the 2002-03 winter storm season.

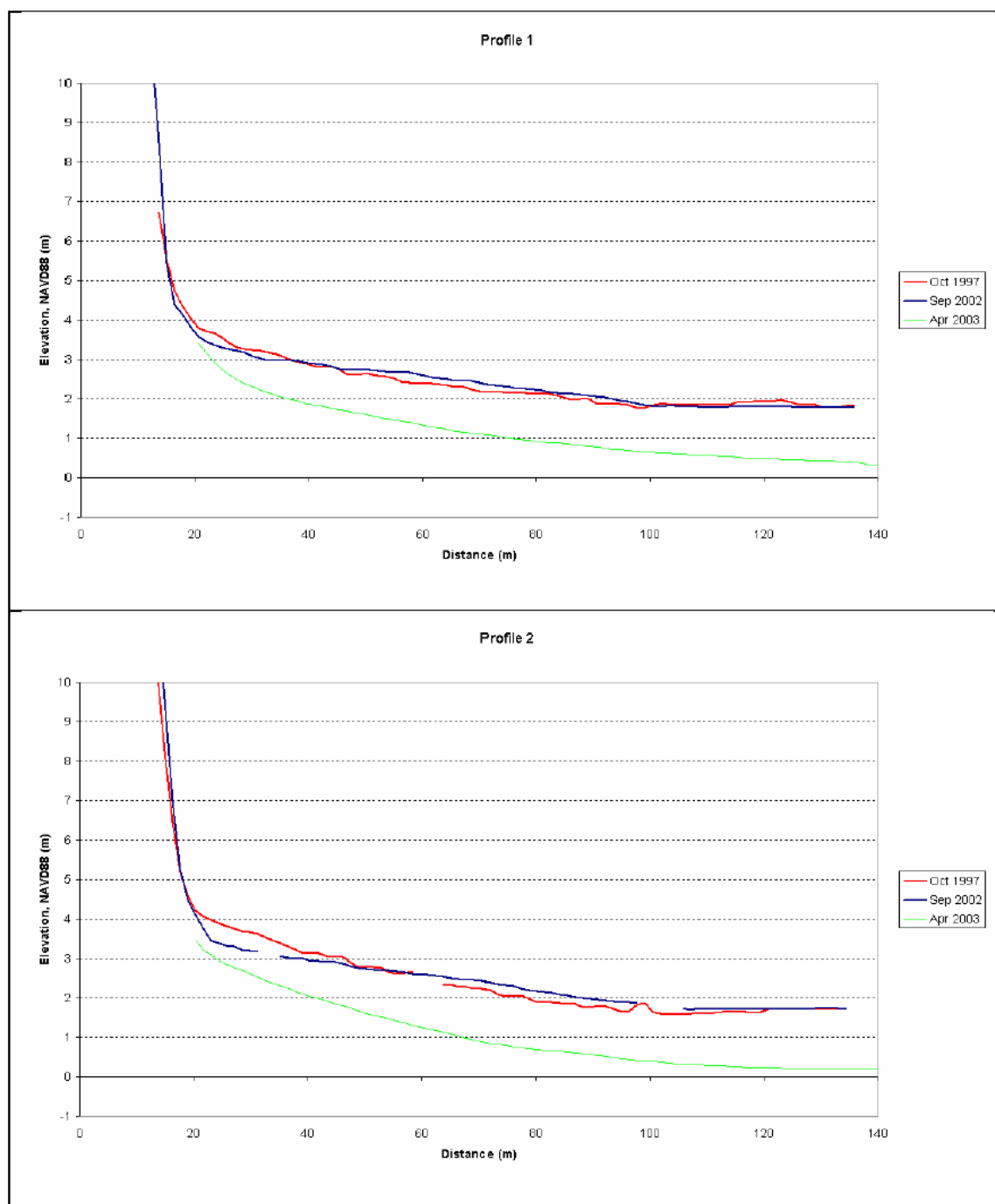


Figure 3A. Beach profile survey derived from LIDAR data and from the April 2003 topographic survey.

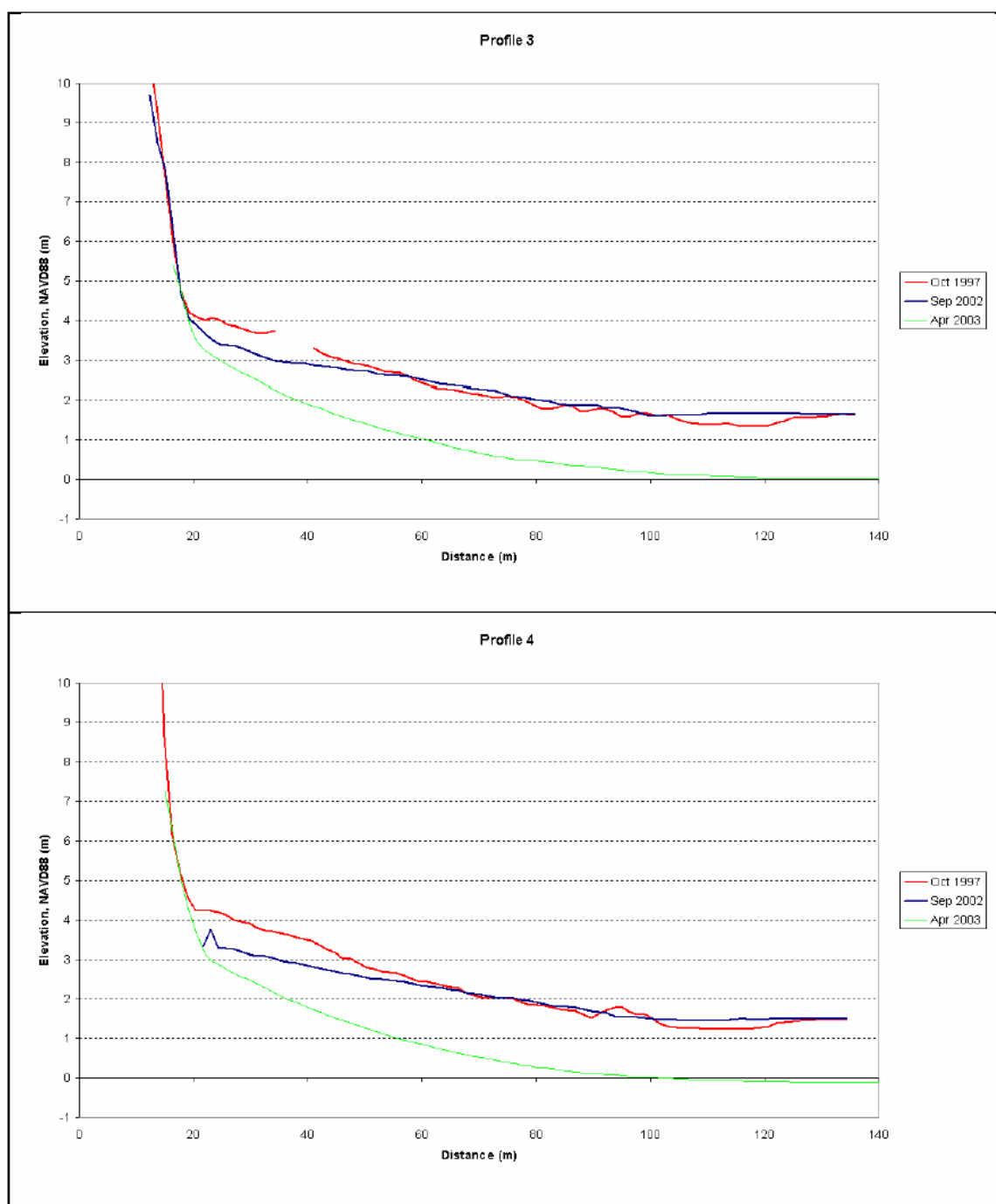


Figure 3B. Beach profile survey derived from LIDAR data and from the April 2003 topographic survey.



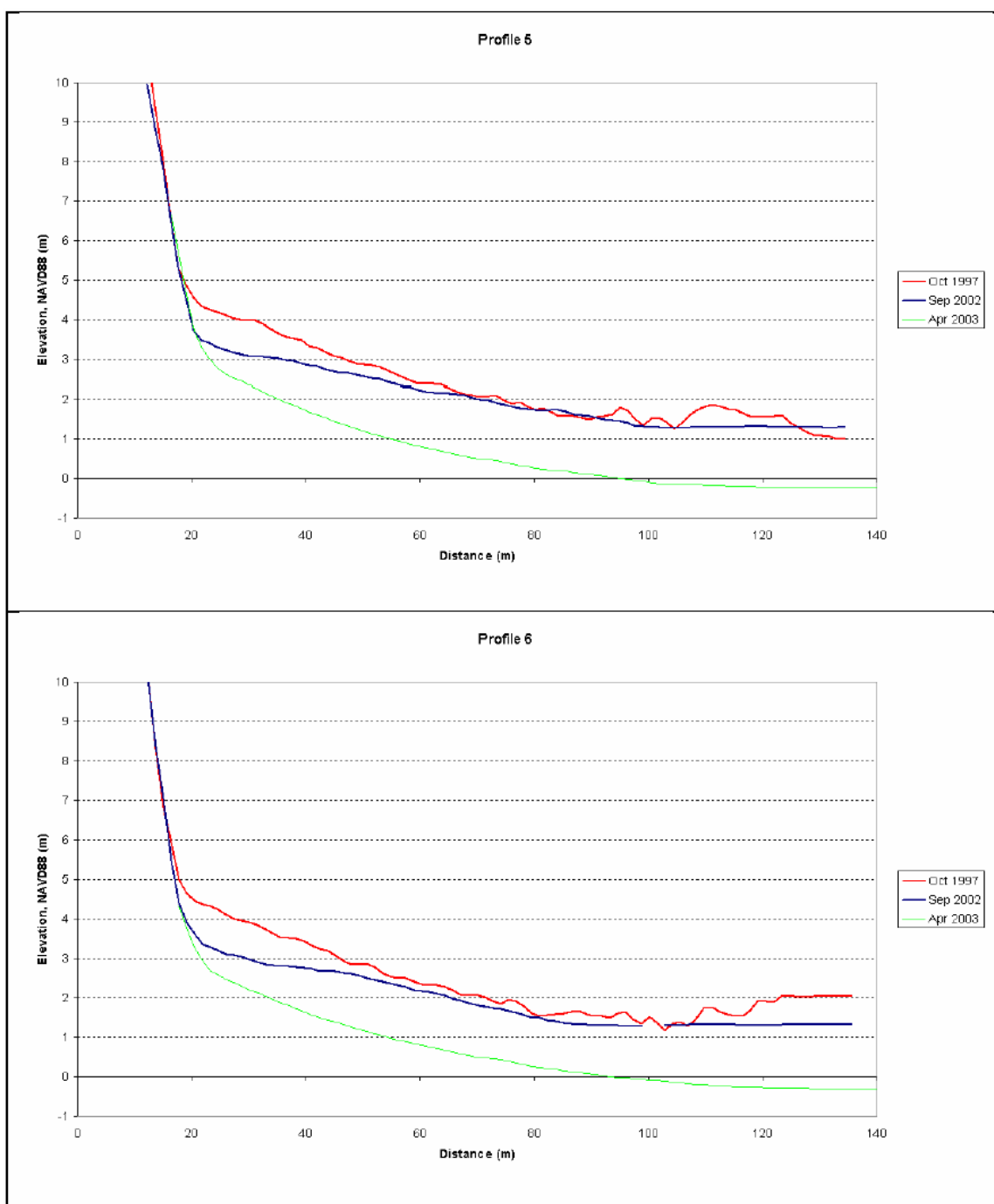


Figure 3C. Beach profile survey derived from LIDAR data and from the April 2003 topographic survey.

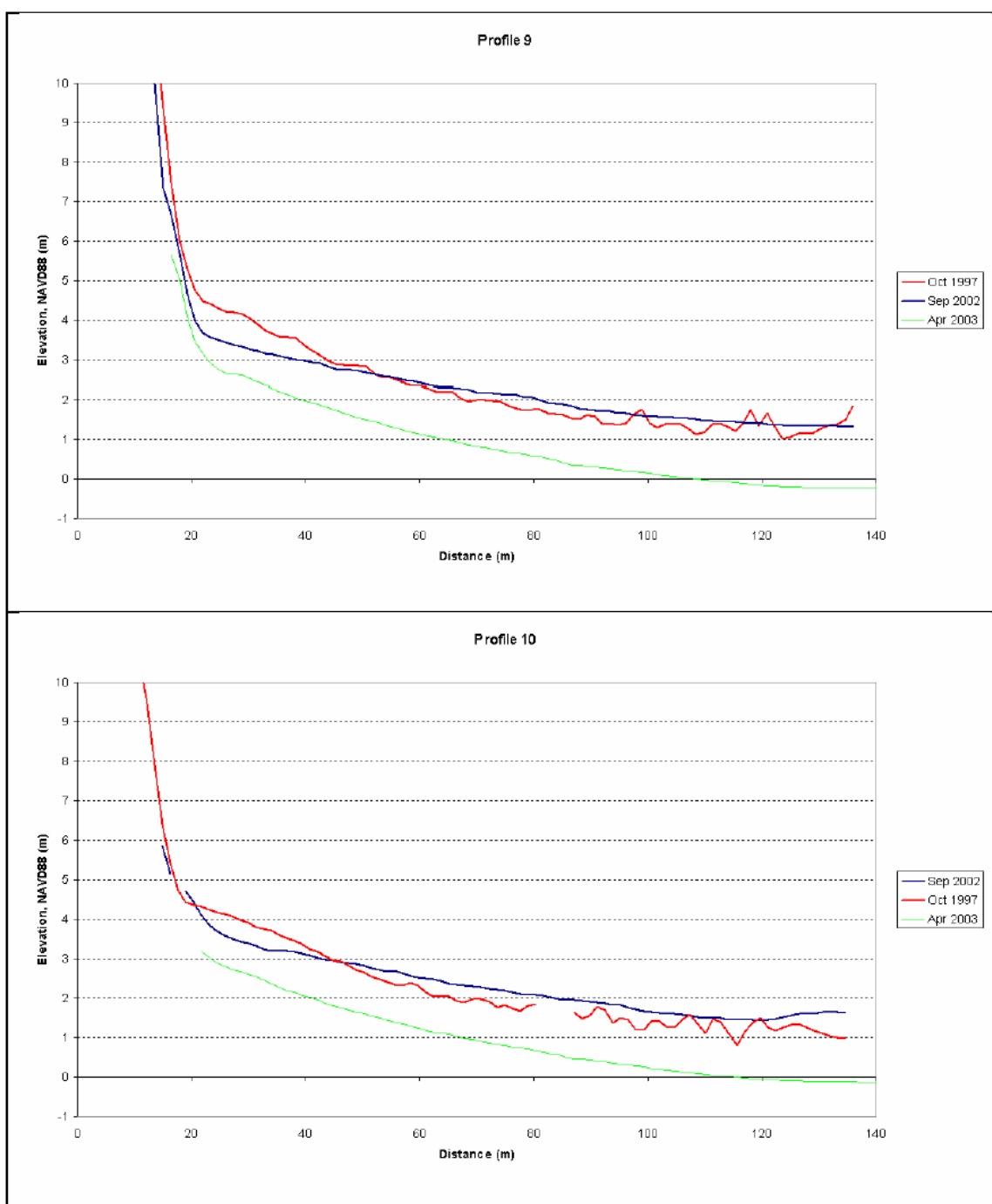


Figure 3D. Beach profile survey derived from LIDAR data and from the April 2003 topographic survey.

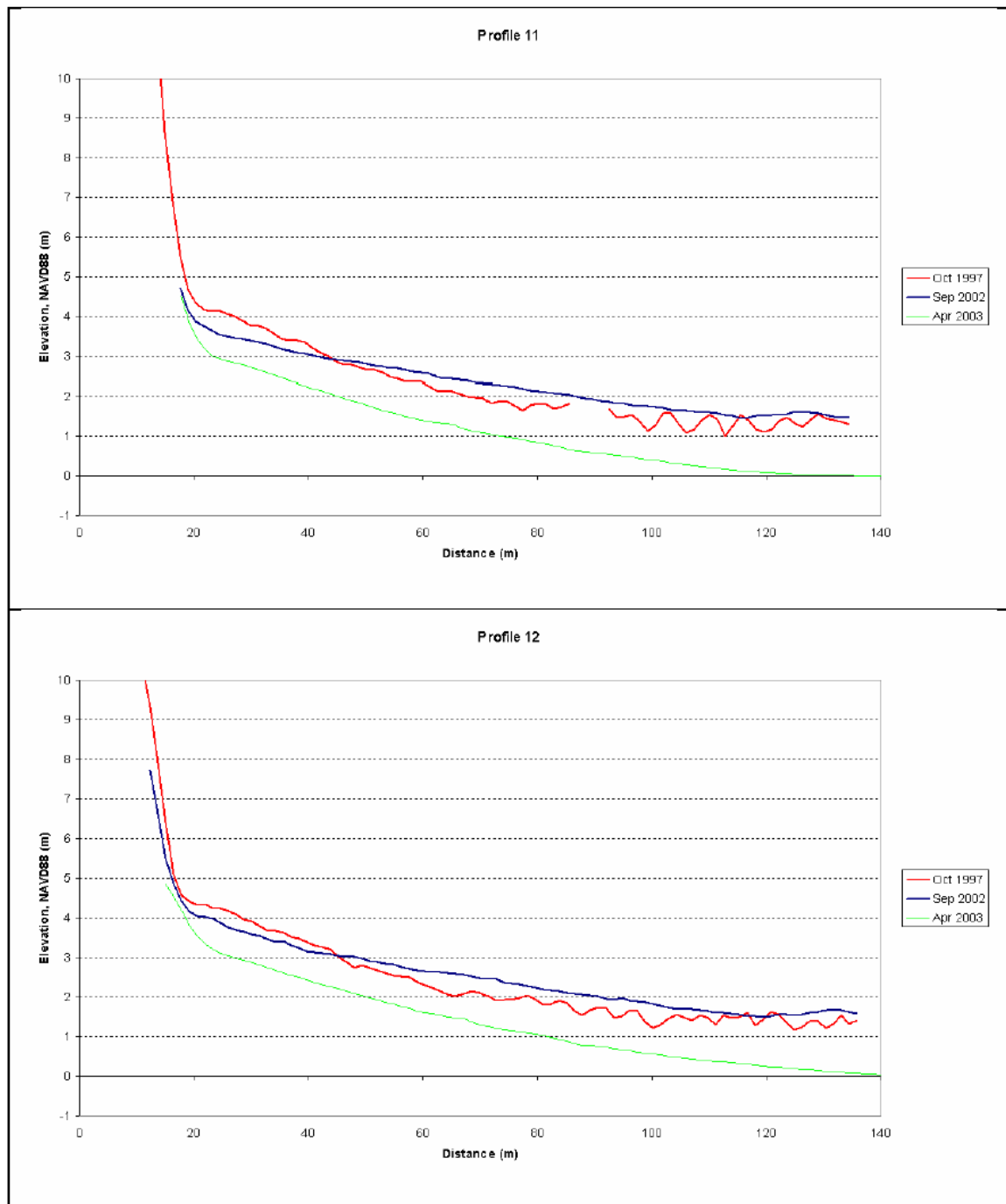


Figure 3E. Beach profile survey derived from LIDAR data and from the April 2003 topographic survey.

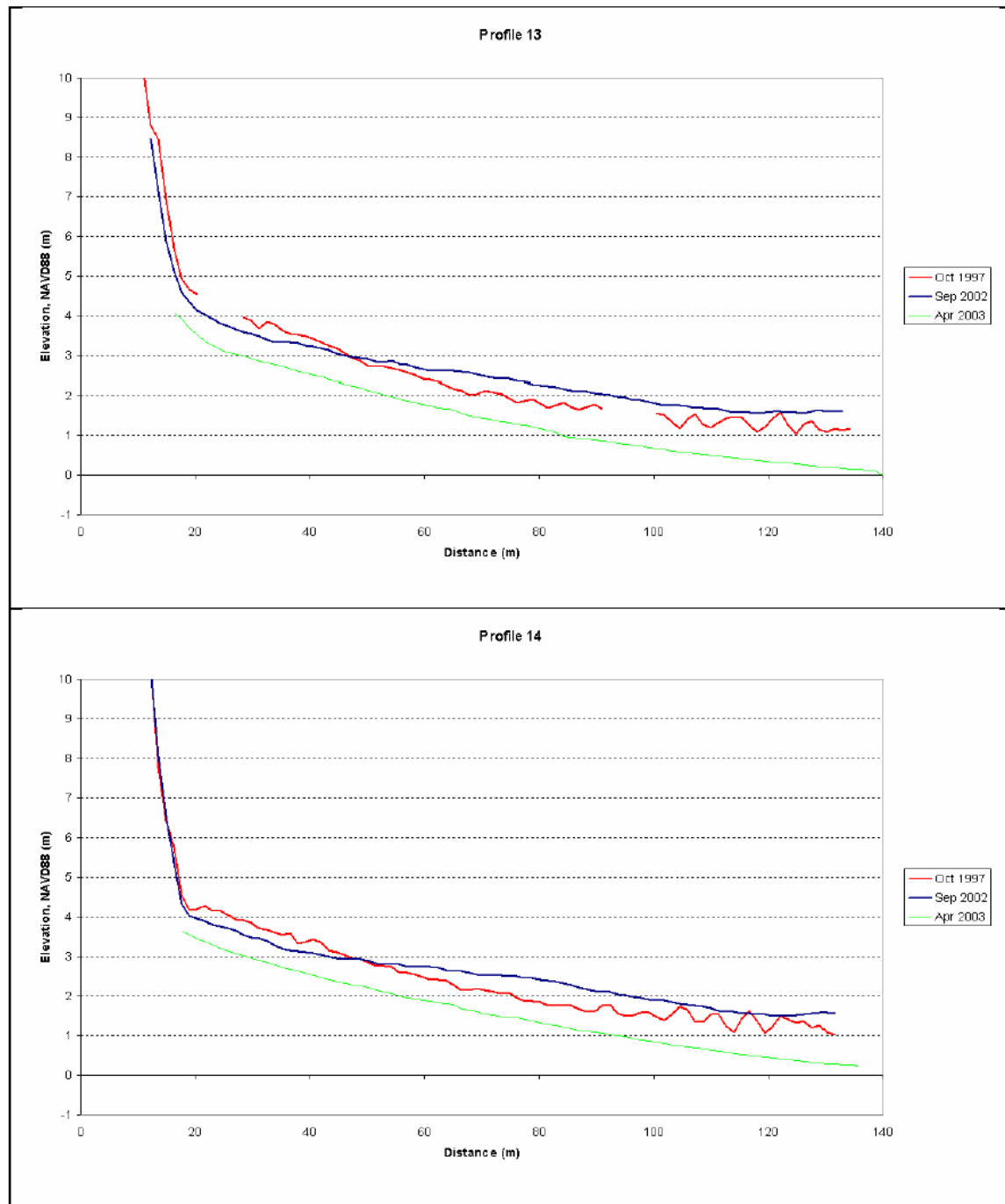


Figure 3F. Beach profile survey derived from LIDAR data and from the April 2003 topographic survey.

## APPENDIX I: RING SHEAR TEST RESULTS

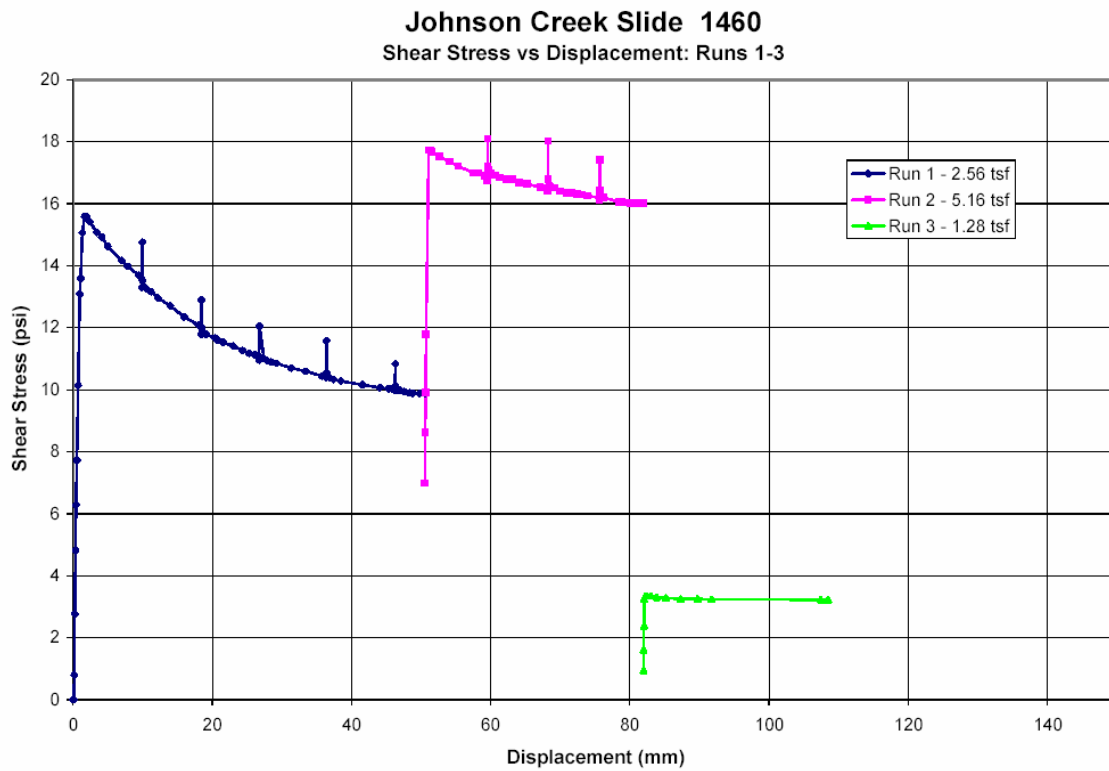


Figure 1. Shear stress versus displacement.



**APPENDIX J:**

**GEOTECHNICAL MODELING OF SLOPE STABILITY  
JOHNSON CREEK LANDSLIDE INVESTIGATION  
LINCOLN COUNTY, OREGON**

**Prepared for DOGAMI by**

**Samuel R. Christie, Graduate Researcher  
Dr. Stephen E. Dickenson, Associate Professor**

**Geotechnical Engineering Group  
Department of Civil, Construction and Environmental Engineering  
Oregon State University**

**June 3, 2005**



## **ABSTRACT**

The Johnson Creek Landslide has become the focus of an extensive, multi-agency investigation, with the goal of identifying internal and external controls on the rate of slide movement. It is anticipated that continued monitoring of this active Coast Range landslide will reveal patterns in slope movement related to factors such as rainfall, groundwater conditions, and toe erosion. As more is learned about the characteristics of the slide more effective methods of remediation can be developed and implemented. The mechanics of the Johnson Creek slide are complicated by the existence of highly weathered and fractured marine sedimentary rocks, complex groundwater hydrology adjacent to the shear zone, highly heterogeneous geotechnical properties, and failure kinematics that involves the interaction of several blocks within the slide mass. Prior geotechnical investigation and stability analyses have focused on one fairly well defined failure surface located near the center of the slide mass. In order to highlight the influence of geotechnical uncertainty on the computed stability of the slide a small project was initiated to supplement the geotechnical stability analyses performed for DOGAMI by Landslide Technology (2004). Additional analyses using standard of practice, limit equilibrium methods for assessing slope stability have been conducted in order to evaluate the influence of the following parameters on overall slide mass stability: (a) drained shear strength parameters, (b) piezometric surface and threshold pore pressure required for slope movement, (c) influence of water-filled tension cracks on toe stability, and (d) evaluation of the impact of translating pore pressure pulses, or waves, on overall stability. The results of these analyses are discussed and compared to those performed by Landslide Technology, where applicable. Additionally, the results are discussed in terms of the inherent limitations, applicability, and overall relevance to the investigation. Recommendations are provided for additional analyses, field investigations, and instrumentation.

## TABLE OF CONTENTS

	<b>Page</b>
1.0 INTRODUCTION.....	J-1
2.0 MODELING EFFORTS .....	J-3
2.1 Model Set Up .....	J-3
2.1.1 Cross Sections.....	J-3
2.1.2 Slope Stability Software .....	J-5
2.2 Parametric Studies .....	J-6
2.2.1 $\phi'$ & $c'$ .....	J-6
2.2.2 Piezometric Surface .....	J-9
2.2.3 Toe Failure & Tension Cracks.....	J-10
2.2.4 Pressure Wave Analysis.....	J-11
3.0 CONCLUSIONS .....	J-13
4.0 RECOMMENDATIONS FOR FUTURE WORK.....	J-14
4.1 Field Investigation and Monitoring .....	J-14
4.2 Laboratory Investigations .....	J-15
4.3 Modeling.....	J-15
ACKNOWLEDGEMENTS .....	J-16
REFERENCES.....	J-16

## LIST OF FIGURES

### Figure No.

- 1 Site Plan
- 2 Cross Section A-A' & Cross Section B-B'
- 3 Cross Section C-C'
- 4 Parametric Study  $c'$ - $\phi'$  A-A'
- 5 Parametric Study  $c'$ - $\phi'$  B-B'
- 6 Parametric Study  $c'$ - $\phi'$  C-C'
- 7 Parametric Study Tension Cracks
- 8 Head Rise Time Lag
- 9 Factor of Safety vs. Piezometric Increase

## **GEOTECHNICAL MODELING OF SLOPE STABILITY JOHNSON CREEK LANDSLIDE INVESTIGATION LINCOLN COUNTY, OREGON**

### **1.0 INTRODUCTION**

The investigation of the Johnson Creek Landslide began in the fall of 2002 with the intention of characterizing the controlling factors that influence the occurrence and rate of slide movement, as well as developing innovative methods of mitigating the slide hazard in a cost effective manner (Priest, et al., 2005). In the summer of 2004, Dr. George Priest of DOGAMI provided a small grant to Professor Stephen Dickenson of the Geotechnical Engineering Group at Oregon State University (OSU) to supplement the slope stability analyses performed by Landslide Technology (2004). The Landslide Technology investigation represents the most thorough geotechnical site characterization and stability investigation that has been performed to date. The analyses were largely confined, due to limited subsurface data, to one cross section located near the center of the slide mass. The strengths and limitations of the initial analyses were well documented, and recommendations were provided for additional investigation. The small pilot study undertaken here is aimed at expanding the slope stability modeling previously performed using standard 2D limit equilibrium methods. Professor Dickenson and two students, working on term projects focused on a critical re-evaluation of the Landslide Technology report, field reconnaissance including both ground traverses and aerial inspection, supplementary review of geotechnical characterizations of regional Coast Range landslides, and an extensive suite of slope stability analyses using the commercially available program XSTABL. The results of this study are intended to supplement the earlier work of Landslide Technology (2004), and to provide guidance for future geotechnical investigations of the Johnson Creek landslide.

A brief description of the slide and history of the investigation is given here based on the main body of the text in this open-file report and on descriptions by Landslide Technology (2004). The Johnson Creek Landslide is located on the Oregon Coast less than 0.5 km south of Otter Rock. The slide consists of three major geologic units, namely a fractured sandstone of the Miocene Astoria Formation to depth and an overlying Pleistocene marine terrace sand deposit approximately 3 to 6 meters thick. The terrace deposits overlie a 0.3- to 2-meter (1- to 6-foot) layer of orange, decomposed Astoria Formation, which in turn, overlies gray, unaltered Astoria Formation bedrock. The structural dip of the Astoria Formation at the site has been measured in nearby exposures at 15 to 20 degrees to the west. The Astoria Formation at the headwall of the landslide strikes N5W  $\pm$  2°, and dips to the west 17°  $\pm$  1.

The recent history of the Johnson Creek Landslide includes a study conducted by ODOT in the 1970s, which included six borings and inclinometers installed from 1972 to 1976 (**Figure 1**). The inclinometers installed by ODOT were pinched off within a few years and provided limited data. A report was prepared by ODOT in 1979 that discussed the results of the investigation and provided options for containing the. In 2002, Landslide Technology conducted an investigation that included three borings with three sets of inclinometers and piezometers. The Landslide Technology report documented three slide events consisting of two slow events and one fast event, which in January 2003 sheared off all three of the inclinometers. Since January 2003 there have been three minor periods of slide movement, all three of which occurred in the winter of 2003-2004.

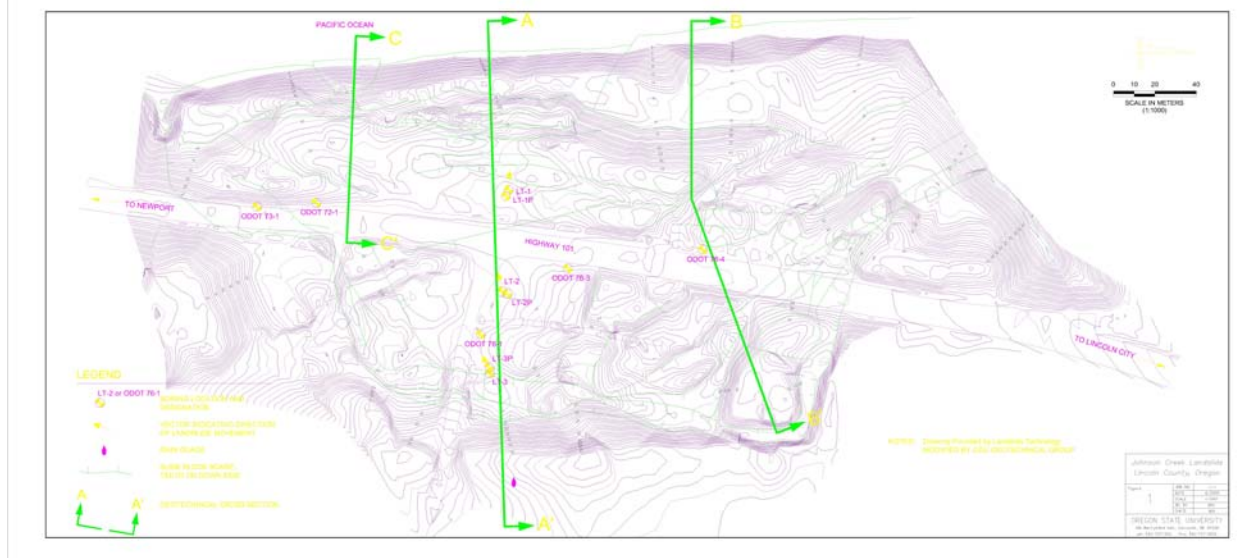


**Figure 1.** Site plan showing locations of cross sections used for analysis.

The investigations to date have identified the key controls on slide initiation and rate of movement, provided estimates of average soil strength parameters across the shear zone, as well as estimates of the threshold pore pressures required for "fast" and "slow" movement. Sensitivity studies by Landslide Technology (2004) have shown that the greatest reduction in factor of safety occurs from severe storm events (-9%) and the loss of toe support (-7%); loss of toe support can be from cliff erosion, sliding at the toe, removal of beach sand due to seasonal wave climate and more long term littoral cell migration. In addition to the analyses mentioned above, insights into the mechanics of the slide have been raised. There is substantial evidence that the slide may be moving as three blocks as opposed to a coherent slide mass. If indeed the slide is moving as separate blocks, the 2D modeling approaches employed thus far are limited in the ability to effectively model the kinematics of the slide. The significance of this is discussed in the Conclusions section of this report.

The DOGAMI investigation has included data collection and monitoring of the slide for a 5-year period. The scope of the extensive investigation:

- Project management, including contracting, reporting and convening periodic meetings of a technical steering committee consisting of ODOT and DOGAMI personnel.
- Field data collection (geologic mapping, logging and stratigraphic interpretation of drill hole samples, collection of piezometer, rainfall, extensometer, and inclinometer data.)
- Geological and geotechnical interpretation of data.
- Publication of three reports, the LT report (Landslide Technology, 2004), an interim report after about two years (Priest et al. 2005), and a final report that will be prepared in 2007 at the end of five years of data collection.

This small study contributes to the comprehensive DOGAMI investigation by confirming the back-calculated residual strength parameters from the 2004 Landslide Technology report, providing

additional stability analyses of other sections of the slide as well as examination of different piezometric surfaces, and by providing recommendations for future geotechnical studies of this landslide.

## 2.0 MODELING EFFORTS

### 2.1 Model Set Up

#### 2.1.1 Cross Sections

To evaluate the portions of the slide that may be moving differentially, three different cross sections were used in our analyses. Cross sections A-A', B-B', and C-C' are intended to represent the slide blocks of the entire slide mass (**Figures 2 and 3**). A brief discussion of the development of each slide follows:

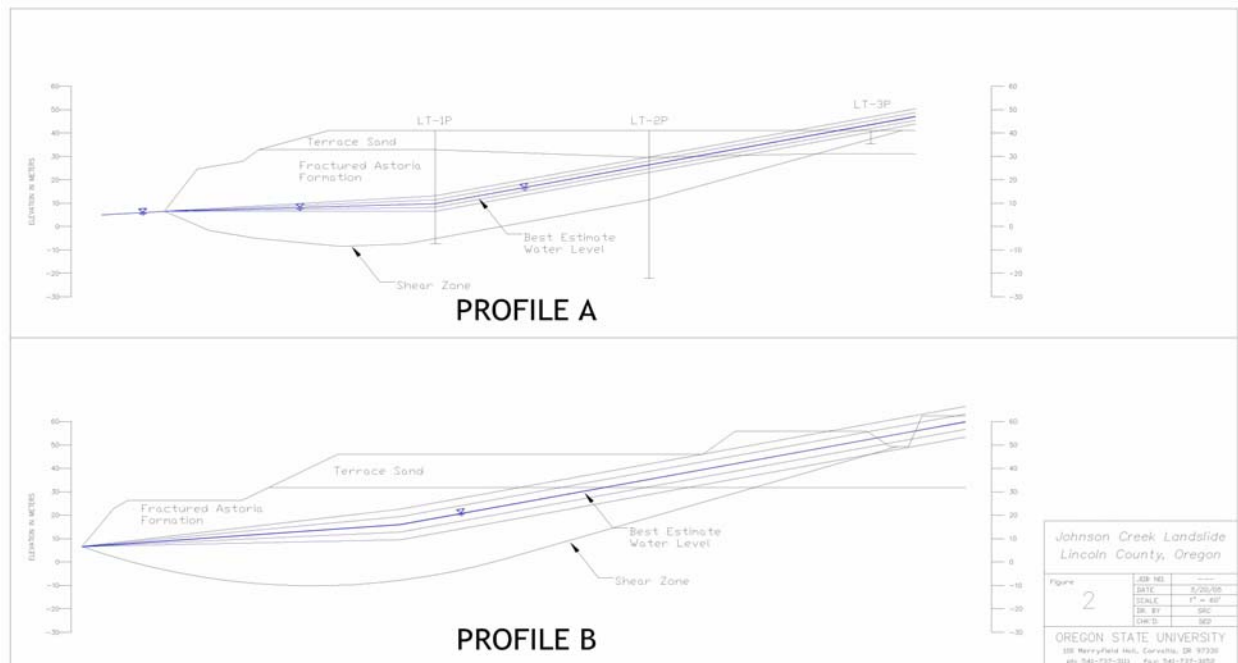


**Figure 2.** Cross Sections A-A' and B-B'.



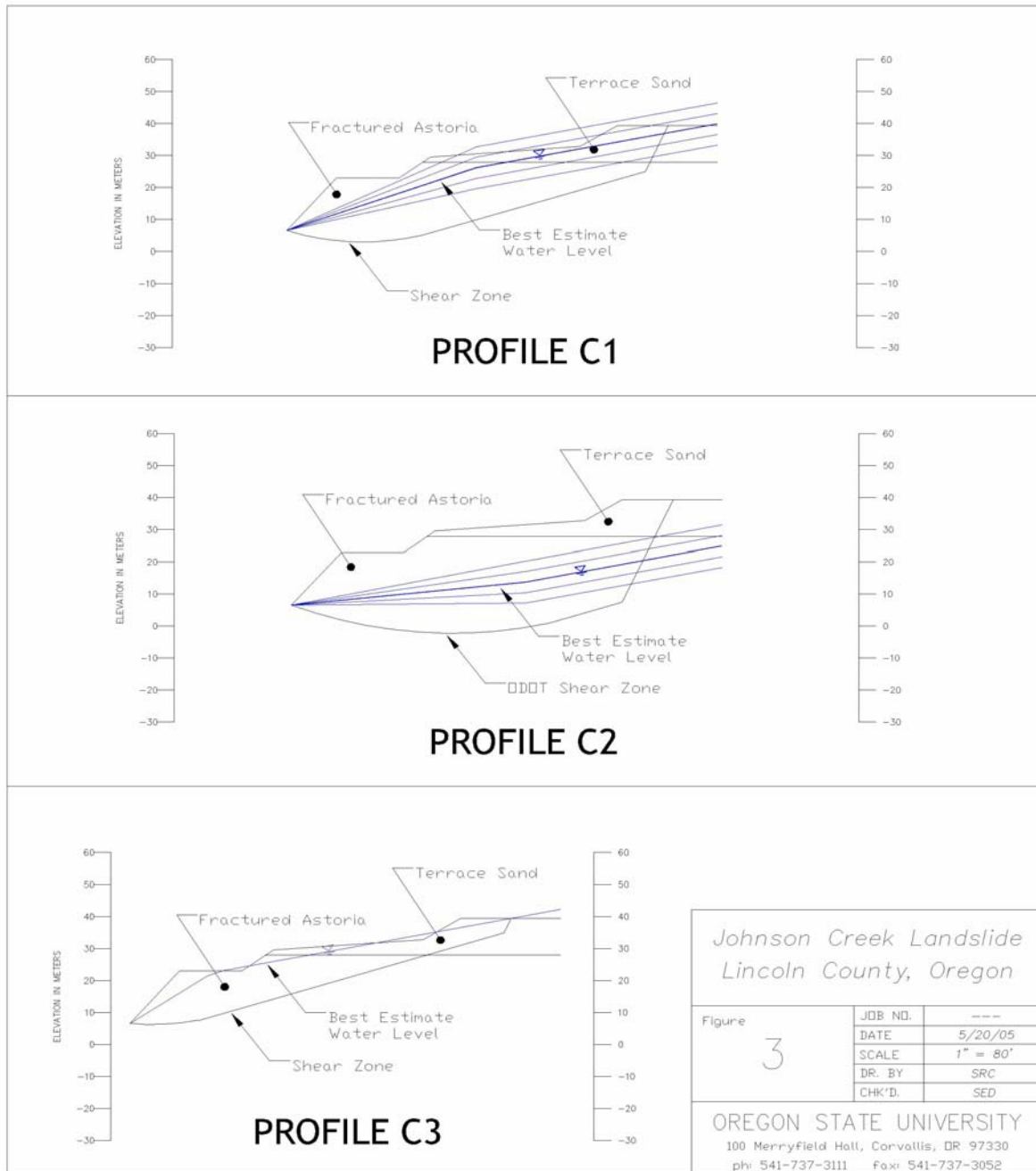


**Figure 3.** Cross Section C-C'.

### Cross Section A-A'

Representing the centermost portion of the slide, cross section A-A' (**Figure 1**) was developed from the Landslide Technology (2004) exploration data. The configuration of the slide plane was established by Landslide Technology and adopted for this study after additional review of available instrumentation data.

### Cross Section B-B'

Representing the northernmost portion of the slide, cross section B-B' (**Figure 1**) was developed to evaluate this area's overall stability and sensitivity to piezometric head increase. The slide geometry is oriented in the direction of the predominant movement of the slope. There is a small bend (approximately 20 degrees) in the section, which follows the movement vectors and the steepest slope gradient obtained from the topographical survey. Although the incorporation of the bend in section is not strictly correct for 2D limit equilibrium analyses, this is considered to impart only a very minor error in the computed margin of safety.

The shear zone associated with this slide plane was extrapolated from the data of Landslide Technology (2004) used in cross section A-A' and an ODOT exploration point (76-4) from a 1976 borehole that produced a boring log and an inclinometer data point. Naturally when data is extrapolated, as is the case here with shear zone and piezometric surfaces, there is some level of uncertainty as to the accuracy of the extrapolated data. However, based on the relative differences observed in the data both could vary by approximately +/-5 feet.

### Cross Section C-C'

This cross section was developed to analyze the southernmost "block" of the slide and intersected a small toe failure. Three different shear zones were analyzed and are designated C1, C2, and C3; all have a common feature of a steeply dipping slide plane at the head scarp. Shear zone C1 was extrapolated using the exploration and inclinometer data from the Landslide Technology report, and is similar in shape to the shear zone used in cross section A-A'. Shear zone C2 was developed using nearby ODOT exploration and inclinometer data points 73-1 and 72-1; this failure surface is more deep seated than C1 and C3. Shear zone C3 represents a shallow failure that is nearly linear along the length of the block.

## **2.1.2 Slope Stability Software**

This study focused on the application of limit equilibrium procedures for evaluating the stability of the Johnson Creek Landslide. Analyses were performed using the commercially available program XSTABL that is the same slope stability program employed by Landslide Technology (2004). XSTABL is a program that employs rigid body mechanics in the solution of circular and wedge slip surfaces. The program searches for the critical surface exhibiting the lowest margin of stability (expressed as the factor of safety against sliding). This approach does not account for the cumulative effect of multiple water-filled tension cracks or interaction between blocks within the overall slide mass.

Spencer's method (1967) was used to evaluate slope stability in our residual strength parameter and piezometric surface parametric study. Spencer's method, in short, is a force and moment equilibrium method that assumes the resultant slide force inclination is the same for every slice. A box search method was used for the stability analysis at the toe of the slope. This is a force and moment equilibrium approach that generates random points within the user specified search box. Details on the XSTABL program can be found at the following website:  
<http://forest.moscowfsl.wsu.edu/4702/xstabl0.html>.

## 2.2 Parametric Studies

In order to evaluate the influence of various parameters and slope configurations on the stability of the slide mass a series of sensitivity analyses were performed. The parameters that were evaluated included:

1. Drained strength parameters ( $\phi'$  and  $c'$ ).
2. Location of the piezometric surface and pore pressures along the failure plane.
3. Influence of water-filled tension cracks on toe stability.
4. Influence of translating pore pressure waves on the stability of the slide.

These evaluations highlighted the relative contributions of the various parameters on overall stability. This work supplements the Landslide Technology's analyses by confirming their back-calculated residual strength parameters, providing analysis of additional cross sections, bounding the residual strength parameters, and evaluating slide toe stability.

### 2.2.1 $\phi'$ & $c'$

The purpose of the parametric study was to bound the "average" Mohr-Coulomb residual strength parameters associated with the shear zone. Analysis was performed using Spencer's method in the computer program XSTABL (Section 3.1.2). Residual strength parameters  $c'$  and  $\phi'$  were back calculated for fixed factor of safety (FOS) value equal to 1 along the three cross sections (**Figures 2 and 3**) used in this study. Residual strength parameters were determined by performing the stability analysis for piezometric surfaces corresponding to the best estimate threshold level and variations of this level from +2 meters to -2 meters.

In order to obtain the representative strength parameters ( $c'$  and  $\phi'$ ) for stability analyses the soils in the shear zone should be sampled and tested. While theoretically advantageous, the variability of the soils along the slide plane, combined with the difficulty and cost associated with obtaining samples, requires that the strength parameters be estimated from back-calculation using the best estimate configuration of the slide plane and 2D limit equilibrium methods. Since unique values of both  $c'$  and  $\phi'$  cannot be determined for a given slide geometry, one approach is to select a value of one and solve for the other in an analysis of the slope stability for marginally stable equilibrium (FOS = 1.0). This method has been employed in this study. The combinations of  $c'$  and  $\phi'$  that yield FOS = 1 are shown in **Figures 4 to 6**. It should be noted that the representative values of  $c'$  for residual strength along slide planes in materials commonly found in the Oregon Coast Range are

very small (commonly less than 50 psf). If this value is assumed, as a maximum upper bound, then appropriate values of  $\phi'$  are in the range of approximately  $5.5^\circ$  to  $6.0^\circ$ . The parametric analyses for  $c'$  values greater than 100 psf were only performed to establish the representative trends in  $c'$  and  $\phi'$ .

The residual strength parameters determined in this study are consistent with those determined by Landslide Technology (2004) along cross section A-A'. The residual strength parameters provided in the Landslide Technology report of  $c'=0$  and  $\phi'=6.5^\circ$  represent an average across the entire shear zone. For comparison, the case of  $c' = 0$  in this study yielded  $\phi' = 5.9^\circ$  at the threshold piezometric surface. Thus, the average friction angle estimate from Landslide Technology and this study are for all intents and purposes equivalent. The small difference in the values is more than likely due to the slight geometric variations in the two respective slope stability models.

The residual strength parameters determined for the shear zone along cross section B-B' are very similar to cross section A-A'. The similarity is not surprising considering that the geometry of cross section B-B' is similar to cross section A-A' and that the shear zone was extrapolated from the Landslide Technology data located along section A-A'. For piezometric surfaces at -4m and +4m of the best estimate level, residual friction angles of  $5.7^\circ$  and  $8.3^\circ$  were calculated (**Figure 5**). The best estimate residual friction angle of  $6.9^\circ$  is consistent with the previous results associated with cross section A-A'.

The residual strength parameters are highly dependent on geometry of the slip surface used in the analysis. Shear zone C1 yields maximum residual friction angles of  $14^\circ$  to  $23^\circ$  (see **Figure 6**) for the extreme water levels of -4m and +4m, respectively. By examining the extrapolated head values used in the stability analysis (**Figure 3**), it is clear that the piezometric surface provides a significant pressure head increase and corresponding reduction in the effective normal stress with each step change in the piezometric surface. As a result, the residual friction angle must be increased to maintain the factor of safety of 1, thereby contributing to the variability of residual strength with these runs. Shear zone C2 was developed from ODOT data and has the deepest shear zone out of the three piezometric surfaces. This, however, tends to reduce the sensitivity of the back calculated strength parameters to increases in the piezometric head due to the large normal stresses over the shear zone. The maximum residual friction angles ranged from  $9^\circ$  to  $11^\circ$  for -4m and +4m fluctuations of the best-estimated piezometric surface, respectively. Shear zone C3 is the shallowest (with respect to the ground surface) of the three cases and subsequently has the largest residual friction angle out of the three cases. Additionally, the piezometric surface approximately follows the surface geometry; this further decreases the normal stress and requires a significant increase in the residual strength to maintain a factor of safety of 1. Generally speaking, the trends associated with the three shear zones are consistent with the model and analysis method.

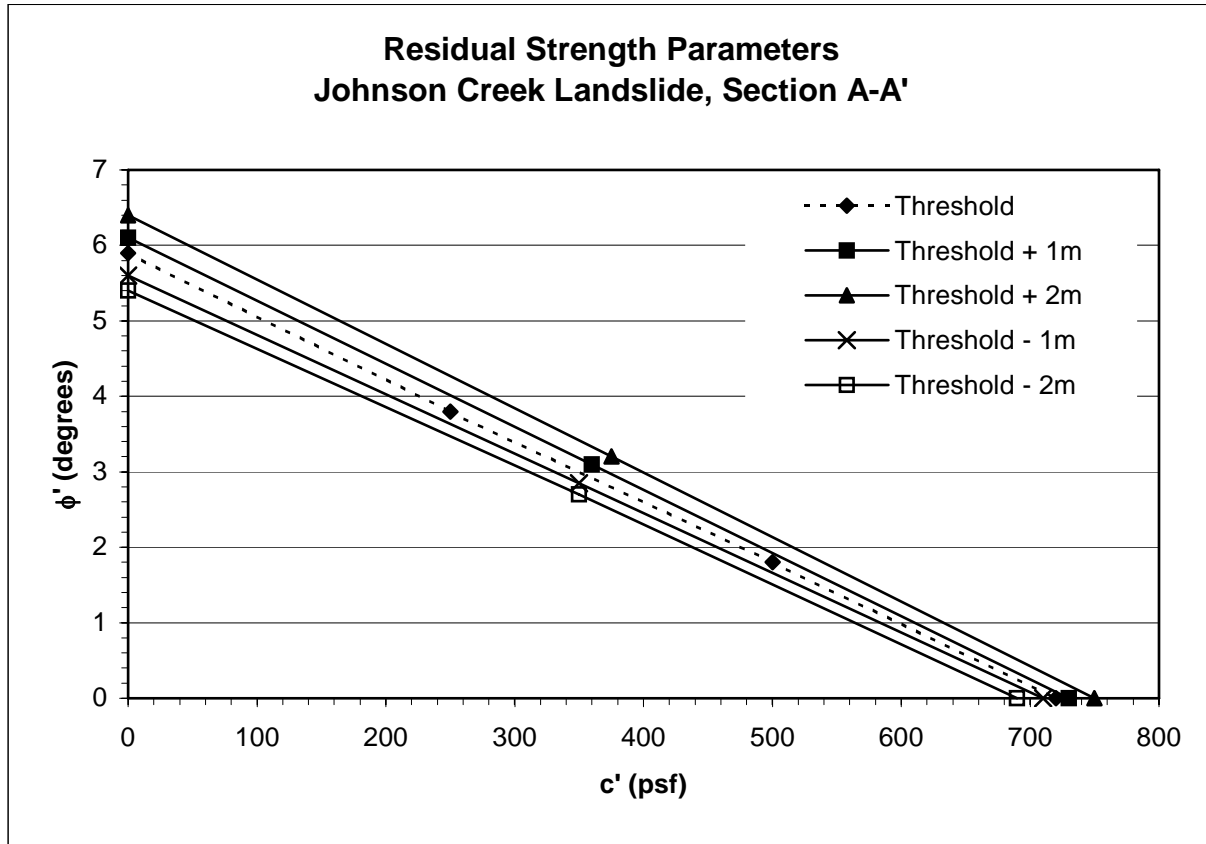


**Figure 4.** Cross Section A-A' Parametric Study.

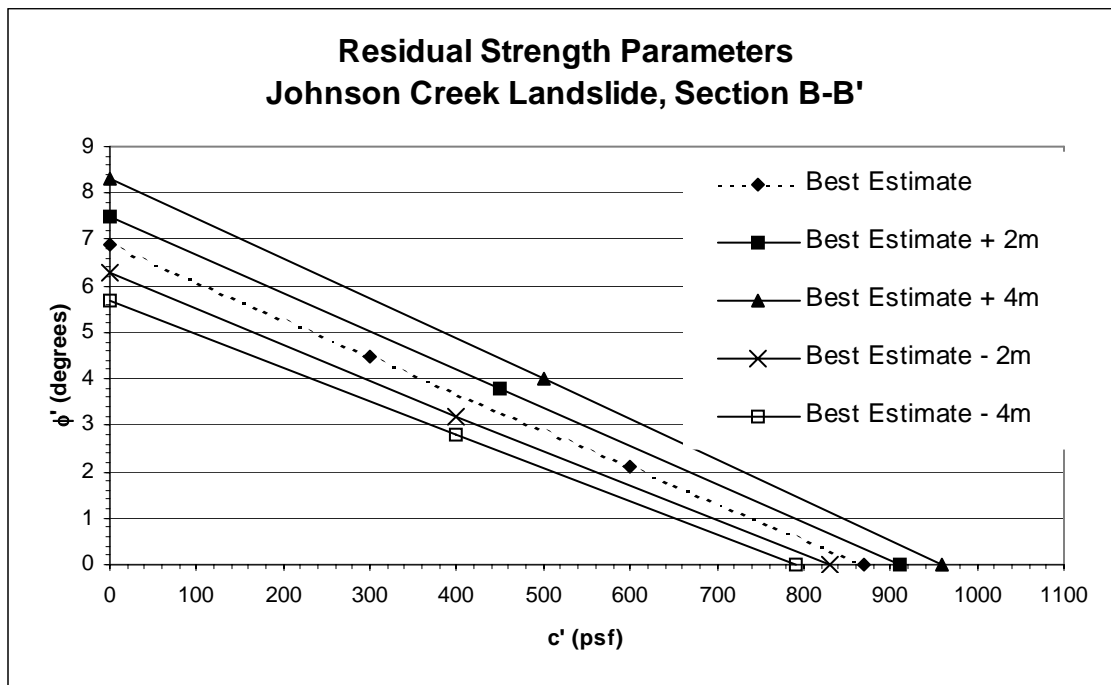


**Figure 5** Cross Section B-B' Parametric Study.

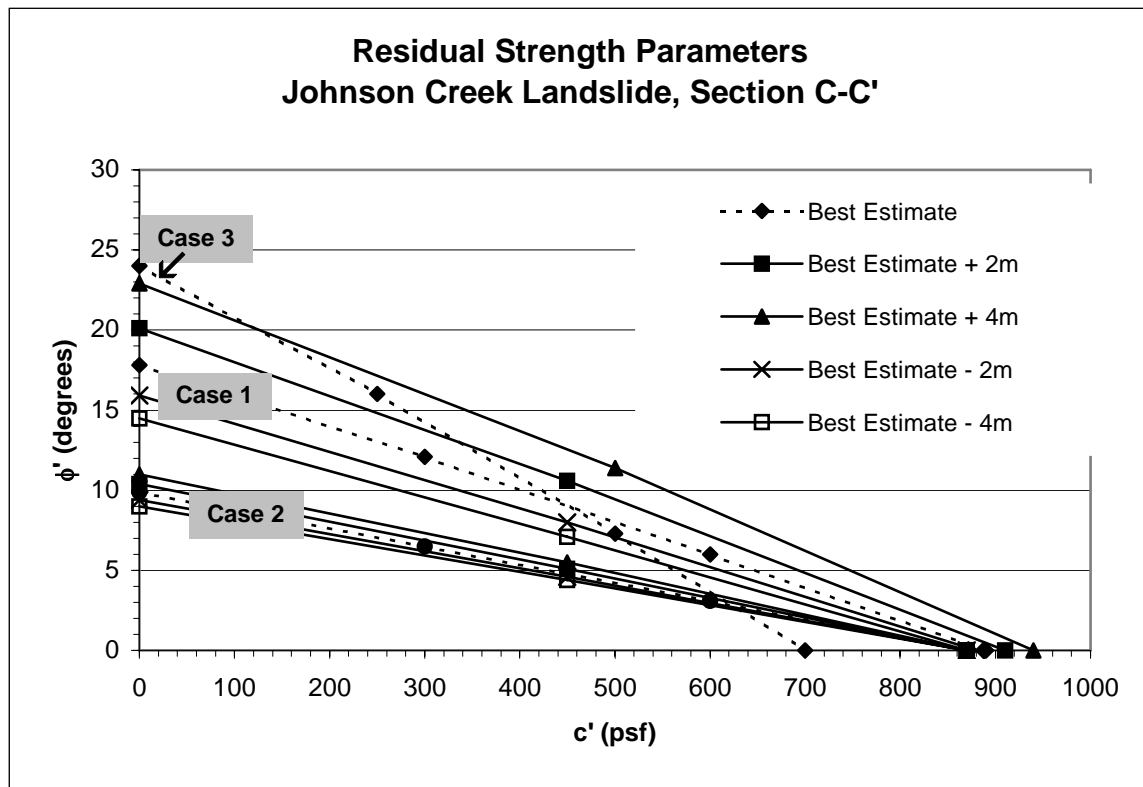


**Figure 6.** Cross Section C-C' Parametric Study.

### 2.2.2 Piezometric Surface

The fractured and interbedded nature of the weathered sedimentary rocks at the site, combined with near-vertical tensional cracks and internal slide planes greatly complicates the groundwater regime in and adjacent to the slide mass. Optimally, an extensive vertical and lateral array of piezometers would be employed to obtain data that could be used to generate real-time, 3-D plots of the pressure heads within the slide mass and immediately beneath the slide plane. As it currently exists there are only three piezometers at the site. The relatively small number of instruments poses significant limitations in the groundwater characterization required for slope stability analyses. The three existing instruments are recording pore pressures above the slide plane. As a result, the pore pressures used in the slope stability calculations may not be truly representative of the conditions across the shear zone. This is particularly important when considering the response of the piezometric surface during storm events may not be representative of what is occurring at the depth of interest.

The piezometric surfaces vary greatly across the shear zone and little data beneath the slip plane exists. It appears that above the slide plane the pore pressures are controlled by infiltration of water through cracks and fissures from above, while below the slide plane the pore pressure is governed by seepage from deeper geologic units. The occurrence of the pore pressure peaks is not coincident. In fact, the peak pore pressures beneath the slide plane may lag rainfall peaks by weeks or months.



Unfortunately, piezometric data does not exist through cross sections B-B' and C-C'. By necessity we estimated the location of the piezometric surfaces at these two locations. To address the considerable uncertainty associated with the piezometric surface estimates, we performed a sensitivity study to evaluate the influence of the piezometric surface elevation on the stability of the slide mass. The piezometric surface was varied from the best estimate value by  $\pm 4\text{m}$ . As previously discussed in 2.2.1, the influence on stability of the piezometric surface was most pronounced at Section C-C' and less pronounced at Section B-B' due to the respective geometries of these sections.

### **2.2.3 Toe Failure & Tension Cracks**

To evaluate the influence of tension cracks in the slide mass slope stability analyses were performed at the toe of cross-sections A-A' and B-B' for varying tension crack depths completely filled with water. The search routine employed in the limit equilibrium model locates all critical surfaces through the tension crack therefore the interaction effects of multiple tension cracks could not be determined from this analysis. However, this analysis did examine the influence of slope stability versus the depth of the tension crack filled with water provided some insight to the threshold tension crack depth.

The results of our analyses indicate there is a bilinear relationship in the percent change FOS for tension crack depths up to 10 feet in cross section A-A' and 15 feet in cross section B-B' (**Figure 7**). Past these respective "threshold" tension crack depths there is an increase in the slope of this curve indicating a relatively rapid loss in stability.

The significance of these results is that the depth of tension crack filled with water at the toe of the slide may be influencing the stability of the larger slide mass. An additional analysis was performed with the critical toe section removed from the previously stated analysis performed on cross section A-A' with best estimate threshold water levels. The factor of safety prior to removing the failed toe section was 1.0. After removing the critical toe section, a stability analysis was performed and the factor of safety against sliding dropped to 0.87. This represents a 13 percent decrease in the factor of safety and implies the performance of the toe has a significant influence on the stability of the slide mass.

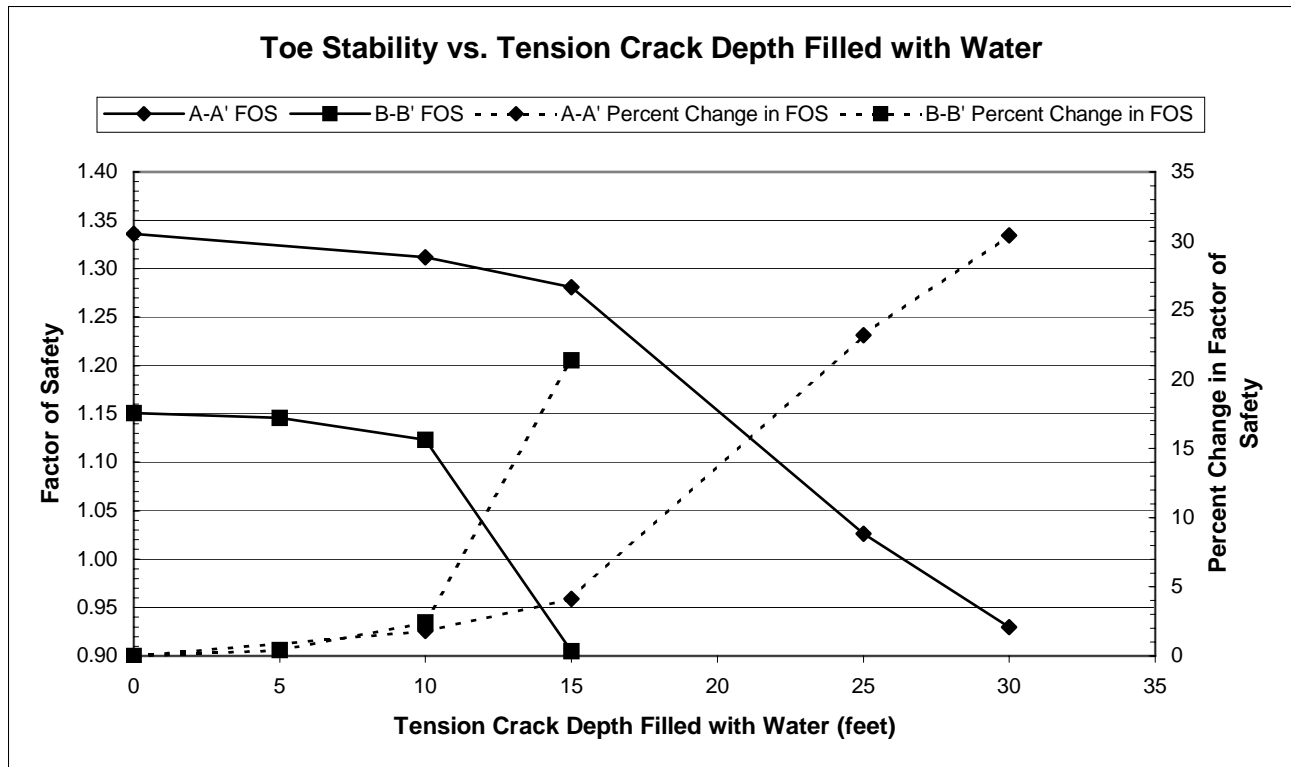


**Figure 7.** Analysis of Toe Stability with Varying Tension Crack Depth Filled with Water.

#### 2.2.4 Pressure Wave Analysis

In depth evaluation of the piezometer data demonstrates that the pore pressures rise first at the top of the slope and progressively increase with distance down slope (see the main body of this open-file report). The rise and fall of pore pressure adjacent to the shear zone moves down slope in the form of a long-period wave. This pulse, or pressure wave, influences the stability of the slide mass by reducing the effective normal stress and shear strength of the section of the slide where this pulse is present.

Based on the analysis of progressive piezometric head increase, a suite of slope stability analyses were performed on cross section A-A' with step increases in the piezometric surface (**Figure 8**). The base model for this analysis was developed from the information provided in **Table 1** for the fast movement case. The initial head values for the analysis were taken from the initial values provided in **Table 1**. All head values used were referenced to the failure plane to ensure consistency throughout the analysis. To model the pressure wave, the piezometric head was increased from normal to "fast movement levels" in increments approximately equal to 1/5 of the total shear zone length. The increases were cumulative and by the end of the analysis the results matched the factor of safety estimates from Landslide Technology (2004) for the extreme storm case. The results of the slope stability analyses are shown in **Figure 9**.

The overall percent change in slope stability from normal winter values to severe storm values is 9 percent, this compares very well to the Landslide Technology estimate of 9.2 percent. The analysis shows that 50 percent of the 9 percent change in factor of safety occurs over the eastern (upslope)

25 percent of the slide plane. As shown in the **Figure 9**, there is a non-linear decrease in factor of safety that transitions to a relatively linear change over the remaining 75 percent of the slide plane. The non-linear decrease in factor of safety is not thought to be a physical phenomenon but rather a manifestation of the computer program's analysis technique with high water pressure levels and low normal stresses. Examining the trend of factor of safety versus incremental pressure increase suggests a linear relationship could be extrapolated back through the point associated with LT-3P to a FOS value equal to 1.0.

Given the relatively high change in factor of safety associated with the head increase associated with the severe storm level, investigating options to maintain the head levels at their normal winter levels appears to be warranted. Although the FOS increase with horizontal drains is 1 percent (Landslide Technology, 2004), this dewatering scheme proposes lowering the normal winter water table by approximately 3 feet. From a limit equilibrium stand point lowering the water table does not improve the FOS significantly, however, if severe water levels could be mitigated or water level could be maintained at "normal" winter levels this option would, in effect, provide an increase in FOS of the 9 percent; the difference associated between normal winter levels and the severe storm levels.

**Table 1.** Threshold values of initial pressure head, pressure head at movement, and depth to elevation head (water table) for slow and fast slide movement. Pressure head is in meters above the slide plane (taken from the main body of this open-file report).

Drill	Initial Head (m)	Initial Head (m)	Pressure Head (m)	Pressure Head (m)	Depth to Elevation Head (m)	Depth to Elevation Head (m)
Site	Slow Mvmt	Fast Mvmt	Slow Movement	Fast Movement	Slow Movement	Fast Movement
LT-1	6.5	6.9	7	~9.0-9.7	19.3	~16.6-17.3
LT-2	9.2	9.4	9.4	~12	8.6	~6
LT-3	4.5	4.6	~5.0	~6.5	~1.6	~0.1

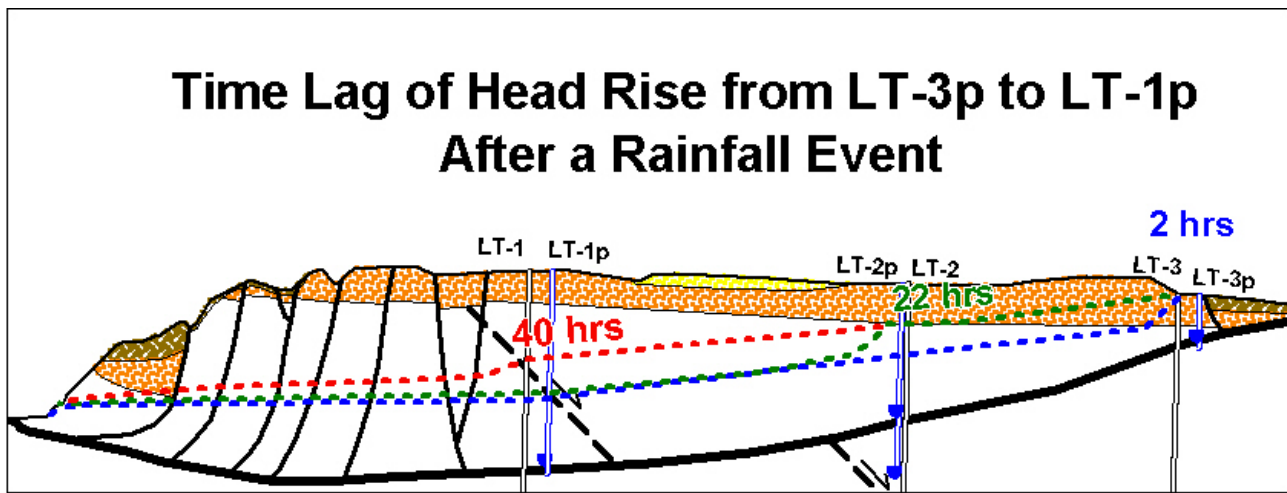


**Figure 8.** Schematic illustration of progressive rise in piezometric head from east-to-west after a typical rainfall event (Priest et al., 2005).

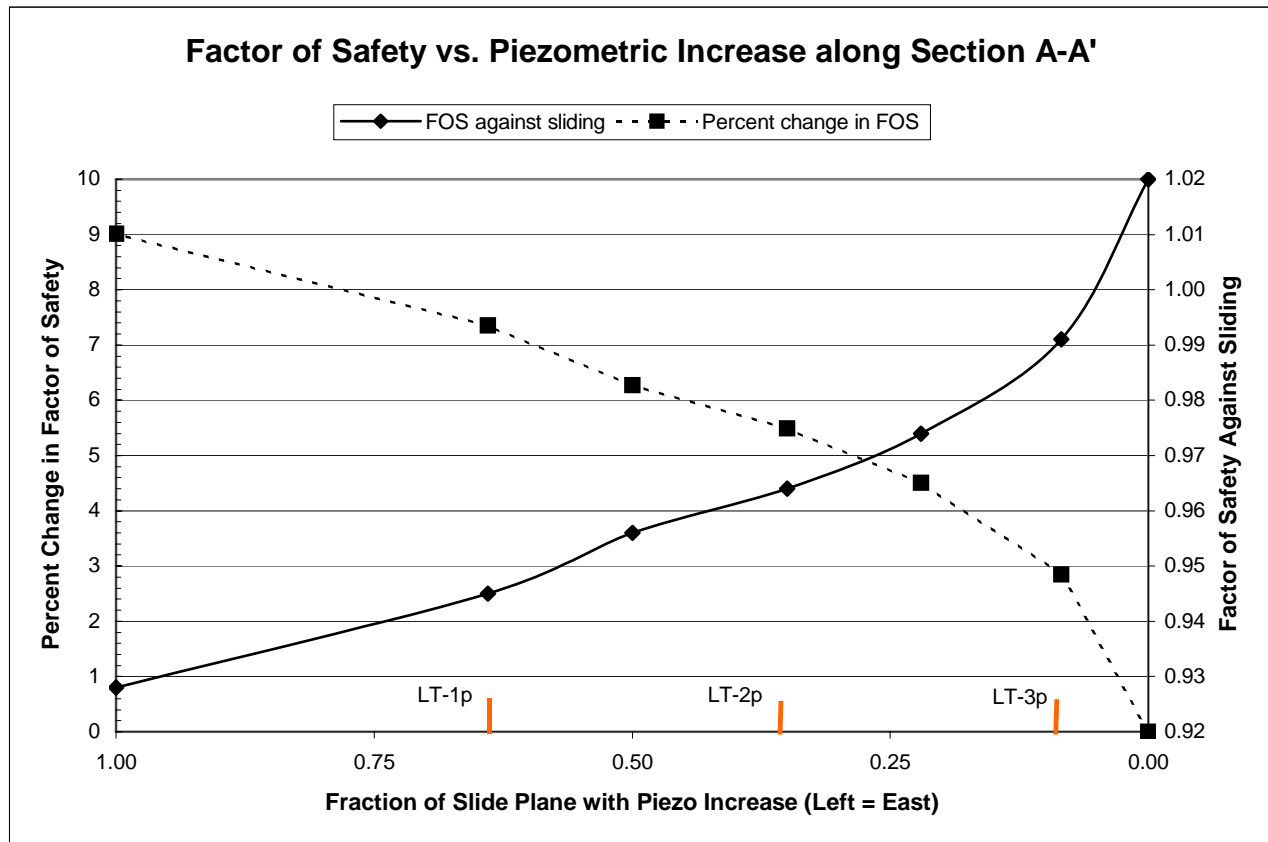


**Figure 9.** Factor of Safety versus Piezometric Increase along Shear Zone A-A'.  
(Note that left is actually west in this diagram).

### 3.0 CONCLUSIONS

On the basis of independent slope stability and parametric analyses the average residual strength parameters provided in the 2004 Landslide Technology report are reasonable for the Johnson Creek Landslide. Furthermore, analysis of a severe storm event yielded the same factor of safety percentage decrease as Landslide Technology's. The residual strength parameter variation for  $c' = 0$  gives  $\phi'$  values do not appear to be extremely sensitive to changes in the piezometric surface. Thus, potential errors in the analytical results based on the range of likely strength parameters are probably small. The sensitivity of the overall decrease in factor of safety associated with an increasing piezometric surface, however, was found to be significant. This observation is consistent with the Landslide Technology's slope stability analysis report and the correlation of movement events with piezometric spikes outlined in the main body of this open-file report.

Tension cracks appear to affect the stability of the toe when cracks are within the 10-foot to 15-foot range and are completely filled with water. Slope stability analysis shows that there is a 13 percent decrease in factor of safety associated with the removal of the critical toe surface obtained in the

tension crack portion of the analysis. Based on the contribution that the toe has on the global stability, the use of a buttress system as recommended in the Landslide Technology report and the in the main body of this open-file report certainly warrants serious consideration.

Given the relative importance of the piezometric surface and toe stability on the overall stability of the slide mass, addressing both of these issues will be critical to successful remediation. Rather than focusing on the modest improvement (1% per Landslide Technology, 2004) lowering the piezometric surface provides, one approach should consider maintaining the "normal winter" levels which ultimately provides a net factor of safety increase of approximately 9 percent over the piezometric surface representing a significant rainfall event. Toe stability, too, should be addressed since there is a significant decrease in the factor of safety associated with the failure/erosion of the toe section. Even if dewatering measures were successfully implemented, the slope would likely become unstable and move regardless of the piezometric water levels.

Although these analysis were performed using standard of practice limit equilibrium methods, there are significant shortcomings associated with these models. For instance, in the case of this landslide there are many factors that influence the stability of the mass concurrently. These variables include the kinematics influence of individual blocks, time dependent increase in the piezometric surface, seepage effects, multiple tension cracks, and the accumulative effects associated with all of these occurring with in a given time frame. In addition to modeling limitations, there is a very limited base of geotechnical data for this landslide. Despite the shortcomings of the limit equilibrium analysis methods, they provide a powerful tool in illustrating the relative influence that hydrologic and geotechnical parameters have on the stability of the slide. In our opinion, these methods are appropriate given the limited data available, and they provide insight into the problem and facilitate the evaluation of potential remediation strategies.

## **4.0 RECOMMENDATIONS FOR FUTURE WORK**

### **4.1 Field Investigation and Monitoring**

In our opinion, there exists the need for additional fieldwork and in situ exploration if the mechanics and causative factors of the slide are to be more completely understood. Given the area of the slide mass, the variable subsurface conditions (e.g. fracturing, soil strengths, stress state, etc.), the complexity of the slide movement, and complex piezometric conditions, there is a need to further investigate these unknowns since they are ultimately influencing the behavior of the slide. Clearly the resources available to this project will dictate the degree to which the various hydrologic and geotechnical controls are characterized. A prioritization strategy is needed.

It appears that a research and monitoring emphasis on the groundwater regime would yield tremendous insights on the initiation and rate of slope movement. A program of extensive instrumentation is highly recommended. As an example, one approach to addressing these unknowns would be to install approximately 10 piezometers and inclinometer tubes throughout the slide. Cross sections B-B' and C-C' would be ideal candidates for 4 piezometer and inclinometer

sets. The two remaining piezometer and inclinometer sets would then be placed along cross section A-A', particularly near the toe where conditions are not well defined to this point in the investigation. Optimally, the piezometers should be placed immediately above and below the shear zone. The assertion that this material may be imposing a confined aquifer type of condition would be of great importance in evaluating the net pressure effect on the slide plane after a storm event.

The long-term survival of the piezometers is a key consideration. This is especially true for instrumentation located below the shear zone. It is recommended that a system of wireless piezometers be used below the slide plane. A wireless system could be used to transmit data across the slide plane even after the slope has moved enough to damage the borehole casing (i.e., slope inclinometer tubing). Data would be transmitted from the piezometer located beneath the slide plane to a receiver suspended in the borehole immediately above the shear zone. Wireless systems such as this have been developed for use in physical model testing using the geotechnical centrifuge. They have been shown to be rugged and reliable for these applications. The Geotechnical Engineering Group at Oregon State University is pursuing field applications for this technology and it appears that the Johnson Creek landslide could be a test bed for evaluating the applicability of this wireless instrumentation.

## **4.2 Laboratory Investigations**

The benefits of additional laboratory testing are judged to be minimal. The heterogeneity of the slide mass materials (lithology, weathering, and pattern of discontinuities) precludes extensive characterization by laboratory tests alone. It appears that a more significant contribution would be made by focusing on drilling and field logging of the materials in order to characterize the locations of the shear zone and piezometric surface, as well as the nature of the soil and rock adjacent to the slide plane. These efforts would be pursued during the placement of the in situ instrumentation.

One aspect of laboratory testing that may be worthwhile would be additional characterization of the porosity and permeability of intact specimens of the weathered rock located near the slide plane. These data would be useful in subsequent hydrologic modeling; however, these properties would have to be modified to account for the rock mass characteristics (i.e. discontinuities, variability in the degree of weathering, etc).

## **4.3 Modeling**

The use of more sophisticated models at this point in the study would not likely provide a better understanding of the behavior of this slide. A 3-D FEM/FDM model could be created based on the surface surveys and subsurface conditions as they are currently understood; however, uncertainties associated with the morphology of the slip surface, the hydrologic regime, geologic structure within the slide mass, and the kinematics of the various blocks within the overall slide mass would significantly limit confidence in the modeling results. If more advanced modeling is pursued, it is recommended that simple models be prepared and validated prior to applications involving all of the relevant parameters that can be reasonably modeled. The application of simple models, along with appropriate simplifications using informed judgment, may yield insights on the kinematic aspects of the slide that are not well defined using the 2-D limit equilibrium models. The ultimate



goal of performing coupled hydrologic-geotechnical stability modeling is considered extremely worthwhile.

## **ACKNOWLEDGEMENTS**

The authors wish to acknowledge the tremendous contributions made to the project by several individuals. Mr. Jason Locke (U.S. Navy, and 2005 graduate of the Department of Construction, Civil, Construction and Environmental Engineering at Oregon State University. In addition to collecting references from DOGAMI, ODOT, and NOAA at the outset of the project, he contributed a great deal to the site reconnaissance by participating in the ground mapping. He also secured the use of an airplane and served as pilot for our aerial reconnaissance. The equipment and services were provided at no cost the project. The authors are grateful to Mr. Locke for his generosity and great interest in the project. Mr. Locke has also provided a collection of his aerial photographs for the DOGAMI archives.

The authors are also grateful to Mr. Andrew Vessely (Cornforth Consultants, Inc.) for sharing his insights on the Johnson Creek Landslide, as well as other Coast Range landslides in the region. His perspectives on the investigations performed to date and the mechanics of the slide were extremely useful.

We also wish to thank Mr. Michael Vail (formerly Graduate Researcher, Geotechnical Engineering Group, OSU) for his preliminary slope stability modeling and figure preparation. His contributions were very useful for highlighting variations in computed stability using different slope stability programs.

## **REFERENCES**

- Landslide Technology, 2004, Geotechnical investigation Johnson Creek Landslide, Lincoln County, Oregon: Oregon Department of Geology and Mineral Industries Open-File Report O-04-05, 115 p, published on CD.
- Priest, G.R., Allan, J.C., Niem, A., 2005, Interim Report: Johnson Creek Landslide Project, Lincoln County, Oregon: Oregon Department of Geology and Mineral Industries unpublished draft report, 04-05.